



Ardley Coal Zone Characterization and Coal-Sandstone Channels Architecture, Pembina CBM Exploration Block, Alberta

**Ardley Coal Zone
Characterization and
Coal-Sandstone Channels
Architecture, Pembina CBM
Exploration Block, Alberta**

Cristina Pana

Alberta Geological Survey

March 2007

©Her Majesty the Queen in Right of Alberta, 2007
ISBN 0-7785-3841-9

The Alberta Energy and Utilities Board/Alberta Geological Survey (EUB/AGS) and its employees and contractors make no warranty, guarantee or representation, express or implied, or assume any legal liability regarding the correctness, accuracy, completeness or reliability of this publication. Any digital data and software supplied with this publication are subject to the licence conditions. The data are supplied on the understanding that they are for the sole use of the licensee, and will not be redistributed in any form, in whole or in part, to third parties. Any references to proprietary software in the documentation, and/or any use of proprietary data formats in this release, do not constitute endorsement by the EUB/AGS of any manufacturer's product.

When using information from this publication in other publications or presentations, due acknowledgment should be given to the EUB/AGS. The following reference format is recommended:

Pana, C. (2007): Ardley Coal Zone characterization and coal-sandstone channels architecture, Pembina CBM exploration block, Alberta; Alberta Energy and Utilities Board, EUB/AGS Earth Sciences Report 2007-04, 153 p.

Published March 2007 by:

Alberta Energy and Utilities Board
Alberta Geological Survey
4th Floor, Twin Atria Building
4999 – 98th Avenue
Edmonton, Alberta
T6B 2X3
Canada

Tel: (780) 422-3767 (Information Sales)

Fax: (780) 422-1918

E-mail: EUB.AGS-Infosales@eub.ca

Website: www.ags.gov.ab.ca

Contents

Acknowledgments	viii
Abstract	ix
1 Introduction	1
2 Geological Framework	2
2.1 Scollard Formation	2
2.2 Paskapoo Formation	5
2.3 Battle Formation	5
3 Ardley Coal Zone in the Pembina CBM Exploration Block	6
3.1 Lithological Description and Facies Association	6
3.1.1 Sandstone.....	6
3.1.2 Mudstone and Siltstone	7
3.1.3 Coal.....	7
3.1.4 Tonstein	9
3.2 Sequence Stratigraphic Model.....	10
3.2.1 Depositional Controls.....	10
3.2.1.1 Tectonic Controls	10
3.2.1.2 Paleoclimatic Controls	11
3.2.2 Stratigraphic Sequences or Cycles in the Scollard-Basal Paskapoo Succession	12
3.2.3 Coal Depositional Model.....	14
3.3 Coal Reservoir Characterization	15
3.3.1 Coal Reservoir Geometry.....	15
3.3.1.1 Depth and Thickness.....	15
3.3.1.2 Internal Structure	16
3.3.1.3 Seals.....	17
3.3.2 Coal Properties	17
3.3.2.1 Coal Quality (Ash Content).....	17
3.3.2.2 Coal Rank and Burial History	19
3.3.3 Fractures Pattern and Infillings.....	20
3.3.4 Reservoir Conditions	22
3.3.4.1 Regional Scale.....	22
3.3.4.2 Pembina CBM Exploration Block	23
3.4 Coal Tonnage and Gas-in-Place	23
4 Coal-Sandstone Architecture and Reservoir Connectivity	24
4.1 Geometry of the Sandstone Channels and their Relationship with the Adjacent Coal Seams	24
4.1.1 Paskapoo Basal Channels Assemblage	25
4.1.2 Arbour-Silkstone Channels Assemblage.....	25
4.1.3 Silkstone-Mynheer Channels Assemblage.....	25
4.2 Discussion on Reservoir Connectivity and CO ₂ -ECBM in Ardley Coal Strata, Pembina Block.....	26
5 Conclusions	27
6 References	29
Appendix 1 Report Figures	34
Appendix 2 Core Photographs	127

Tables

Table 1	Equivalence of coal subzones between the Edson and Pembina CBM exploration blocks	4
Table 2	Lithotype correlation table (after Bustin et al., 1983).....	8
Table 3	Coal volume, coal mass and volume of gas-in-place	24

Figures

Figure 1	Coalbed methane production wells from the Ardley Coal Zone.....	37
Figure 2	Stratigraphic chart of the Upper Cretaceous–Tertiary formations in the Alberta foreland basin.....	38
Figure 3	Chart of the stratigraphic models of the Scollard–Paskapoo sequence.....	39
Figure 4	Isopach map of the Scollard Formation.....	40
Figure 5	Alberta bedrock.....	41
Figure 6	Isopach map of the upper member of the Scollard Formation (Ardley Coal Zone)	42
Figure 7	Isopach map of the Paskapoo Formation and Quaternary deposits	43
Figure 8	Structural contour map of the top of the Scollard Formation (Ardley Coal Zone)	44
Figure 9	Structural contour map of the base of the Scollard Formation	45
Figure 10	Isopach map of cumulative coal in the Ardley Coal Zone	46
Figure 11	Schematic correlation of Edson and Pembina coal sub-basins (Scollard Formation).....	47
Figure 12a)	Digital elevation model (DEM) of the Pembina study area.....	48
Figure 12b)	Wells considered during the study.....	49
Figure 13	Location of the examined drillcores in the Pembina study area.	50
Figure 14	Vertical lithological profile of the Ardley Coal Zone in the Pembina study area	51
Figure 15	Locations of structural cross-sections, Pembina study area	52
Figure 16	A–A' Structural cross-section, Pembina study area	53
Figure 17	B–B' Structural cross-section, Pembina study area	54
Figure 18	C–C' Structural cross-section, Pembina study area	55
Figure 19	D–D' Structural cross-section, Pembina study area.....	56
Figure 20	E–E' Structural cross-section, Pembina study area.....	57
Figure 21	F–F' Structural cross-section, Pembina study area	58
Figure 22	H–H' Structural cross-section, Pembina study area.....	59
Figure 23	I–I' Structural cross-section, Pembina study area	60
Figure 24	J–J' Structural cross-section, Pembina study area	61
Figure 25	L–L' Structural cross-section, Pembina study area	62
Figure 26	M–M' Structural cross-section, Pembina study area	63
Figure 27	Schematic representation of the distribution of subzones in the Ardley Coal Zone	64
Figure 28	Section illustrating consistency of the vertical lithological profile of the Ardley Coal Zone in the Pembina study area.....	65
Figure 29	Thin tonstein strata recognized on the geophysical log, Pembina study area.....	66
Figure 30	Sequence stratigraphic model, Pembina study area	67
Figure 31	Schematic reconstruction of the peat environment during deposition of the Ardley Coal Zone	68
Figure 32	Depth to the top of the Ardley Coal Zone, Pembina study area.....	69
Figure 33	Depth to the base of the Ardley Coal Zone, Pembina study area.....	70
Figure 34	Depth to the base of the lower Scollard Formation, Pembina study area.....	71
Figure 35	Structure contours on the top of the Ardley Coal Zone, Pembina study area.....	72
Figure 36	Structure contours on the base of the Ardley Coal Zone, Pembina study area.....	73
Figure 37	Structure contours on the base of the Lower Scollard Formation, Pembina study area	74

Figure 38	Isopachs of the Ardley Coal Zone, Pembina study area.....	75
Figure 39	Isopachs of the lower Scollard Formation, Pembina study area.....	76
Figure 40	Isopachs of the Battle Formation, Pembina study area	77
Figure 41	Isopachs of Ardley cumulative coal, Pembina study area.....	78
Figure 42	Number of Ardley coal seams, Pembina study area.....	79
Figure 43	Isopachs of the Mynheer coal subzone, Pembina study area	80
Figure 44	Isopachs of Mynheer cumulative coal, Pembina study area	81
Figure 45	Number of Mynheer coal seams, Pembina study area	82
Figure 46	Isopachs of the Silkstone coal subzone, Pembina study area.....	83
Figure 47	Isopachs of Silkstone cumulative coal, Pembina study area	84
Figure 48	Number of Silkstone coal seams, Pembina study area.....	85
Figure 49	Isopachs of the Arbour coal subzone, Pembina study area	86
Figure 50	Isopachs of Arbour cumulative coal, Pembina study area	87
Figure 51	Number of Arbour coal seams, Pembina study area	88
Figure 52	Isopachs of the Val D’Or coal subzone, Pembina study area	89
Figure 53	Isopachs of Val D’Or cumulative coal, Pembina study area	90
Figure 54	Number of Val D’Or coal seams, Pembina study area	91
Figure 55	Distribution of ‘clean coal’ (in per cent) in the Val D’Or subzone, Ardley Coal Zone, Pembina study area.....	92
Figure 56	Distribution of ‘clean coal’ (in per cent) in the Arbour subzone, Ardley Coal Zone, Pembina study area.....	93
Figure 57	Distribution of ‘clean coal’ (in per cent) in the Silkstone subzone, Ardley Coal Zone, Pembina study area.....	94
Figure 58	Distribution of ‘clean coal’ (in per cent) in the Mynheer subzone, Ardley Coal Zone, Pembina study area.....	95
Figure 59	Coal rank chart	96
Figure 60	Distribution of vitrinite reflectance in the Ardley Coal Zone, Alberta.....	97
Figure 61	Distribution of vitrinite reflectance in the Ardley Coal Zone in the Pembina study area	98
Figure 62	Structural cross-section, Brazeau River area, central foothills of Alberta	99
Figure 63	Interpretation of surface lineaments from the Alberta digital elevation model.....	100
Figure 64	Interpretation of surface lineaments from the digital elevation model of the Pembina CBM exploration block.....	101
Figure 65	Potentiometric contours of hydraulic head data for the Paskapoo Formation plotted on the digital elevation model.....	102
Figure 66	Potentiometric contours of hydraulic head data for the Scollard Formation plotted on the digital elevation model.....	103
Figure 67	Formation pressure versus depth, Scollard and Paskapoo formations, regional scale.....	104
Figure 68	Formation pressure versus depth, Paskapoo Formation, regional scale.....	104
Figure 69	Formation pressure versus depth, commingled Paskapoo basal sandstone channels and upper Ardley coal beds, regional scale.....	105
Figure 70	Formation pressure versus depth, upper Ardley coal subzones	105
Figure 71	Formation pressure versus depth, lower Ardley coal subzones.	106
Figure 72	Formation pressure versus depth, Paskapoo Formation, well 02/07-32-036-03W5/0	106
Figure 73	Formation pressure versus depth, Paskapoo basal sandstone channels, well 00/06-34-052-09W5/0	107
Figure 74	Formation pressure versus depth, upper Paskapoo and Paskapoo basal channels.....	107
Figure 75	Formation pressure versus depth, MU and MI coal subzones, well 02/11-06-056-19W5/0, Edson coalbed methane exploration block.....	108

Figure 76	Formation pressure versus depth, Val D’Or, Arbour and Silkstone coal subzones, well 00-10-16-048-14W5/0, Pembina coalbed methane exploration block.....	108
Figure 77	Formation pressure versus depth, ‘S’ , ‘Ml’ and ‘N’ coal subzones, well 00/11-01-056-19W5/0, Edson coalbed methane exploration block	109
Figure 78	Total dissolved solids (TDS), Quaternary, Paskapoo and Scollard succession, regional data.....	109
Figure 79	Potentiometric surface, Paskapoo Formation, Pembina study area.	110
Figure 80	Potentiometric surface, Scollard Formation, Pembina study area	111
Figure 81	Formation pressure versus depth, Paskapoo Formation, Pembina study area	112
Figure 82	Total dissolved solids (TDS), Pembina study area	112
Figure 83	Total dissolved solids (TDS), regional scale including the TDS trend.....	113
Figure 84	Isopachs of the Paskapoo basal sandstone channels (>10 m), Pembina study area.....	114
Figure 85	Isopachs of the Arbour-Silkstone sandstone channels (>5 m), Pembina study area	115
Figure 86	Isopachs of the Silkstone-Mynheer sandstone channels (>5 m), Pembina study area	116
Figure 87	Isopachs of the upper sandstone channels (>5 m) of the lower Scollard Formation, Pembina study area.....	117
Figure 88	Locations where Paskapoo basal channels are in direct contact with the uppermost Ardley coal seams (indicated in red), Pembina study area	118
Figure 89	Locations where Arbour-Silkstone channels are in direct contact with the Silkstone coal seams (indicated in red), Pembina study area.....	119
Figure 90	Locations where upper channels are in direct contact with the lowermost Mynheer coal seams (indicated in red), Pembina study area	120
Figure 91	Locations where Silkstone-Mynheer channels are in direct contact with the Mynheer coal seams (indicated in red), Pembina study area	121
Figure 92	Three-dimensional image of the channel succession, Pembina study area	122
Figure 93	Isopachs of the lower channels of the lower Scollard Formation, Pembina study area.	123
Figure 94	Multiple small gas accumulations in the basal Paskapoo and Arbour-Silkstone sandstone channels, well 03/14-27-048-08W5, Pembina study area	124
Figure 95	Small gas accumulation in the lower sandstone channel of the Scollard Formation, Pembina study area.....	125
Figure 96	Shallow gas wells map.....	126

Plates

Plate 1	Core photographs of sandstone units.....	132
Plate 2	Core photographs of sandstone units.....	133
Plate 3	Core photographs of paleosoil units	134
Plate 4	Core photographs of paleosoil units	135
Plate 5	Core photographs of coal seams.....	136
Plate 6	Core photographs of coal seams.....	137
Plate 7	Core photographs of coal seams.....	138
Plate 8	Core photographs of coal seams.....	139
Plate 9	Core photographs of coal seams.....	140
Plate 10	Core photographs of coal seams.....	141
Plate 11	Core photographs of coal seams.....	142
Plate 12	Core photographs tonstein beds	143

Acknowledgments

I extend special thanks to the following present and former colleagues for their invaluable help during this study (all of whom are with the Alberta Geological Survey unless otherwise indicated):

- Andrew Beaton for leadership support,
- Natalyia Lyublimova (stratigraphic and coal picks), Energy and Utilities Board,
- Dr. Karsten Michael (hydrogeological data and guidance in hydrogeological interpretation),
- Tony Lemay (water chemistry data and GIS),
- Andre Lytviak (basin stratigraphic and reservoir data),
- Desmond Wynne (database management),
- Dennis Chao (GIS),
- Dr. Shilong Mei (DEM),
- Dan Magee (artistic drafting),
- Mike Berhane (LAS files),
- Dr. Magda Ciulavu (paleosol literature), Canadian Natural Resources Ltd.,
- Hanne Csanyi (publications),
- Maryanne Protz and Gisela Hippolt-Squair (internal editing).

Special consideration goes to the external reviewers Dr. Tony Hamblin (Geological Survey of Canada) and Dr. David Marchioni (Petro-Logic Services Ltd.) for the dedicated and competent effort shown to improve the content of the report.

I also thank AERI (Alberta Energy Research Institute) for funding components of this work through a research grant.

Abstract

This study was motivated by the economic importance of coalbed methane (CBM) exploration and development in the Ardley Coal Zone and emerging interest in CO₂ sequestration associated with enhanced CBM production (CO₂-ECBM) in the Pembina CBM exploration block. The purpose was to assist exploration by providing a better understanding of the relationship between the coal sequences and reservoir characteristics.

The study integrates the new detailed coal and stratigraphic picks for the Pembina CBM exploration block with the publicly available formation-pressure and water chemistry data. The resulting detailed interpretation of the Pembina exploration block indicates those areas with high CBM potential (coal thickness and continuity, coal quality, optimum depth, fracture pattern) and outlines the potential long-term risk associated with CO₂ storage in the Ardley coal strata.

The report consists of three parts:

1. the first part presents an overview of the Scollard–Paskapoo succession interpreted in light of the adjacent tectonic activity and climatic regime;
2. the second part focuses on the Pembina CBM exploration block and systematically analyzes the Ardley Coal Zone with respect to coal properties, coal zone internal structure, hydrogeology and fracture patterns;
3. the last part discusses the channel intervals, the coal-channels architecture and potential pathways of fluid migration.

As the result of this study, five fluvial sequences have been recognized in the Pembina exploration block and interpreted as dynamic responses to the cyclic slow thrusting tectonic stages in the sediment source area followed by isostatic rebound. The depositional environments favourable for coal accumulation migrated from the west-northwest during Mynheer depositional time to the west-east central area during Silkstone time and to the west-southeast in Arbour and Val D’Or time. Coal subzones can be considered individual reservoirs due to the particular geometry and sealing of the coal packages. The examined drillcores have shown that the ‘banded coal’ lithotype is the dominant category of coal in the Pembina block. Coal cleats free of mineral infilling are dominant. Vitrain reflectance ranges from 0.54% to 0.59%, within the onset of hydrocarbon generation. Interpretation of the fracture system suggests two areas of potential ‘two-face-cleat’ systems, on each side of the North Saskatchewan River. In addition, differential compaction may locally amplify the existing cleats or generate additional fractures at the contacts of the coal seams with adjacent sandstone channels. The Scollard–Paskapoo succession in the Pembina exploration block is considered an aquifer system, based on formation-pressure and water-salinity data. The Ardley Coal Zone contains a total of approximately $323 \times 10^9 \text{ m}^3$ gas-in-place, with estimated gas content increasing from the uppermost coal subzone, Val D’Or ($62 \times 10^9 \text{ m}^3$) to the lowermost coal subzone, Mynheer ($104 \times 10^9 \text{ m}^3$). The sandstone channels are in direct stratigraphic contact with the underlying coal seams in some locations, which may have allowed to methane to migrate. Both types of reservoirs, coal and sandstone, may have inherent permeability; therefore on a geological time scale, the direct stratigraphic contacts can be considered potential gas migration pathways in CO₂-ECBM strategy.

1 Introduction

Current demand for new sources of hydrocarbons, including the unconventional types, requires a re-evaluation of all potential coalbed methane (CBM) zones in Alberta at a greater level of detail. One of the important CBM targets in the Alberta foreland basin is the early Tertiary coal accumulation, referred to as the Ardley Coal Zone. Another emerging interest, that of CO₂ storage in coal to reduce the amount of gas emissions, makes the Ardley Coal Zone an environmentally attractive target associated with enhanced CBM production (CO₂-ECBM). Both potential targets require a better understanding of the reservoir characteristics of the Ardley Coal Zone.

Analogous to the concept of petroleum systems (Magoon and Dow, 1994), the ‘coal system’ (Warwick, 2005) approach considers an evaluation of the source rock, thermal maturation and generation, and an assessment of gas entrapment. The coal system model is used in this study as a tool for assessing the Ardley Coal Zone as a CBM potential target and indicates long term risk regarding CO₂ storage in the coal seams. The modern approach to evaluation of the Ardley Coal Zone as a source rock for hydrocarbons integrates the coal formation processes, coal quality and reservoir characteristics into a more accurate description of the succession.

The present report presents: 1) an overview of the Scollard Formation, reinterpreted based on sequence analysis; 2) an updated regional characterization of the Ardley Coal Zone with a brief comparison of two CBM exploration blocks (Edson and Pembina); and 3) a detailed coal zone characterization within the Pembina block. In addition, a detailed interpretation of the channel systems and their proximity to the underlying coal seams is presented for the Pembina block to assist in defining the entrapment characteristics of the coal reservoir.

Comprehensive coalbed methane resource estimates are generally not rigorous at this time because CBM testing of the Ardley Coal Zone is in the preliminary stages (Figure 1). Thus, the coal resource evaluation of the Ardley Coal Zone has relied on the subsurface drilling data to obtain information on coal thickness, quality, depth and tonnages, and volume of gas-in-place estimates. The hydrogeological data publicly available for the Scollard–Paskapoo sequence, at the basin scale, comprise a very small number of formation-pressure values and water chemistry results. Also, coal petrography and vitrain reflectance data are very limited. Under these circumstances, the interpretation of Ardley reservoir heterogeneity depends mainly on stratigraphic characteristics combined with the associated limited reservoir data and detailed coal analyses. Considering the architecture of the sandstone channels and their proximity to the underlying coal seams, the study assessed the potential hydraulic connectivity through geological time and the open system character of the Ardley Coal Zone as a part of Scollard–Paskapoo aquifer system. Locally, small quantities of methane are trapped in the Paskapoo basal channels or in the Ardley inter–coal seam sandstone channels, which possibly represent present-day reservoirs for methane that migrated from the underlying coal seams.

Sequence-stratigraphic principles and paleoclimatic and tectonic depositional control factors in coal-bearing units have been used to define and demonstrate the ‘Ardley coal system’ attributes as a part of the Scollard–Paskapoo clastic prism. The interpretation presented in this report provides a solid stratigraphic framework of the Scollard and basal Paskapoo clastic succession in the Pembina exploration block, which assists in CBM reservoir characterization issues, such as coal-reservoir internal structure, geometry and methane trapping. The new dataset used for producing the present stratigraphic framework is associated to the report.

2 Geological Framework

The Rocky Mountains foreland basin in Alberta consists of a thick sedimentary succession dominated by clastic sediments during Cretaceous and Tertiary time. The source of the abundant clastic sediments transported into the foreland basin was the Cordilleran Orogen, during stages of uplift associated with the Laramide Orogeny. The entire clastic succession dips westerly to the thrust-and-fold belt. Post-Tertiary uplift of the Alberta foreland basin generated the partial erosion of the Upper Cretaceous–Tertiary formations in the distal area and induced the strong asymmetry of the basin. The Upper Cretaceous–Tertiary sequence is well preserved in proximity, and parallel, to the foothills. The influx of sediments was deposited mainly in fluvial environments, discontinuously associated with coal strata.

2.1 Scollard Formation

The Scollard Formation (Gibson, 1977) represents the clastic succession spanning the end of the Cretaceous and beginning of the Tertiary (Figure 2). The Cretaceous–Tertiary boundary corresponds to the initiation of coal deposition within the upper part of the Scollard Formation.

The definition of the late Maastrichtian–early Paleocene stratigraphic interval has been improved during the last four decades (Figure 3). The stratigraphic model proposed here (Figure 3) is based on Gibson's model (1977) and includes the later-documented Maastrichtian–Paleocene boundary (Sweet and Braman, 1992) at the base of the coal zone. The model recognizes the unconformities at the base and at top of the Scollard Formation, and applies the foothills informal nomenclature to the four subunits of the Ardley Coal Zone (Dawson et al., 2000).

The present-day architecture of the foreland basin in Alberta shows that the Scollard Formation, described in publications as a 'molasse type' succession (Eisbacher et al., 1977) or 'clastic prism' (Dawson et al., 1994) that infilled the foredeep trough along the foothills area, is an asymmetric sedimentary succession dipping towards the deformation belt. The preserved thickness varies from several metres in the outcrop, along the northern and eastern erosional edge, to about 420 m in the subsurface, near the deformation belt (Figure 4). The Scollard Formation covers an elongated area in front of, and parallel to, the foothills between townships 20 and 62 (Figure 5), mostly west of the 5th Meridian, encompassing approximately 130 000 km². Towards south, the Scollard Formation gradually changes lithologically, by loss of the coal component and becoming more enriched in 'caliche' (Jerzykiewicz and Sweet, 1986). The stratigraphic equivalent of the Scollard Formation south of township 20 is the Willow Creek Formation (Figures 2 and 5).

The Scollard Formation is separated from the underlying Horseshoe Canyon Formation to the south and southeast, and from the clastic wedge of the Wapiti Group to the west and northwest, by a thin and consistent unit of interbedded layers of tonstein and mudstone named the Battle Formation (Allan and Sanderson, 1945). After an interruption considered diachronic, the clastic deposition continued in middle and upper Paleocene with the Paskapoo succession, also of fluvial origin. The hiatus between the Scollard and Paskapoo formations is described as the 'pre-Paskapoo unconformity' (Jerzykiewicz, 1997) and spans more than 1.2 m.y., as documented in outcrop (Lerbekmo et al., 1990).

The top of the Scollard Formation is generally considered the top of the uppermost coal seam of the regionally continuous coal unit known as the Ardley Coal Zone, with some exceptions where the upper coal strata had not been deposited or had been eroded. The isopachs of the Scollard Formation show that it thinned northward and eastward even before the pre-Paskapoo hiatus (Figure 4). The preservation of the uppermost coal seam indicates that, in most of the basin, the erosional processes were still limited during the pre-Paskapoo hiatus.

The Scollard Formation consists of medium-coarse to very fine clastic sediments, represented by sandstone, mudstone and siltstone associated with coal strata. Occasionally and with different regional distributions, thin layers of diagenetic volcanic ash are recognized as tonstein beds. The sequence stratigraphic principles applied in this study have allowed the separation of five major cycles or sequences that are regionally mappable within the Scollard succession, as will be discussed in section 3.

The Scollard Formation can be informally divided into a lower and an upper member. The lower member consists of siltstone and mudstone with several thin tonstein beds, most of them discontinuous, associated with moderately thin and clean sandstone units. Coal is absent. Where the succession is preserved, the lower member represents an accumulation of 40–200 m thickness, thinning easterly. The thickness and the number of stacked sandstone channels gradually increase towards the deformation belt, close to the source area of the sediments. The lower part of the Scollard Formation is considered to be latest Maastrichtian in age, based on the palynological data (Sweet et al., 1990; Sweet and Braman, 1992). The upper member of the Scollard Formation, informally referred to as the Ardley Coal Zone, contains several economically significant coal seams, grouped in subzones intimately associated with thin, distinctive and laterally quasi-continuous layers of tonstein. Other lithological components of the upper member are mudstone, siltstone and sandstone. The lower Paleocene age of the upper member of the Scollard Formation is documented by the palynomorphs associated with the coal strata (Sweet et al., 1990; Demchuck, 1990; Sweet and Braman, 1992).

Upper Member of the Scollard Formation (Ardley Coal Zone)

The upper member of the Scollard Formation, lower Paleocene in age and commonly referred to as the Ardley Coal Zone, contains important coal and coalbed methane resources (Dawson et al., 1994). A content of approximately 53 Tcf of methane was recently estimated for the entire Ardley Coal Zone (Beaton et al., 2002; Beaton, 2003). Nevertheless, Ardley Coal Zone has remained an important subject for stratigraphic and reservoir studies.

The Ardley Coal Zone has an area of distribution similar to that of the lower Scollard member north of township 20. The thickness of the upper Scollard member or Ardley Coal zone ranges from a few metres along the erosional edge up to 217 m in subsurface close to the thrust-and-fold belt (Figure 6), and commonly represents half of the Scollard Formation thickness. The isopachs of the Ardley Coal Zone (Figure 6) show a narrow area with significant increase of thickness (<200 m) located in the northern part of the basin.

The thickness of the overlying Paskapoo Formation is illustrated by the map showing depth to the top of the Ardley Coal Zone (Figure 7). The isopachs of the overburden succession (Paskapoo Formation and Quaternary deposits) mimic the present-day topography and depict a gradual westerly increase in thickness up to 800 m in front of the central foothills. In addition, a maximum of 600 m is shown along the Athabasca River valley. Quaternary deposits range in thickness from 10 to 50 m (L. Andriashek, personal communication, 2006).

Comparison of the present-day thickest depositional areas of the Ardley Coal Zone (Figure 6) with the overlying Paskapoo Formation (Figure 7) indicates that a more active subsidence migrated from the front of the northern foothills during the lower Paleocene to the central part of the foothills during the middle–upper Paleocene.

The present-day geometry of the basin is suggested by the structural contour maps at the top and the base of the Ardley Coal Zone (Figures 8 and 9). The structural contours of both surfaces depict a similar dipping gradient towards the west and mainly in front of the central foothills.

At the regional scale, the map of cumulative coal thickness (Figure 10) displays two areas of greater coal concentration within the upper part of the Scollard Formation, both located north of township 42. They indicate the presence of two divergent areas of coal accumulation that can be referred to as coal sub-basins. The northern coal sub-basin, informally known as the Edson CBM exploration block, is oriented perpendicular to the deformation front and pinches out towards the Swan Hills. The southern major area of coal accumulation is known as the Pembina CBM exploration block and is oriented obliquely to the deformation front.

The Edson and Pembina sub-basins of the Scollard Formation represent the two main Tertiary CBM exploration areas and potential targets for CO₂ storage and enhanced CBM (ECBM) production. Deciphering the depositional models for the two coal sub-basins, including vertical zonation and lateral reservoir characteristics, is important for CBM exploration and development.

Detailed stratigraphic and sedimentological analysis of the two CBM exploration blocks has revealed that they represent two almost synchronous coal sub-basins, interconnected to the west and defined by similar depositional characteristics (Figure 11). The Edson CBM exploration block has been recently interpreted based on new coal, stratigraphic and sedimentological data, which are presented in a complementary report (Edson CBM Exploration Block, Alberta, Ardley Coal Zone Characterization and Sandstone Channels Geometry, C. Pana, work in progress, 2007).

The schematic presentation of both coal sub-basins is constructed based on a distal northwest-southeast regional cross-section. The chart shows the similarity of the lithological components, the synchronicity of the coal deposition time, and potential coal correlation throughout the basin. The coal in both sub-basins accumulated in response to similar tectonic and climatic cyclic conditions in the sediment source area. The Ardley Coal Zone in the Pembina block is defined by four distinct coal subzones with a consistent area of distribution. In contrast, the variable number (1–4) of discontinuous coal subunits in the Edson block generally makes it difficult to correlate at the regional scale. In the Pembina block, sandstone channels associated with the Ardley Coal Zone show locally superficial erosion at the top of the underlying coal seams in contrast to the deeper erosion recorded in some places in the Edson block (Edson CBM Exploration Block, Alberta, Ardley Coal Zone Characterization and Sandstone Channels Geometry, C. Pana, work in progress, 2007).

In the northern part of the Ardley basin, the following arbitrary nomenclature for the coal subzones has been set up in the Edson CBM exploration block (from top to bottom): 'S,' 'Mu' (upper M), 'Ml (lower M)' and 'N' (Edson CBM Exploration Block, Alberta, Ardley Coal Zone Characterization and Sandstone Channels Geometry, C. Pana, work in progress, 2007). Based on the tentative extension of the stratigraphic model across the basin, the preliminary equivalents in the Pembina CBM exploration block are given in Table 1.

Table 1. Equivalence of coal subzones between the Edson and Pembina CBM exploration blocks.

Pembina sub-basin		Edson sub-basin
Mynheer coal subzone	—	'N' coal subzone
Silkstone coal subzone	—	'ML' coal subzone
Arbour coal subzone	—	'MU' coal subzone
Val D'Or coal subzone	—	'S' coal subzone

2.2 Paskapoo Formation

The Scollard Formation is overlain by the middle and upper Paleocene Paskapoo Formation, after a diachronous hiatus of approximately 1.2 m.y., as documented in the eastern part of the basin (Lerbekmo et al., 1990; Lerbekmo et al., 1992). During the period of time with no or very limited sediment supply, minor and local erosional processes took place at the basin scale, in some places changing the geometry and continuity of the uppermost coal strata of the Scollard Formation. The Paskapoo thick clastic wedge represents the response to the renewed Tertiary tectonic activity in the adjacent orogen. The cross-section through the central part of the foothills, Brazeau River area, (LeDrew, 1997; Langenberg et al., 2002) shows that, within 'The Triangle Zone,' the Paskapoo Formation is the youngest sequence disrupted by thrusting. This leads to the observation that the last stage of thrusting in the adjacent orogen took place sometime during the upper Paleocene.

The Paskapoo Formation overlies most of the Scollard sequence and played an important role in preservation and maturation of the vegetal organic matter within the upper part of the Scollard Formation. Its erosional edge is within the outcrop belt of the Scollard Formation (Figure 5).

The boundary with the underlying Scollard Formation has been placed at the base of the "thick, massive, coarse-grained sandstone" (Demchuck and Hills, 1991) that generally overlies the uppermost coal seam of the Scollard Formation. The basal part of the Paskapoo Formation consists of thick, stacked sandstone channels, deposited in response to the uplifting of the adjacent tectonic source area, that are well distributed across the basin.

The Paskapoo Formation has been divided into three clastic members, based on the dominant lithological components (Demchuck and Hills, 1991). The Paskapoo basal thick sandstone channels, which occur rarely in association with discontinuous coal seams, are referred to as the Haynes Member. The middle and the upper parts of the Paskapoo sequence are defined as the Lacombe and Dalehurst members, respectively; their main components are mudstone, siltstone, sporadic thin and argillaceous coal seams, and subordinate sandstone and/or conglomerate. The entire Paskapoo succession is documented as middle–upper Paleocene in age, based on palynological and paleobotanical content and faunal remains (Demchuck and Hills, 1991).

The persistence of a semi-arid climatic zone south of township 20 during the middle and upper Paleocene is indicated by some lateral changes in the typical Paskapoo facies association, which led to the separation of the Porcupine Hills Formation (Dawson, 1883) as the stratigraphic equivalent of the Paskapoo Formation (Figures 2 and 5).

The top of the Scollard Formation was locally eroded in the distal part of the basin due to the basal Paskapoo fluvial systems (Haynes Member). A more aggressive effect of erosion of the base of the Paskapoo basal channels occurs in the northern part of the basin (Edson CBM block).

2.3 Battle Formation

The Battle Formation, which underlies the Scollard Formation, is defined as a thin, continuous and distinct stratigraphic interval made up of a group of several thin tonstein layers interbedded in silty-mudstone strata (Irish and Harvard, 1968), averaging 10 m thickness.

Easy to recognize on the geophysical logs due to the high gamma-ray response, the Battle Formation is present throughout the entire Scollard distribution area.

The Battle Formation originated in the tectonically induced changes in the foreland basin that were initiated about 68 Ma and accompanied by volcanism (Jerzykiewicz, 1997). Near the deformation front, the Battle Formation loses its distinct character due to the presence of multiple tonstein beds, at different stratigraphic levels within the lower part of Scollard Formation, interfingering with the mudstone and sandstone strata. The Scollard–Battle stratigraphic contact is considered to be disconformable throughout much of the basin (Jerzykiewicz, 1997).

The physico-chemical properties of the lithological components of the Battle Formation give the unit the characteristics of an aquitard, which plays an important role in the subsurface hydrodynamics. The Battle Formation represents the confine unit between two successive aquifer systems. The lower aquifer system is represented by the Wapiti Group and its uppermost equivalent in southwest, the Horseshoe Canyon Formation. The upper aquifer system consists of the Scollard–Paskapoo clastic succession.

3 Ardley Coal Zone in the Pembina CBM Exploration Block

The primary objectives of this study are to document the sequence stratigraphic model of Scollard-basal Paskapoo clastic succession, including the coal-favourable depositional conditions, and to delineate the general characteristics of the Ardley coal reservoir.

The Pembina CBM exploration block encompasses Townships 45–52, Ranges 6–12, west of the 5th Meridian, an area of approximately 540 km². The surface topography in the drainage basin of the North Saskatchewan and Pembina rivers varies in elevation from 1197 m in the southwest to 695 m in the northeast (Figure 12a).

Interpretation of the coal stratigraphy and sedimentology in the Pembina CBM exploration block is based on 254 oil and gas exploration wells (Figure 12b). The new descriptive dataset presented in this report consists of stratigraphic, lithological and detailed coal picks. The density of the wells varies from high in the east-central part of the study area (up to five wells per township) to low in the western part (approximately one well per township). The associated database reflects the architecture of the strata defined in the sequence stratigraphic model of the Scollard Formation.

In addition to the log interpretation, three drillcores (Figure 13) were examined within the study area:

- 02/10-10-047-07W5 (366–380 m and 419–435 m)
- 02/09B-26-047-11W5 (433–547 m)
- 00/14-15-046-10W5 (486–580 m)

3.1 Lithological Description and Facies Association

The vertical profile of the Ardley Coal Zone in the study area shows a cyclic succession of the main lithological components: sandstone, siltstone-mudstone, coal and tonstein (Figure 14).

3.1.1 Sandstone

In the examined cores, the sandstone is lithic with a ‘salt-and-pepper’ aspect, medium to fine grained, poorly sorted, poorly to well cemented and contains subangular lithic fragments (Plate 2, Figures A and B). Their occurrence and characteristics attest to the high energy environment in which the fluvial sequences were deposited (Plate 1, Figures A–G; Plate 2, Figures A and B).

Thick sandstone channels in the Pembina CBM block represent an amalgamation of individual units that produced stacked, widespread sand units of almost uniform composition. In stacked sandstone units,

which can reach 50 m thickness, several thin fining-upward units alternate occasionally with coarsening-upward units. The sandstone has an overall massive texture. Simple sets of sedimentary structures, dominated by low-angle or tabular stratification, are rarely observed (Plate 1, Figure E). Coarse sediments are atypical in the study area, but local scour surfaces or discontinuous lag sediments (Plate 1, Figures A and B) may occur sporadically within the sandstone body. The matrix is represented by mud.

On the geophysical logs, the sandstone units generally have a ‘cylindrical shape’ signature with abrupt base and more or less gradual transition to finer grained sediments (fining upward point-bar deposits signature). Occasionally, channels with sharp change at the top and at the base are also recorded by the gamma-ray log trace. The lateral variability of each channel on the gamma-ray record is shown on the regional cross-sections (Figures 15–26).

3.1.2 Mudstone and Siltstone

In the Pembina CBM block, mudstone and siltstone are usually medium to dark brownish grey with frequent slickensides, frequent carbonaceous vegetal debris, and root traces. Soil structures and the presence of root traces led to the interpretation of the mudstone and siltstone units as paleosols (Retallack, 1990).

Generally, two thin (approximately 1–3 m thick) paleosol units have been recognized in each cycle. Every recognizable unit in the examined drillcores can be associated with a stage of paleosol genesis (Mack et al., 1993) (Plate 4, Figure A1 and A2). The lower unit is usually massive, structureless, medium to dark brownish grey with rare or no root traces or vegetal debris (Plate 3, Figures A–C). The top unit is considered the mature paleosol unit (Plate 3, Figures D1–2; Plate 4, Figures B–C). Usually the upper unit has a darker colour, multiple root traces and slickensides, and is overlaid by coal beds. This recognizable paleosol profile from the drillcores and the lateral distribution of the paleosol sequences constitute a preliminary description of the Scollard paleosol series in the Pembina block. The paleosol units mark the time intervals of landscape stability associated with isostatic rebound, in most cases preceding the peat swamp environments during the humid climate of the lower Paleocene (Reinhardt and Sigleo, 1988; Diessel, 1992).

‘Slickensides’ are the distinctive structural feature of paleosol units. They originated in soil peds formed initially by the disruption (swelling and shrinking associated with wetting and drying) of relict laminar clay bedding on top of an impermeable layer of soil. As a result, the lentil peds are separated by slickensides. The clay swelling depends upon the mineralogical content. The disruption behaviour is most common in soils enriched in smectite, which has 28% linear extensibility (Krishna and Perumal, 1948; Wright, 1992). In the Pembina CBM block, the more mature paleosol units have frequent slickensides which form particularly in soils rich in smectitic clays (Plate 4, Figures A1–2, B and D).

Grey to dark brownish grey colour indicates reducing and wet soil units, which correspond to waterlogged environments favourable for the development of peat (Wright, 1986).

Because the paleosol units in the Pembina block represent thin strata (~3 m), it is difficult to recognize them on the geophysical log record without core examination.

3.1.3 Coal

Lateral and vertical distribution of the coal lithotypes in the Pembina CBM exploration block reflects the original peat plant association and the modifications of the physical and chemical conditions during peat development.

Diessel (1965), Britten and Smyth (1973) and Mackowsky (1982) demonstrated close correspondence between the macroscopically observed lithotype profile of coal beds and the petrographic composition of their macerals. In this report, coal is described based on examination of the drillcores and interpretation of the geophysical logs.

The description of coal in the examined cores followed the Australian coal lithotype divisions (Table 1) (Bustin et al., 1983). The Ardley coals in the Pembina block vary from bright to banded and dull types (Plates 5–8 and 10–11). The dominant coal lithotype is banded, followed by banded dull and more rarely banded bright coal.

Table 2. Lithotype correlation table (after Bustin et al., 1983).

Division (after Stopes)	Division used in Australia	Macroscopic description
Vitrain	Bright coal	<10% dull
Clarain	Banded bright coal	10–40% dull
	Banded coal	40–60% dull
	Banded dull coal	10–40% bright
Durain	Dull coal	<10% bright
Fusain	Fibrous coal	Charcoal

‘Banded bright’ and ‘banded dull’ coals comprise successive layers of vitrinite and liptinite or fusinite (Diessel, 1965; Bustin et al., 1983; Diessel, 1992). Macroscopically, the bright lustre is associated with the vitrinite component, which contrasts with the bands of less bright to matte lustre that are considered to be liptinite or fusinite. The presence in the Ardley coals of bright components, in varying proportions and interlayered with other groups of macerals, suggests a consistent presence of woody tissue, in association with other sources of vegetal matter, when the peat began to form. Also, the vitrain group is considered to have a high potential for methane generation under specific conditions of coalification. The banded coals rich in vitrain have high cleat or fracture response. The frequency of the ‘face-cleat’ system ranges from less than 1 cm in thick vitrain bands to 3 cm in banded dull coals (Plate 10, Figures D–F). The ‘butt-cleat’ system seems to be more continuous in thick vitrain layers than in banded dull coals. The variable distribution of the cleats in the examined cores is illustrated in Plates 5–11.

The coal description based on the geophysical log signature has been also added to that from the core examination. The complementary gamma-ray and density logs are sensitive to major fluctuations of mineral matter content in the coal seams. The resolution of the log interpretation is still generic, but allows the separation into layers or coal seams thicker than 33 cm of

- clean coal (60%–80% organic matter; includes generically all categories of bright, banded, dull and fibrous coal);
- shaly coal (~60% organic matter; mudstone or siltstone intimately mixed with coal debris or separate thin coal bands); and
- coaly shale (~40% organic matter; finely dispersed or agglomerated in bands).

The photographs of the coal seams in the examined cores (Plates 5–11) show multiple vertical changes, from banded coal to the other coal categories over intervals of a few centimetres. The geophysical log records the dominant category existing in the coal intervals thicker than 33 cm.

In the Pembina block, some of the macroscopically visible layers of mineral matter that originated as airfall tuff associated to the coal seams display considerable lateral continuity and become an integral part of the coal lithotype profile (Figures 14 and 27). Thus, the vertical arrangement of successive lithotypes, including the layers of mineral matter (Bustin et al., 1983), represents the vertical profile or signature of the Ardley coal subzones in the Pembina exploration block. Geophysical log correlation of coal strata in the Pembina block, including the comparison of the vertical profiles in adjacent wellbores, was the basis for identifying the coal petrological cycles in each of the coal subzone (Figure 28).

Vertical changes in the macroscopic characteristics of coal seams, recorded on the geophysical logs for each of the Ardley coal subzones, correspond to the alternating low ash and high ash content in coal seams (Figures 14 and 28).

The most common vertical profile of the Val D'Or coal subzone shows the following succession (from top to bottom; Figures 28 and 29): tonstein thin layer (<1 m), shaly coal (<75 cm), coal (up to 1 m), shaly coal or coaly shale (<75 cm), coal (up to 1 m), coaly shale or mudstone or tonstein (~1–1.5 m), coal (up to 1 m), tonstein and associated mudstone-siltstone (up to 1–1.5 m). The lateral consistency of the Val D'Or vertical components recorded the stabilized peat-forming pattern conditions. The vertical profile of the Arbour coal subzone shows the following succession (from top to bottom; Figure 14): tonstein (<1 m), shaly coal or coaly shale (<1 m), coal (up to 1.2 m), very thin shaly –coal (~50 cm), coal (up to 1 m), shaly coal, coal (up to 1 m), shaly coal or coaly shale, mudstone (>1 m) and shaly coal or coaly shale (up to 60 cm). The Silkstone coal subzone vertical profile shows two continuous coal seams with a fairly consistent thickness, each of which can be up to 1 m in thickness. The coal seams are separated by a thin laterally variable interval of mudstone, coaly shale or carbonaceous shale. A less consistent vertical and lateral profile is shown by the Mynheer coal subzone. The vertical separation of the unit into three intervals, based on the presence of four tonstein thin layers, aims in areal correlation of the coal subzones (Figure 29).

3.1.4 Tonstein

In the Pembina block, tonstein generally occurs as thin layers (a few centimetres to a few tens of centimetres thick) associated with the coal seams (Plate 12, Figures B, C and F). Occasionally, the thin tonstein beds may contain detrital and carbonaceous material. In the regional correlation the tonstein layers were used as stratigraphic markers or timelines.

Bohr and Triplehorn (1993) have shown that tonstein represents an alteration product of volcanic ash that has fallen into an acidic environment, such as a coal swamp or an inland waterlogged area. Under advanced diagenesis, the tonstein beds contain predominately kaolinite.

Soils based on volcanic ash show a low record on bulk density trace (if thicker than 3 to 5 m), high water and organic matter retention and on core samples weakly developed soil structures, and a high content of amorphous alteration products and complexes of Al, Fe and humus. They develop clayey soils (Wright, 1986) in which the outlines of volcanic shards are preserved by replacement with other minerals.

The coal-tonstein contact can present occasionally clusters of fine calcite infillings atypical for the regulate coal cleat pattern. The infilling interval is generally lenticular in shape, as it is observed on the examined drillcores, with a 'spider web' aspect and thickness in the apex of maximum 5 cm

(Plates 5–7). The extremely fine, dense, reticular design suggests a different stage of infilling possibly more premature than that of cleat genesis and possibly contemporaneous with sediment compaction.

3.2 Sequence Stratigraphic Model

3.2.1 Depositional Controls

The Scollard Formation represents an entirely fluvial succession with no traces of marine deposits. The last marine event recorded in the Alberta foreland basin coincides with the last transgression of the Bearpaw Sea (Maastrichtian; Figure 2).

It has been demonstrated that fluvial systems in nonmarine domains respond to a number of allocyclic controls on sedimentation, which include climate, active tectonics in the source area and basin subsidence (Miall, 1996). In this study it is considered that during Uppermost Cretaceous–Lower Tertiary in the Alberta foreland basin, the drainage systems responded primarily to a combination of tectonic and climatic mechanisms as the dominant control factors on sedimentation.

3.2.1.1 Tectonic Controls

The relationship between tectonic movements and clastic sedimentation was re-examined by Miall (1996). The conventional idea that wedges of coarse sediment are syntectonic in origin (Heller et al., 1988; Blair and Bilodeau, 1988) has become more integrated into the interpretation of the dynamics of ancient fluvial deposits. The concept is based on the observation that sedimentation is related to fault pulses or growth of faults and folds in the source area (Van Wagoner et al., 1988). The rejuvenated relief represents the main factor in the generation and transportation of clastic debris in large quantities that relate to the basinal and depositional response to uplift and subsidence. The most obvious effects of tectonic controls are the changes in sedimentary accommodation space and in the quantity and calibre of the sediment load. Coarsening and fining units of alluvial successions, in the form of cycles or sequences have long been interpreted in tectonic terms (Heward 1978; Heller et al., 1988; Miall, 1984; Miall, 1996).

During the late Maastrichtian–early Paleocene, weak cycles of subsidence and uplift superimposed on a long-term humid climatic background led to the development of fluvial cyclicity in the Scollard Formation deposits. Five major cycles (C1–C5), presented as one of the results of the present study and consisting of repetitive successions of fluvial sequences, are separated by subaerial intraformational unconformities (Figure 30). The main characteristic of each clastic cycle of the Scollard Formation is an overall fining-upward profile. The subaerial unconformities are marked locally by superficial fluvial incisions, sediment bypass, and extensive paleosols associated with coal strata. The subaerial unconformities can be traced along the tops of the paleosol horizons (Galloway and Hobday, 1996) and thus considered here as sequence boundaries.

The deposition of the Scollard Formation was mainly controlled by the foreland drainage systems. Each sequence represents the response to an initial stage of thrusting in the adjacent orogen, accompanied by flexural subsidence in the foredeep. The next stage was associated with isostatic rebound, which generated sequence boundaries related to the timing of fluvial aggradation. The intensity of the tectonic pulses was different from one cycle to another based on the interpretation of the associated drainage systems. Source-area tectonism controlled the topographic gradients of the fluvial landscape during uplift. Differential subsidence controlled the sedimentary processes during orogenic unloading stages (Miall, 1996). The fining-upward profile displayed by each Scollard foreland fluvial sequence reflects the change in fluvial pattern from high to low energy.

The upper four cycles of the Scollard Formation are capped by coal beds. Coal deposition was therefore closely tied to the tectonic, structural and depositional settings because peat accumulation and preservation as coal requires a delicate balance of vegetal mass accumulation, subsidence rate and optimum level of water table, but exclude clastic sediment influx in-excess (Reinhardt and Sigleo, 1988).

Following the relative tectonic stability in the source area during coal deposition, the last stage of renewed tectonism (thrusting) during the middle and upper Paleocene (LeDrew, 1997; Langenberg et al., 2002) resulted in the high-energy, thick clastic deposits of the Paskapoo Formation.

3.2.1.2 Paleoclimatic Controls

During the late Cretaceous–early Tertiary in the Alberta foreland basin, the prevailing humid climate resulted in extensive drainage systems and therefore fluvial-type sedimentation. Climate was interpreted in the Scollard sedimentary succession mainly on the basis of vegetation, paleosol units and syndiagenetic minerals. Abundant rainfall and positive values of temperature represented two important attributes of the recorded climate during Scollard Formation deposition time. Production, dispersal and deposition of terrigenous detrital sediment as a result of tectonic activity in the sediment source area were facilitated by quantity, continuity and distribution with time of rainfalls. In addition, the positive values of temperature maintained the mobile stage of water and initiated syndepositional diagenesis. The level of rainfall and temperature together controlled the amount and type of vegetation (Potter et al., 1980; Moore and Reynolds, 1997).

During deposition of the Scollard Formation, climate and tectonic changes modified the loading index of the river systems. The excess of sediment load during massive rainfalls correlated with uplift of the source area, which leads to a considerable increase in river discharge (Lyons and Rice, 1986). During the late Cretaceous–early Tertiary, five cycles of massive discharge events were recorded. Every fluvial cycle of the Scollard Formation shows an initial stage of high energy followed by stages when the discharge of rivers decreased dramatically and fluvial aggradation dominated (Figure 30). Thickness and lateral extent of the coal-bearing sequences of the Scollard Formation depended on the geometry of the fluvial systems and the geographic extent of the humid climate.

Different stages of the humid climate during little or no sediment influx were also responsible for the high growth rate of plants. The upper Scollard coal strata are the result of the abundance of botanical colonies characterized by declining gymnosperms, ascending angiosperms, deciduous trees and shrubs (Demchuck and Hills, 1991).

During the late Maastrichtian–early Paleocene, the paleoclimatic zonation restricted the extent of the environmentally favourable conditions for plant ecosystems to the north-central part of the basin (humid climate). At the same time, the southern part of the basin was dominated by semi-arid conditions, which generated ‘caliche paleosols’ (Jerzykiewicz and Sweet, 1986; Jerzykiewicz and Sweet, 1988). This different sedimentological character of the southern part of the basin is referred to as the Willow Creek Formation (Figure 5). Caliche paleosols are specific to high alkaline soils generated by warm climate with low supplies of H₂O and CO₂ and high pH (8–9), where calcium is precipitated as ‘caliche’ or ‘calcrete’ (Wright, 1992). The pedogenesis associated with the peat-forming conditions in the central and northern parts of the basin was dependent on a humid environment with a slightly acidic pH (Wright, 1992).

The climatic difference between the north-central and southern parts of the basin (Jerzykiewicz and Sweet, 1986), with profound paleoenvironmental and sedimentological consequences, has an approximate line of demarcation that can be traced north of Calgary (Figure 5).

3.2.2 Stratigraphic Sequences or Cycles in the Scollard-Basal Paskapoo Succession

One of the objectives of this study is to document in detail the geometry and internal structure of the Scollard–Lower Paskapoo succession in the Pembina exploration block to obtain a better understanding of the coal reservoir geometry.

The sequence stratigraphic model, presented in this report (Figure 30) as an approach to sequence stratigraphy applied to nonmarine sequences, had initially been defined in a previous report on a smaller area within the Pembina CBM exploration block (Alberta Energy and Utilities Board, 2005). The schematic sequence stratigraphic model was tentatively extended to the entire coal sub-basin and became a more comprehensive illustration of the Scollard Formation style of sedimentation in the Pembina exploration block. Within the Scollard Formation, the regionally mappable units bounded by extensive intraformational unconformities represent five primarily fluvial depositional cycles (Figure 30). The unconformities correspond to five short quiescent tectonic stages of no thrusting in the adjacent orogen. Every cycle interpreted on the geophysical logs reflects a stage of tectonic uplift followed by a time interval of tectonic quiescence accompanied by isostatic rebound in the foredeep.

The paleosol sequences and the adjacent coal strata document the stratigraphic breaks in fluvial facies (Heward, 1978; Heller et al., 1988; Wright, 1992). The association of paleosols with unconformities required long-term landscape stability in the sedimentary regime, characterized by almost no deposition or erosion, which allowed the parental material to go through the pedogenesis process (Wright, 1992). The final stage of each of the upper Scollard cycles is marked by coal accumulation, which indicates a more mature stage of pedogenesis, when the paleosols are populated by plants ecosystems.

The changes in thickness and of the lateral distribution of the Battle and Scollard formations including the Haynes Member as the lower part of the Paskapoo Formation are shown by the structural cross-sections oriented west-east and north-south (Figure 15). Generally, the structural cross-sections (Figures 16–24) show that the Pembina sub-basin dips to the west and to the south. The Battle Formation is consistently present as a thin lithological interval with the same specific signature on the induction log. The thickness of the Scollard Formation declines from 150 m in the southern part of the study area to approximately 75 m in the north (Figures 16–26). The regional northward thinning trend of the Scollard Formation is accentuated by erosion. In the central part of the study area, the formation has an east-west zone of consistent thickness of about 100 m (Figure 19). The lateral continuity of the coal seams is remarkable at the scale of the Pembina study area, especially in this west-east central zone. Some changes in the distribution of the coal subzones are observed to the west: the Arbour and Val D’Or subzones pinch out and the Silkstone and Mynheer split in two or three thin coal subunits (Figures 19 and 25). The north-south structural cross-sections (Figures 25 and 26) show that the greater thickness of the lower coal subzones is compensated by thinner upper coals, in contrast to the thinner lower coals, which are overlain by the thicker upper coals. The migration of the peat depocentres from the north during the lower coal subzones to the south during the upper coal units indicates the rebalance of the accommodation space during lower Paleocene time.

The major lithological components of the upper four cycles are sandstone, mudstone-siltstone, coal and tonstein (Figure 30). The succession of lithological components in every cycle interpreted from the geophysical logs shows an initial stage characterized by higher energy at the base, marked by sandstone, channels, generally followed by a gradational decrease in energy, recorded as fining-upward units, accompanied by pedogenesis sequences that are capped by coal beds (Figure 30). The intensity of the fluvial drainage processes varies from one cycle to the next. Cycles C3 and C5 are weaker than cycles

C1, C2 and C4, and all Scollard cycles are weaker than the basal clastic cycle (Haynes Member) of the Paskapoo Formation. Miall (1984) demonstrated the direct relationship between the higher level of energy and the greater thickness, grain size and areal extent of the sandstone channels. In most cases, the Scollard cycles with relatively lower energy during the initial stage (C3 and C5) have a restricted area of sandstone channel occurrence, mainly closer to the sediment source area (deformation belt). Distally, these cycles are thinner and can be exclusively characterized by mudstone-siltstone (paleosol) units capped by coals (Figure 25).

Each of the last four major fluvial cycles (C2, C3, C4 and C5) or fluvial sequences regionally recognizable within the upper part of the Scollard Formation is capped by coal strata (Figure 30).

The top coal of every sequence (Figure 30) corresponds to the informal names associated with the Ardley coal subzones (Val D'Or, Arbour, Silkstone and Mynheer), which have become more frequent used in publications without a solid stratigraphic foothills-foreland stratigraphic correlation (Figure 30). Some of the examined drillcores show the abrupt stratigraphic contact between the underlying coal seams and the overlying sandstone channels, and depict the sequence boundaries (Plate 2, Figures C and D).

Regionally, the C2 cycle represents the Mynheer coal subzone genetic cycle. The drainage system shows a stage of decrease in drainage energy towards the top. The Mynheer subzone consists of several (up to nine) coal seams, which are areally discontinuous, with an increase in consistency and organic content towards the top of the coal subzone. The coal-seams package represents an inconsistent succession of coaly shale, shaly coal and coal. The coal seams of the C2 cycle are sometimes separated by thick coal-barren intervals up to 10 m thick. Generally, the coal seams of C2 have cumulative higher ash content, which demonstrates that the sediment influx was significantly reduced but still persistent during the first peat-forming stage within the Ardley Coal Zone in the Pembina block (Figures 21, 23 and 30).

The C3 cycle (pre-Silkstone coal subzone) represents a lower energy drainage system. Only in some areas, the sandstone channels between the Mynheer and Silkstone coal subzones are present (Figures 17 and 19–22). The Silkstone subunit consists mainly of two coal seams that are generally grouped together, each of them averaging 1 m in thickness, characterized by relatively consistent high organic content (~70%–80% organic matter) (Plate 6, Figure F; Plate 9, Figure G; Plate 10, Figure E; Plate 11, Figure K). The Silkstone coal seams are separated by a thin layer of mudstone that laterally change into carbonaceous shale or coaly shale in the southern part of the basin. The regional occurrence of the Silkstone coal subzone as a distinctive stratigraphic unit reflects the stability of the peat-forming conditions during a period of time when the sediment supply was absent.

The next cycle up-section, C4, represents the response to the genetic conditions that generated the Arbour coal subzone. The cycle has a stronger drainage signature, marked by thick (up to 56 m) stacked sandstone channels (Figures 16–26). At the top, a paleosol unit of variable thickness is capped by several thick coal seams that are usually packed together. The paleosol unit may include one or two pre-Arbour coal seams with local occurrence (Figures 19–21). Regionally, the Arbour coal subzone is made up of a tight package of coal seams with higher organic content that ranges between shaly coal and clean coal (~60%–80% organic matter) (Plate 11, Figures B, D and H).

The last cycle of the Scollard Formation in the Pembina block is C5, representing the genetic conditions of the Val D'Or coal subzones. Cycle 5 has a very weak signature of drainage processes, except the area proximal to the foothills where the sandstone channels are present (Figure 25). Regionally, it represents paleosol units rarely up to 10 m in thickness, capped by relatively thick and grouped coal seams. The

general organic content varies vertically between shaly coal and clean coal (Plate 8, Figures A–D; Plate 9, Figures A–C, E, H, J; Plate 11, Figures A, C, E). The thickness of the coal package can reach 5–6 m.

3.2.3 Coal Depositional Model

The coal depositional model in the Pembina block represents the simplified assemblage of the most frequent lithological and stratigraphic observations on the Scollard–Paskapoo succession. The model was built based on analysis of the structural and stratigraphic cross-sections of the study area (Figures 15–26).

The accumulation and preservation of peat as coal required a delicately balanced subsidence rate, during minimum or no sediment supply that maintained an optimum water-table level and abundant vegetation. Coal strata occupy specific positions within the genetic sequences of the Scollard Formation and represent reference horizons for analysis of the uppermost Cretaceous–Tertiary sequence in the Alberta foreland basin. The regional correlation framework has used the correlatable tonstein strata located at the top and base of the coal subzones as selected timelines. The structural cross-sections in the Pembina block depict the general present-day architecture of the sub-basin, variations of dip direction, lateral continuity of the coal seams, distribution of sandstone channels and the proximal relationship of different lithological units (Figures 19, 20 and 25).

The lateral continuity of the Ardley Coal Zone in the Pembina block over an area of approximately 540 km² represents an unusual character for the common fluvial environments in which the peat units occupy the interfluvial spaces. The relative stratigraphic position of the successive lithological units shows a distinctive cyclic succession from sandstone to mudstone-siltstone (paleosol units) to coal. No sandstone channels contemporaneous with the coal strata have been identified in the study area (Figure 27).

The primary factor influencing the extensive distribution of peat is the topographic surface and the nature of the substrate on which the peat evolved. The topographic surface was almost flat and horizontal over a wide area of more than 500 km², allowing a consistent distribution of the peat. We assume that the mud-rich nature of the substrate is sensitive to the differential compaction and imposed the relocation of the depocentre of the peat-swamp domains. The higher rate of compaction was found in the mud-rich substrate (peat-swamp sediments) than in the sandy substrate (sandstone channels).

The paleo-reconstruction model in the Pembina area (Figure 31) shows that the favourable conditions for peat development were met four times in the depositional history of the southern Ardley sub-basin. The synergistic effect of low topographic gradient, water-saturated mudstone and regular rainfalls is interpreted to have cyclically developed peat-swamp environmental conditions within the upper part of the Scollard Formation. The uniform low topographic gradient is inferred from the absence of any relict of drainage channel contemporaneous with the coal strata in the study area. The tectonic quiescence, due to the rebounding stage, induced a very low influx of sediments during the time of peat formation. The water level was maintained by the underlying water-saturated mudstone-siltstone of the paleosol units. Vegetal growth was stimulated by the humid climate and possibly by thin volcanic layers as fertile soils (Retallack, 1990). The source of water is considered to be the rainfalls in the absence of any indication of contemporaneous drainage systems to the peat units in the study area. The water table in the peat area remained at or near the ground surface, with no pronounced seasonal lowering and with a pH higher than 5.0 (Retallack, 1990).

The distribution of swamp facies varies somewhat with time, but the overall succession of the major lithological components is similar. This observation suggests that the quasi-horizontal position of the substrate remained fairly constant at the scale of the Pembina block during deposition of the lower Paleocene coal strata (Figure 27).

3.3 Coal Reservoir Characterization

Coal is a unique type of rock due the dual attributes of source rock and reservoir for methane. The major coal reservoir components for gas exploration can be listed as: *coal reservoir geometry* referring to depth, thickness, internal structure and seals of coal seams or groups of coal seams, *coal properties* such as coal rank, ash content and fracture systems, and *reservoir conditions* controlled by the hydrogeological characteristics.

3.3.1 Coal Reservoir Geometry

The geometry of the coal reservoir is deciphered through interpretation of thickness, internal structure, lateral continuity, relationship with adjacent lithological components and structural position. This initial set of parameters is important for estimation of the volume of gas and identification of trap conditions. Thickness and extent are important criteria for estimating the economic scale of the coal reservoir; internal structure defines how many individual coal reservoirs make up the coal zone and the degree of their lateral continuity; the relationships with the adjacent lithological components are important for identifying the types of reservoirs in possible contact with the coal strata and characterization of the traps. Structural contours show the present-day stratigraphic position and attitude of coal reservoir.

3.3.1.1 Depth and Thickness

The thickness of the Ardley Coal Zone equivalent to the informal upper member of the Scollard Formation is defined arbitrarily as the stratigraphic interval between the base of the lowermost coal seam and the top of the uppermost coal seam. This stratigraphic interval corresponds with the coal deposition time from the initiation to the final stage. Regionally, the thickness of the Ardley Coal Zone ranges from a few metres along the erosional edge up to 217 m in subsurface, close to the deformation front (Figure 6). The isopachs show a uniform distribution in thickness intervals that thins gradually to the east. The coal cumulative thickness of the Ardley Coal Zone is mainly concentrated in two distinct areas (Figure 10) considered in this report as coal sub-basins. The coal deposition interval appears to be almost synchronous across the basin.

In the Pembina block, the thickness of the overburden succession Paskapoo Formation and Quaternary deposits, is only 196 m in the present-day North Saskatchewan-Pembina rivers drainage basin, in the northeastern part of the study area, and becomes three times thicker (>600 m) to the southwest (Figure 32). The change in thickness occurs gradually over a distance of approximately 100 km. A similar pattern is shown by the maps of depth to base of Ardley Coal Zone (equivalent with the lower member of the Scollard Formation) and the base of the lower member of the Scollard Formation (Figures 33 and 34).

The set of structural maps generated for the major surfaces (e.g., top of the Ardley Coal Zone, base of the Ardley Coal Zone and based of the lower Scollard Formation) depicts a consistent dip direction toward the southwest (Figures 35–37).

In the Pembina CBM exploration block, the isopach map of the Ardley Coal Zone shows a westward increase in thickness up to 112 m, from only 5 to 13 m in the northeastern part of the study area (Figure 38). The coal-barren part of the Scollard Formation (equivalent to the top of the lower Scollard member) shows a consistent increase in thickness to the southwest (Figure 39), which implies a more accentuated subsidence in the same direction. The Battle Formation isopachs show two areas of thicker strata in the north and southwest separated by a central zone of smaller thickness (Figure 40). Comparison of the three isopach maps led to the interpretation that the depocentres of sedimentation migrated from the north and extreme southeast during deposition of the Battle Formation to the southwest during deposition of the lower Scollard and to the west during deposition of the upper Scollard (Ardley Coal Zone).

The cumulative coal thickness (Figure 41) and the number of coal seams (Figure 42) show, respectively, the same east-west trend of thickness greater than 11–12 m and a range of 11–20 coal seams.

There is a weak relationship between the maximum thickness of the Ardley Coal Zone and 1) the area of maximum coal cumulative thickness, and 2) the distribution of maximum number of coal seams (Figures 38, 41 and 42). The westward increase of the Ardley Coal Zone thickness in the Pembina block is the result of the more accentuated subsidence that created accommodation space for sediments closer to the thrust-and-fold belt. This effect diminishes farther to the southeast, so the coarser clastic sediments at the base of cycles C5 and C3 are absent (Figures 25 and 26). Distally, the favourable conditions of peat environments were mainly stimulated by tectonic quiescence.

Inside the wide peat-forming platform, differential compaction of underlying sediments locally induced syn-sedimentary changes in the thickness of some of the coal seams (e.g. Figure 21) Areas where the peat substrate included significant proportions of clay and organic material subsided more rapidly than the sand channels (Retallack, 1990). The subsidence rate was not higher than the rate of vegetal matter supply, this maintaining the peat conditions for a considerable period of time.

3.3.1.2 Internal Structure

In the Pembina block, the Ardley Coal Zone includes the following subzones (from bottom to top): Mynheer, Silkstone, Arbour and Val D'Or. Each of the coal subzones can be considered an independent coal reservoir with distinct extent, sealing characteristics and coal properties controlled by depositional settings. The informal nomenclature used in this report for the four coal subzones has no certain stratigraphic correlation with the names of the Foothills coal zones.

The Ardley coal subzones in the Pembina block are relatively thin and laterally continuous, rarely thinning or splitting. The middle and upper coal subzones in particular, show a relatively consistent lateral ash content for a specific coal seam.

Mynheer Coal Subzone Geometry

The Mynheer coal subzone is the lowest coal unit and represents the onset of peat-forming conditions in the Scollard Formation. Numerous coal seams characterized by inconsistent lateral extent and high variability of ash content are the main characteristics of the Mynheer coal subzone. The lateral continuity and coal quality increase towards the top of the coal subzone. The recorded variability of the lowermost Mynheer coal seams can be interpreted as 1) the initiation stage of peat-forming conditions as a transition stage, 2) local irregularities of the substrate, and 3) low sediment supply. Up to eight coal seams are vertically distributed in three coal sub-packages that easy to correlate laterally due to the presence of four tonstein beds associated with the top, base and middle part of the coal subzone. The Silkstone lower marker and the Mynheer top marker sometimes coalesce to form a unique bed-marker (Figures 29 and 30).

The isopach map of the Mynheer coal subzone shows that it is thickest in the west-central part of the study area, with a range of 11–13 m (Figure 43). This subzone is absent in the southern part of the area (Figures 21, 23 and 24). Occasionally, it can either reach maximum thickness of 24 m or be absent, thus emphasizing its lateral variability (Figure 43). In the west-central part of the area, the coal cumulative thickness can be greater than 5–6 m and consist of up to 12 coal seams (Figures 44 and 45).

Silkstone Coal Subzone Geometry

The isopach map of the Silkstone coal subzone (Figure 46) shows a change in the coal distribution from the south-central to the north-central part of the study area; it is thin to absent in the south (Figure 22).

This subzone is commonly 6–10 m thick but can locally reach 22 m. The coal cumulative thickness ranges from 2 to 4 m, locally reaching a maximum of 7 m (Figure 47), which corresponds to an increase in the number of coal seams from three to six (Figure 48). The local vertical profile shows mainly coal, with almost no shaly coal or coaly shale as no peat-transition stages associated with the initial or final stages of the peat development (Diessel, 1992) (Figures 14, 28 and 29).

Arbour Coal Subzone Geometry

The maximum thickness of the Arbour coal subzone is 28 m, making it the thickest subzone in the Pembina block due to the local occurrence of one or two additional coal seams (Figures 19, 21, 22 and 24). In plan view the inconsistent occurrence of the lowermost coal seams induces an abrupt and discontinuous increase in thickness (Figure 49). The most common thickness range is of 12–16 m. The isopach map shows that this subzone is thickest in the south-central part of the study area. It was either not deposited or had been eroded in the northeastern part. Coal cumulative thickness is generally 3–4 m, with local increases from 6 to 7 m (Figure 50). The number of coal seams associated with the greater coal accumulation is generally three, but can locally reach five or six (Figure 51).

Val D'Or Coal Subzone Geometry

The Val D'Or coal subzone represents the last record of peat-forming conditions in the lower Paleocene within the Pembina sub-basin (Figures 14 and 29). This youngest coal subzone is thickest mainly in the southern half of the study area, locally reaching a maximum thickness of 13 m (Figure 52). It is absent due to erosion or nondeposition in the northeastern part of the area (Figures 16, 17, 19, 21–23). The cumulative coal thickness shows a similar distribution to that of the Arbour coal subzone in the southern part of the Pembina block. Cumulative coal thickness is generally 2–3 m, increasing locally to 6 m (Figure 53). The subzone contains generally four coal seams, and only locally can present up to six individual coal seams (Figure 54).

3.3.1.3 Seals

The Scollard–Paskapoo succession consists of two types of reservoir: the Ardley coal subzones as unconventional CBM reservoirs and the adjacent sandstone channels as conventional reservoirs. Most of the Ardley unconventional reservoirs are sealed by thin beds of tonstein intimately associated with the coal packages. Also, thick successions of mudstone and siltstone may occur associated with the tonstein beds. Of the maximum of four thin tonstein beds recognized, the more important are those localized at the top and the base of every coal subzone, which ensure sealing of the coal strata (Figure 29).

Locally, the overlying sandstone channels have superficially eroded the tops of these coal seals and may also have eroded parts of the coal seams. Thus, some of the reservoir characteristics of the coal subzones have been modified by changes in pressure regime and geo-fluids content (Plate 2, Figures C and D; Figures 16 and 17).

3.3.2 Coal Properties

The potential for high gas content is directly controlled by coal rank and burial history, coal quality or maceral composition, and ash content (Diessel, 1992; Scott, 2001). In addition, coal permeability (inferred from coal-cleat systems) is an important criterion in gas production.

3.3.2.1 Coal Quality (Ash Content)

Coal quality (or ash content) reflects the original depositional conditions (Diessel, 1992; Scott, 2001) and influences the CBM potential of the Ardley coal reservoirs.

It is always a problem considering all the coal seams identified on the geophysical logs as having minimum ash content and defining them generically as 'coal.' A distinction among the subcategories of the generic term of 'coal' reflecting the variability of the organic content vs. ash content such as 'shaly coal,' 'coaly shale' and 'coal' itself can be made by detailed description of drillcores and petrographic analysis. Unfortunately, the drillcores in the Scollard Formation are rare and usually incomplete. An alternative, used in this study, is to estimate the ash content, relative to the coal subcategories, based on gamma ray–density readings (coal <1.7 g/cm³, shaly coal 1.7–1.9 g/cm³ and coaly shale 1.9–2.1 g/cm³) compared with the deep induction record. In this way, the coal sub-categories data presented in this study were obtained from the interpretation of the geophysical logs, which are always available. The associated detailed core descriptions compiled during this study were necessary for calibrating the resolution of the geophysical log interpretation and for improving the quality of coal classification. The new coal datasets for the Pembina exploration block (associated to the report) and for the Edson block (Edson CBM Exploration Block, Alberta, Ardley Coal Zone Characterization and Sandstone Channels Geometry, C. Pana, work in progress, 2007) utilize the descriptive coal subcategories, thereby allowing more detailed interpretation of coal quality.

The variability in ash content in coal seams is the result of internal and external factors, the most important of which is the sediment supply. Depending on quantity, the sediment supply induces contamination of organic matter with inorganic components and can also lead to splitting of the coal seams. The margins of the peat-forming environment are always more prone to enrichment in inorganic components or splitting than the central part (Diessel, 1992) (Figure 21).

The improved resolution of coal quality (ash content) for the Ardley Coal Zone in the Pembina exploration block reveals a substantial vertical and lateral variability that is sensitive to fluctuations in depositional conditions. Analysis of the generic vertical succession of coal lithotypes (Bustin et al., 1983) within the block resulted in the definition of a lithotype pattern that can be considered representative of the study area (Figure 28). The initial and final stages of the peat-forming environment are marked by a lower content of organic matter relative to the increased organic content of the middle stages when favourable conditions prevailed. The record of these stages is well depicted by the vertical profiles of the Arbour and Val D'Or coal subzones in the Pembina block. The transition stages in the Silkstone subzone are very short or almost nonexistent.

The upper parts of the Arbour and Val D'Or coal subzones consist mainly of 'clean coal,' with subordinately amounts of 'shaly coal' or 'coaly shale' (Figures 14 and 28). In general, within the Ardley Coal Zone, thicker coal seams tend to have a greater concentration in organic matter (Figure 29).

The typical vertical succession for the Val D'Or subzone shows the following variability (from top to bottom): shaly coal, coal, shaly coal (or coaly shale), coal, coaly shale (or mudstone or tonstein) and coal. The coal interlayers (e.g., shaly coal, coaly shale, carbonaceous shale or carbonaceous silt) have a lower organic content and reflect changes in the peat environment with respect to the vegetation community (macerals), the influx of fine sediment or the presence volcanic ash falls. The Arbour vertical profile shows the following succession (from top to bottom; Figures 14 and 29): shaly coal (or coaly shale), coal, shaly coal, coal, shaly coal, coal, shaly coal (or coaly shale), mudstone and shaly coal (or coaly shale). The consistency of the Val D'Or and Arbour components in the vertical succession recorded the variability of the peat environmental conditions from high to low ash content (Figures 14 and 28).

The vertical profile of the Silkstone subzone shows two continuous coal seams, each with a fairly consistent thickness of approximately 1 m (Figures 14 and 28). The coal seams are separated by a thin interval of mudstone, coaly shale or carbonaceous shale. The Mynheer vertical profile is less consistent

due to lateral variability in the occurrence of the coal seams. The gradual increase in the organic content towards the top is noticeable where most of the coal seams are present.

The margins of the peat environment have been interpreted based on radical lateral changes in the vertical profiles. Coal seams grouped together in the middle part of the swamp split into a similar or lesser number of individual coal beds, which become thinner, are enriched in ash content, and vary from less continuous to totally absent to the peat margins.

The depositional settings controlled both the geometry of the Ardley coals in the Pembina block and the types of organic matter (macerals) present, which in turn affected the intimate reservoir properties or reservoir anisotropy, as well as the quantity of hydrocarbons generated by the coal.

A set of percentage distribution maps was generated to emphasize the geographical repartition of 'clean coal' in each of the coal-zone (Figures 55–58). 'Clean coal' category is defined in this report as 100% and consists of coal and shaly coal beds. Any record of coaly shale per coal subzone will diminish proportionally the total percentage of 100% of 'clean coal.'

The maps for Silkstone, Arbour and Val D'Or coal subzones (Figures 55–57) show that the percentage of coaly shale increases mainly where the number of coal seams increases, possibly as the result of a more sensitive response to the depositional conditions such as more sediment influx during instable peat-forming conditions. The coal categories distribution-map of the Mynheer subzone shows a persistent occurrence of coaly shale component, of varying percentages with a random distribution (Figure 58).

3.3.2.2 Coal Rank and Burial History

Coal Rank

The diagenetic process of peat coalification occurs with increasing burial depth (temperature and pressure) and higher geothermal gradient, and can be accelerated by tectonics (Teichmüller and Teichmüller, 1982). One of the most commonly used methods to estimate the stage of coalification is the evaluation of coal rank by measuring the reflectance of vitrinite. The direct correlation between the coal rank and the vitrinite reflectance can be seen on the standard coal rank chart (Figure 59) (Bustin et al. (1983).

Only a few vitrinite reflectance ($R_{o,ran}$) data are publicly available for the Ardley coal strata at the regional scale. The vitrinite reflectance dataset presented in Beaton et al. (2002) has been updated with only four new measurements regionally distributed. The data vary east to west from 0.39% to 0.63%, but most fall in the interval of 0.51%–0.57% (Figure 60). The Ardley Coal Zone can be characterized by the persistent vitrinite reflectance range 0.51%–0.59%, which classifies the Ardley coal strata as 'sub-bituminous A - high volatile sub-bituminous C' (Figure 59), approaching the lower limit of thermogenic gas generation (Rice, 1993). The additional data from this study are consistent with the earlier data.

The basin-wide map of Ardley vitrinite reflectance distribution shows a regional zonation of coal maturation, decreasing from the foothills to the erosional edge (Figure 60). Southwest of the Swan Hills area, the vitrinite reflectance data show a less organized pattern of distribution. In this area, vitrinite reflectance values reach only 0.52%, much lower than values in adjacent areas. The sporadic atypical values of the Ardley coal vitrinite reflectance could be due to suppression of vitrinite reflectance (Marchioni, 1983), a process that is sometimes observed in weathered coal seams.

In the study area, the vitrinite reflectance ranges between 0.54% and 0.59% (Figure 61) in the domain of the 'high volatile sub-bituminous C' (Figure 59), approaching the lower limit of thermogenic gas generation (Rice, 1993). The three vitrinite reflectance values found within the outline of the Pembina study area suggest a slight increase of the coal rank from east to west in accord with the regional trend.

Burial History

Burial history of the Ardley Coal Zone began with the deposition of the overlying Paskapoo clastic sediments. Thick, coarse clastic deposits were accumulated on the Scollard Formation during the middle and upper Paleocene following a diachronous hiatus. More than 1600 m of sediments were assumed to be deposited in the Alberta foreland basin (Nurkowski, 1984; Bustin, 1991) during the middle–upper Paleocene. An important part of the thick succession has been removed by erosion since the end of Paleocene. Today, the Paskapoo Formation represents only a few metres along the erosional edge, increasing gradually to 836 m in the subsurface (Figure 7), close to the deformation front.

Present interpretation suggests that a period of tectonic compression and uplift synchronous with the upper Paskapoo clastic sedimentation led to the deposition of stacked fluvial-channel sandstone units. The west-east cross-section through 'The Triangle Zone,' Brazeau River area, (LeDrew, 1997 and Langenberg, et al., 2002) shows that the latest displacement to have affected the Scollard and Paskapoo formations took place sometime during the upper Paleocene (Figure 62). The thick clastic succession that overlays the Scollard Formation for a relatively short period of time and the tectonic compression were possibly responsible for the coalification process of the Ardley coals, which was more intense to the west.

The post-Paleocene massive erosion caused cooling of the basin by uplift, with important consequences for the Ardley coal reservoirs. One of the major hypothetical consequences is the change to a slightly underpressured status, allowing the recharge-discharge hydro-system, accompanied by complex coal degassing processes, to be active within this particular stratigraphic interval (Littke and Leythaeuser, 1993).

3.3.3 Fractures Pattern and Infillings

The presence of coal fracture systems or an orthogonal system of cleats is an important characteristic of the coal strata and a criterion in coal reservoir characterization. Variations in cleat attributes, such as orientation, abutting, spacing, lateral and vertical connectivity and infilling, govern coal permeability and regulate the fluid transport within the coal and from the coal to adjacent reservoirs.

The prediction of the cleat-system orientation is thus critical for coal permeability. Tyler et al. (1994) have shown that cleat-system orientation is predictable from models of simple-deformation foreland basins. In this report, the dominant cleat pattern in the Ardley Coal Zone was interpreted from the surface structural lineaments on the Alberta digital elevation model and compared with the regional structural pattern (Figure 63). As in coal basins in the western United States (Raton, San Juan and Piceance basins), the more continuous type of coal fractures, known as the 'face-cleat system,' is inferred to be approximately perpendicular to the Cordilleran deformation front (Scott, 2001).

The surface lineaments map shows a zonal distribution (Figure 63). The northern part of the Scollard basin has multiple lineament systems, in contrast to the central and southern parts, which are dominated by a northwest-southeast system composed of two groups. The most frequent group trends 335°, approximately parallel to the deformation front, and is distributed mainly in the central part of the Scollard basin. A secondary group of lineaments trends 300°, oblique to the deformation front, and is more frequent south of the North Saskatchewan River. Occasionally, both of these groups are either intersected by or intersect minor lineaments with different orientations. As the result of the interpretation

of the major surface lineaments, the coal face-cleat system of the Ardley Coal Zone is inferred to trend 030°, almost perpendicular to the dominant 300° trend of the lineaments. In some areas of the central part of the basin, where both groups of surface lineaments are present and well defined, the Ardley Coal Zone possibly has a ‘two-face coal-creat’ system. A ‘two-face coal-creat system’ (Scott, 2001) defines a system in which both cleat components, the face and the butt sets, are almost equally developed. The two-face-creat system is assumed to have orientations of 030° and 060° at the basin scale. These areas are interpreted as having the highest potential permeability. Comparison with the distribution of the CBM production wells (Figure 1) shows that the central part of the basin (south of North Saskatchewan River) has the greatest density of CBM wells in production, which might be a confirmation of the higher coal permeability (‘two-face-creats’).

Prior to this study, the coal-creat systems related to the major stress trajectories, S_{Hmax} and S_{Hmin} , within the Alberta foreland basin (Bell et al., 1994; Bell and Bachu, 2003) were generally considered to trend 030°–060° and 300°–330°, respectively. The additional observations on surface lineaments presented in this report are in agreement with the previous analyses of stress orientation in the Alberta foreland basin and represent a more detailed image of the potential zonal distribution of coal-creat systems within the basin.

Interpretation of surface lineaments at the regional scale (Figure 64) shows that the Pembina exploration block is dominated by the northwest-southeast lineament system (i.e., 300° and 335°).

This interpretation reveals the presence of a group of surface lineaments consistently trending 300°–330° and considered here as the major group of surface lineaments. From this, the orientation of the coal-face-creat system is estimated to be 030–060°. The predicted orientation of the coal-face cleats of the Ardley Coal Zone in the Pembina study area is consistent with that measured in the mines (Campbell, 1979).

Northwest of the North Saskatchewan River, the major group of surface lineaments is consistently intersected by a set of lineaments trending 290°. The strong presence of the second system of lineaments may suggest the presence of a ‘two-face-creat’ system. This area coincides with a good distribution of the Mynheer and Silkstone coal subzones.

Southeast of the Saskatchewan River, the major surface lineaments are intersected by a lineament pattern trending 030°–050°. Their presence may also imply a ‘two-face-creat’ system affecting mainly the Arbour and Val D’Or coal subzones. The upper coal subzone recorded the dominant area of distribution almost in the same part of the Pembina sub-basin.

Differential compaction of underlying sediments can locally generate additional cleats or favour the amplification of the existing coal cleats. Areas sensitive to this type of development are defined by the proximal relationship between sandstone channels and coal seams. These relationships are difficult to observe through the analysis of cross-sections, but the vertical relationship between the coal seams and the sandstone units may, in some cases, indicate potential increase in permeability. Two of the cross-sections, C–C’ (00/16-18-045-06W4; Figure 18) and E–E’ (0/08-22-045-07W4; Figure 20), locally show the coal-sand contact. In the first case, additional cleats may evolve at the top of the uppermost Mynheer coal seam due to the overlying sandstone channel. In the second case, the Silkstone lower coal seam may develop additional cleats due to draping over the underlying sandstone.

Another aspect of the coal cleats is revealed by local obstructions of cleat spaces due to calcitic infillings (Plates 5–11). Examination of the drillcores showed that the most frequent infillings with calcite along the cleat systems occur in the Mynheer coal subzone, likely due the higher content of clay and tonstein. The

Val D'Or and Arbour coal subzones are mostly free of calcitic infillings, except for localized occurrences of small lenses (Plate 5, Figure I; Plate 7, Figure C; Plate 8, Figures A–D; Plate 9, Figures A–C, E, H and J; Plate 11, Figures A–E and H).

3.3.4 Reservoir Conditions

Reservoir conditions are inferred from hydraulic gradient, pressure and temperature regime. Several regional hydrogeological studies have shown that the Scollard–Paskapoo succession can be considered an aquifer system (Michael and Bachu, 2001; Bachu and Michael, 2002). The publicly available data on formation pressure, water chemical analysis and reservoir temperature for the Scollard and Paskapoo formations at the regional scale are very limited. Also, the data quality is variable. In support of the little data available, modelled regional grid maps of groundwater table, pressure and temperature were generated by Bachu (2005a, b).

Aquifer characteristics of the Scollard–Paskapoo succession can be summarized as follows: topographically driven recharge-discharge hydrogeological system, normal to slightly underpressured with low salinity (Michael and Bachu, 2001). The Scollard–Paskapoo aquifer is confined at the base by the group of thin layers of tonstein and mudstone of the Battle Formation. Vertical hydraulic communication within the Scollard–Paskapoo aquifer system is not restricted at the basin scale by any laterally consistent confining lithological interval. Nevertheless, discontinuous aquitards, consisting of mudstone and tonstein beds, can locally obstruct the vertical flow between sandstone aquifers.

The coal reservoir properties of the Ardley Coal Zone have required a more detailed analysis of the pressure data than the regional interpretation previously published (Michael and Bachu, 2001; Bachu and Michael, 2002). Re-analysis of the available formation –pressure data involved assigning the data to specific stratigraphic intervals. In this study, the generic Paskapoo-Scollard formation-pressure data have been separated in data correspond to the upper Scollard Formation coal subzones Val D'Or, Arbour, Silkstone and Mynheer and their northern equivalents 'S,' 'MU,' 'MI' and 'N'(Edson CBM Exploration Block, Alberta, Ardley Coal Zone Characterization and Sandstone Channels Geometry, C. Pana, work in progress, 2007) and to the Paskapoo Formation (lower or upper Paskapoo) (Figures 65 and 66). In addition, it was found that three of the datasets represent the commingled intervals of the upper part of the Scollard Formation and basal channels of the Paskapoo Formation.

3.3.4.1 Regional Scale

The potentiometric map of the Paskapoo Formation shows hydraulic head values ranging from 936 m to 761 m, decreasing easterly towards the discharge area of the Pembina and North Saskatchewan rivers (Figure 65). Hydraulic head values for the upper Scollard Formation have a different distribution but show a similar range of values (>1000 m to 778 m) and a similar flow direction (Figure 66). The distribution of calculated hydraulic head elevations in the Scollard–Paskapoo aquifer mimics the present-day topography (Bachu, 2005 a, b).

Scatterplots of the stratigraphically re-assigned formation-pressure data versus depth (Figures 67–71) consistently show slightly lower values than the equivalent freshwater hydrostatic pressures (shown as line joining red data points). Beyond a depth of 400 m, the pressure data show an increase in underpressuring.

Another important type of data display used in this report, is the scatterplot sets of two or more pressure values from the same lithostratigraphic unit in the same well (Figures 72–77). Six wells were found across the basin that had two or three pressure values from the same lithological unit. These scatterplots

also show the slightly underpressured status of the plotted values relative to the freshwater hydrostatic pressure for each lithological unit within the upper Scollard–Paskapoo succession.

Salinity in the Upper Cretaceous–Tertiary succession in the Alberta basin increases with depth (Figure 83). Salinity is low in the Scollard–Paskapoo aquifer, in the range 400–1500 mg/L (Figure 78). The water samples (Lemay, 2003) were taken at depths ranging from 15 to >325 m, with one sample from a depth of 725 m. The scatterplot shows a slight increase in total dissolved solids (TDS) with depth. Most of the water samples come from the Quaternary, the upper Paskapoo, the upper Scollard–basal Paskapoo commingled interval and just the upper Scollard at the very shallow depths of 15 to -100 m. The TDS data are distributed between 200 and 1000 mg/L except for one sample that contains >1500 mg/L. The water samples from the Upper Scollard–Basal Paskapoo and just the Upper Scollard interval are from greater depths and show slightly higher TDS concentrations (>1000 mg/L).

3.3.4.2 Pembina CBM Exploration Block

In the Pembina exploration block, the Scollard and Paskapoo potentiometric surfaces have similar values and northeasterly flow directions towards the Pembina-Saskatchewan drainage basin (Figures 79 and 80). The scatterplots of the stratigraphically re-assigned formation-pressure data from the 200 to 300 m depth interval in the Pembina study area show slightly consistent lower values than the equivalent freshwater hydrostatic pressures. At depths greater than 300 m, the data show an increase in underpressuring (Figures 81 and 82).

The scatterplots of two or more formation pressure data from the same stratigraphic unit measured in the same well show similarly to the scatterplots across the basin, the underpressured status relative to freshwater hydraulic pressures (Figures 73 and 74).

The selected salinity (TDS) values for Quaternary deposits, the upper and lower Paskapoo and the upper Scollard in the study area (Figure 82) are mainly grouped between 300 and 800 mg/L in the depth range of 20–75 m. There is a slight increase to 1100–1400 mg/L at depths of 275–325 m for water samples from the lower Paskapoo and upper Scollard.

The data indicate that, within the Pembina block, the Scollard–Paskapoo succession can be characterized as slightly underpressured with low salinity content and a general northeasterly flow direction toward lower topography. These observations are in agreement with those of previous published regional interpretation. The vertical hydraulic communication within the Scollard–Paskapoo aquifer system at the basin scale is not lithologically restricted by any laterally consistent confining unit, which leads to the conclusion that the Scollard–Paskapoo succession behaves in the Pembina area as an aquifer system with lateral variability.

3.4 Coal Tonnage and Gas-in-Place

Coal mass and gas-in-place (GIP) were calculated using following formulas:

$$\text{coal mass} = \text{density} \times \text{volume}$$

where in situ density is 1.44 g/cm³ (Beaton et al., 2002) and the volume of coal was obtained from the application of the surface-volume utility in ArcMap[®] GIS to the coal cumulative thickness grid.

$$\text{GIP} = \text{volume} \times \text{density} \times \text{gas content/unit}$$

where gas content/unit in the Pembina exploration block is 3.50 cm³/g (Beaton et al., 2002).

Coal volume, coal mass and volume of gas-in-place calculated for the Pembina block are shown in Table 3.

Table 3. Coal volume, coal mass and volume of gas-in-place.

Coal subzone	Coal volume (x 10 ⁹ m ³)	Coal mass (x 10 ⁹ t)	Gas-in-place (x 10 ⁹ m ³)
Val D'Or	12.3	17	62
Arbour	15.1	22	76
Silkstone	16.2	23	81
Mynheer	20.7	30	104
Ardley (total)	64.3	92	323

4 Coal-Sandstone Architecture and Reservoir Connectivity

The Scollard–Paskapoo clastic succession is described as an aquifer system consisting of lithological components, such as sandstone units and coal strata, with attributes of aquifers. Mudstone and siltstone beds are discontinuous aquitards (Michael and Bachu, 2001; Bachu and Michael, 2002).

Interpretation of the Scollard–Paskapoo succession based on a sequence stratigraphic model provides an improved framework for correlation of the reservoir units. The two types of reservoirs considered here are the coal subzones as an unconventional type of reservoir and the adjacent fluvial sandstone channels of the Scollard and lower Paskapoo formations as conventional reservoirs. In some conditions, both coal and sandstone reservoirs may have inherent permeability. The reservoir units have distinct facies, characteristic geometries and specific interrelationships.

The present interpretation focuses on defining major reservoir characteristics, such as geometry and inter-reservoir potential connectivity.

The succession of coal reservoirs within the Pembina CBM exploration block consists of the Val D'Or, Arbour, Silkstone and Mynheer coal subzones. These can be characterized as small-scale heterogeneous reservoirs, thin but laterally continuous and naturally fractured (cleated). The coal subzones are sealed by thin and continuous tonstein beds that are sometimes associated with thick mudstone strata.

The adjacent fluvial sandstone channels are considered potential conventional reservoirs. They represent the maximum sediment supply of every fluvial cycle. The channel succession recognized in the Pembina block consists of the lower and upper channels of the lower Scollard Formation, followed by Silkstone-Mynheer, Arbour-Silkstone and basal Paskapoo channels. The examined drillcores have shown that sandstone reservoir heterogeneity is mainly the result of changes in grain size, degree of sorting, amount of clay minerals and local diagenesis. Overall, decreasing permeability corresponds to the fining-upward stage of the fluvial sequences when the depositional energy and sediment supply declined.

Occasionally, the overlying sandstone channels eroded the sealing tonstein beds at the top of the coal seams, allowing direct contact between the two types of reservoirs. The degree of connectivity between the sandstone channels and the coal strata varies considerably, both vertically and laterally.

4.1 Geometry of the Sandstone Channels and their Relationship with the Adjacent Coal Seams

A key component in defining coal reservoir characteristics is the geometry of the channels and their proximity to the coal seams. Locally in the Pembina block, the direct contact between the coal seams and the overlying sandstone channels may allow the exchange of mobile phases and leads to the consideration of a unique coal-sandstone system.

Detailed geological mapping of the Scollard–Paskapoo sequence provides the architecture of the fluvial channels (Figures 84, 85, 86 and 87), which should be considered in the development of a CO₂ injection–ECBM strategy.

The three important channel intervals in the Pembina block mentioned before infer reservoir connectivity with the adjacent coal strata:

- 1) Paskapoo basal channels and the Val D’Or or Arbour coal subzones,
- 2) Arbour-Silkstone channels and the Silkstone coal subzone,
- 3) Silkstone-Mynheer channels and the Mynheer coal subzone.

4.1.1 Paskapoo Basal Channels Assemblage

The Paskapoo basal channels, consisting of one or several stacked channels, are continuous over large distances and locally cut down to the top of the Val D’Or coal subzone (Plate 2, Figures C and D) or may erode completely the top coal unit of the Ardley Coal Zone (Figures 16, 17, 19, 21 and 22).

In the study area, the basal Paskapoo channels can be thicker than 65 m (Figure 84). The northwest-southeast axis of the maximum thickness of the Paskapoo basal channels overlies the thickest parts of the Val D’Or and Arbour coal subzones. Gradational compaction may have induced the vertical stacking of fluvial-channel sand units along the area of subsidence. The basal Paskapoo channels are in direct contact at their base with the uppermost Ardley coal strata in numerous locations (Figure 88).

4.1.2 Arbour-Silkstone Channels Assemblage

The sandstone channels within the Arbour-Silkstone interval can exceed 30 m in thickness (Figure 85). The fluvial style of the Arbour-Silkstone is one of stacked channels. The isopach map of the Arbour-Silkstone channels shows a dominant distribution in the eastern part of the study area. Distribution of the Arbour-Silkstone channels overlying the Silkstone peat-swamp was possibly induced by the rapid compaction of the underlying peat. In some areas shown on the structural cross-sections, the base of the Arbour-Silkstone channels is in direct contact, possibly erosional, with the Silkstone coal seams (Figures 16–18 and 21–23).

Direct contact between coal seams and the overlying sandstone channels is more frequent in the east-central part of the study area (Figure 89).

4.1.3 Silkstone-Mynheer Channels Assemblage

The Silkstone-Mynheer interval is up to 25 m in thickness. The area of maximum of thickness reveals at least two to three generations of stacked channels. The channel reconstruction map shows dominant northwest-southeast axis of channels (Figure 86). The channels are absent in the northeastern part of the study. The orientation of the Silkstone-Mynheer channels doesn’t show a strong dependence upon the compaction of the underlying mud and peat-swamp sediments, but could be the result of subtle tectonic control.

Direct contact between the channels and the underlying Mynheer coal strata occurs in several places in the southeastern part of the map (Figure 89). Some of the structural cross-sections identify a few of the locations where the coal seams and the overlying sandstone channels are in direct contact (Figures 18, 20

and 22). Also, the basal coal seam of the Mynheer coal-zone can be in direct contact with the underlying sandstone channels (Figure 90).

A few locations grouped in townships 48–49, ranges 7–8, west of the 5th Meridian represent the contact of the lowermost Mynheer coal strata and the underlying upper channels of the lower Scollard Formation (Figure 91).

Evaluation of the channel episodes in the Pembina block with respect to their placement within the uppermost Maastrichtian to Lower–Middle Paleocene shows that the axis of the drainage systems had changed with time (Figure 92). For instance, in the lower part of the Scollard Formation, the channels (Figures 90 and 93) had a consistent west-southeast orientation and the area of maximum thickness changed from the southern part (Figure 87) of the study area to the western part (Figure 93). Later, during deposition of the Ardley Coal Zone, the Mynheer-Silkstone channels and the Arbour-Silkstone channels have a northwest-southeast flow axis and north-south respectively (Figures 85 and 86). The isopachs of the Paskapoo basal channels (Figure 84) show a pronounced northwest-southeast axis. The thinner sandstone succession with a north-south axis may belong to a secondary, possibly younger drainage system.

Detailed interpretation of the relationship among the lithological components in the Pembina CBM exploration block, such as a) erosional contact surfaces at the base of the overlying sandstone channel and the underlying coal seam and b) differential compaction of the underlying sediments indicates areas of reservoir connectivity and therefore potential long-term risk associated with CO₂ storage in the Ardley coal strata.

4.2 Discussion on Reservoir Connectivity and CO₂-ECBM in Ardley Coal Strata, Pembina Block

The changes in basin temperature are very important for preserving methane in coal reservoirs. An overpressured accumulation can evolve into an underpressured one if the basin undergoes cooling as a result of uplift and overburden removal (Law and Dickinson, 1985) and enables small quantities of methane to migrate (Scott, 2001). Gas migration within coal may occur as a result of combined factors such as decrease in reservoir pressure and hydrogeological dynamics. The decreasing level of pressure favours the combination of gas desorption, diffusion and free-phase flow processes (Littke and Leythaeuser, 1993). Inside of the coal matrix, gas migration takes place through the coal fractures (cleats). From the coal fractures, the gas migration may continue updip in the adjacent sandstone channels through the areas of direct stratigraphic contact between coal and sandstone. The present-day slightly underpressured status of the Ardley coal reservoir was induced by the significant erosion of the overlying Paskapoo sequence. During basin uplift stages accompanied by cooling, the coal cleats of the Ardley coal units as permeability index have become more open and, thus subject to more intense geo-fluid transfer within the coal reservoirs and/or outside to the adjacent permeable sandstone through the places where the sealing strata were eroded. In favourable conditions, geo-fluid migration can take place laterally updip within laterally continuous and permeable coal strata or downdip if the coal is underpressured allowing the recharge of meteoric water and generating the biogenic methane. Also the migration can take place vertically from other sources and into the coal reservoirs or from coal seams into adjacent reservoirs such as permeable sandstone. The distribution and orientation of the coal zone and sealing are important in gas trapping. In the Pembina block, geo-fluid migration within the Scollard-basal Paskapoo succession is assumed to be obstructed by permeability barriers or by changes in the pressure-temperature status of the reservoirs. In the Scollard–Paskapoo succession, the permeability barriers can occur as the result of high level of coal anisotropy or lithofacies changes, grain size, sorting and diagenetic processes in the adjacent sandstone. Possibly the small gas pools identified in different associated sandstone channels to the Ardley Coal Zone in the Pembina CBM exploration block represent

evidences of gas migration from adjacent coal strata (Figures 94 and 95). The geo-fluid migration from Ardley coal strata into the adjacent sandstone channels is assumed to be a complex multi-step process that requires further study to be fully understood.

Two well logs from the Pembina block are used to demonstrate the presence of small methane accumulations in the adjacent sandstone channels located at different stratigraphic intervals such as: basal Paskapoo, Arbour-Silkstone and lower Scollard sandstone channels (Figures 94 and 95). Similarly, other small methane accumulations within the upper Paskapoo Formation (Figure 96) may possibly originate in the Ardley coal seams.

Carbon dioxide storage in coal strata as a new strategy for reducing greenhouse gas emissions has, as consequence, the potential to increase coalbed methane (CBM) production. The Scollard–lower Paskapoo stratigraphic framework presented in this report indicates locations where the Ardley coal seams are in direct stratigraphic contact with the adjacent sandstone channels, which may result in vertical connectivity of the two types of reservoir if permeability in the coalbeds and the sandstone channels is inherent. The connectivity of the reservoirs can lead in undefined geological time to gas leakage from the coal strata within the adjacent reservoirs.

5 Conclusions

The following conclusions can be drawn regarding characterization of coal in the Pembina CMB exploration block:

- Five fluvial sequences have been recognized and interpreted as dynamic responses to the cyclic slow thrusting tectonic stages followed by isostatic rebounding. The depositional environments favourable for coal accumulation migrated from northwestern part of the block during deposition of the Mynheer to the central part during Silkstone deposition and to the southeastern part during Arbour and Val D’Or deposition time.
- Banded coal is the dominant type of coal in the Pembina block, followed by banded dull coal and more rare banded bright coal.
- Vitrain reflectance is 0.54%–0.59%, approaching the lower limit of hydrocarbon generation.
- Interpretation of the fracture system suggests two areas of potential ‘two-face-cleat’ systems, northwest and southeast of the North Saskatchewan River.
- Coal-cleats are generally free of calcitic infillings at the macroscopic scale.
- Differential compaction may locally amplify the existing cleats or generate additional fractures at the contact of coal seams with sandstone channels.
- Coal subzones can be considered individual reservoirs due to the unique geometry of each subzone and to the thin layers of tonstein at the top and base that act as seals for the coal packages.
- The Ardley Coal Zone in the study area has a total gas-in-place volume of $323 \times 10^9 \text{ m}^3$, with gas content steadily increasing from the Val D’Or ($62 \times 10^9 \text{ m}^3$) to the Mynheer coal subzone ($104 \times 10^9 \text{ m}^3$).

The following conclusions can be drawn regarding coal-sandstone architecture and reservoir connectivity:

- Two types of reservoir are recognized: coal as an unconventional coalbed methane reservoir

and sandstone channels as a conventional reservoir; both types of reservoirs may have inherent permeability.

- The Scollard–Paskapoo succession can be considered a slightly underpressured, aquifer system. Variations in the degree of underpressuring in different locations can be caused by the anisotropy of facies.
- The sandstone channels and the underlying coal seams are in direct stratigraphic contact in some locations, which may have allowed to methane to migrate under certain reservoir conditions (pressure, hydrogeology and temperature).
- Small accumulations of methane within the adjacent sandstone channels might be the result of methane migration from the coal strata suggesting vertical reservoir connectivity.

6 References

- Alberta Environment (2005): Water well database <http://www.telusgeomatics.com/tgpub/ag_water>, May 2005.
- Alberta Energy and Utilities Board (2005): 2004 Alberta coalbed methane activity summary and well locations; Alberta Energy and Utilities Board, 81 p.
- Allan, J.A. and Sanderson, J.O.G. (1945): Geology of Red Deer and Rosebud sheets, Alberta, Part 1, General geology and economic geology by J. A. Allan and J. O. G. Sanderson; Part 2, Historical geology and sedimentation, by J. O. G. Sanderson; Alberta Research Council, Annual Report 47, 116 p.
- Bachu, S. (2005a): Carbon dioxide storage capacity in uneconomic coal beds in Alberta: potential and site identification; Alberta Energy and Utilities Board, EUB/AGS unpublished client report, 94 p.
- Bachu, S. (2005b): Carbon dioxide storage capacity in Upper Cretaceous–Tertiary Ardley coals in Alberta; Alberta Energy and Utilities Board, EUB/AGS unpublished client report, 50 p.
- Bachu, S. and Michael, K. (2002): Hydrogeology and stress regime of the Upper Cretaceous–Tertiary coal-bearing strata in Alberta; Alberta Energy and Utilities Board, EUB/AGS Earth Sciences Report 2002-04, 73 p.
- Beaton, A. (2003): Production potential of coalbed methane resources in Alberta; Alberta Energy and Utilities Board, EUB/AGS Earth Sciences Report 2003-03, 58 p.
- Beaton, A., Pana, C., Chen, D., Wynne, D. and Langenberg, C.W. (2002): Coalbed methane potential of Upper Cretaceous–Tertiary strata, Alberta Plains; Alberta Energy and Utility Board, EUB/AGS Earth Sciences Report 2002-06, 75 p.
- Bell, J.S. and Bachu, S. (2003): In situ stress magnitude and orientation estimates for Cretaceous coal-bearing strata beneath the plains area of central and southern Alberta; *Bulletin of Canadian Petroleum Geology*, v. 51, no. 1, p. 1–28.
- Bell, J.R., Price, P.R. and McLellan, P.J. (1994): In-situ stress in the Western Canada Sedimentary Basin; *in* Geological Atlas of the Western Canada Sedimentary Basin, G.D. Mossop and I. Shetson (comp.), Canadian Society of Petroleum Geologists and Alberta Research Council, Special Report 4, p. 439–446.
- Blair, T.C. and Bilodeau, W.L. (1988): Development of tectonic cyclothems in rift, pull-apart, and foreland basins; sedimentary response to episodic tectonism; *Geology (Boulder)*, v. 16, no. 6, p. 517–520.
- Bohr, B.F. and Triplehorn, D.M. (1993): Tonstein: altered volcanic-ash layers in coal-bearing sequences; Geological Society of America, Special Paper 285, 44 p.
- Britten, R.A. and Smyth, M. (1973): The Bayswater coal member of the Singleton coal measures of New South Wales; *in* Proceedings, Australasian Institute of Mining and Metallurgy, v. 248, p. 37–47.
- Bustin, R.M. (1991): Organic maturation in the Western Canada sedimentary basin; *Bulletin of Canadian Petroleum Geology*, v. 39, no. 2, p. 207.
- Bustin, R.M., Cameron, A.R., Grieve, D.A. and Kalkreuth, W.D. (1983): Coal petrology: its principles, methods and applications; Geological Association of Canada, Short Course Notes, v. 3, 230 p.
- Bustin, R.M. and Ross, J.V. (1988): Anisotropy of vitrain under differential stress and high confining pressure and temperature; implications for strain analysis; *American Geophysical Union, EOS Transactions*, v. 69, n. 44, p. 1418.

- Campbell, J.D. (1979): Major cleat trends in Alberta Plains coals; Canadian Institute of Mining and Metallurgy Bulletin, v. 72, n. 802, p. 69–75.
- Dawson, F.M., Marcioni, D.L., Anderson, T.C. and McDougall, W.J. (2000): An assessment of coalbed methane exploration projects in Canada; Geological Survey of Canada, Bulletin 549, 217 p.
- Dawson, G.M. (1883): Preliminary report on the geology of the Bow and Belly River region, North West Territories, with special reference to the coal deposits; Geological Survey of Canada, Reports of Progress 1880-82, Part B, 23 p.
- Dawson, F.M., Evans, C.G., Marsh, R. and Richardson, R.R., (1994): Uppermost Cretaceous and Tertiary strata of the Western Canada Sedimentary Basin; *in* Geological Atlas of the Western Canada Sedimentary Basin, G.D. Mossop and I. Shetson (comp.), Canadian Society of Petroleum Geologists and Alberta Research Council, Special Report 4, p. 387–406.
- Demchuck, T.D. (1990): Palynostratigraphic zonation of Paleocene strata in the central and south-central Alberta Plains; Canadian Journal of Earth Sciences, v. 27, n. 10, p. 1263–1269.
- Demchuck, T.D. and Hills, L.V. (1991): A re-examination of the Paskapoo Formation in the central Alberta Plains: the designation of the three new members; Canadian Society of Petroleum Geologists Bulletin, v. 39, no. 3, p. 270–282.
- Diessel, C.F.K. (1965): Correlation of macro- and micropetrography of some New South Wales coals; Proceedings of the 8th Commonwealth Mining and Metallurgical Congress, v. 6, p. 669–677.
- Diessel, C.F.K. (1992): Coal-bearing Depositional Systems; Springer-Verlag, Berlin, Germany, 721 p.
- Eisbacher, G.H., Carrigy, M.A. and Campbell, R.B. (1977): Paleodrainage pattern in late-orogenic basins of the Canadian Cordillera; *in* Tectonics and Sedimentation, W.R. Dickinson (ed.), Society of Economic Paleontologists and Mineralogists, Special Publication 22, p. 143–166.
- Galloway, W. E. and Hobday, D. A. (1996): Terrigenous clastic depositional systems (2nd ed.); Heidelberg, Springer-Verlag, 483 p.
- Gibson, D.W. (1977): Upper Cretaceous and Tertiary coal-bearing strata in the Drumheller-Ardley region, Red Deer River Valley, Alberta; Geological Survey of Canada, Paper 76-35, 41 p.
- Heller, P.L., Angevine, C.L., Burns, B.A. and Paola, C. (1988): Origin of pre-, syn-, and post-orogenic alluvial gravels in foreland basins; examples from the Western Interior; Geological Society of America, Abstracts with Programs, v. 20, no. 7, p. 378.
- Heward, A.P. (1978): Alluvial fan sequence and megasequence models, with examples from Westphalian D-Stephanian B coalfields, northern Spain; Canadian Society of Petroleum Geologists, Memoir, no. 5, p. 669–702.
- Holter, M. E., Yurko, J. R. and Chu, M. (1975): Geology and coal reserves of the Ardley coal zone of central Alberta. Program with Abstracts-Geological Association of Canada; Mineralogical Association of Canada; Canadian Geophysical Union, Joint Annual Meeting.1; Publisher: Geological Association of Canada; Waterloo, 74 p.
- Irish, E.J.W. and Harvard, C.J. (1968): The Whitemud and Battle formations (“Kneehills Tuff Zone”), a stratigraphic marker; Geological Survey of Canada, Paper 67-63, 51 p.
- Jerzykiewicz, T. (1997): Stratigraphic framework of the uppermost Cretaceous to Paleocene strata of the Alberta Basin; Geological Survey of Canada, Bulletin 510, 121 p.

- Jerzykiewicz, T. and Sweet, A.R. (1986): Caliche and associated impoverished palynological assemblages: an innovative line of paleoclimate research into the uppermost Cretaceous and Paleocene of southern Alberta; *in* Current Research, Part B, Geological Survey of Canada, Paper 86-1B, p. 653–663.
- Jerzykiewicz, T. and Sweet, A.R. (1988): Sedimentological and palynological evidence of regional climatic changes in Campanian to Paleocene sediments of the Rocky Mountain Foothills, Canada; *Sedimentary Geology*, v. 59, p. 29–76.
- Krishna, P G. and Perumal, S. (1948): Structure in black cotton soils of the Nizamsagar project area, Hyderabad state, India. *Soil Science*, vol.66, no.1, p.29-38.
- Langenberg, C.W., Beaton, A. and Berhane, H. (2002): Regional evaluation of the coalbed methane potential of the foothills/mountains of Alberta (2nd edition); Alberta Energy and Utilities Board, EUB/AGS Earth Sciences Report 2002-05, 125 p.
- Law, B.E. and Dickinson, W.W. (1985): Conceptual model for origin of abnormally pressured gas accumulations in low-permeability reservoirs; *AAPG Bulletin*, v. 69, no. 8, p. 1295–1304.
- LeDrew, J. (1997): Three-dimensional geometry and evolution of the Lovett River Triangle Zone, central Alberta Foothills; M.Sc. thesis, University of Calgary, 113 p.
- Lemay, T.G. (2003): Chemical and physical hydrogeology of coal, mixed coal-sandstone and sandstone aquifers from coal-bearing formations in the Alberta Plains region; Alberta Energy and Utilities Board, EUB/AGS Earth Sciences Report, 2003-04, 370 p.
- Lerbekmo, J.F., Evans, M.E. and Hoye, G.S. (1990): Magnetostratigraphic evidence bearing on the magnitude of the sub-Paskapoo disconformity in the Scollard Canyon–Ardley area of the Red Deer Valley, Alberta; *Bulletin of Canadian Petroleum Geology*, v. 38, p. 197–202.
- Lerbekmo, J.F., Demchuk, T.D., Evans, M.E. and Hoye, G.S. (1992): Magnetostratigraphy and biostratigraphy of the continental Paleocene of the Red Deer Valley, Alberta, Canada; *Bulletin of Canadian Petroleum Geology*, v. 40, p. 24–35.
- Littke, R. and Leythaeuser, D. (1993): Migration of oil and gas in coals; *in* Hydrocarbons from Coal, B.E. Law and D.D. Rice (ed.), American Association of Petroleum Geologists, Studies in Geology, v. 38, p. 219–236.
- Lyons, P.C. and Rice, C.L., ed. (1986): Paleoenvironmental and tectonic controls in coal-forming basins of the United States; Geological Society of America, Special Paper 210, 200 p.
- Mack, G.H., James, W.C. and Monger, H.C. (1993): Classification of paleosols; Geological Society of America, *Bulletin*, v. 105, p. 129–136.
- Mackowsky, M.-Th. (1982): Methods of coal examination; *in* Coal Petrology (3rd edition), E. Stach, M.-Th. Mackowsky, M. Teichmüller, G. H. Taylor, D. Chandra, and R. Teichmüller (ed.), Gebrüder Borntraeger, Berlin-Stuttgart, p. 300–348.
- Magoon, L.B. and Dow, W.G. (1994): The petroleum system; *in* The Petroleum System — from Source to Trap, L.S. Magoon and W.G. Dow (ed.), American Association of Petroleum Geologists, Memoir 60, p. 3–24.
- Marchioni, D.L. (1983): The detection of weathering in coal by petrographic, rheologic and chemical methods; *International Journal of Coal Geology*, v. 2, p. 231–259.
- Miall, A.D. (1984): Principles of Sedimentary Basin Analysis; Springer-Verlag, New York, 490 p.

- Miall, A.D. (1996): *The Geology of Fluvial Deposits: Sedimentary Facies, Basin Analysis and Petroleum Geology*; Springer-Verlag, New York, 582 p.
- Michael, K. and Bachu, S. (2001): Fluids and pressure distribution in the foreland-basin succession in the west-central part of the Alberta Basin, Canada: evidence for permeability barriers and hydrocarbon generation and migration; *AAPG Bulletin*, v. 85, no. 7, p. 1231–1252
- Moore, D. M. and Reynolds, R. C., (1997): *X-ray diffraction and the identification and analysis of clay minerals*: New York, Oxford University Press, 378 p.
- Nurkowski, J.R. (1984): Coal quality, coal rank variation and its relation to reconstructed overburden, Upper Cretaceous and Tertiary plains coals, Alberta, Canada; *AAPG Bulletin*, v. 68, no. 3, p. 285–295.
- Potter, P. E., Maynard, J. B. and Pryor, W. A. (1980): *Sedimentology of Shale*; Springer Verlag, New York, 303 p.
- Reinhardt, J. and Sigleo, W.R., ed. (1988): *Paleosols and weathering through geologic time*; Geological Society of America, Special Paper 216, 181 p.
- Retallack, G.J. (1990): *Soils of the Past: An Introduction to Paleopedology*; Unwin Hyman, Boston, 520 p.
- Rice, D.D. (1993): Composition and origins of coalbed gas; *in Hydrocarbons from Coal*, B.E. Law and D.D. Rice (ed.), American Association of Petroleum Geologists, Studies in Geology, v. 38, p. 159–184.
- Scott, A.R. (2001): A coalbed methane producibility and exploration model: defining exploration fairways; 2001 International Coalbed Methane Symposium, Tuscaloosa, Alabama, Short Course Notes, 448 p.
- Sweet, A.R., Braman, D.R. (1992): The K-T boundary and contiguous strata in western Canada: interactions between paleoenvironments and palynological assemblages; *Cretaceous Research*, v. 13, p. 31–79.
- Sweet, A.R., Braman, D.R. and Lerbekmo, J.F. (1990): Palynofloral response to K/T boundary events: a transitory interruption within a dynamic system; *in Global Catastrophes in Earth History*, V.L. Sharpton and P.D. Ward (ed.), Geological Society of America, Special Paper 247, p. 457–469.
- Teichmüller, M. and Teichmüller, R. (1982): The geological basis of coal formation; *in Coal Petrology* (3rd edition), E. Stach, M.-Th. Mackowsky, M. Teichmüller, G.H. Taylor, D. Shandra and R. Teichmüller (ed.), Gebrüder Borntraeger, Berlin-Stuttgart, p. 5–86
- Tyler, R., Roger, W., Laubach, S.E., Scults-Ela, D.D. and Tremain, C.M. (1994): Variations in Cretaceous and Tertiary coal fracture pattern, Rocky Mountain Foreland, western United States; Geological Society of America, Annual Meeting, Seattle, Washington, Abstracts, v. 26, no. 7, p. A–209.
- Van Wagoner, J. C., Posamentier, H. W., Mitchum, R. M., Vail, P. R., Sarg, J. F., Loutit, T. S., Hardenbol, J. (1988); An overview of the fundamentals of sequence stratigraphy and key definitions; *in: Wilgus, C. K., Hastings, B. S., Kendall, C. G. St. C., Posamentier, H. W., Ross, C. A., Van Wagoner, J. C. (Eds.), Sea-Level Changes: and Integrated Approach*, SEPM Spc. Publ., vol.42, p. 39-40.
- Warwick, P.D. (2005): Coal systems analysis: a new approach to the understanding of coal formation, coal quality and environmental considerations, and coal as a source rock for hydrocarbons; p. 1–8; *in Coal Systems Analysis*, P.D. Warwick (ed.), Geological Society of America, Special Paper 387, 238 p.

Wright, V.P., ed. (1986): *Paleosols: Their Recognition and Interpretation*; Blackwell Scientific Publications, Oxford, United Kingdom, 315 p.

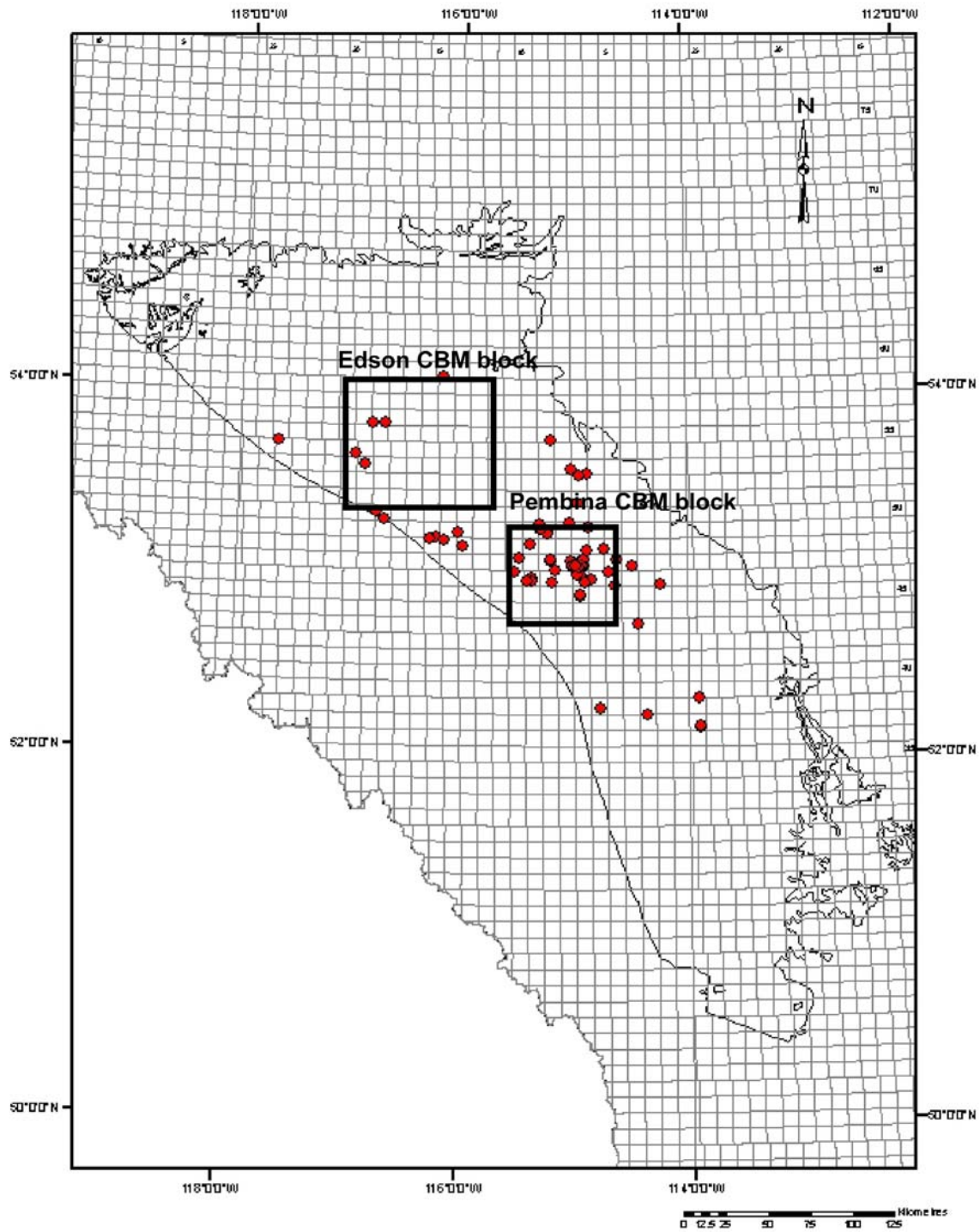
Wright, V.P. (1992): Paleosol recognition: a guide to early diagenesis in terrestrial settings; *in* *Diagenesis III*, K.H. Wolf and G.V. Chilingarian (ed.), Elsevier, *Developments in Sedimentology* 47, p. 591–619.

Appendix 1. Report Figures

- Figure 1 Coalbed methane production wells from the Ardley Coal Zone (Alberta Energy and Utilities Board, 2005)
- Figure 2 Stratigraphic chart of the Upper Cretaceous–Tertiary formations in the Alberta foreland basin
- Figure 3 Chart of the stratigraphic models of the Scollard–Paskapoo sequence (after Holter et al., 1976).
- Figure 4 Isopach map of the Scollard Formation.
- Figure 5 Alberta bedrock.
- Figure 6 Isopach map of the upper member of the Scollard Formation (Ardley Coal Zone).
- Figure 7 Isopach map of the Paskapoo Formation and Quaternary deposits.
- Figure 8 Structural contour map of the top of the Scollard Formation (Ardley Coal Zone).
- Figure 9 Structural contour map of the base of the Scollard Formation.
- Figure 10 Isopach map of cumulative coal in the Ardley Coal Zone.
- Figure 11 Schematic correlation of Edson and Pembina coal sub-basins (Scollard Formation).
- Figure 12 a) Digital elevation model (DEM) of the Pembina study area. b) Wells considered during the study.
- Figure 13 Location of the examined drillcores in the Pembina study area.
- Figure 14 Vertical lithological profile of the Ardley Coal Zone in the Pembina study area.
- Figure 15 Locations of structural cross-sections, Pembina study area.
- Figure 16 A–A' Structural cross-section, Pembina study area.
- Figure 17 B–B' Structural cross-section, Pembina study area.
- Figure 18 C–C' Structural cross-section, Pembina study area.
- Figure 19 D–D' Structural cross-section, Pembina study area.
- Figure 20 E–E' Structural cross-section, Pembina study area.
- Figure 21 F–F' Structural cross-section, Pembina study area.
- Figure 22 H–H' Structural cross-section, Pembina study area.
- Figure 23 I–I' Structural cross-section, Pembina study area.
- Figure 24 J–J' Structural cross-section, Pembina study area.
- Figure 25 L–L' Structural cross-section, Pembina study area.
- Figure 26 M–M' Structural cross-section, Pembina study area.
- Figure 27 Schematic representation of the distribution of subzones in the Ardley Coal Zone.
- Figure 28 Section illustrating consistency of the vertical lithological profile of the Ardley Coal Zone in the Pembina study area.
- Figure 29 Thin tonstein strata recognized on the geophysical log, Pembina study area.
- Figure 30 Sequence stratigraphic model, Pembina study area.
- Figure 31 Schematic reconstruction of the peat environment during deposition of the Ardley Coal Zone.
- Figure 32 Depth to the top of the Ardley Coal Zone, Pembina study area.
- Figure 33 Depth to the base of the Ardley Coal Zone, Pembina study area.
- Figure 34 Depth to the base of the lower Scollard Formation, Pembina study area.
- Figure 35 Structure contours on the top of the Ardley Coal Zone, Pembina study area.
- Figure 36 Structure contours on the base of the Ardley Coal Zone, Pembina study area.
- Figure 37 Structure contours on the base of the Lower Scollard Formation, Pembina study area.
- Figure 38 Isopachs of the Ardley Coal Zone, Pembina study area.
- Figure 39 Isopachs of the lower Scollard Formation, Pembina study area.
- Figure 40 Isopachs of the Battle Formation, Pembina study area.
- Figure 41 Isopachs of Ardley cumulative coal, Pembina study area.
- Figure 42 Number of Ardley coal seams, Pembina study area.

- Figure 43 Isopachs of the Mynheer coal subzone, Pembina study area.
- Figure 44 Isopachs of Mynheer cumulative coal, Pembina study area.
- Figure 45 Number of Mynheer coal seams, Pembina study area.
- Figure 46 Isopachs of the Silkstone coal subzone, Pembina study area.
- Figure 47 Isopachs of Silkstone cumulative coal, Pembina study area.
- Figure 48 Number of Silkstone coal seams, Pembina study area.
- Figure 49 Isopachs of the Arbour coal subzone, Pembina study area.
- Figure 50 Isopachs of Arbour cumulative coal, Pembina study area.
- Figure 51 Number of Arbour coal seams, Pembina study area.
- Figure 52 Isopachs of the Val D'Or coal subzone, Pembina study area.
- Figure 53 Isopachs of Val D'Or cumulative coal, Pembina study area.
- Figure 54 Number of Val D'Or coal seams, Pembina study area.
- Figure 55 Distribution of 'clean coal' (in per cent) in the Val D'Or subzone, Ardley Coal Zone, Pembina study area.
- Figure 56 Distribution of 'clean coal' (in per cent) in the Arbour subzone, Ardley Coal Zone, Pembina study area.
- Figure 57 Distribution of 'clean coal' (in per cent) in the Silkstone subzone, Ardley Coal Zone, Pembina study area.
- Figure 58 Distribution of 'clean coal' (in per cent) in the Mynheer subzone, Ardley Coal Zone, Pembina study area.
- Figure 59 Coal rank chart (Bustin et al., 1983)
- Figure 60 Distribution of vitrinite reflectance in the Ardley Coal Zone, Alberta.
- Figure 61 Distribution of vitrinite reflectance in the Ardley Coal Zone in the Pembina study area.
- Figure 62 Structural cross-section, Brazeau River area, central foothills of Alberta (LeDrew, 1997).
- Figure 63 Interpretation of surface lineaments from the Alberta digital elevation model.
- Figure 64 Interpretation of surface lineaments from the digital elevation model of the Pembina CBM exploration block.
- Figure 65 Potentiometric contours of hydraulic head data for the Paskapoo Formation plotted on the digital elevation model.
- Figure 66 Potentiometric contours of hydraulic head data for the Scollard Formation plotted on the digital elevation model.
- Figure 67 Formation pressure versus depth, Scollard and Paskapoo formations, regional scale. Trend line represents equivalent freshwater hydrostatic pressures.
- Figure 68 Formation pressure versus depth, Paskapoo Formation, regional scale. Trend line represents equivalent freshwater hydrostatic pressures.
- Figure 69 Formation pressure versus depth, commingled Paskapoo basal sandstone channels and upper Ardley coal beds, regional scale. Trend line represents equivalent freshwater hydrostatic pressures.
- Figure 70 Formation pressure versus depth, upper Ardley coal subzones. Trend line represents equivalent freshwater hydrostatic pressures.
- Figure 71 Formation pressure versus depth, lower Ardley coal subzones. Trend line represents equivalent freshwater hydrostatic pressures.
- Figure 72 Formation pressure versus depth, Paskapoo Formation, well 02/07-32-036-03W5/0. Trend line represents equivalent freshwater hydrostatic pressures.
- Figure 73 Formation pressure versus depth, Paskapoo basal sandstone channels, well 00/06-34-052-09W5/0. Trend line represents equivalent freshwater hydrostatic pressures.
- Figure 74 Formation pressure versus depth, upper Paskapoo and Paskapoo basal channels. Trend line represents equivalent freshwater hydrostatic pressures.

- Figure 75 Formation pressure versus depth, MU and MI coal subzones, well 02/11-06-056-19W5/0, Edson coalbed methane exploration block.
- Figure 76 Formation pressure versus depth, Val D'Or, Arbour and Silkstone coal subzones, well 00-10-16-048-14W5/0, Pembina coalbed methane exploration block.
- Figure 77 Formation pressure versus depth, 'S' , 'MI' and 'N' coal subzones, well 00/11-01-056-19W5/0, Edson coalbed methane exploration block.
- Figure 78 Total dissolved solids (TDS), Quaternary, Paskapoo and Scollard succession, regional data
- Figure 79 Potentiometric surface, Paskapoo Formation, Pembina study area
- Figure 80 Potentiometric surface, Scollard Formation, Pembina study area
- Figure 81 Formation pressure versus depth, Paskapoo Formation, Pembina study area
- Figure 82 Total dissolved solids (TDS), Pembina study area
- Figure 83 Total dissolved solids (TDS), regional scale including the TDS trend
- Figure 84 Isopachs of the Paskapoo basal sandstone channels (>10 m), Pembina study area
- Figure 85 Isopachs of the Arbour-Silkstone sandstone channels (>5 m), Pembina study area
- Figure 86 Isopachs of the Silkstone-Mynheer sandstone channels (>5 m), Pembina study area
- Figure 87 Isopachs of the upper sandstone channels (>5 m) of the lower Scollard Formation, Pembina study area
- Figure 88 Locations where Paskapoo basal channels are in direct contact with the uppermost Ardley coal seams (indicated in red), Pembina study area
- Figure 89 Locations where Arbour-Silkstone channels are in direct contact with the Silkstone coal seams (indicated in red), Pembina study area
- Figure 90 Locations where upper channels are in direct contact with the lowermost Mynheer coal seams (indicated in red), Pembina study area
- Figure 91 Locations where Silkstone-Mynheer channels are in direct contact with the Mynheer coal seams (indicated in red), Pembina study area
- Figure 92 Three-dimensional image of the channel succession, Pembina study area
- Figure 93 Isopachs of the lower channels of the lower Scollard Formation, Pembina study area
- Figure 94 Multiple small gas accumulations in the basal Paskapoo and Arbour-Silkstone sandstone channels, well 03/14-27-048-08W5, Pembina study area
- Figure 95 Small gas accumulation in the lower sandstone channel of the Scollard Formation, Pembina study area
- Figure 96 Shallow gas wells map



Legend

● *CBM production wells*

Figure 1. Coalbed methane production wells from the Ardley Coal Zone (Alberta Energy and Utilities Board, 2005).

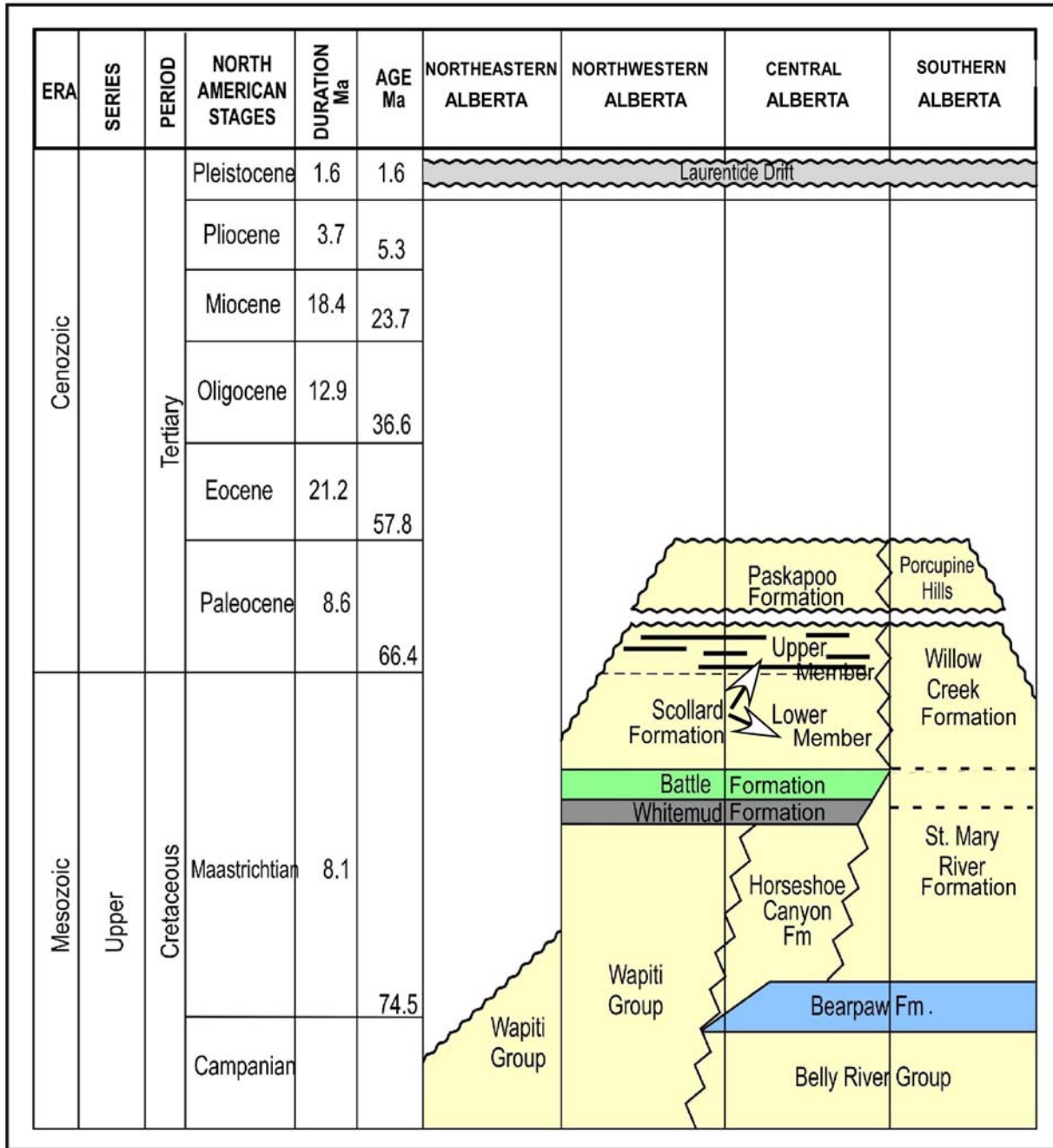


Figure 2. Stratigraphic chart of the Upper Cretaceous–Tertiary formations in the Alberta foreland basin.

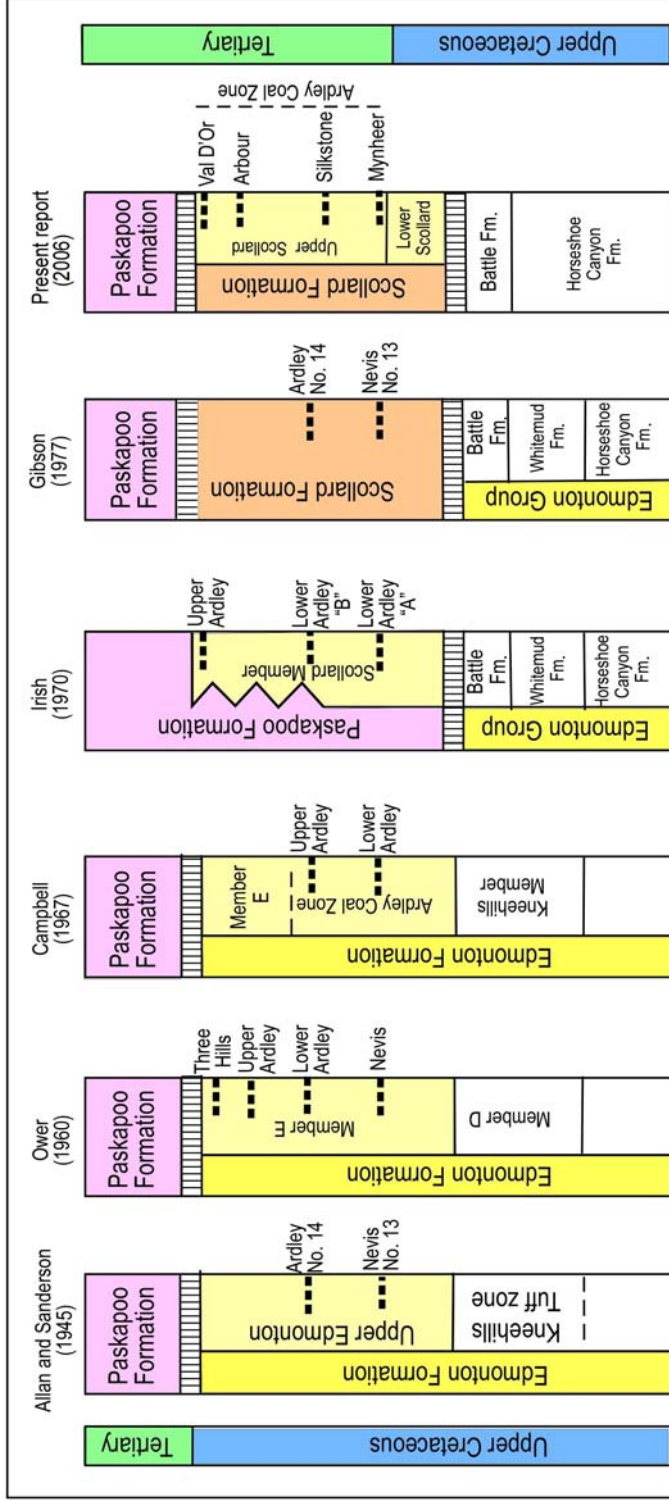


Figure 3. Chart of the stratigraphic models of the Scollard-Paskapoo sequence (after Holter et al., 1976).

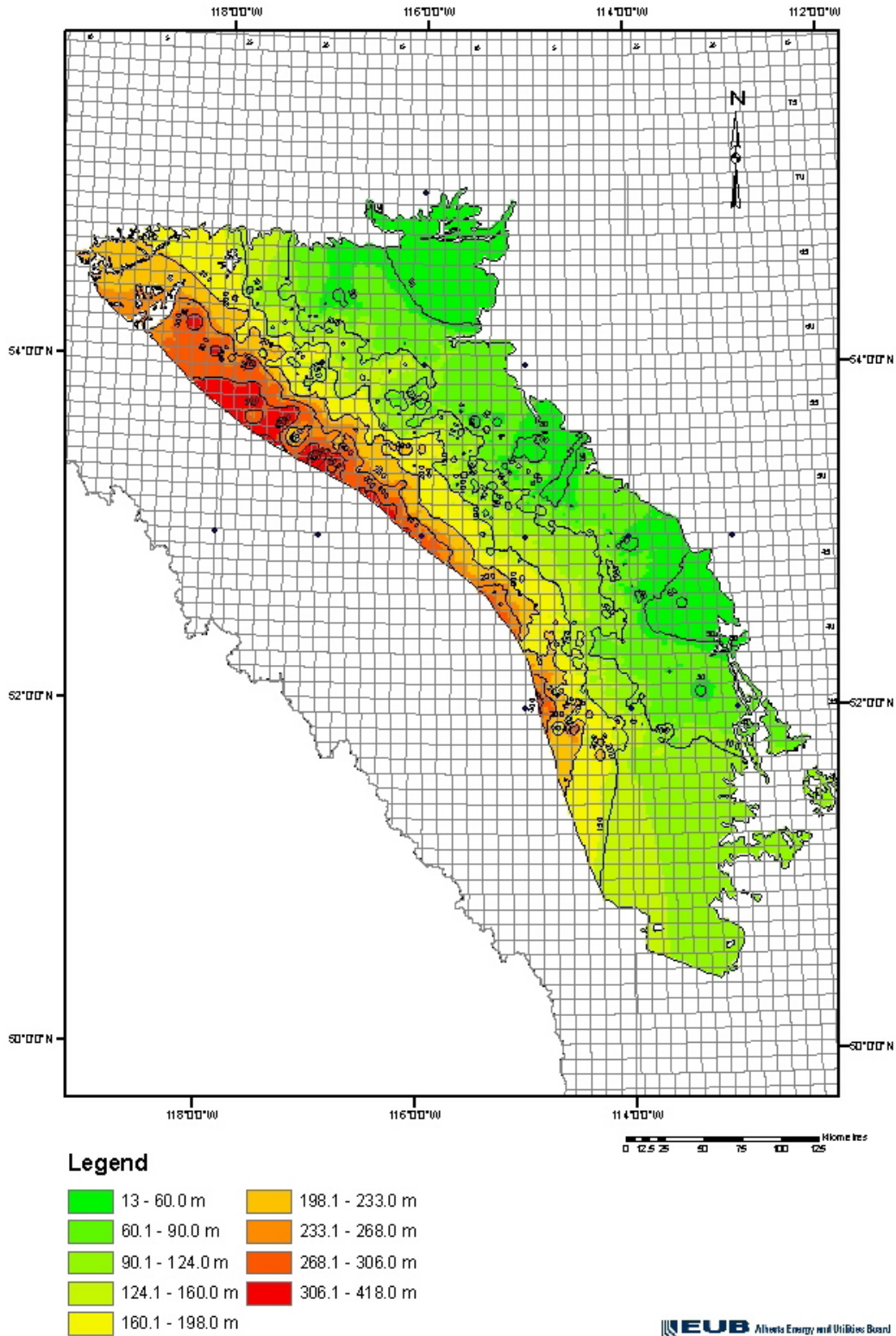


Figure 4. Isopach map of the Scollard Formation.

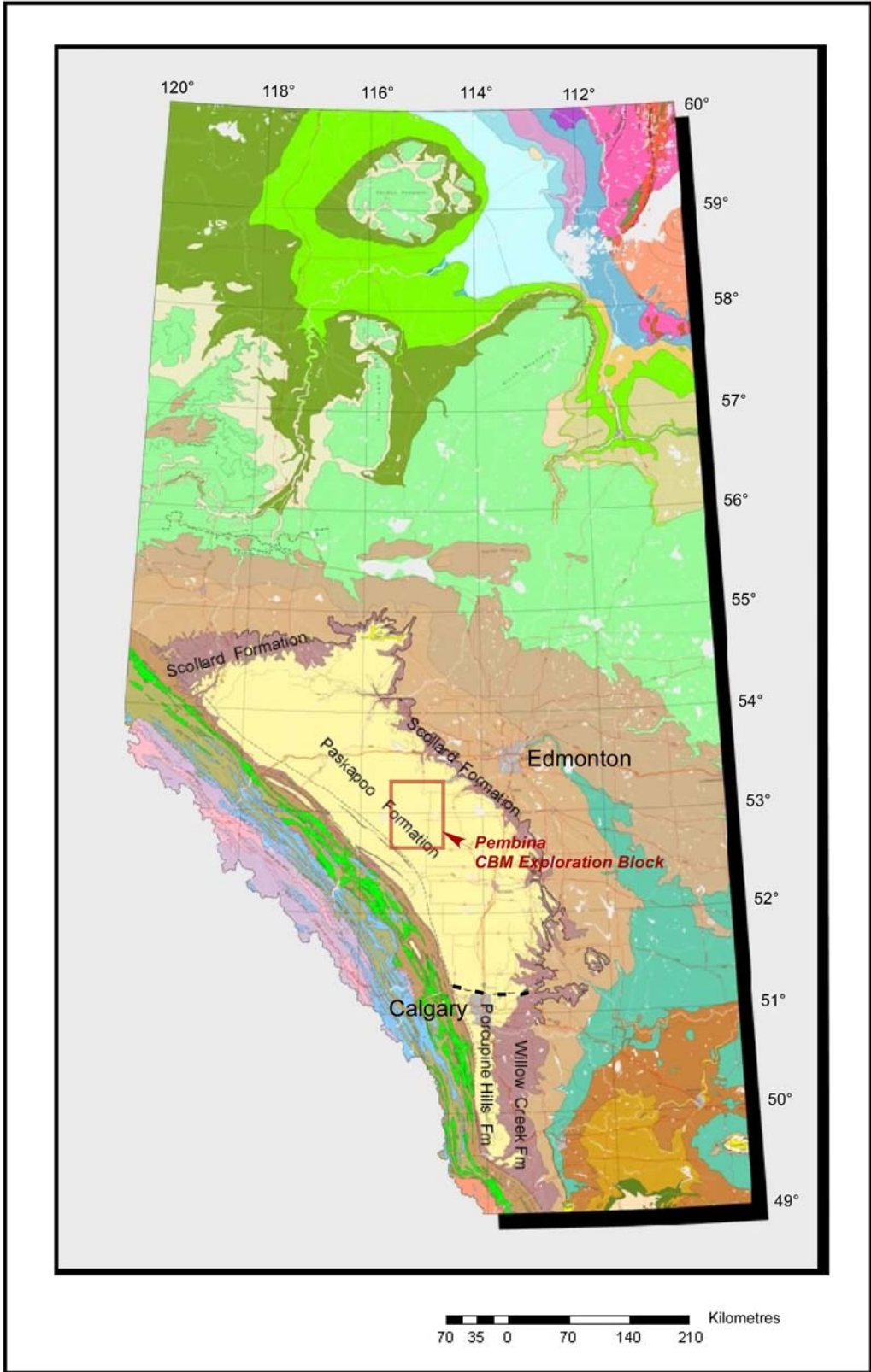
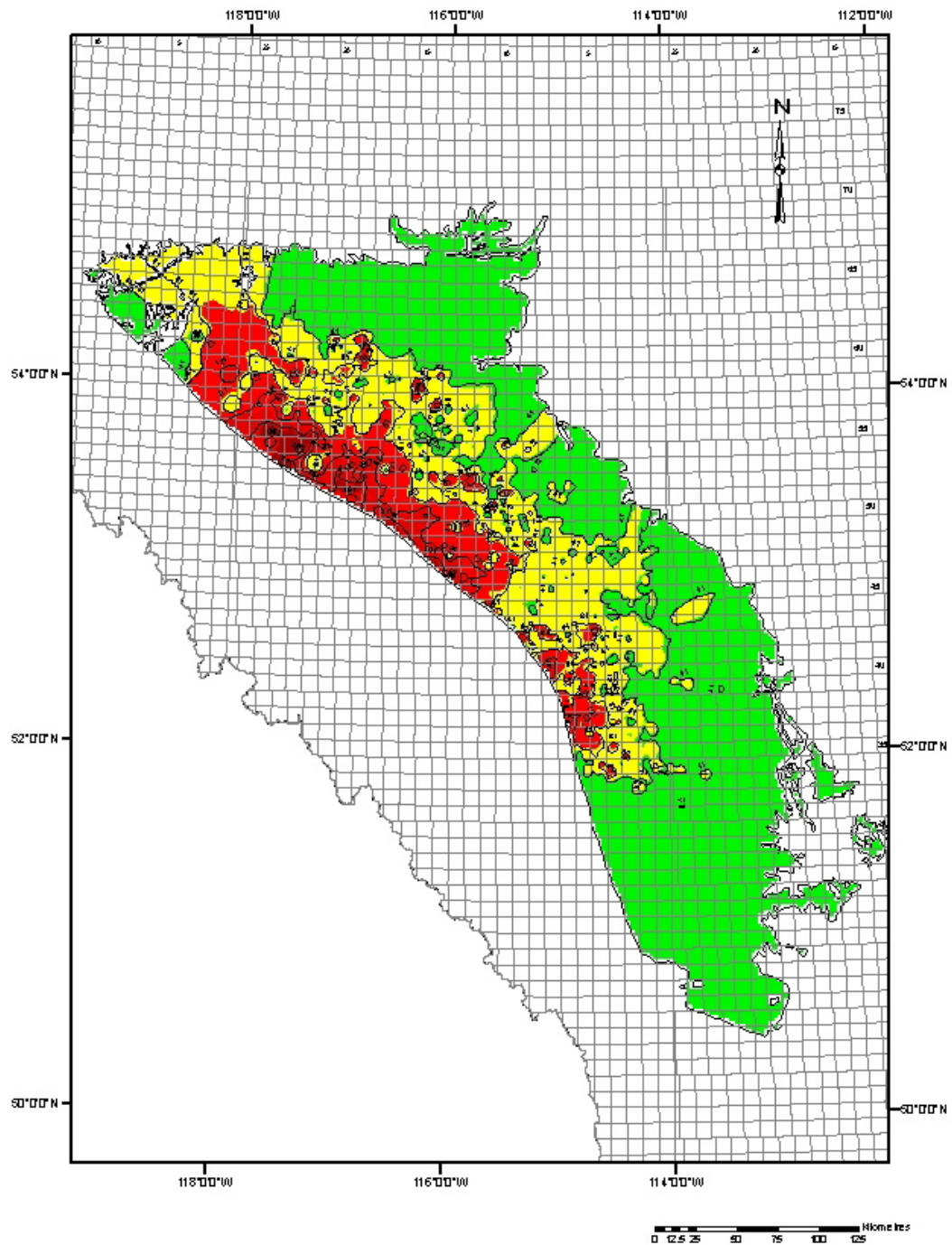


Figure 5. Alberta bedrock.



Legend

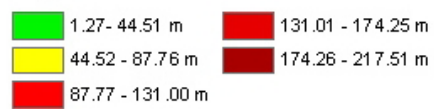
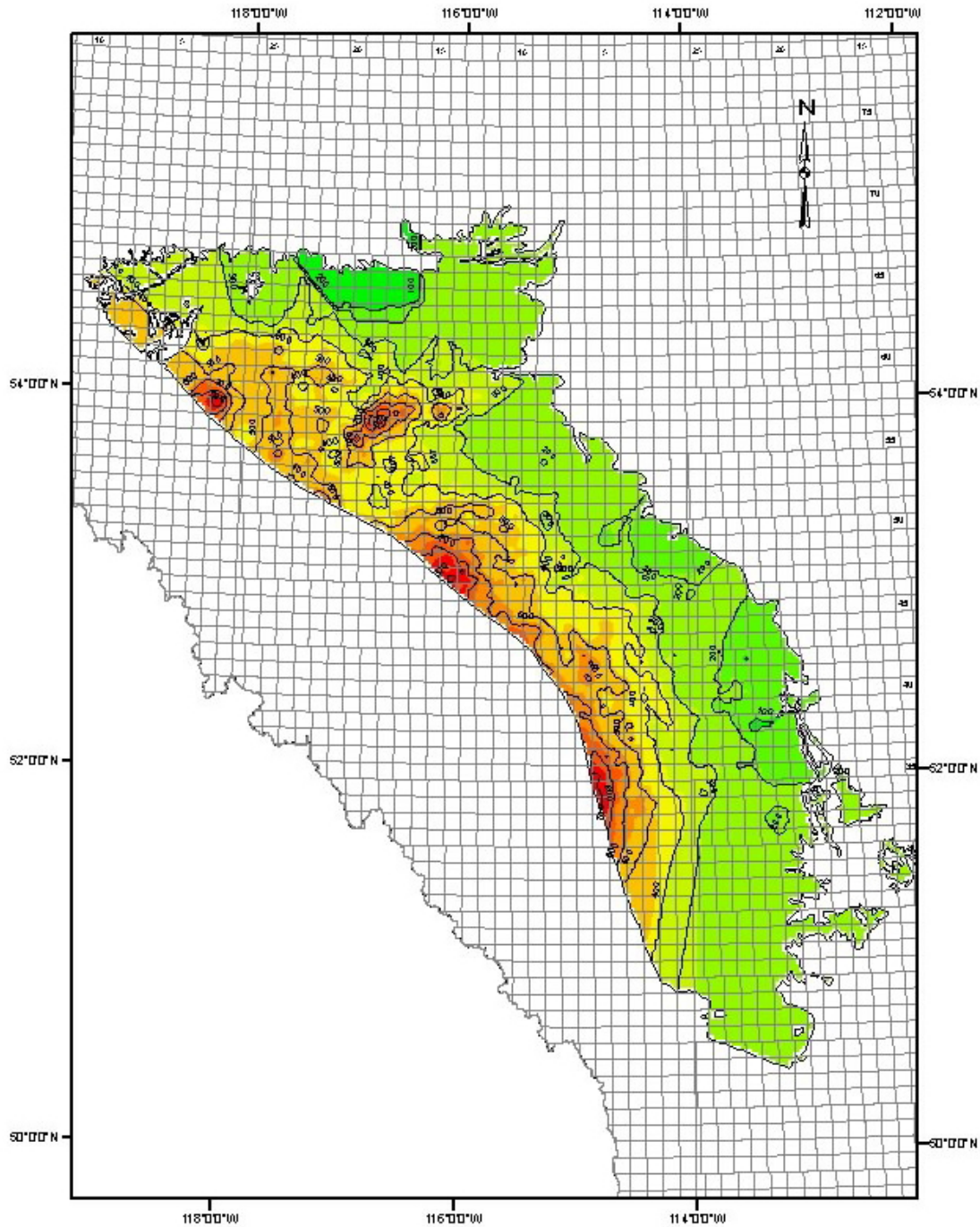
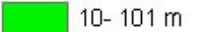

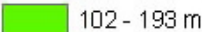

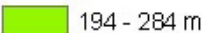



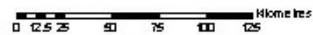


Figure 6. Isopach map of the upper member of the Scollard Formation (Ardley Coal Zone).



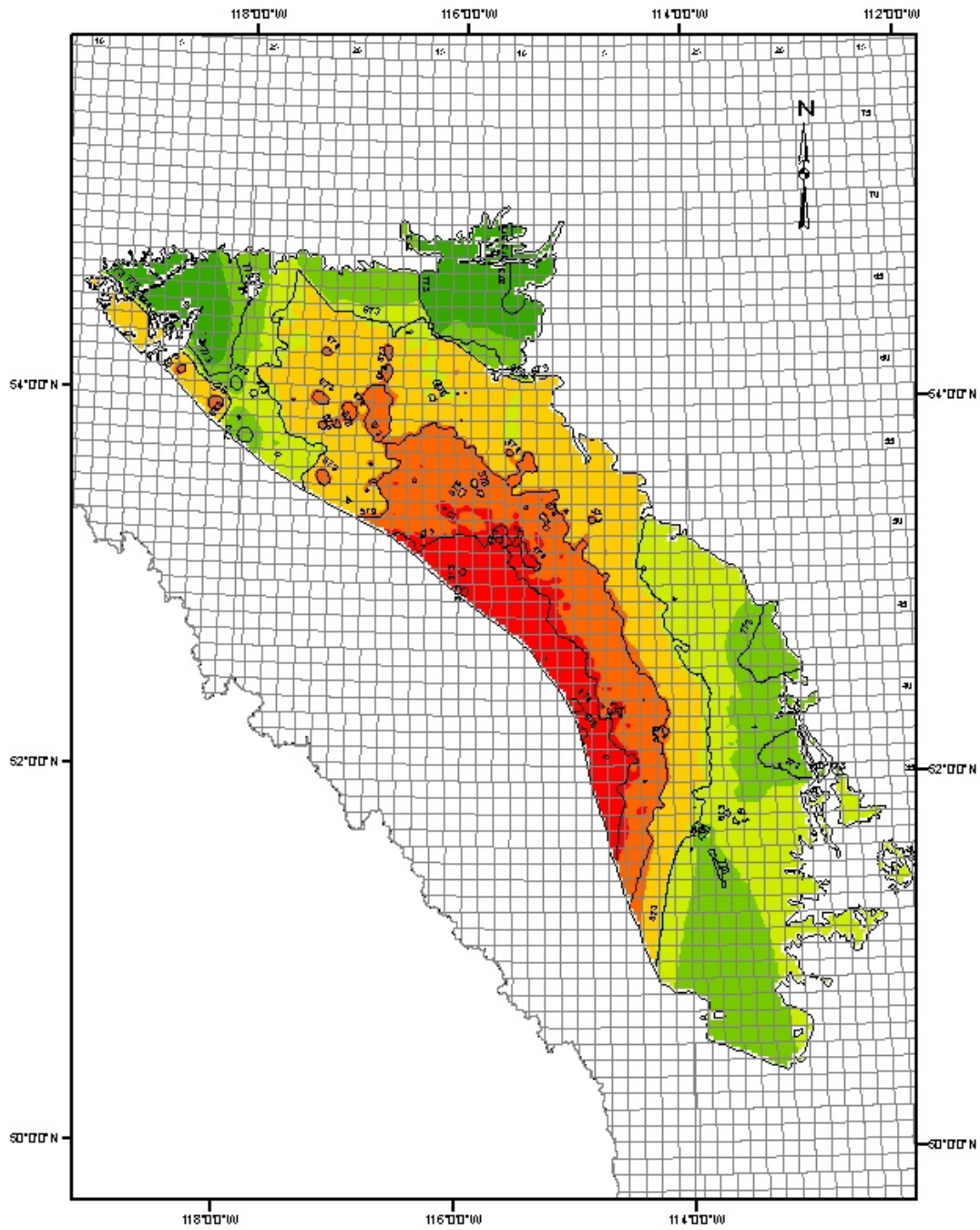
Legend

	10- 101 m		469- 560 m
	102 - 193 m		561 - 652 m
	194 - 284 m		653 - 744 m
	285- 376 m		745 - 836 m
	377 - 468 m		



EUB Alberta Energy and Utilities Board
AGS

Figure 7. Isopach map of the Paskapoo Formation and Quaternary deposits.



Legend







	273 - 494m		658 - 728 m
	495 - 580 m		729 - 800 m
	581 - 657 m		801 - 923 m

Figure 8. Structural contour map of the top of the Scollard Formation (Ardley Coal Zone).

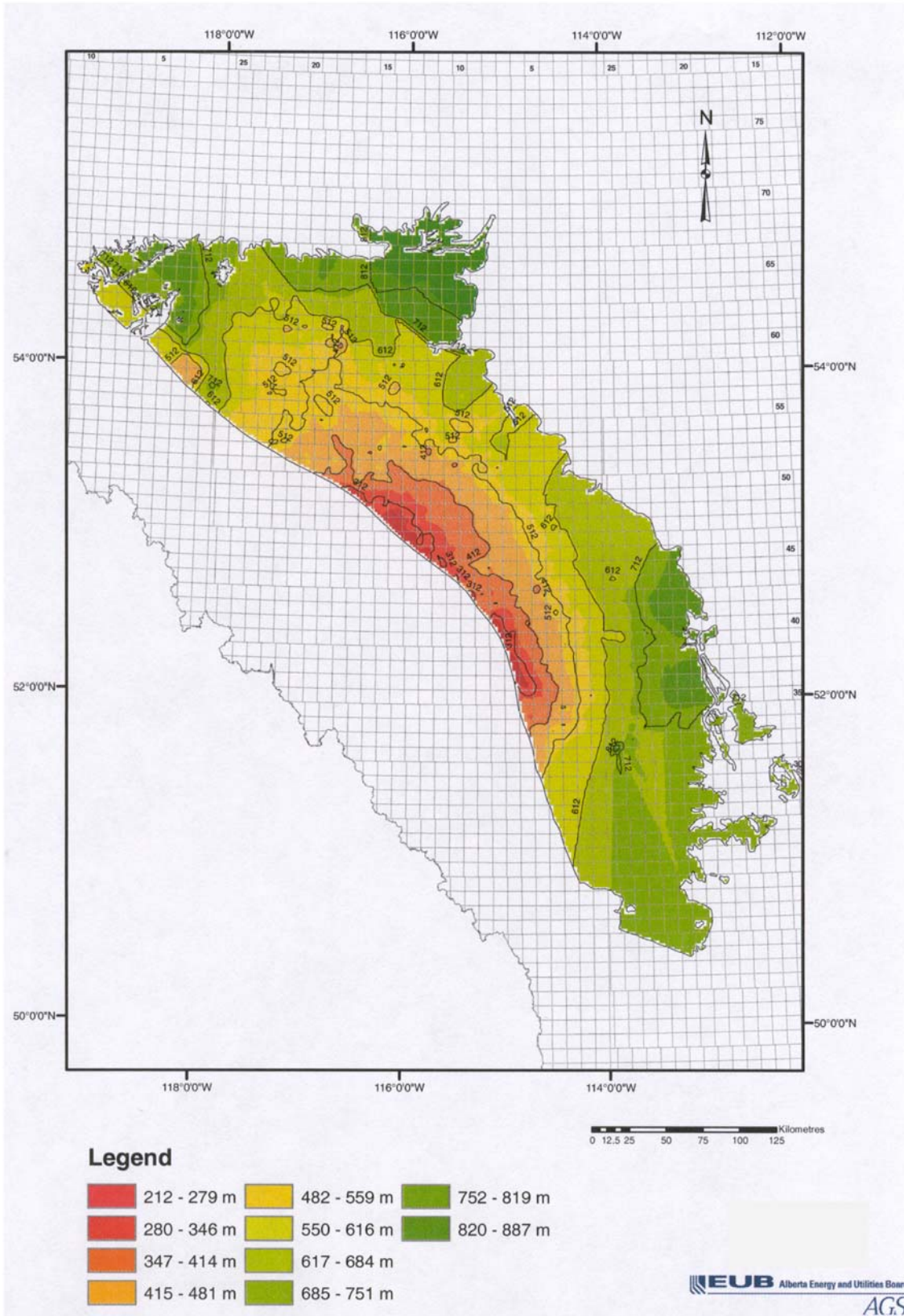


Figure 9. Structural contour map of the base of the Scollard Formation.

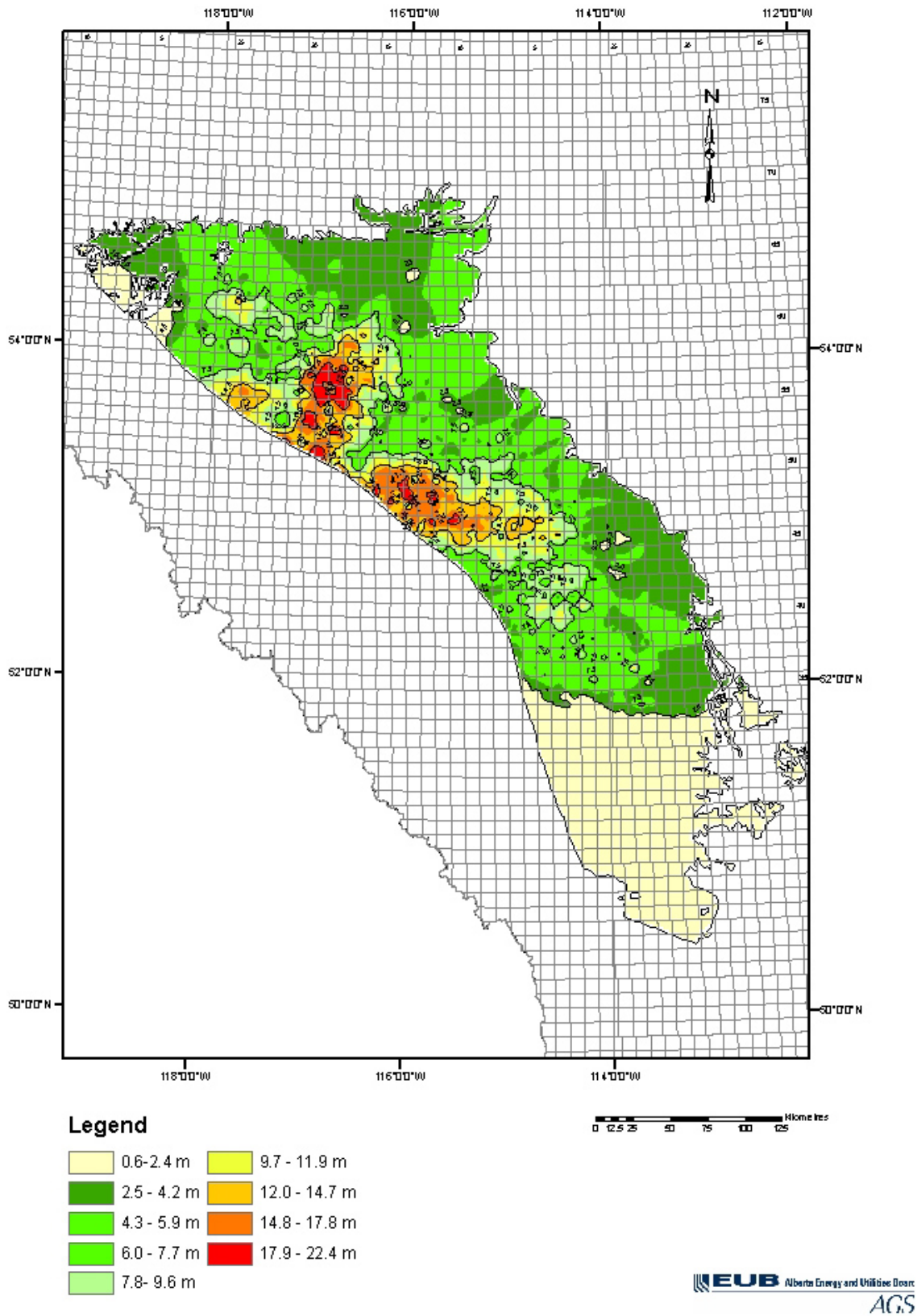
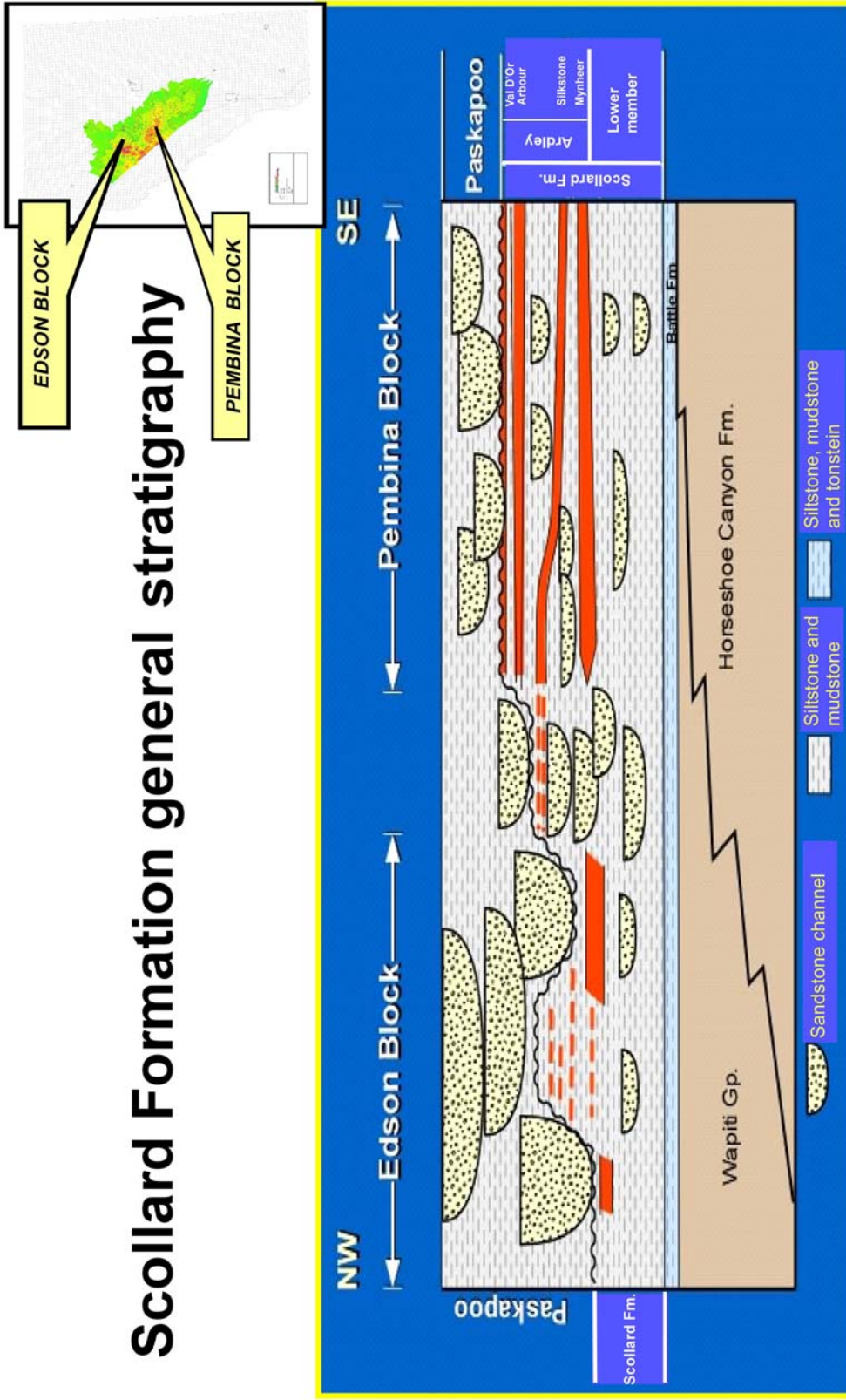


Figure 10. Isopach map of cumulative coal in the Ardley Coal Zone.

Scollard Formation general stratigraphy



Variable number of coal sub-zones (1-4)
Discontinuous coal seams
Deep channel erosion

Four distinct coal sub-zones
Consistent coal sub-zones
Superficial channel erosion

Figure 11. Schematic correlation of Edson and Pembina coal sub-basins (Scollard Formation).

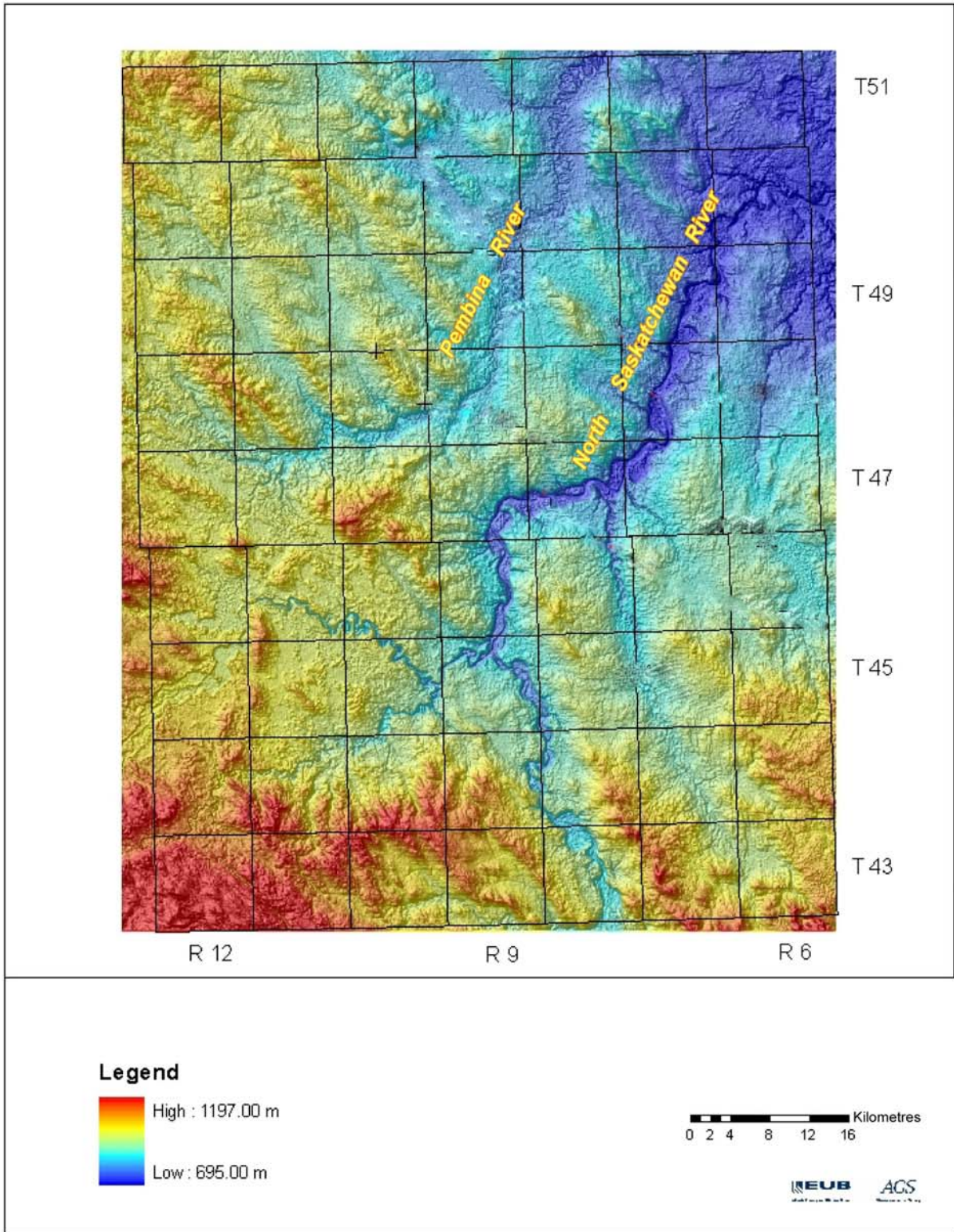


Figure 12a). Digital elevation model (DEM) of the Pembina study area.

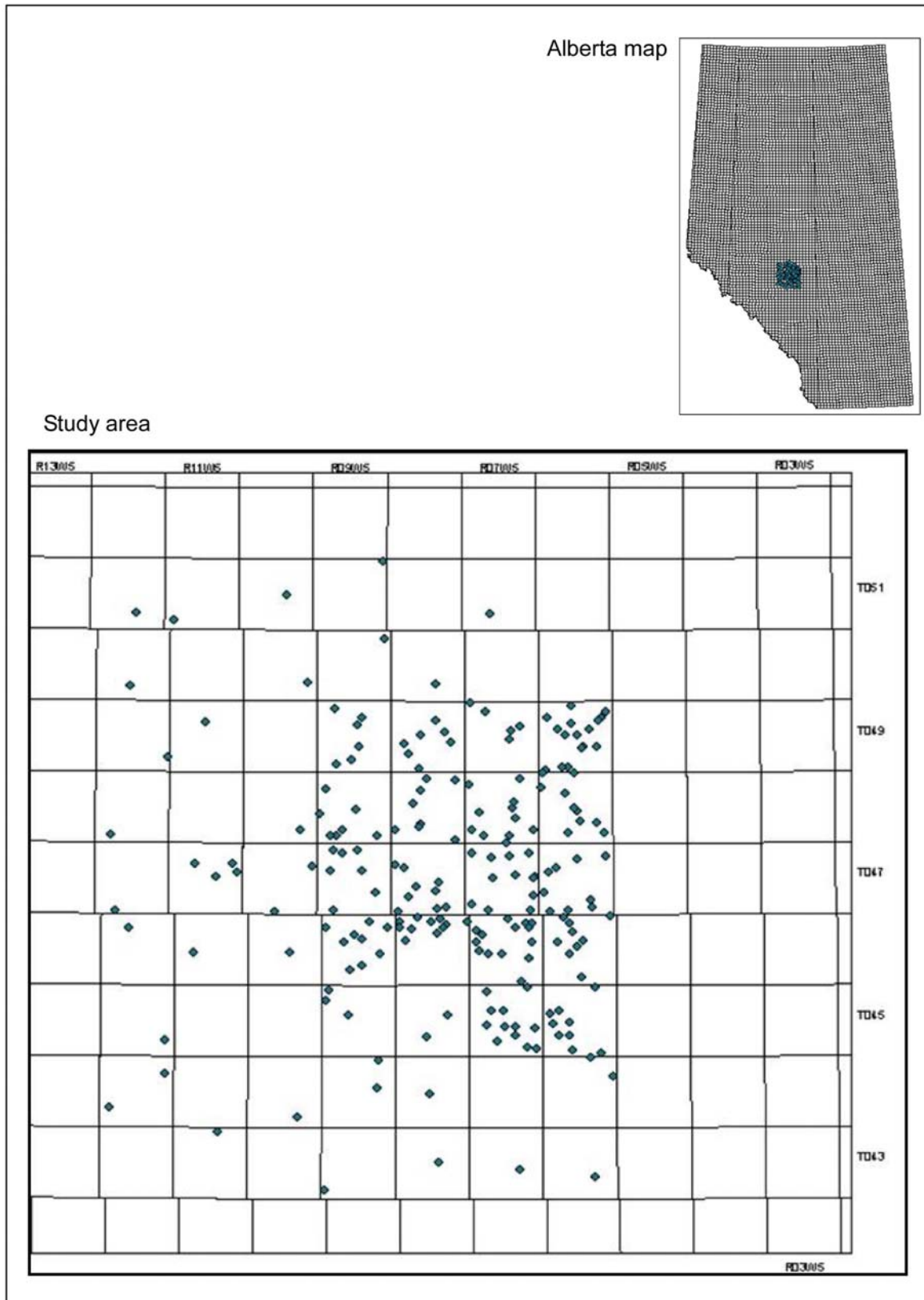


Figure 12b). Wells considered in the study.

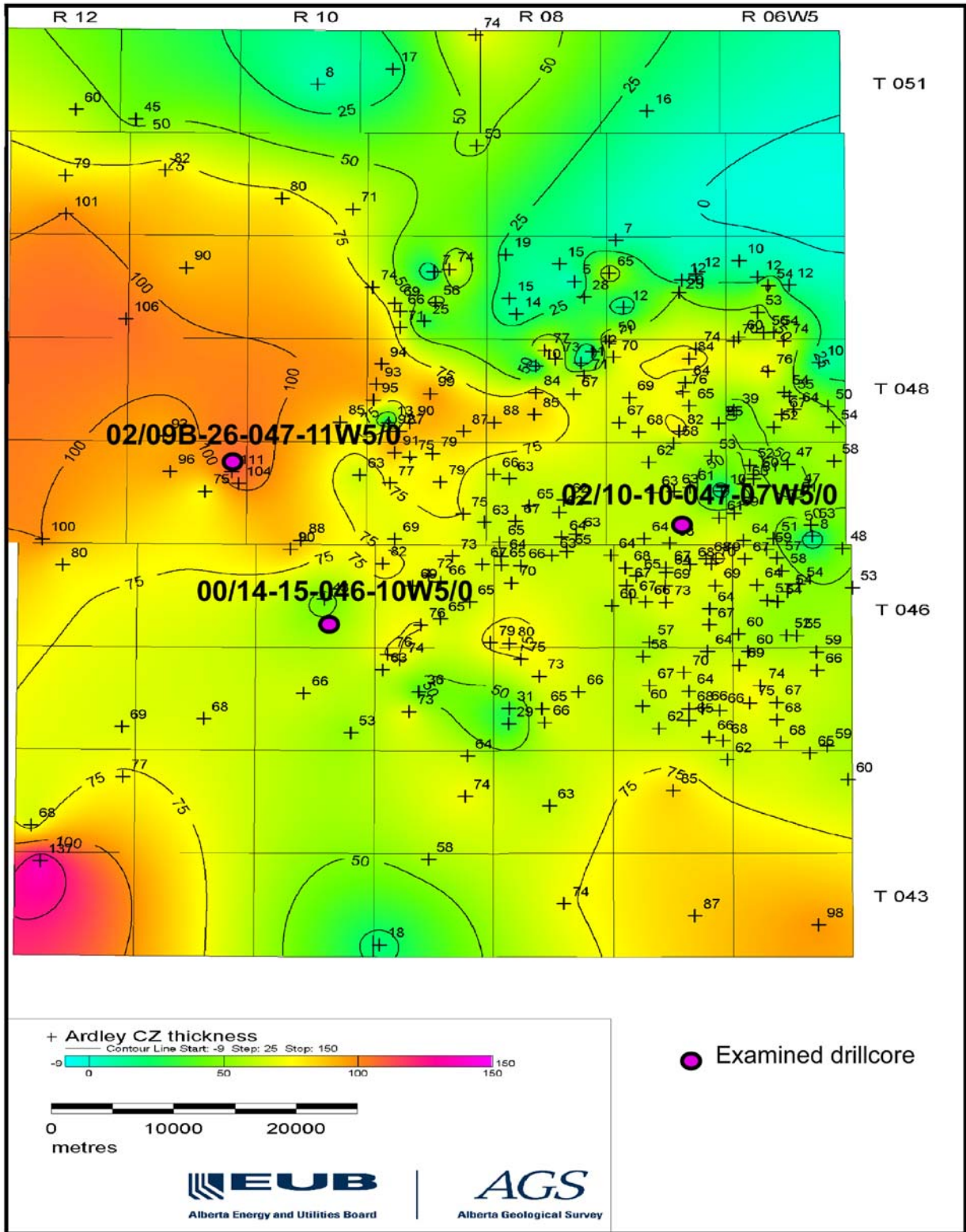


Figure 13. Location of the examined drillcores in the Pembina study area.

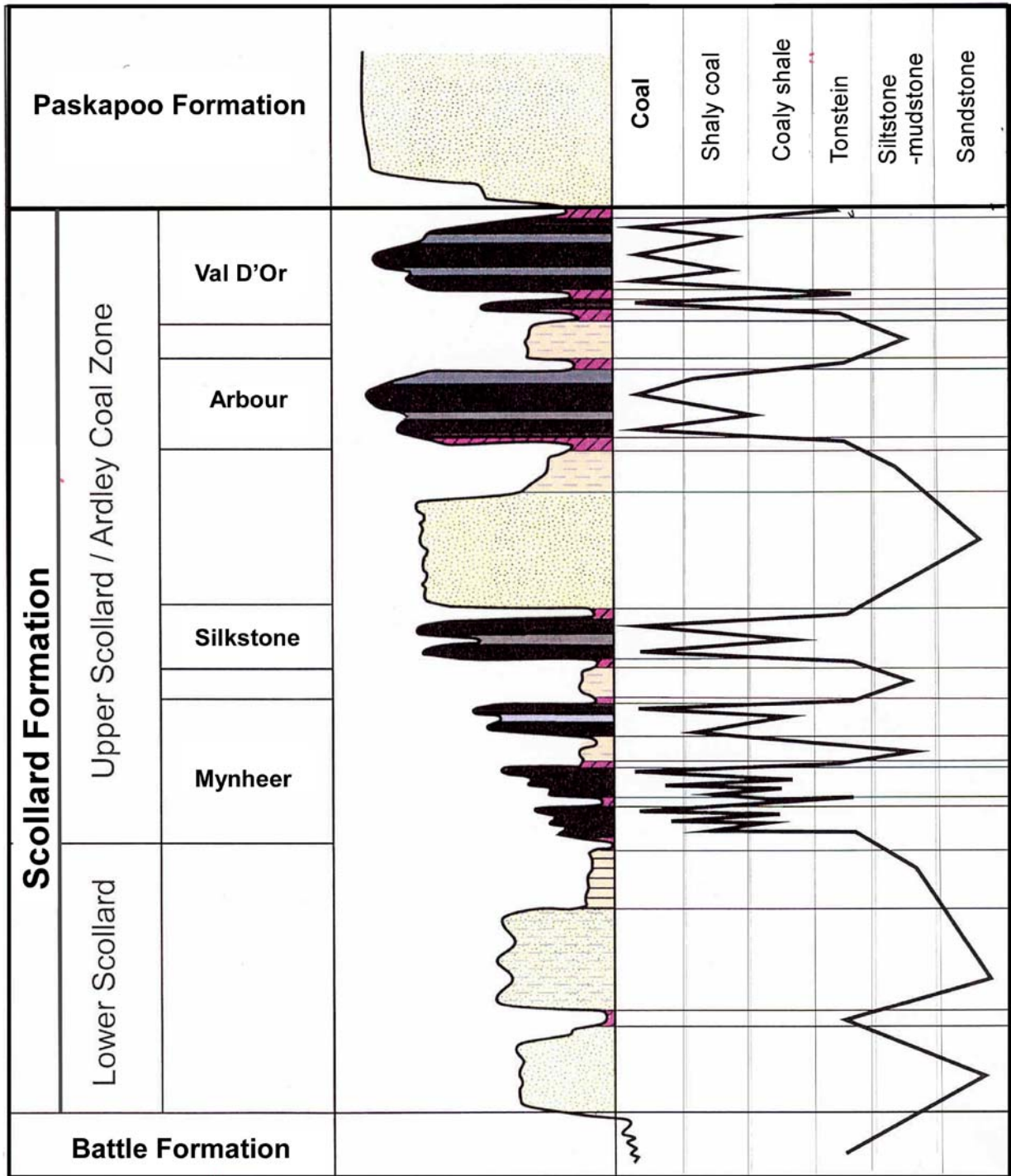


Figure 14. Vertical lithological profile of the Ardley Coal Zone in the Pembina study area.

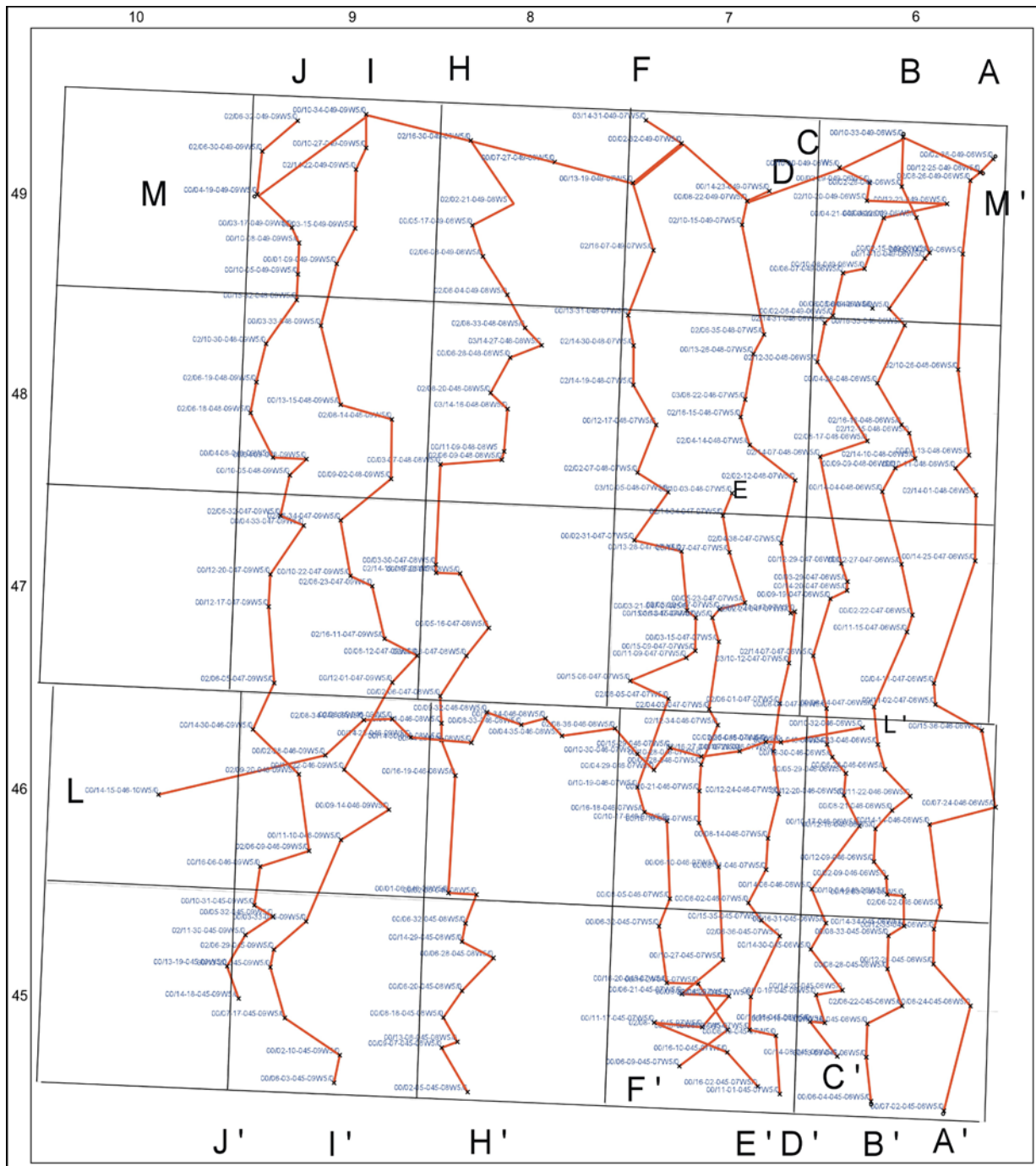
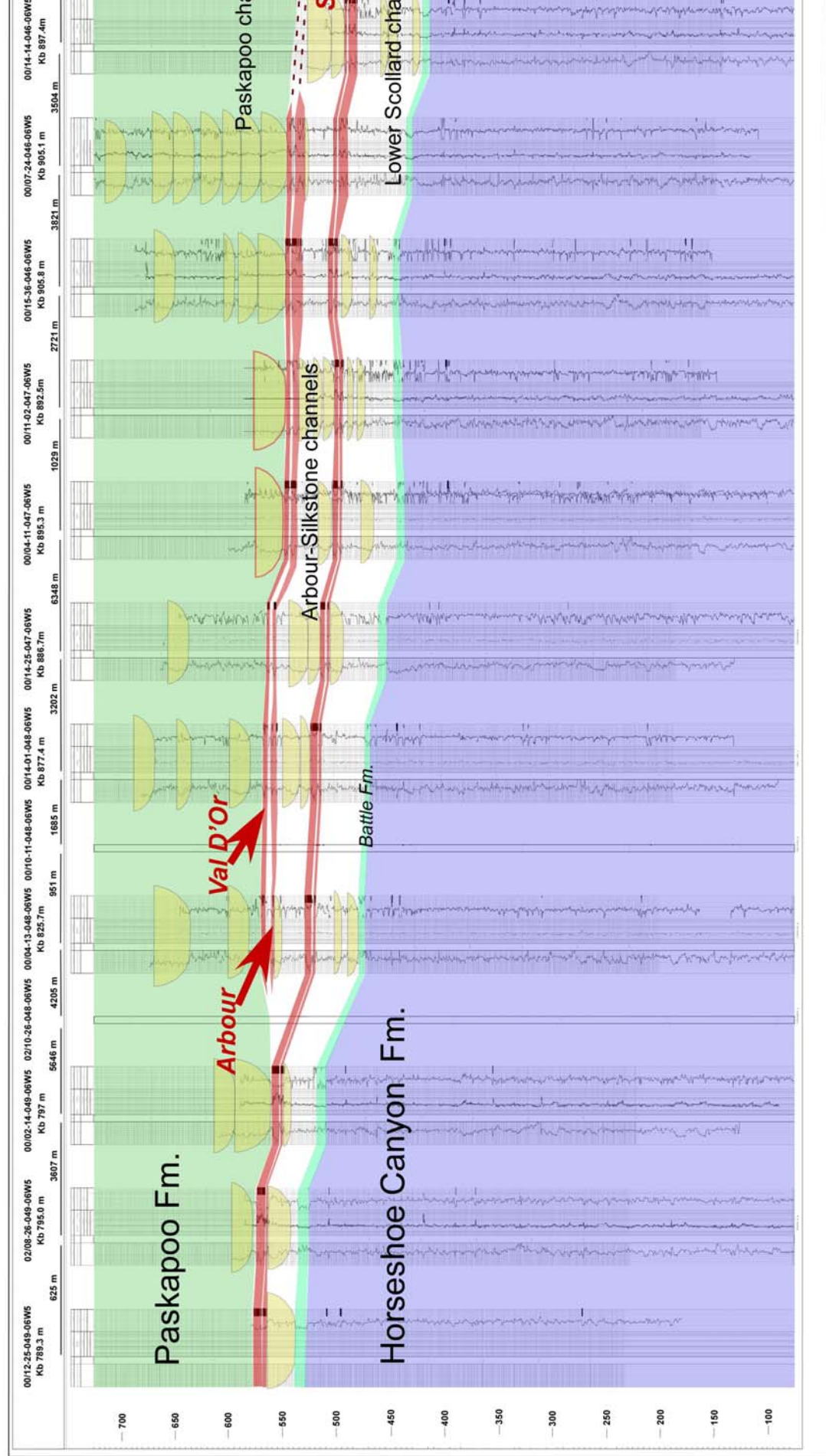


Figure 15. Locations of structural cross-sections, Pembina study area.

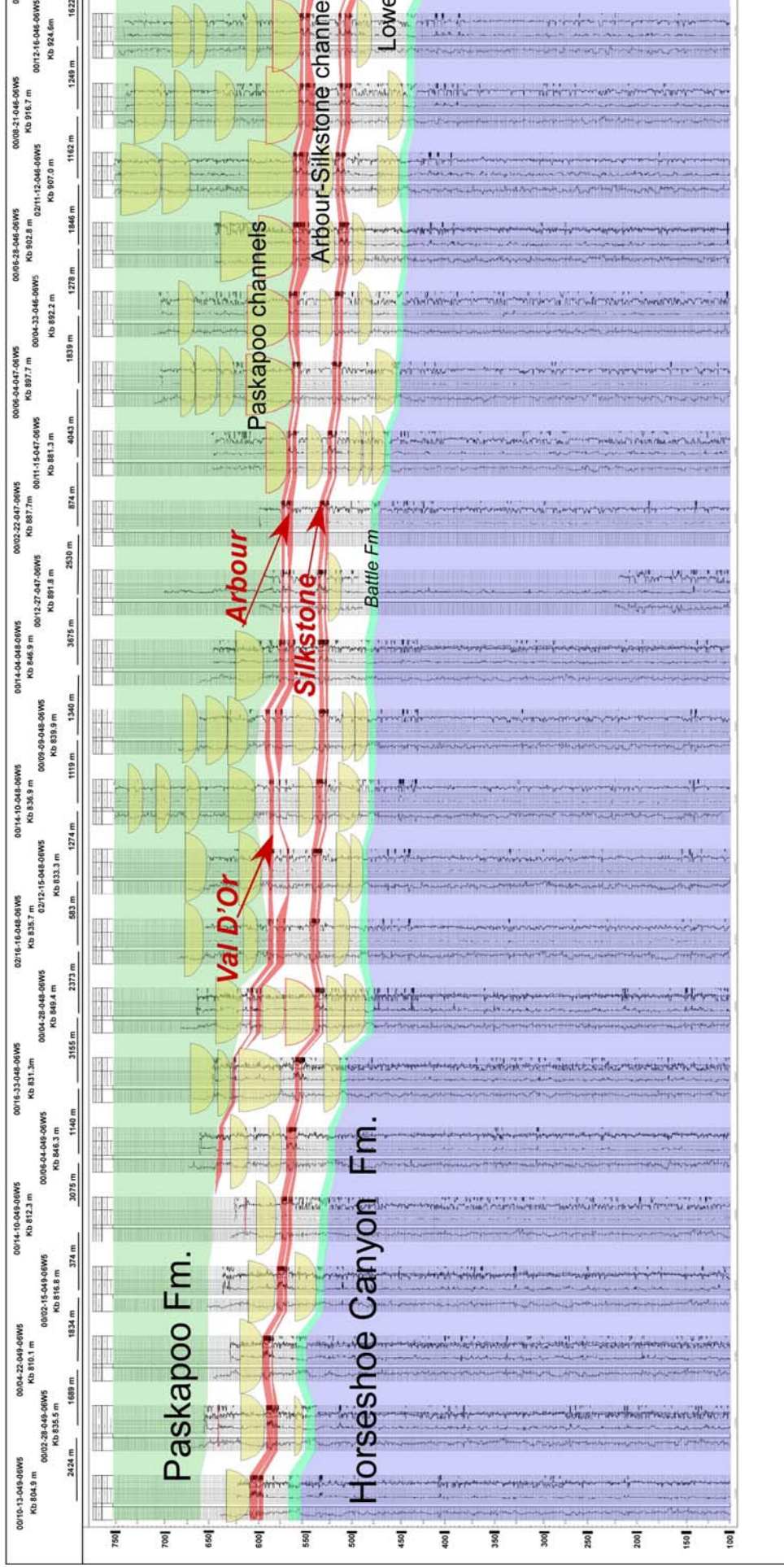
A-A' STRUCTURAL CROSS-SECTION

N



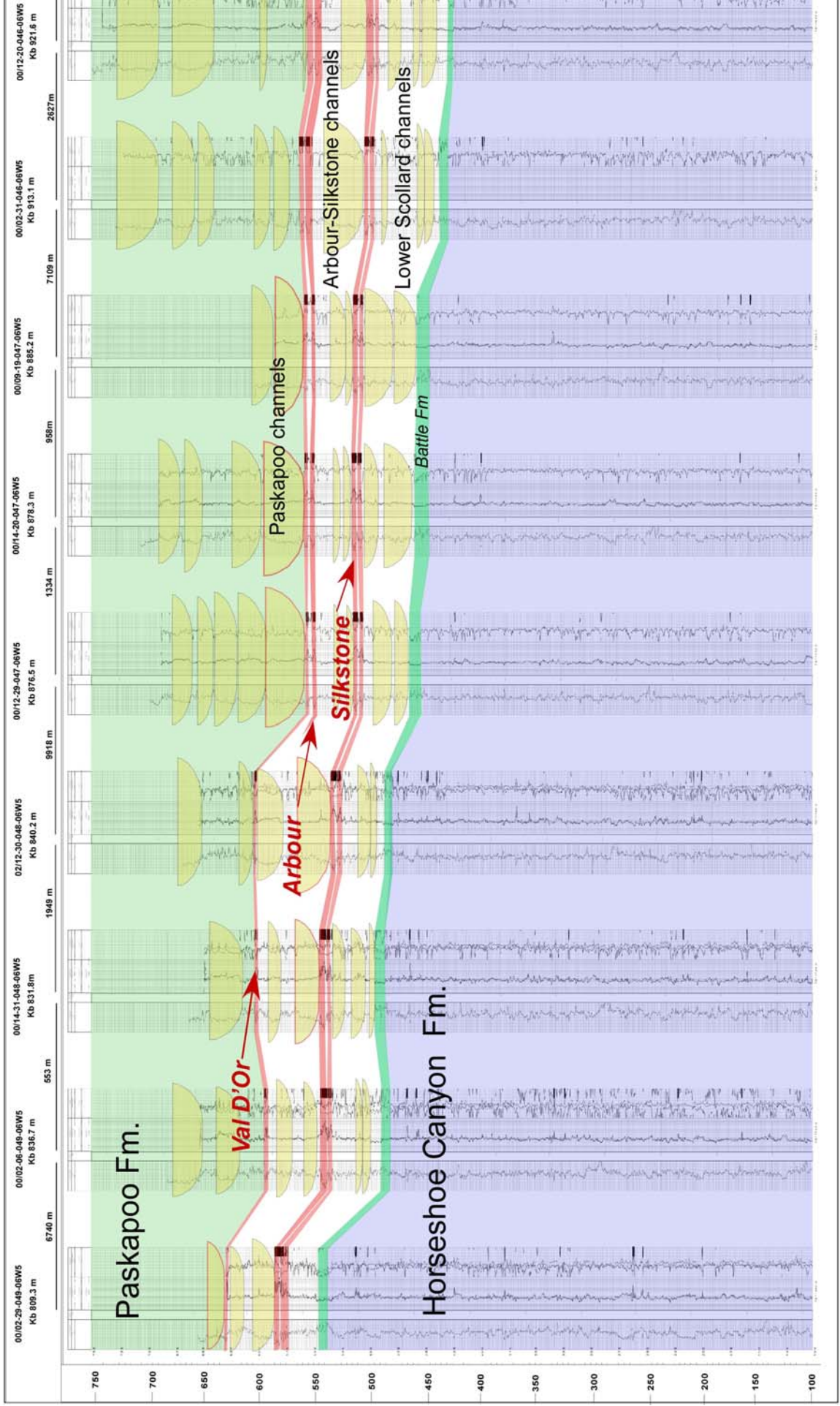
B-B' STRUCTURAL CROSS-SECTION

N



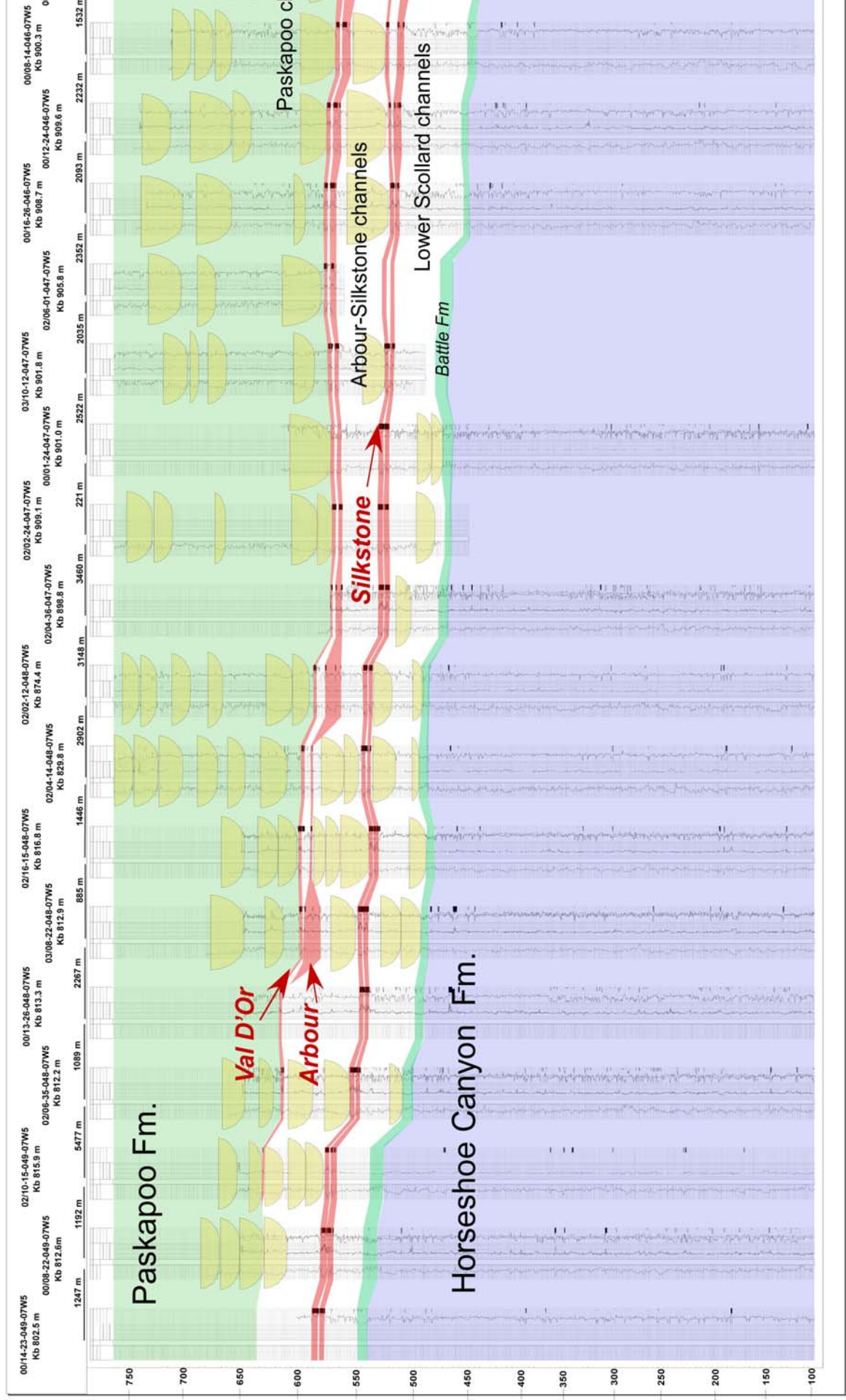
C-C' STRUCTURAL CROSS-SECTION

N



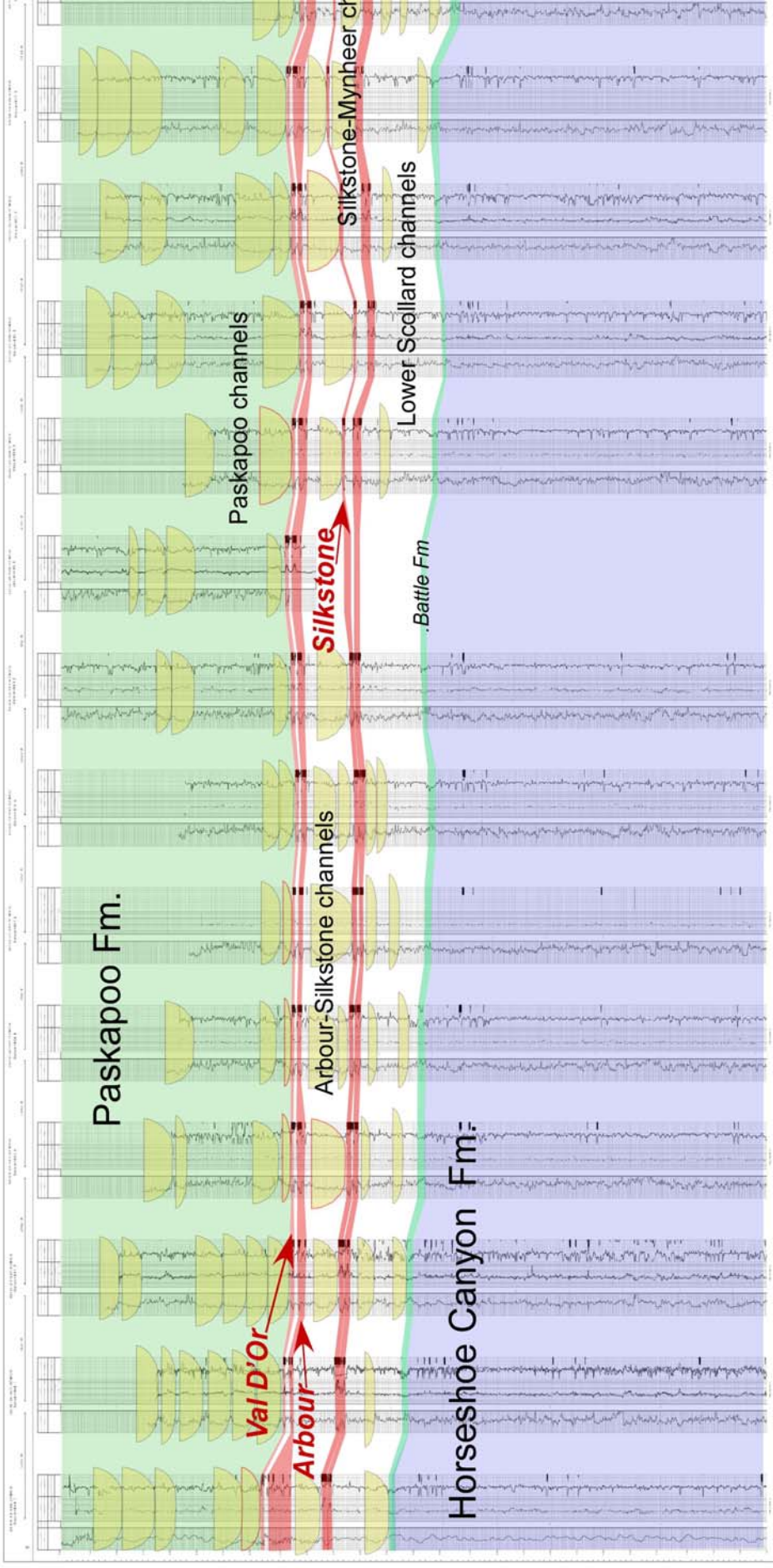
D-D' STRUCTURAL CROSS-SECTION

N



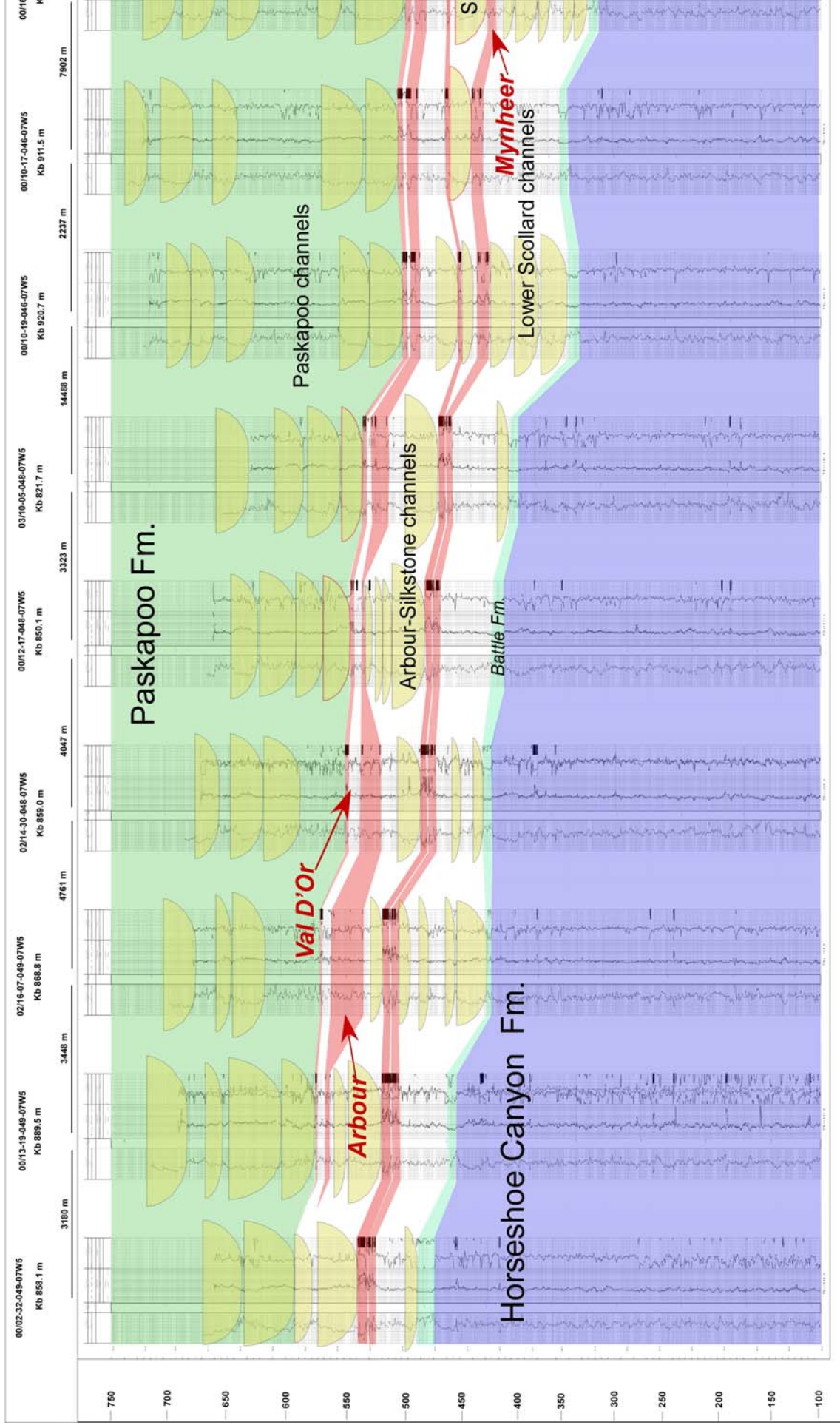
E-E' STRUCTURAL CROSS-SECTION

N

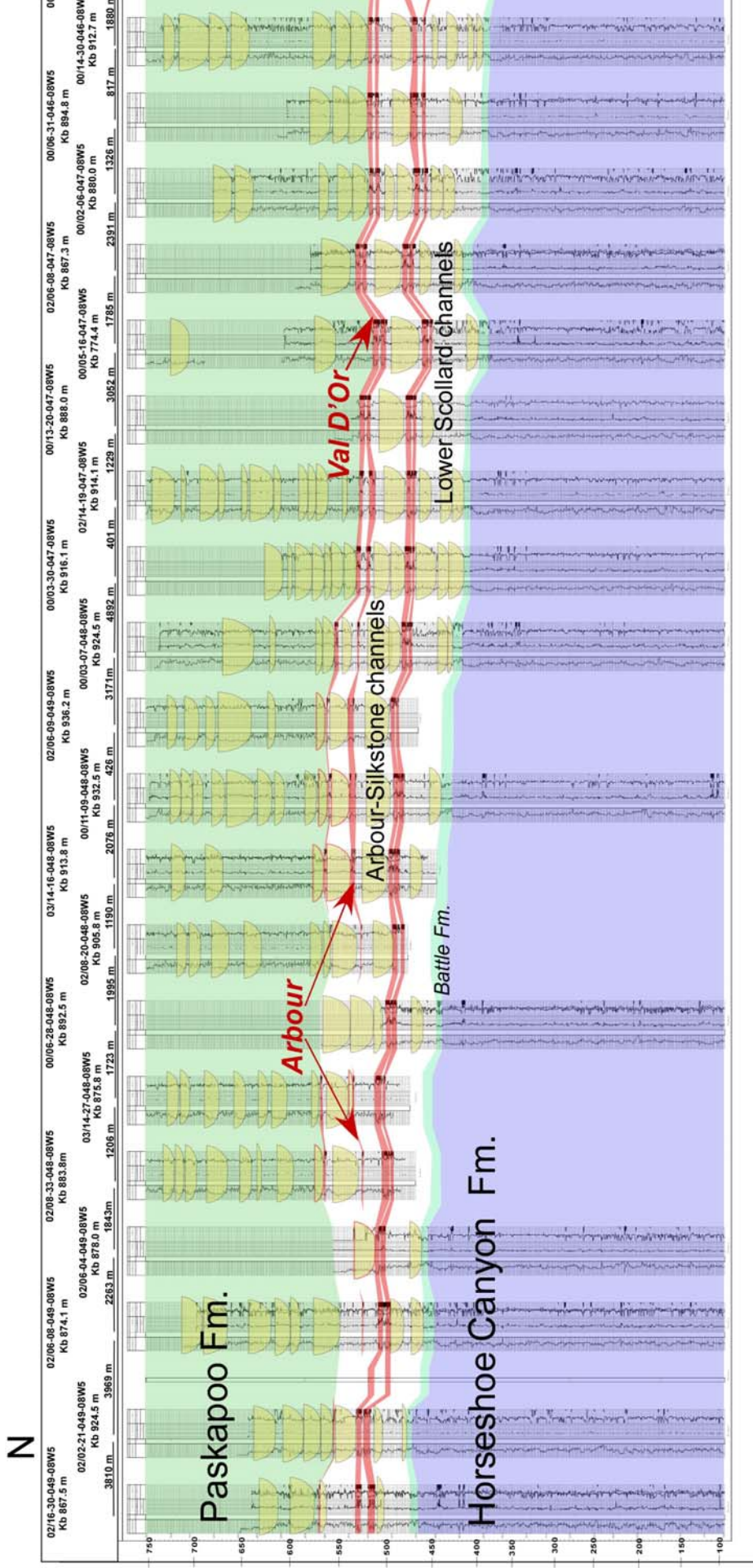


F-F' STRUCTURAL CROSS-SECTION

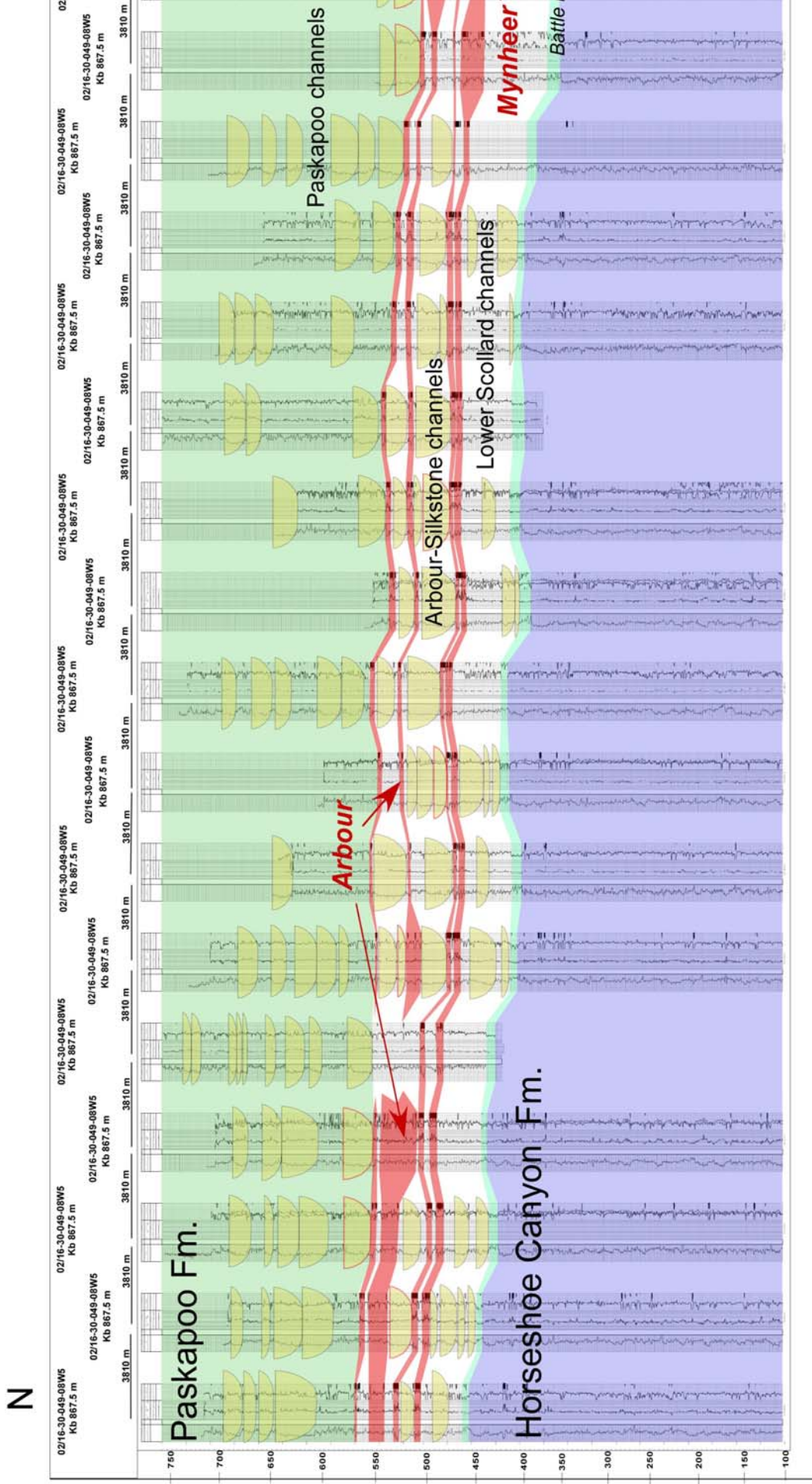
N



H-H' STRUCTURAL CROSS-SECTION

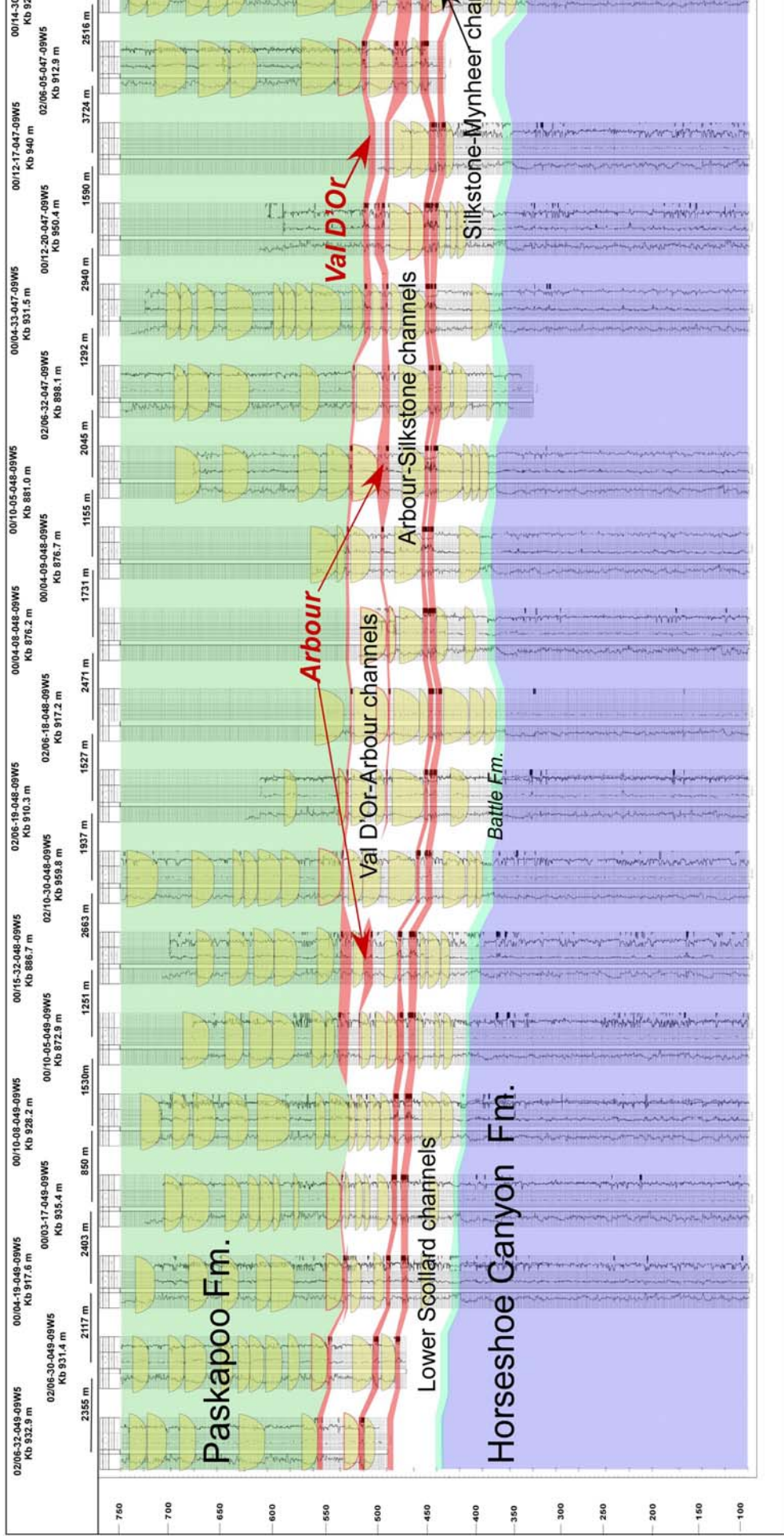


I-I' STRUCTURAL CROSS-SECTION



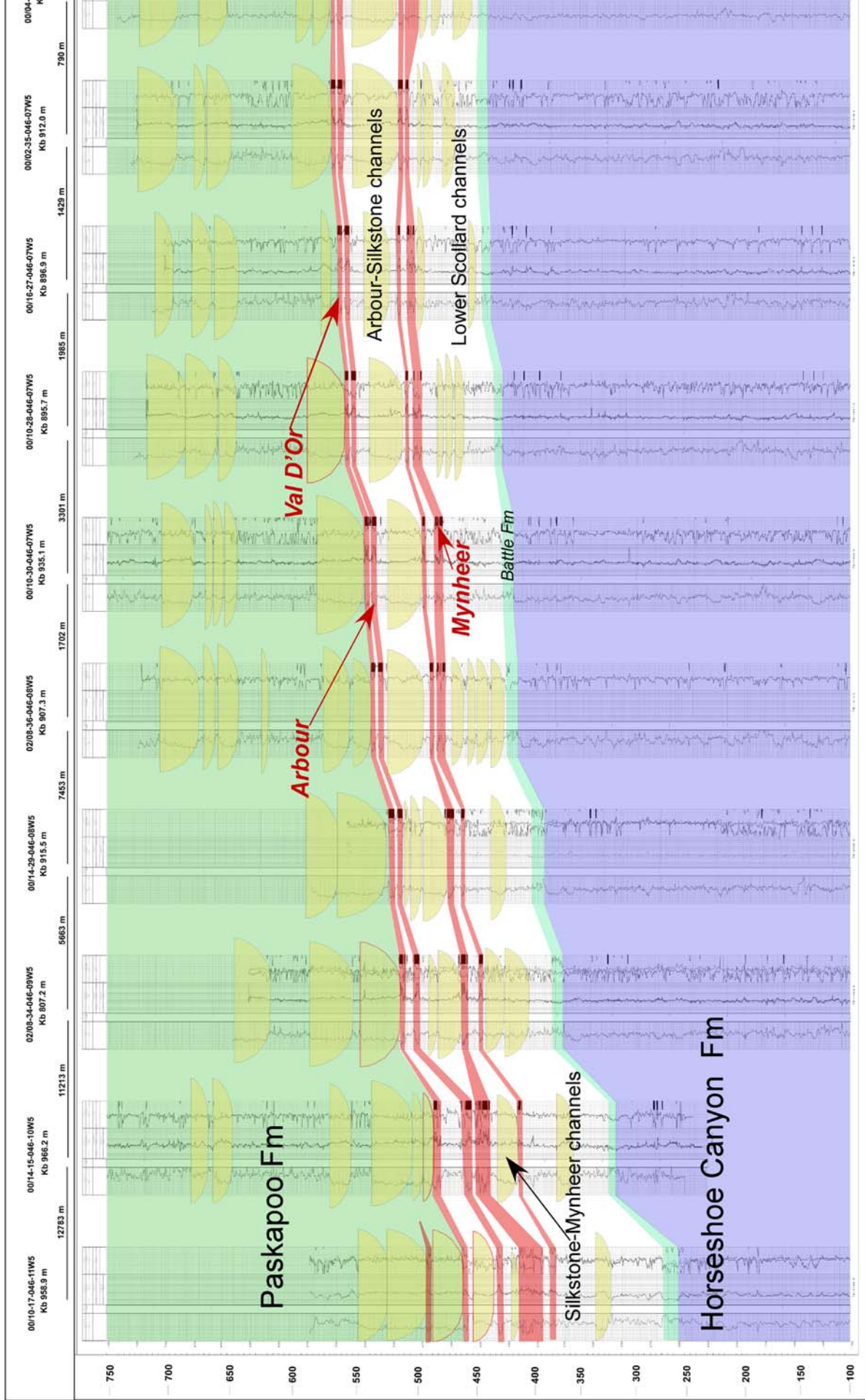
J-J' STRUCTURAL CROSS-SECTION

N



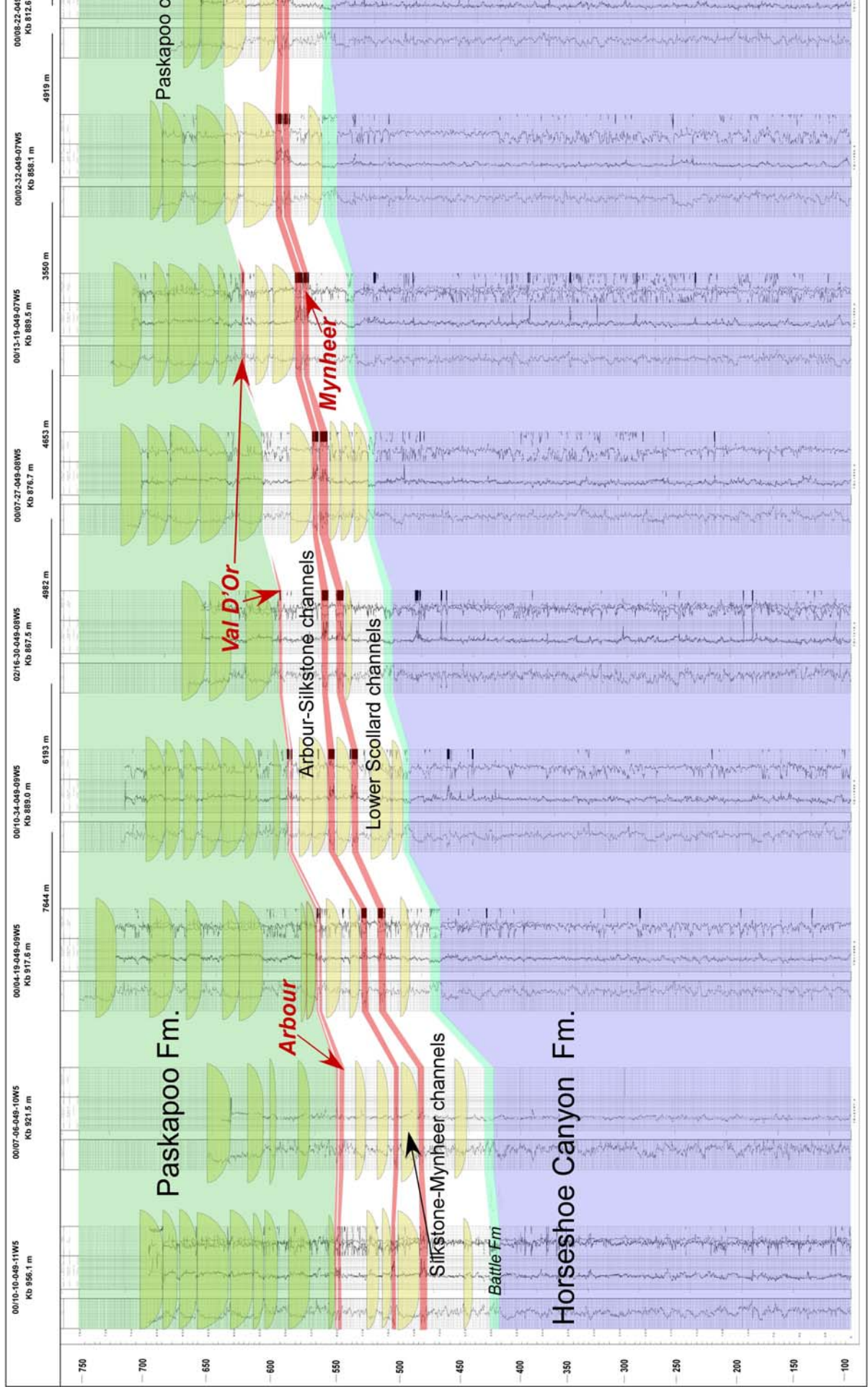
L-L' STRUCTURAL CROSS-SECTION

W



M-M' STRUCTURAL CROSS-SECTION

W



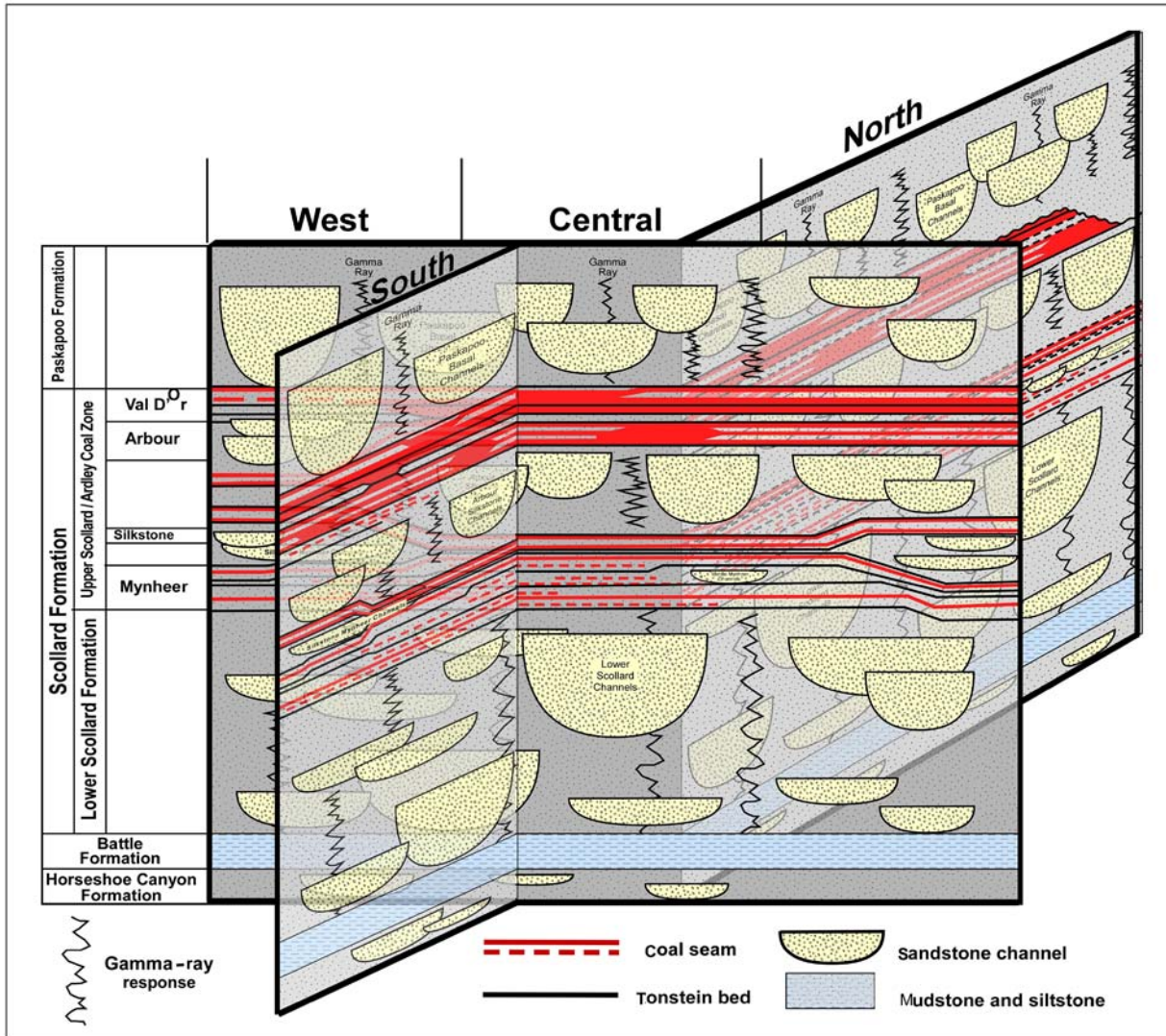


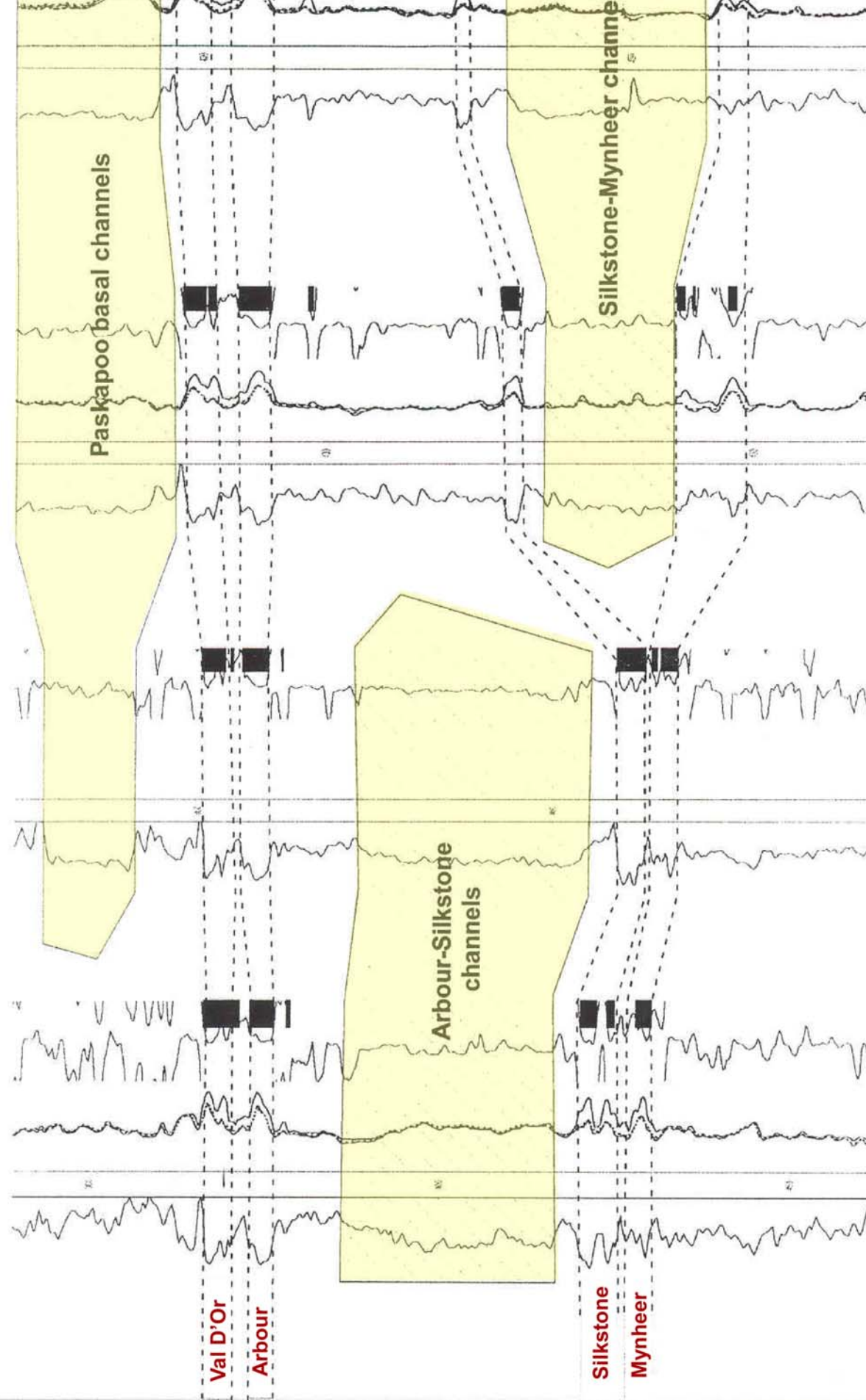
Figure 27. Schematic representation of the distribution of subzones in the Ardley Coal Zone.

12-20-046-06W5

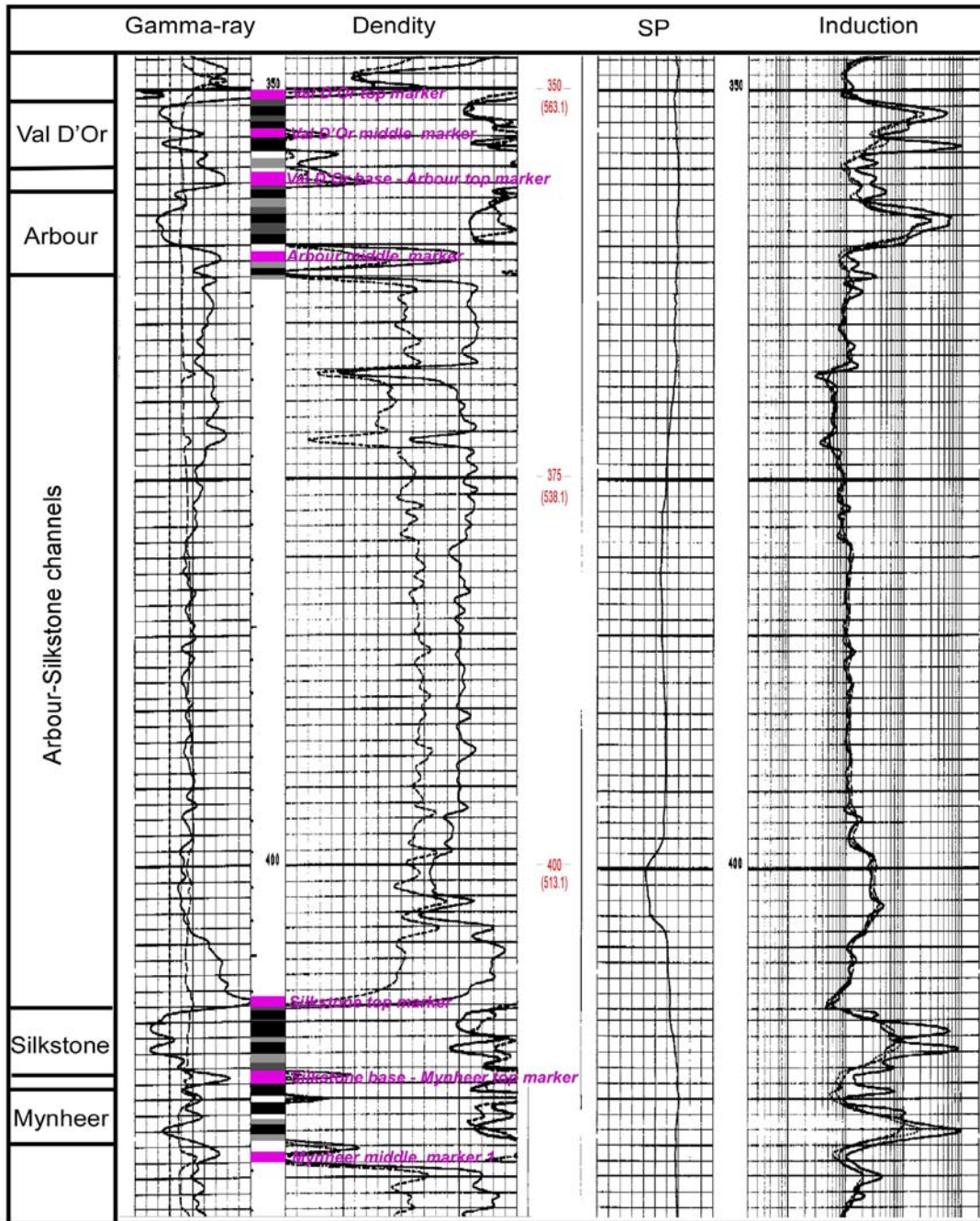
02-31-046-06W5

10-17-046-07W5

16-20-045-



00/02-31-046-06W5
 Tonstein strata and coal sub-zones markers



- Tonstein bed (marker)
- Coaly shale
- Shaly coal
- Coal

Figure 29. Thin tonstein strata recognized on the geophysical log, Pembina study area.

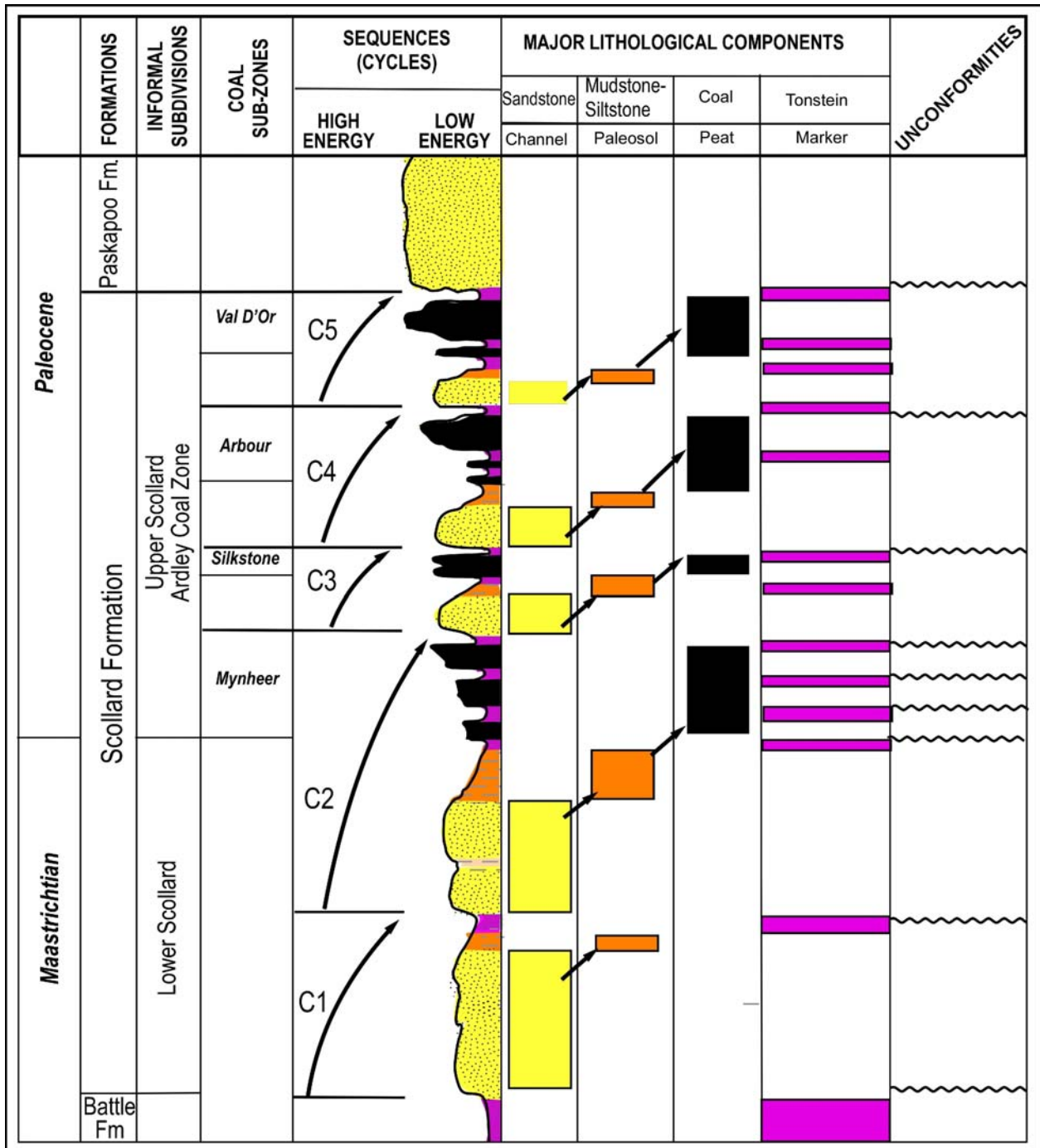


Figure 30. Sequence stratigraphic model, Pembina study area.

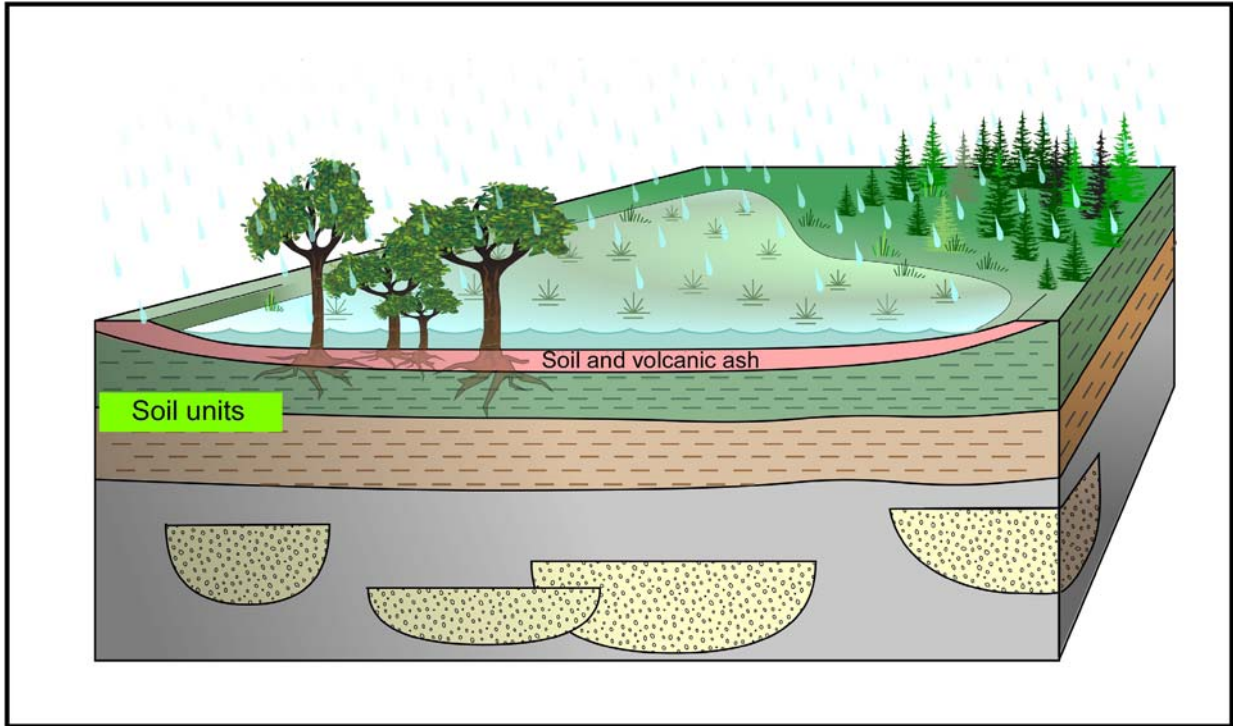


Figure 31. Schematic reconstruction of the peat environment during deposition of the Ardley Coal Zone.

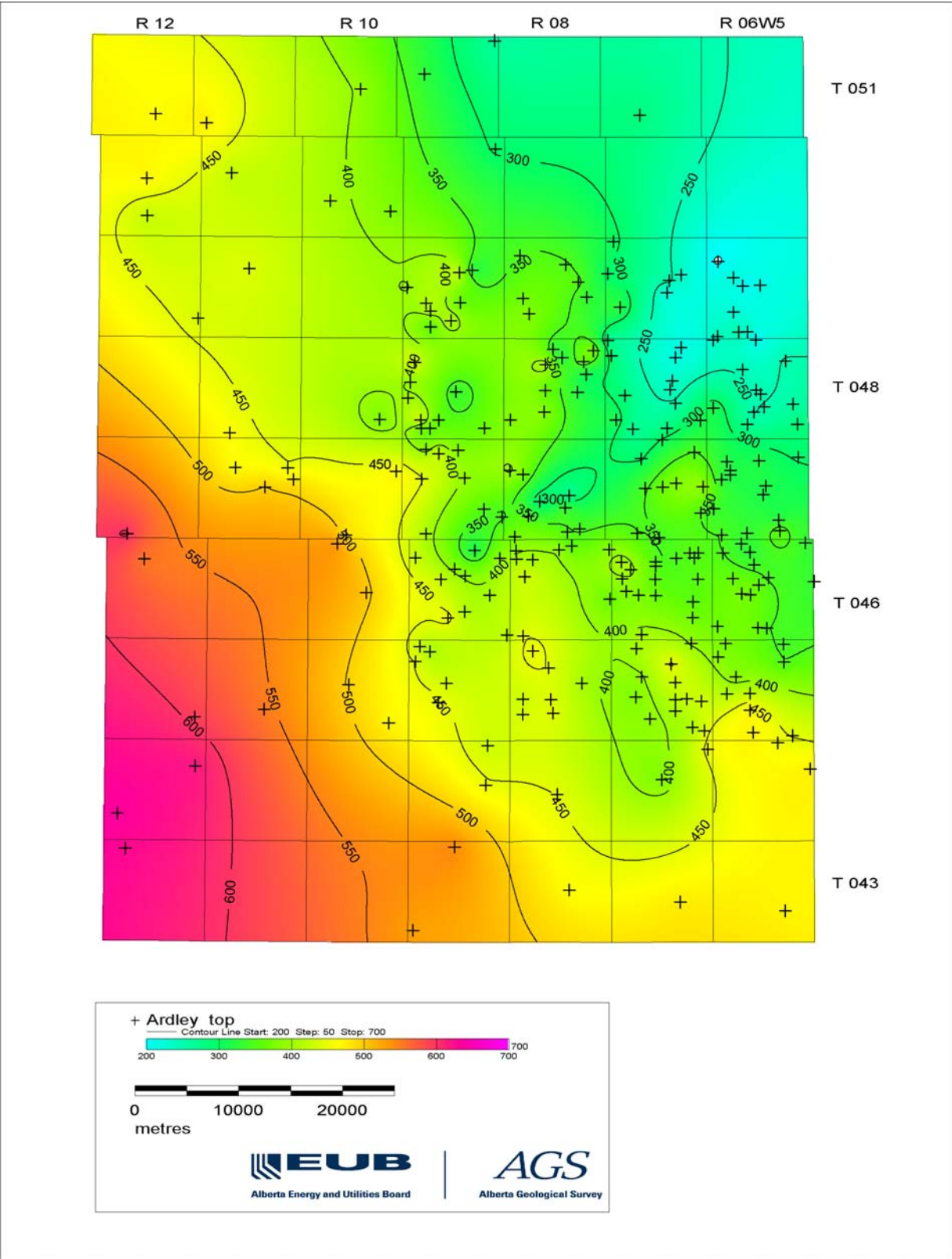


Figure 32. Depth to the top of the Ardley Coal Zone, Pembina study area.

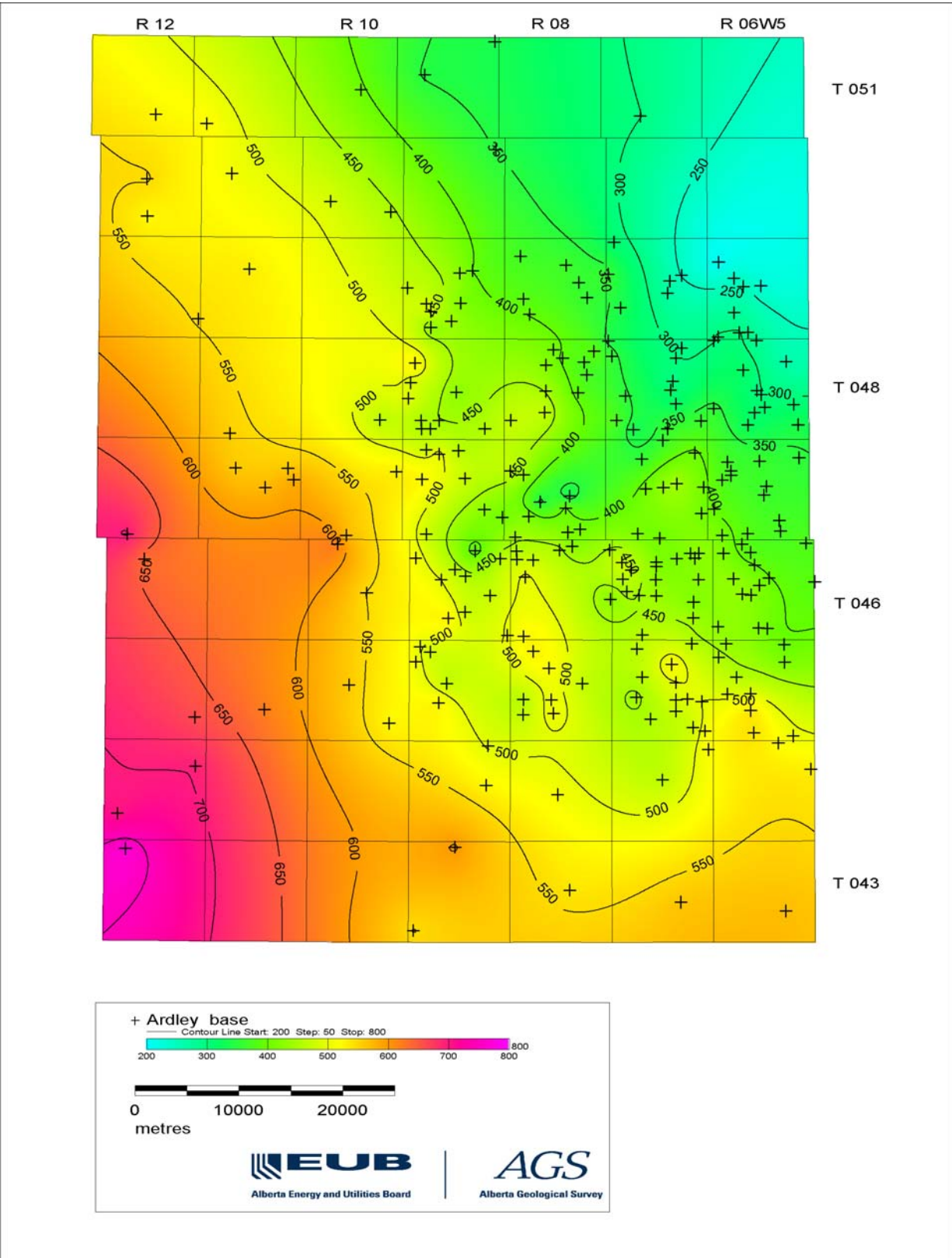


Figure 33. Depth to the base of the Ardley Coal Zone, Pembina study area.

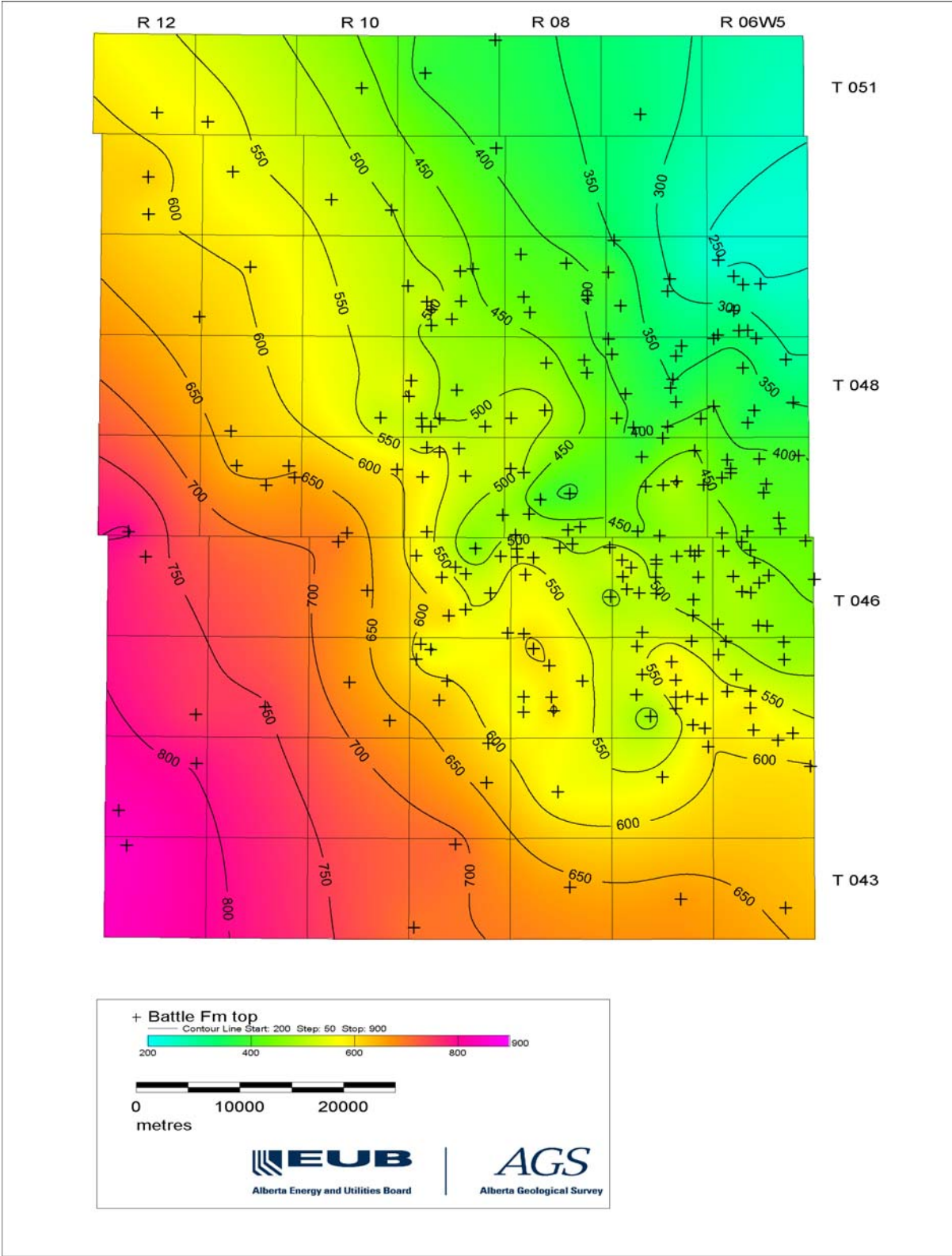


Figure 34. Depth to the base of the lower Scollard Formation, Pembina study area.

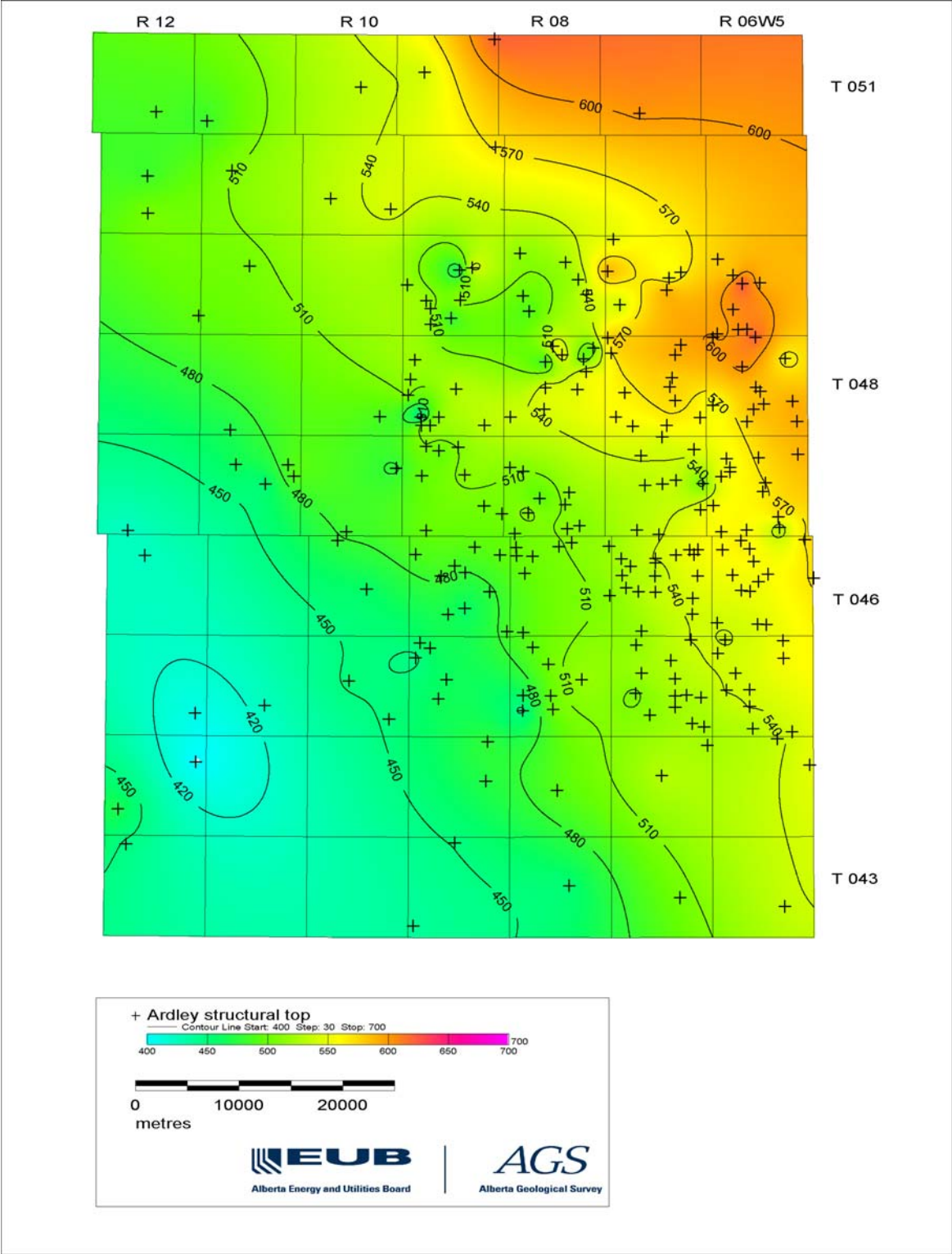


Figure 35. Structure contours on the top of the Ardley Coal Zone, Pembina study area.

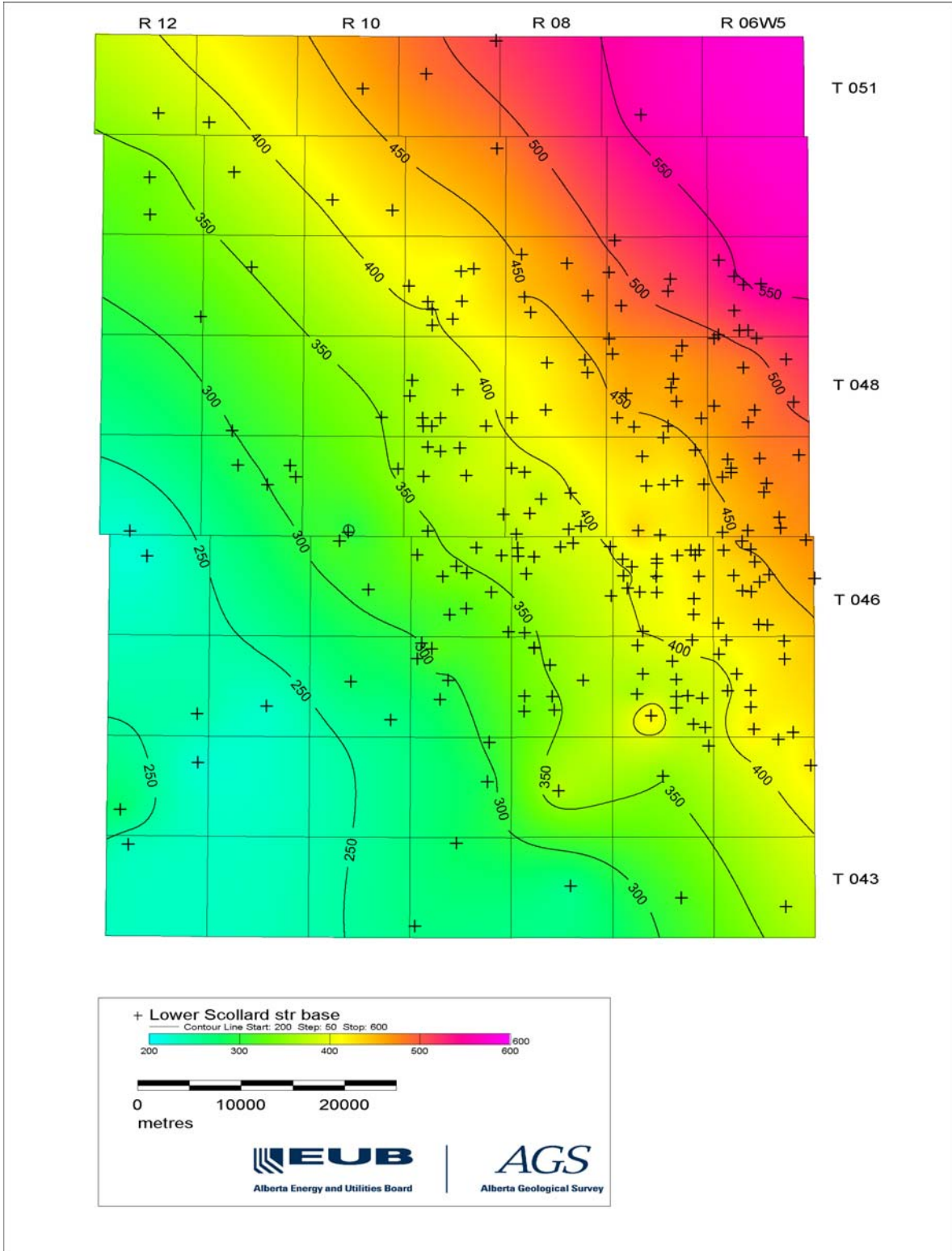


Figure 36. Structure contours on the base of the Ardley Coal Zone, Pembina study area.

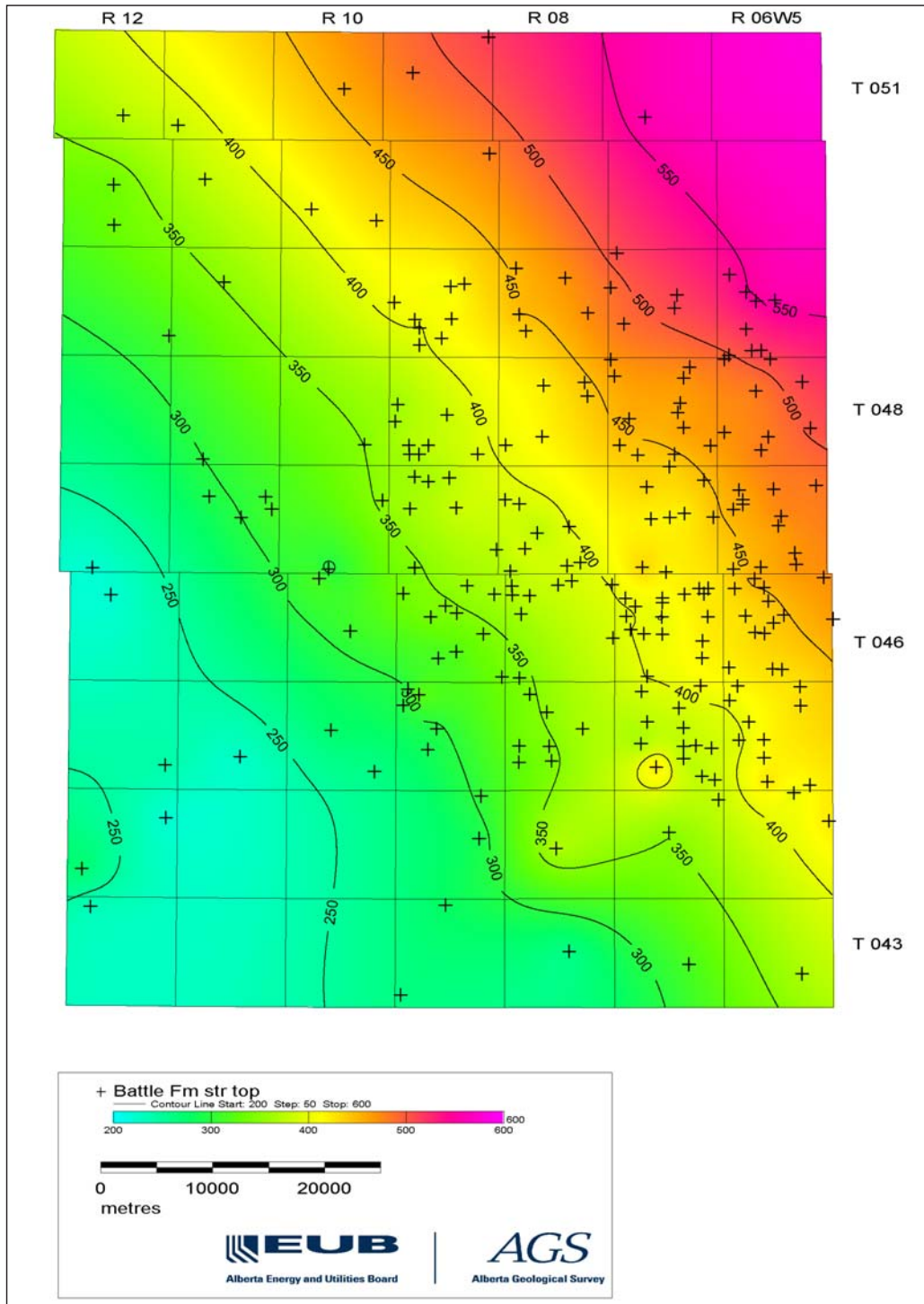


Figure 37. Structure contours on the base of the Lower Scollard Formation, Pembina study area.

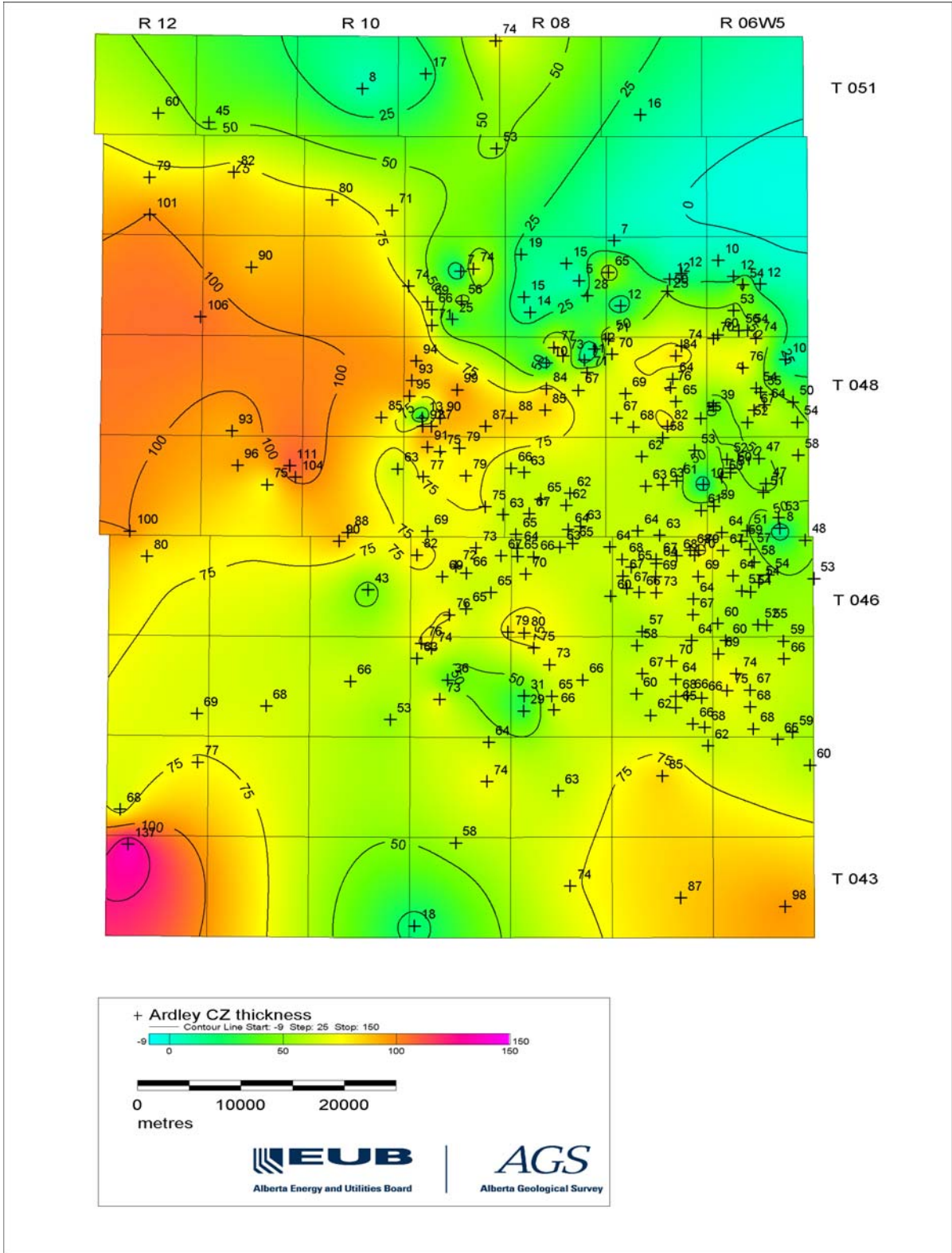


Figure 38. Isopachs of the Ardley Coal Zone, Pembina study area.

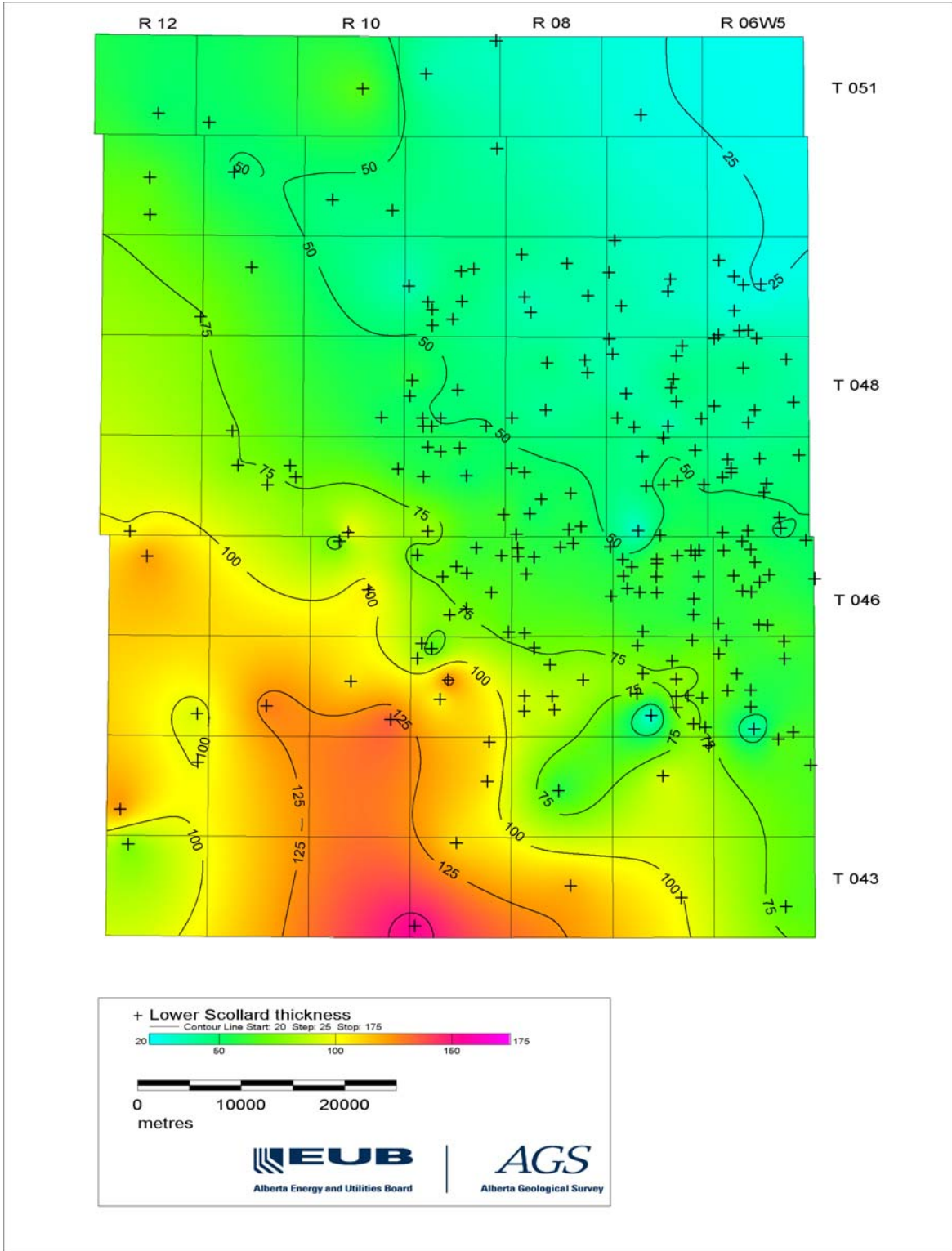


Figure 39. Isopachs of the lower Scollard Formation, Pembina study area.

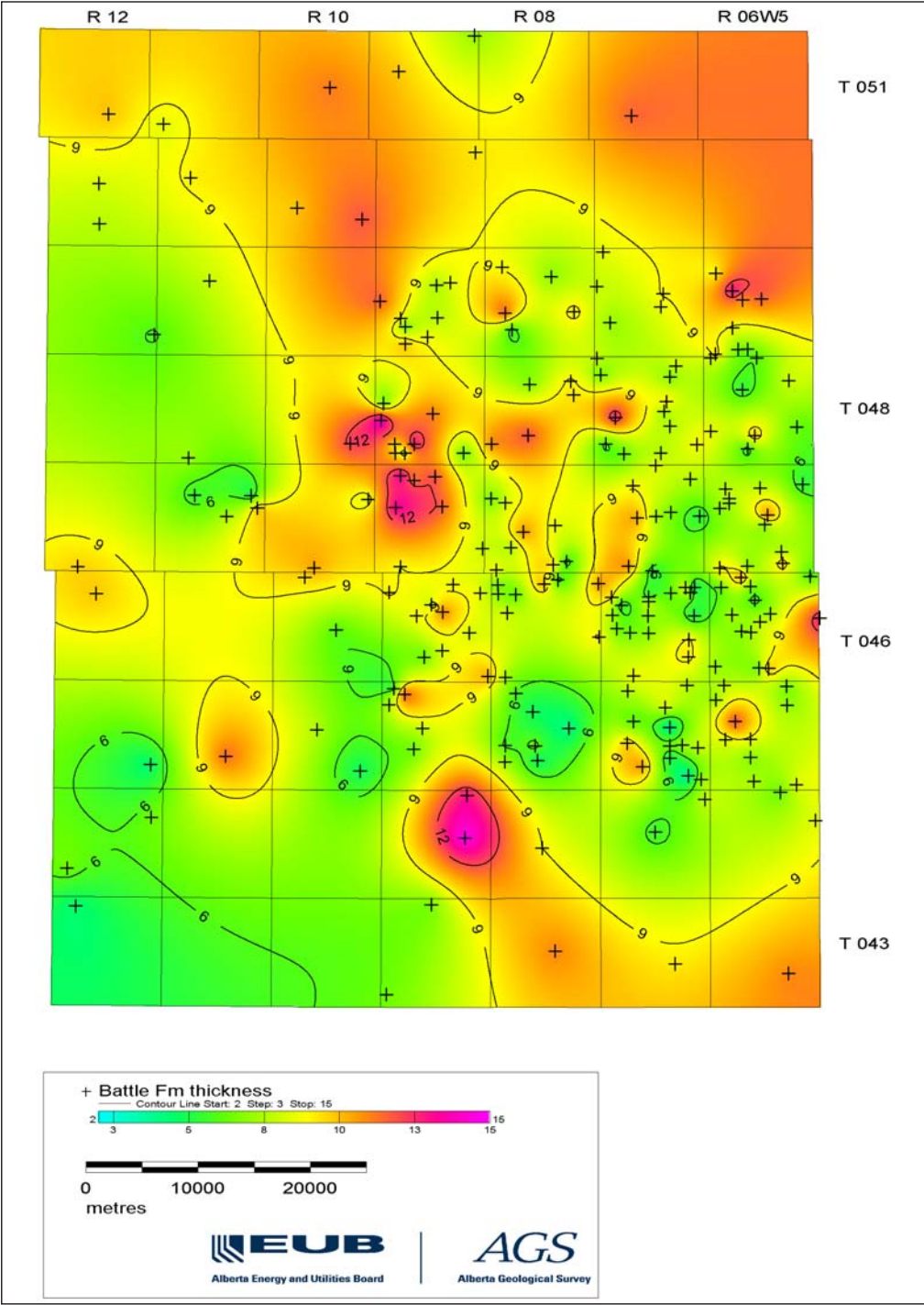


Figure 40. Isopachs of the Battle Formation, Pembina study area.

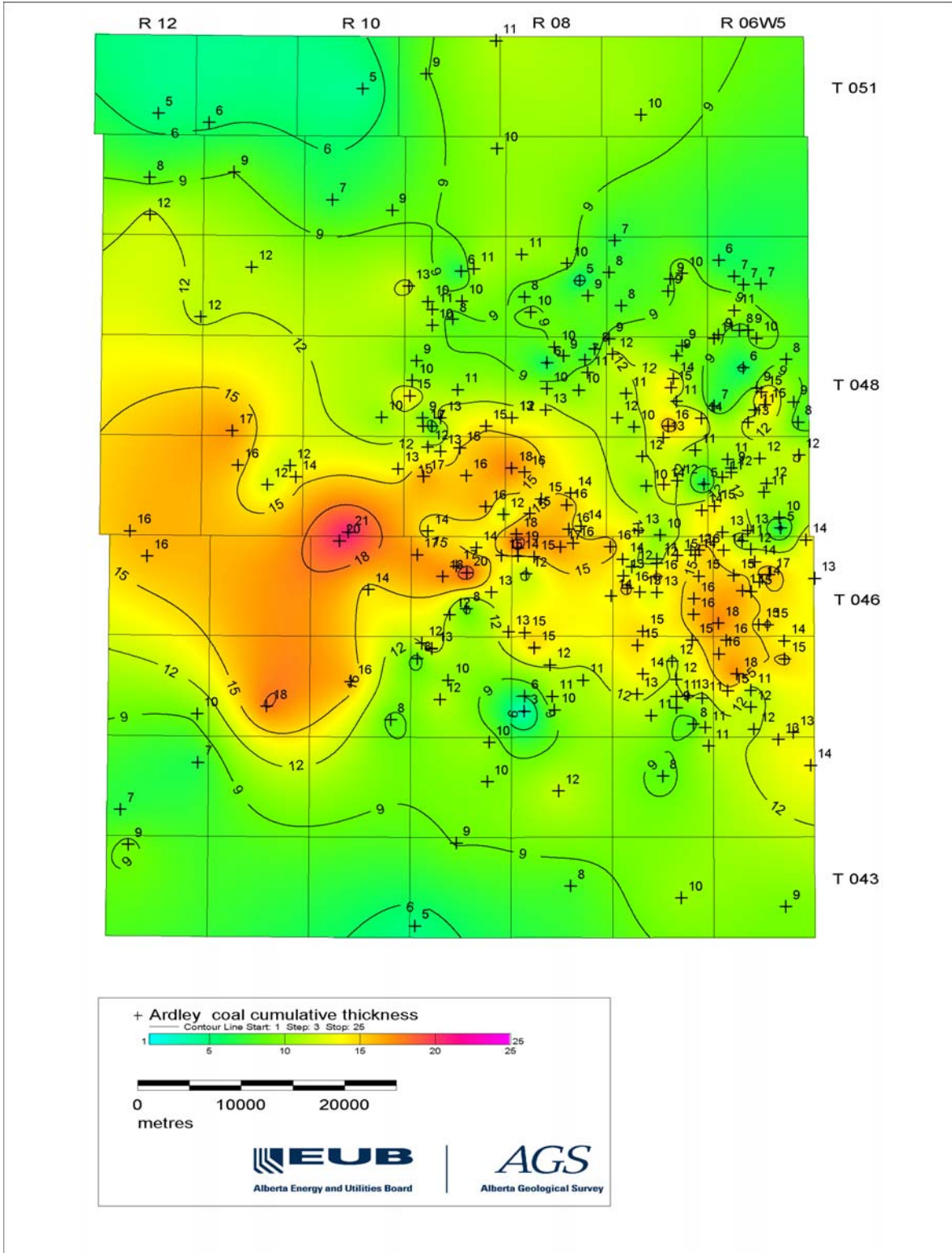


Figure 41. Isopachs of Ardley cumulative coal, Pembina study area.

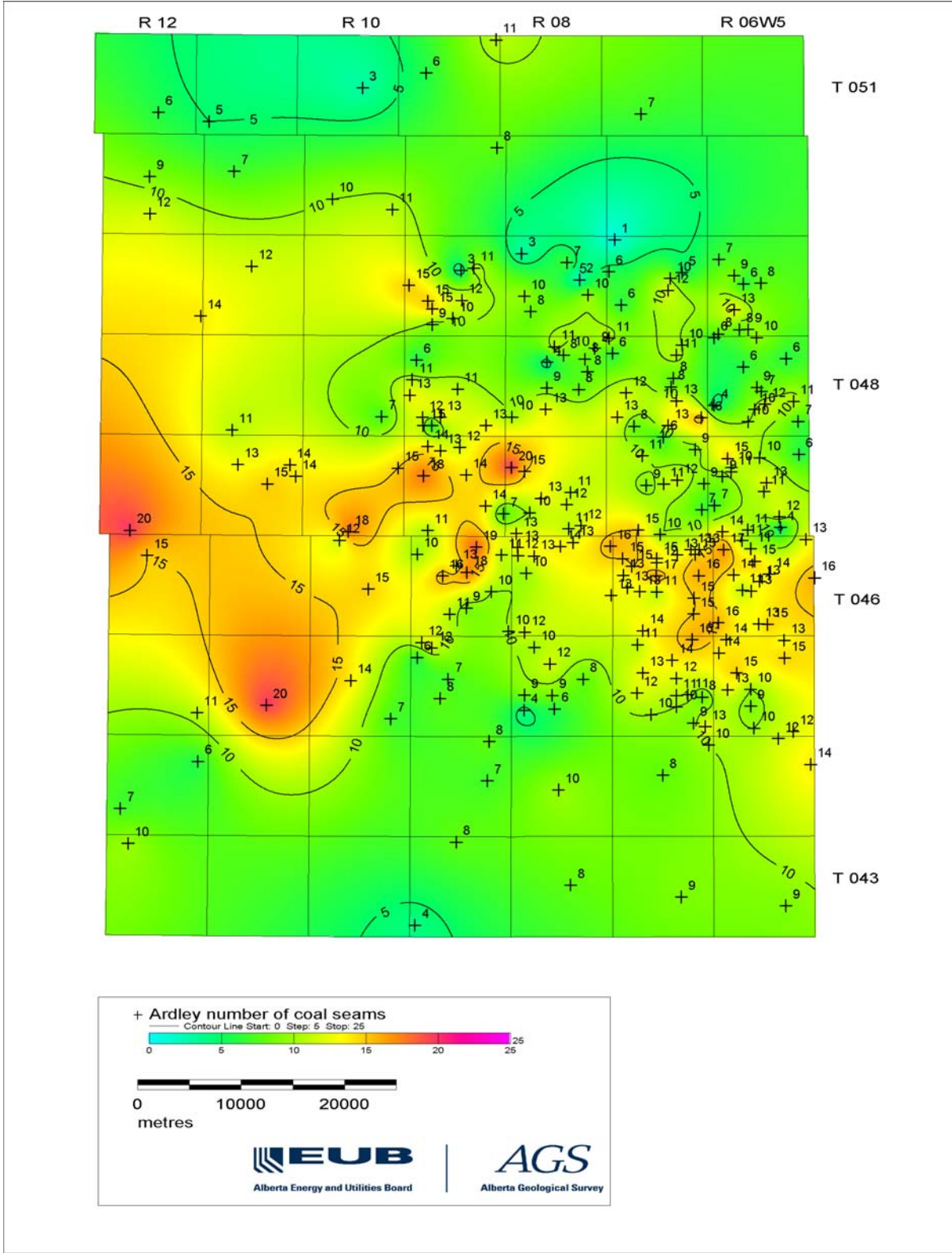


Figure 42. Number of Ardley coal seams, Pembina study area.

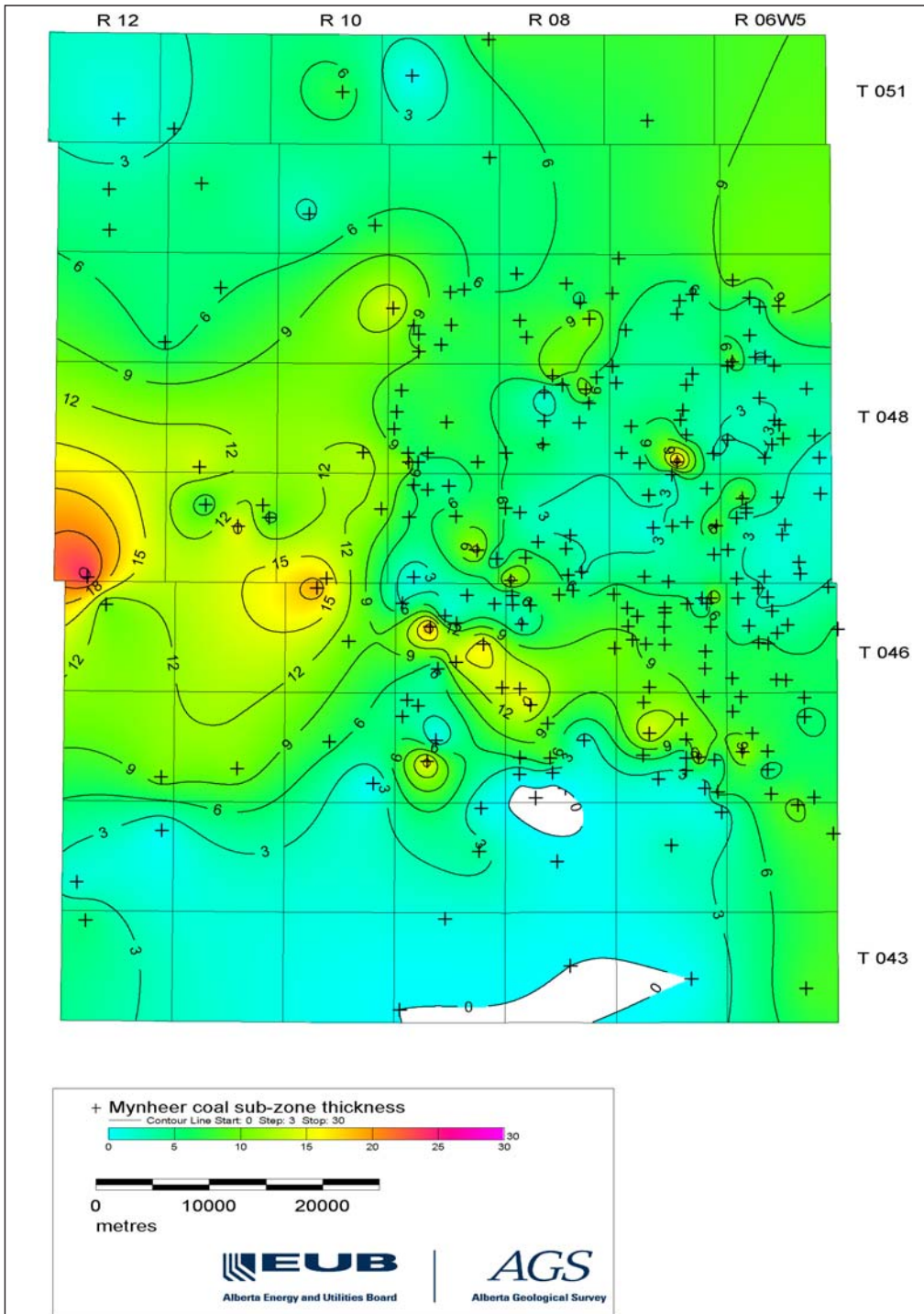


Figure 43. Isopachs of the Mynheer coal subzone, Pembina study area.

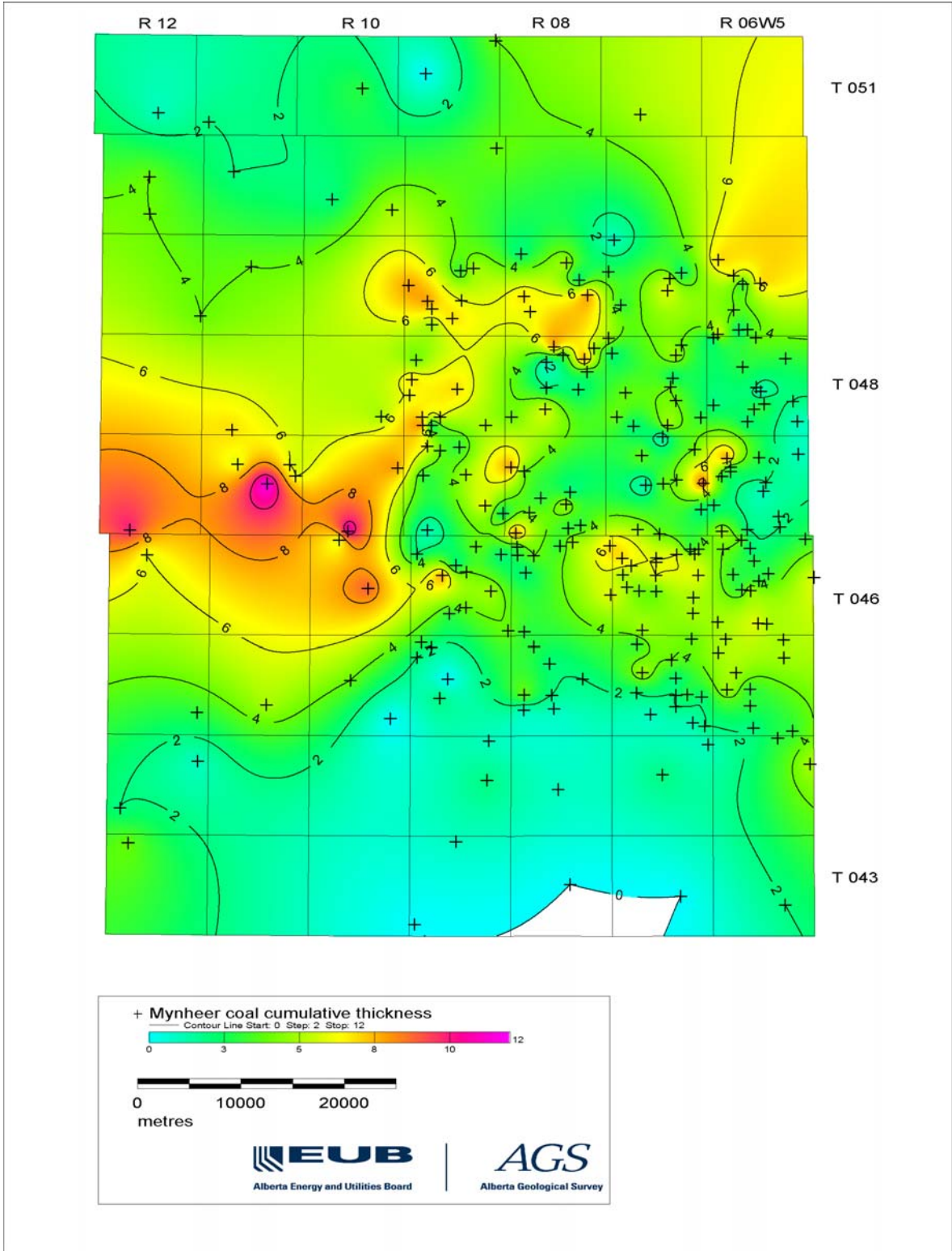


Figure 44. Isopachs of Mynheer cumulative coal, Pembina study area.

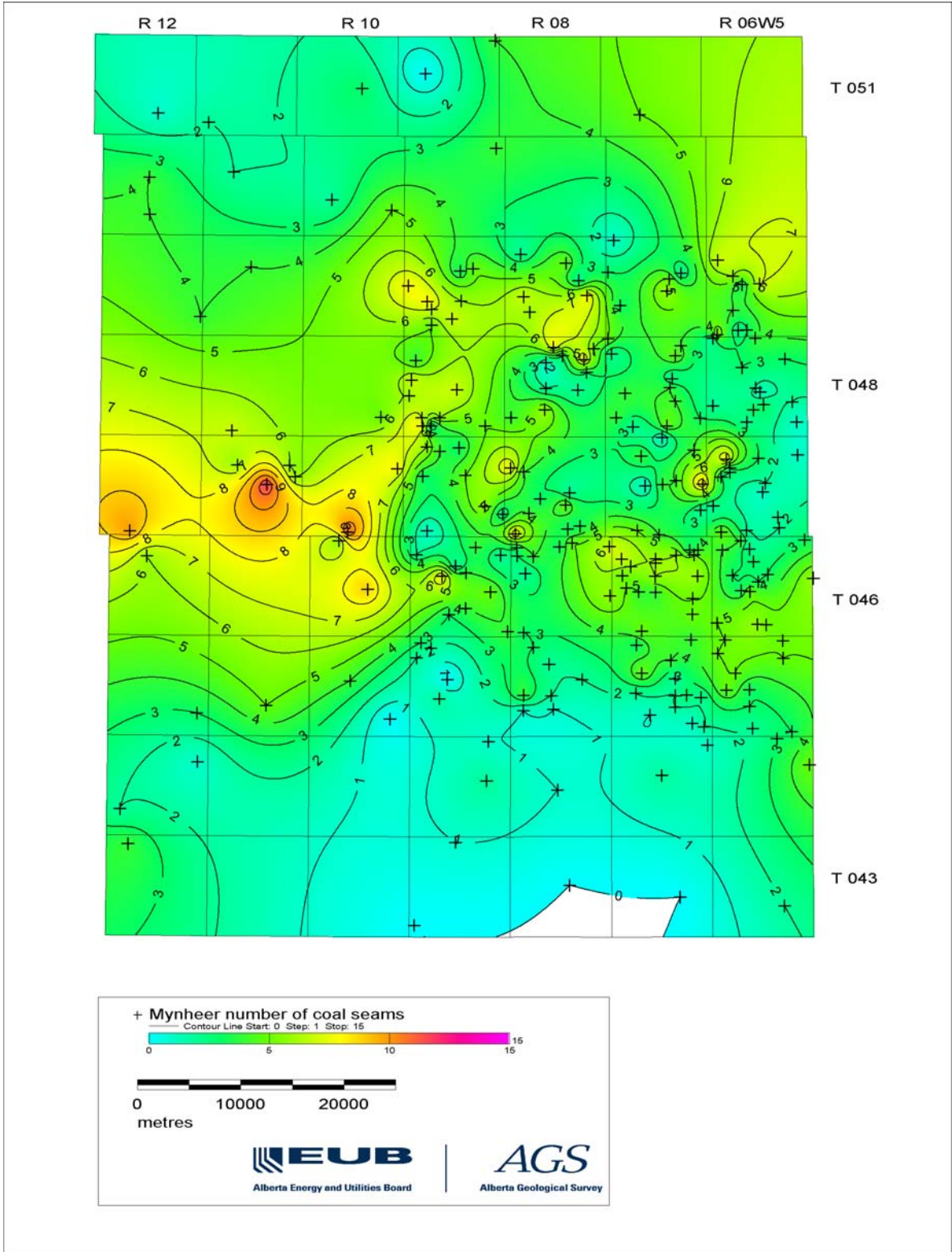


Figure 45. Number of Mynheer coal seams, Pembina study area.

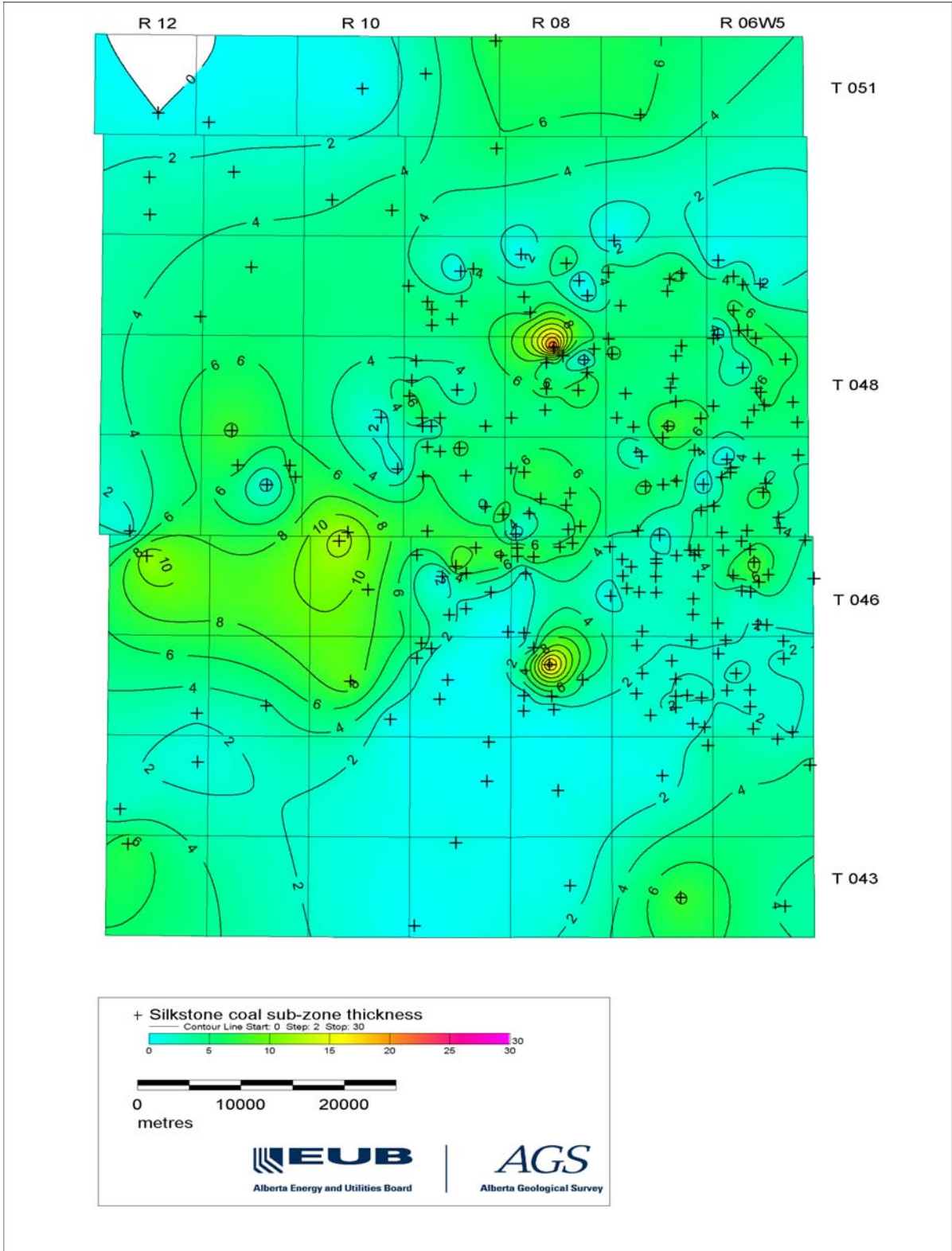


Figure 46. Isopachs of the Silkstone coal subzone, Pembina study area.

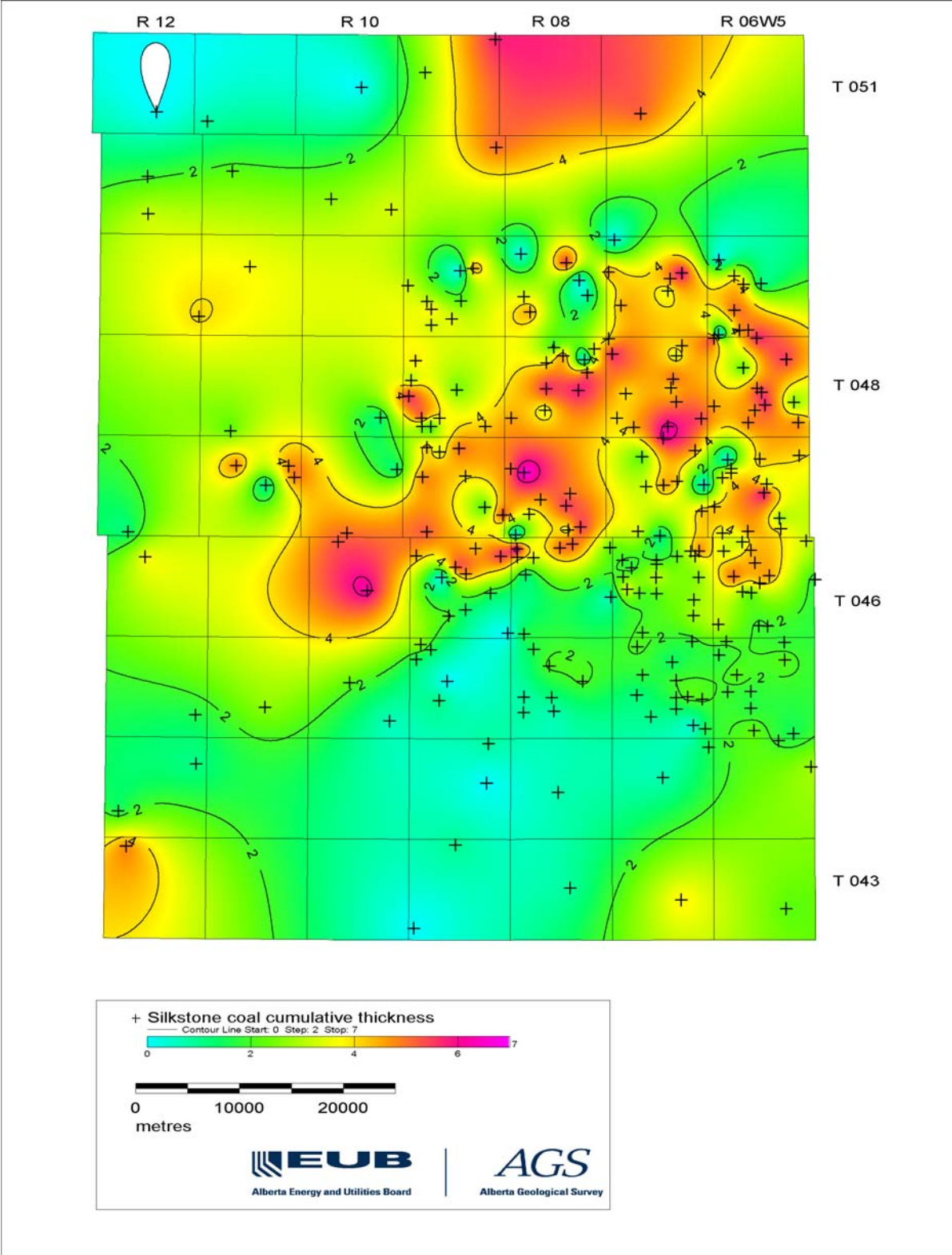


Figure 47. Isopachs of Silkstone cumulative coal, Pembina study area.

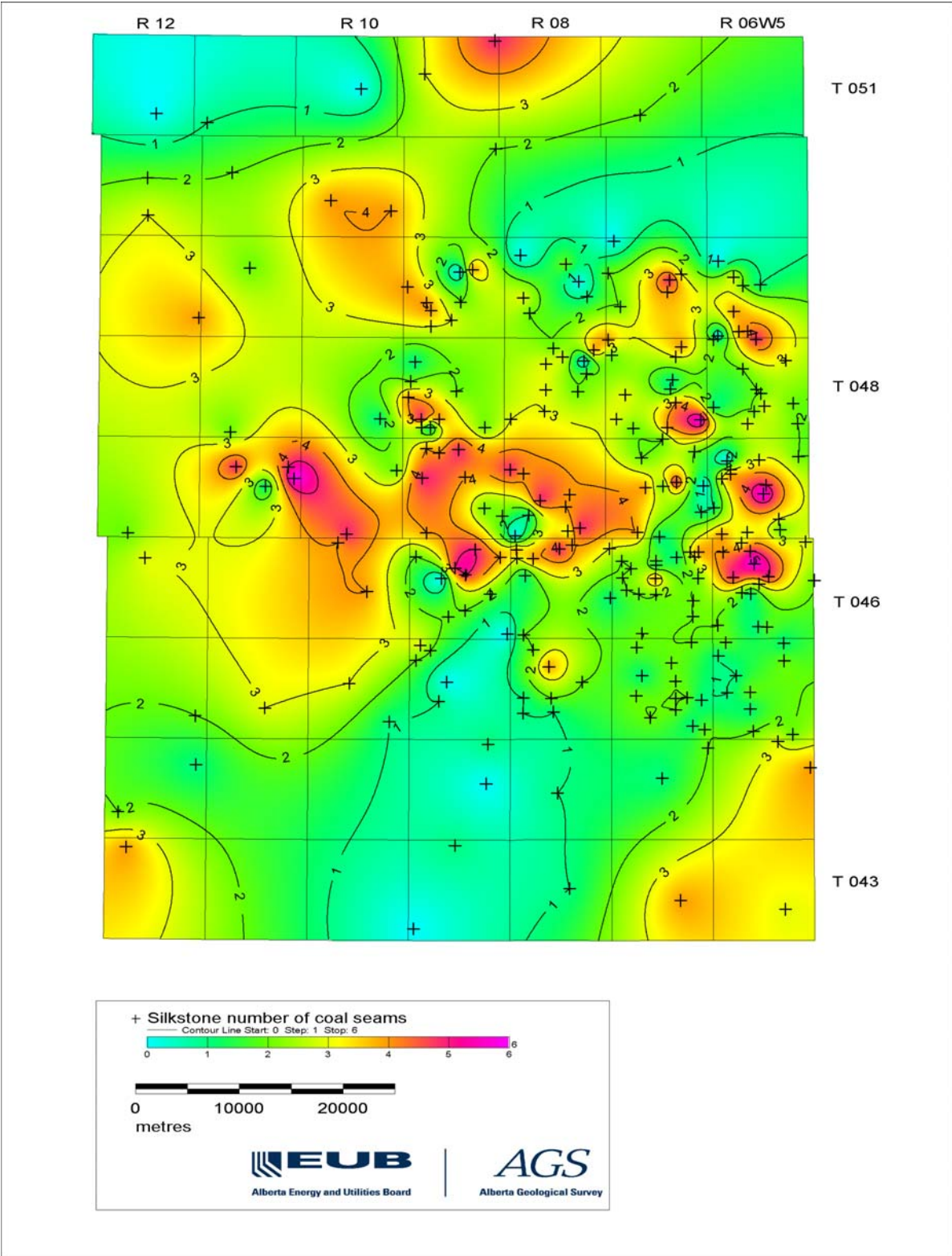


Figure 48. Number of Silkstone coal seams, Pembina study area.

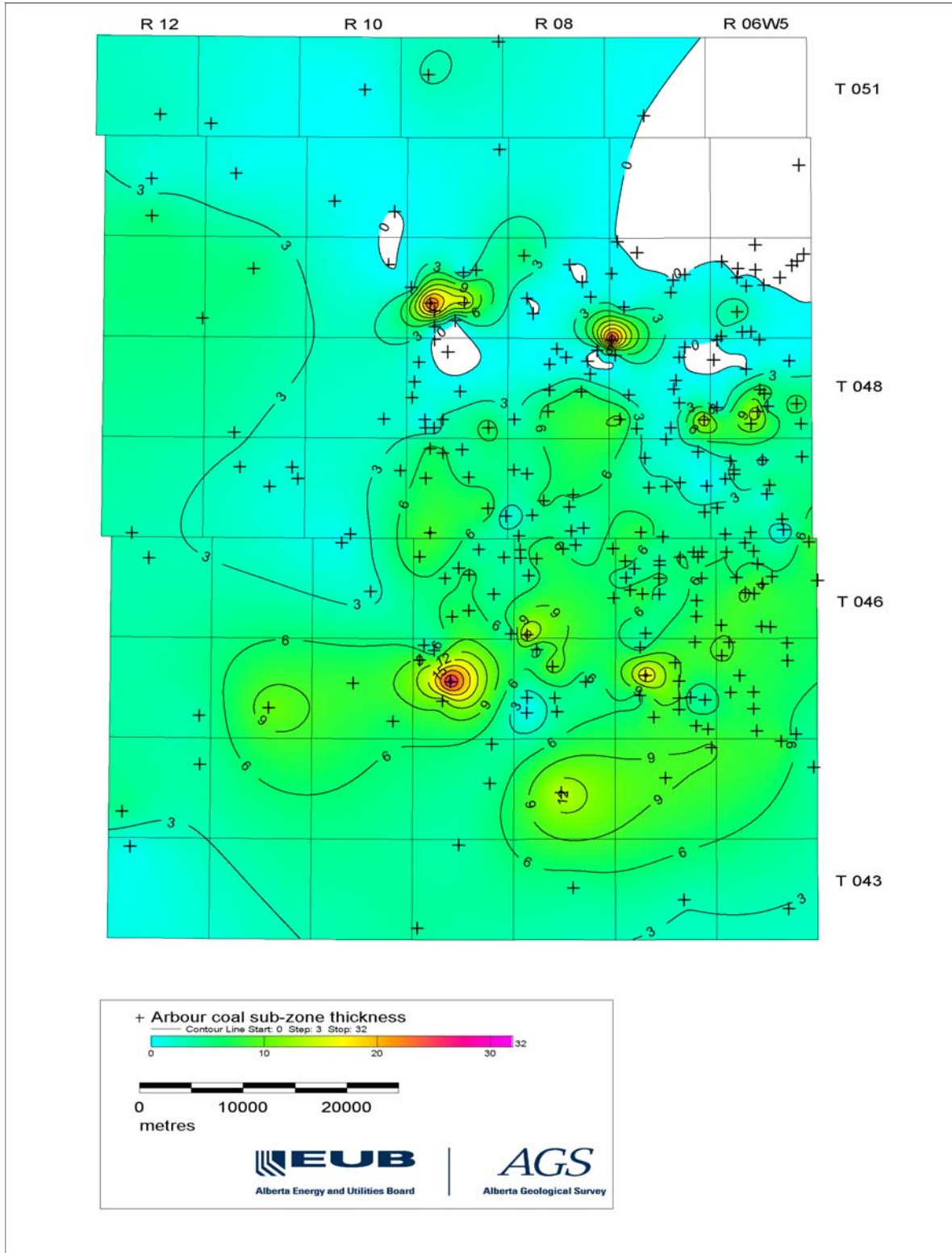


Figure 49. Isopachs of the Arbour coal subzone, Pembina study area.

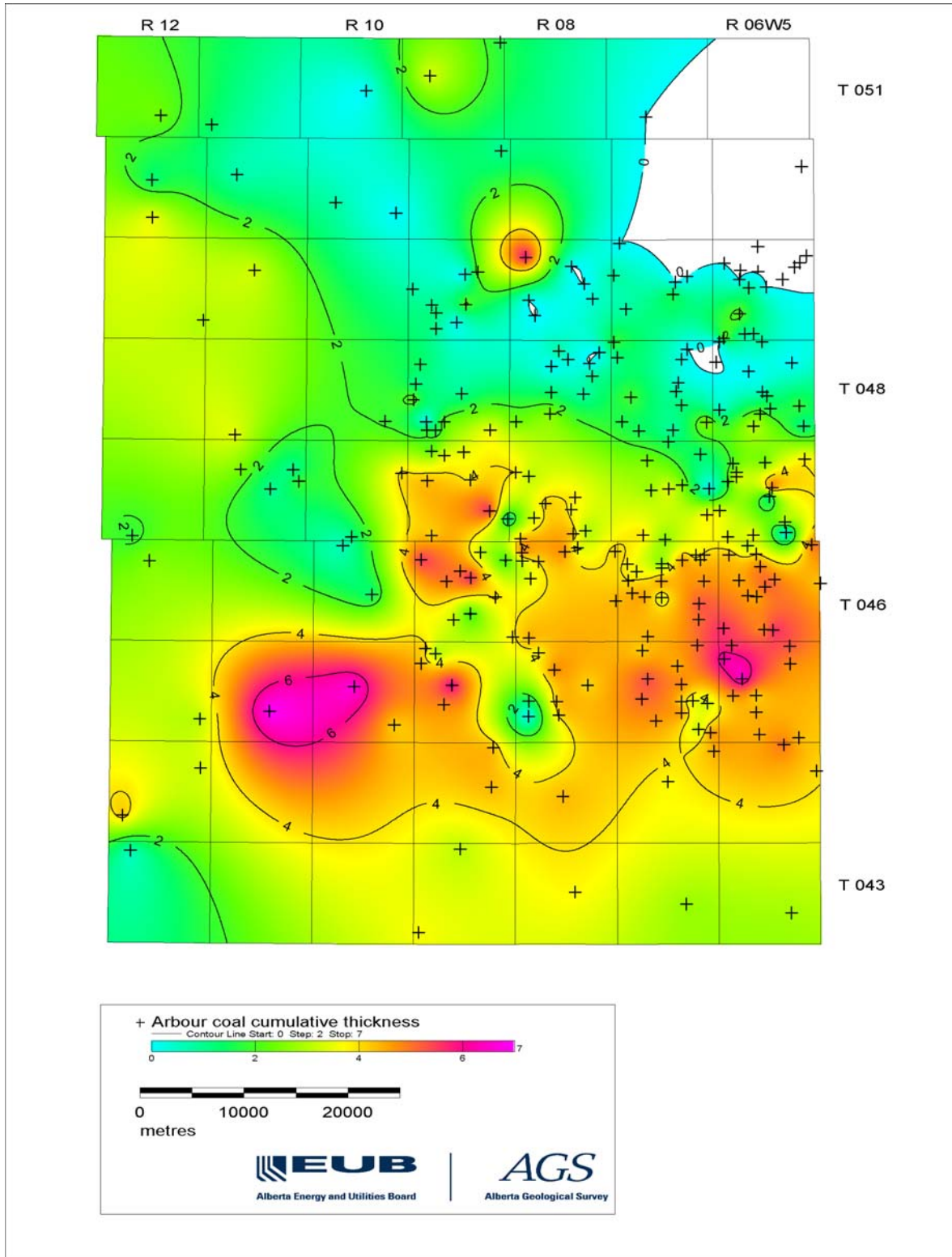


Figure 50. Isopachs of Arbour cumulative coal, Pembina study area.

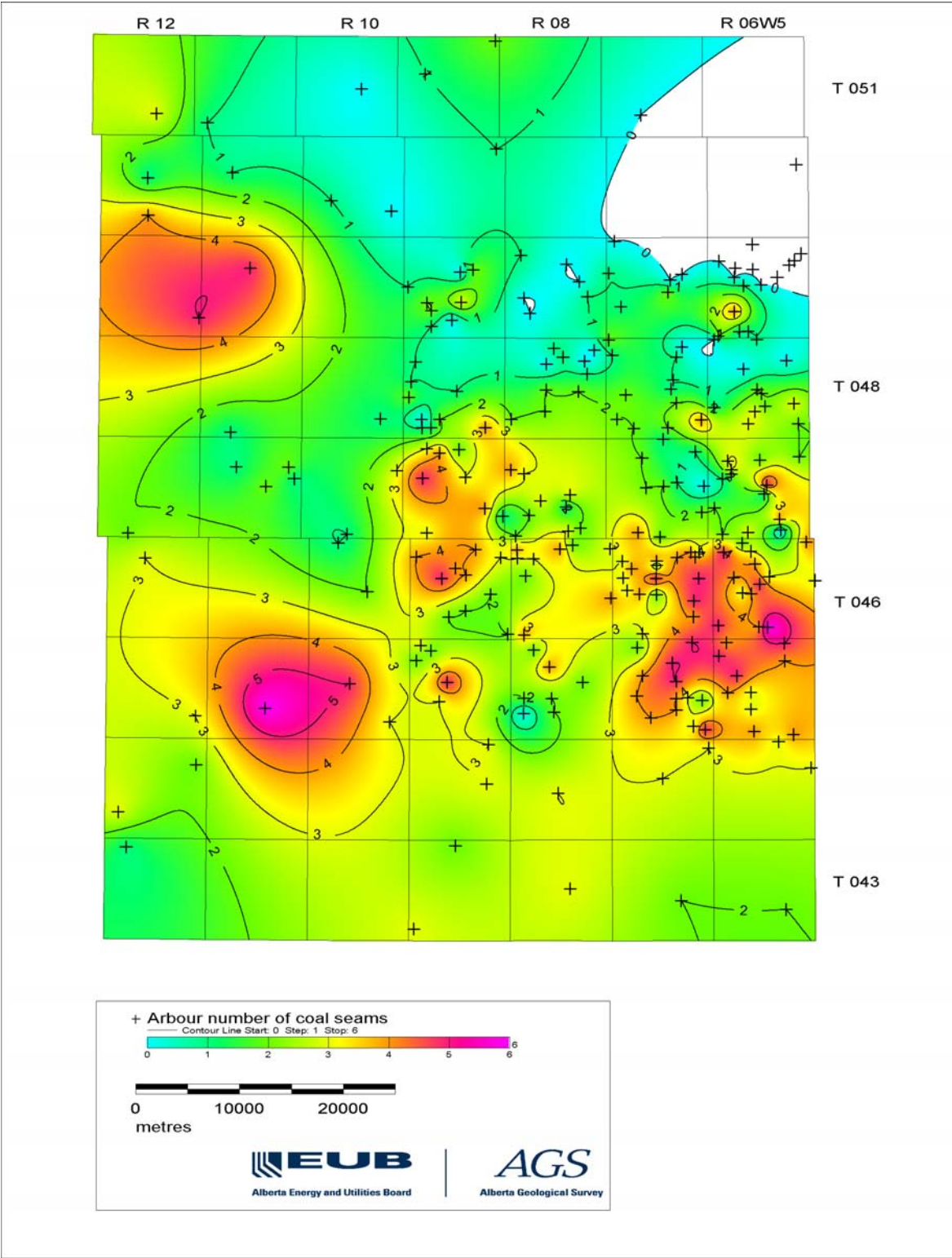


Figure 51. Number of Arbour coal seams, Pembina study area.

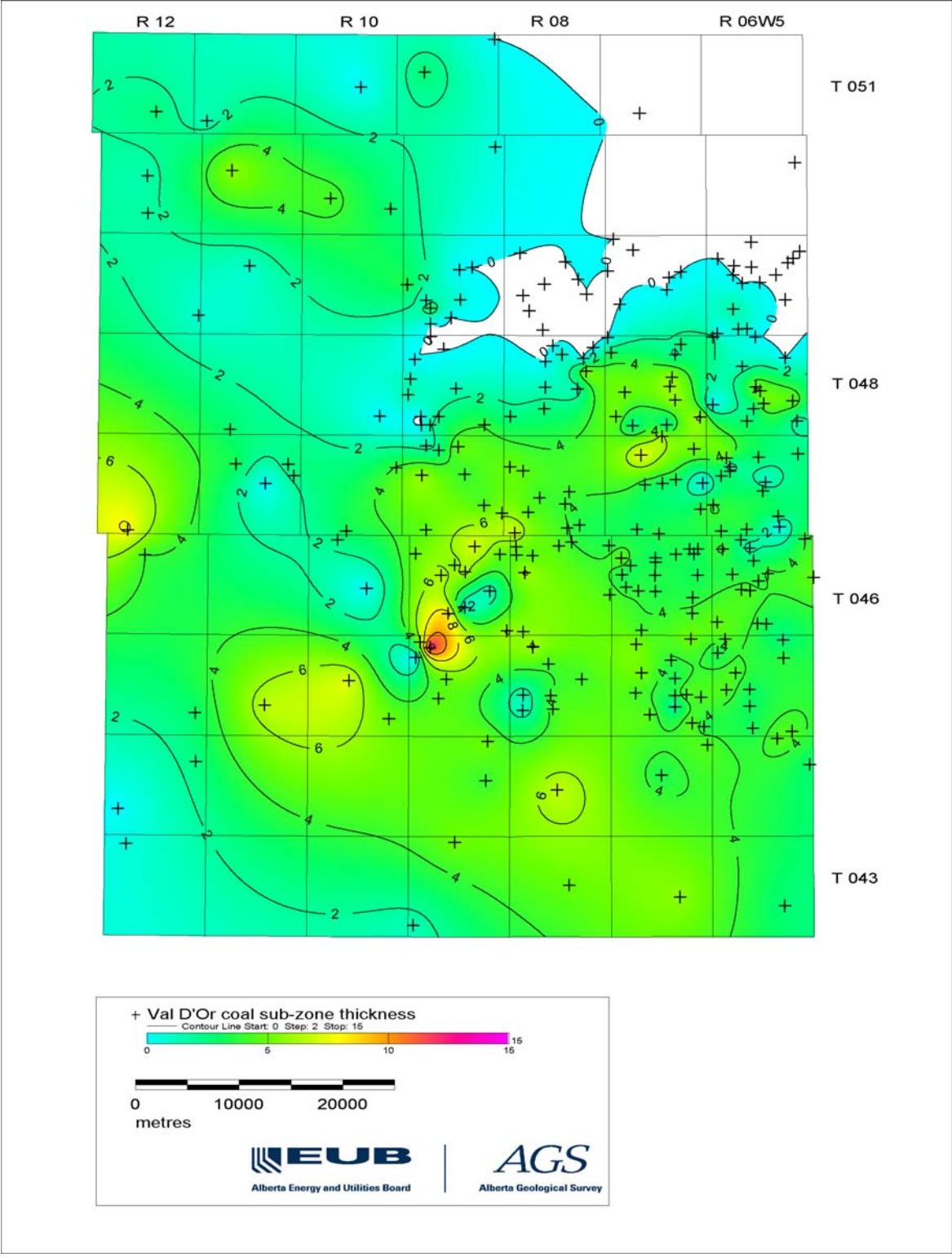


Figure 52. Isopachs of the Val D'Or coal subzone, Pembina study area.

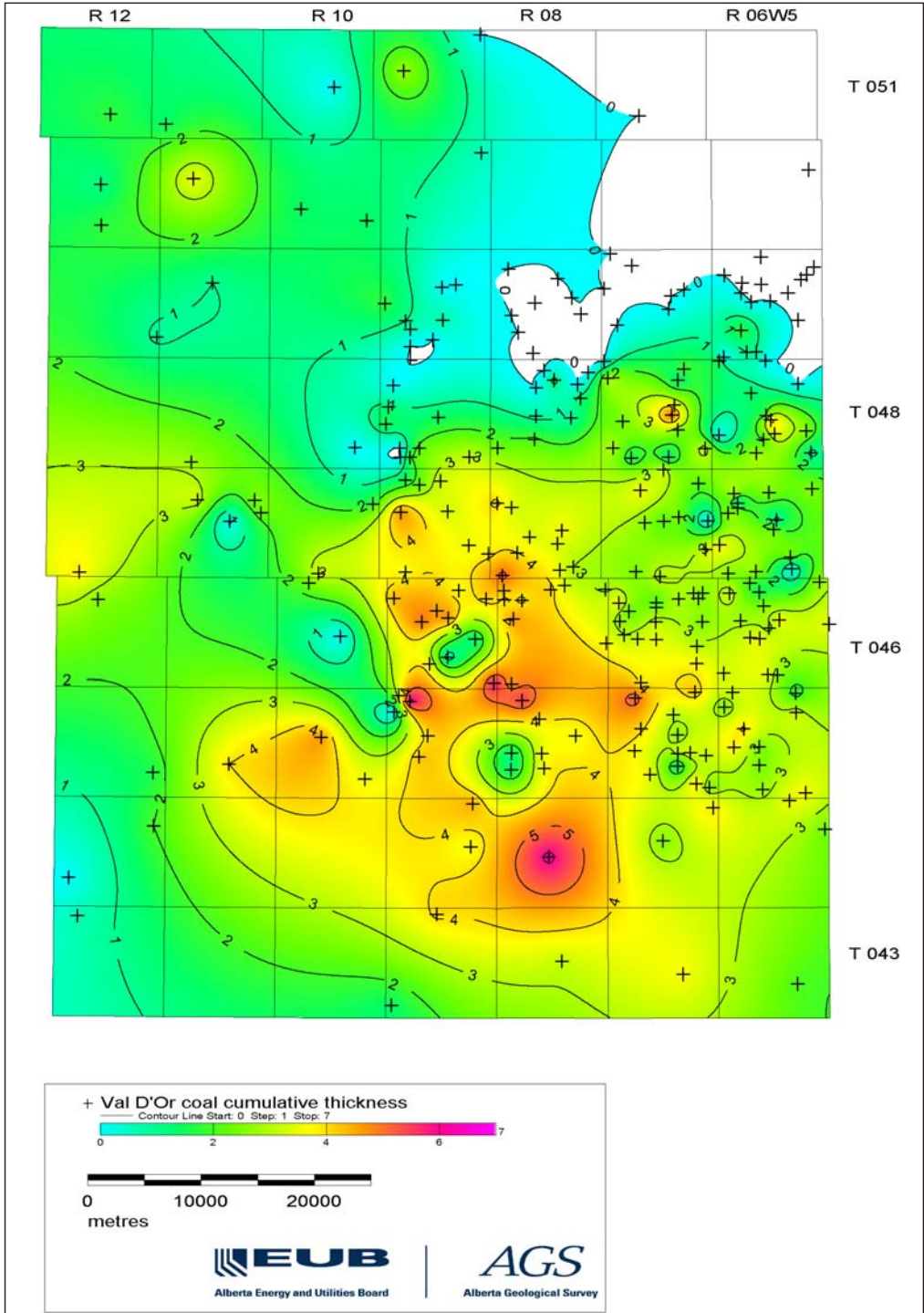


Figure 53. Isopachs of Val D'Or cumulative coal, Pembina study area.

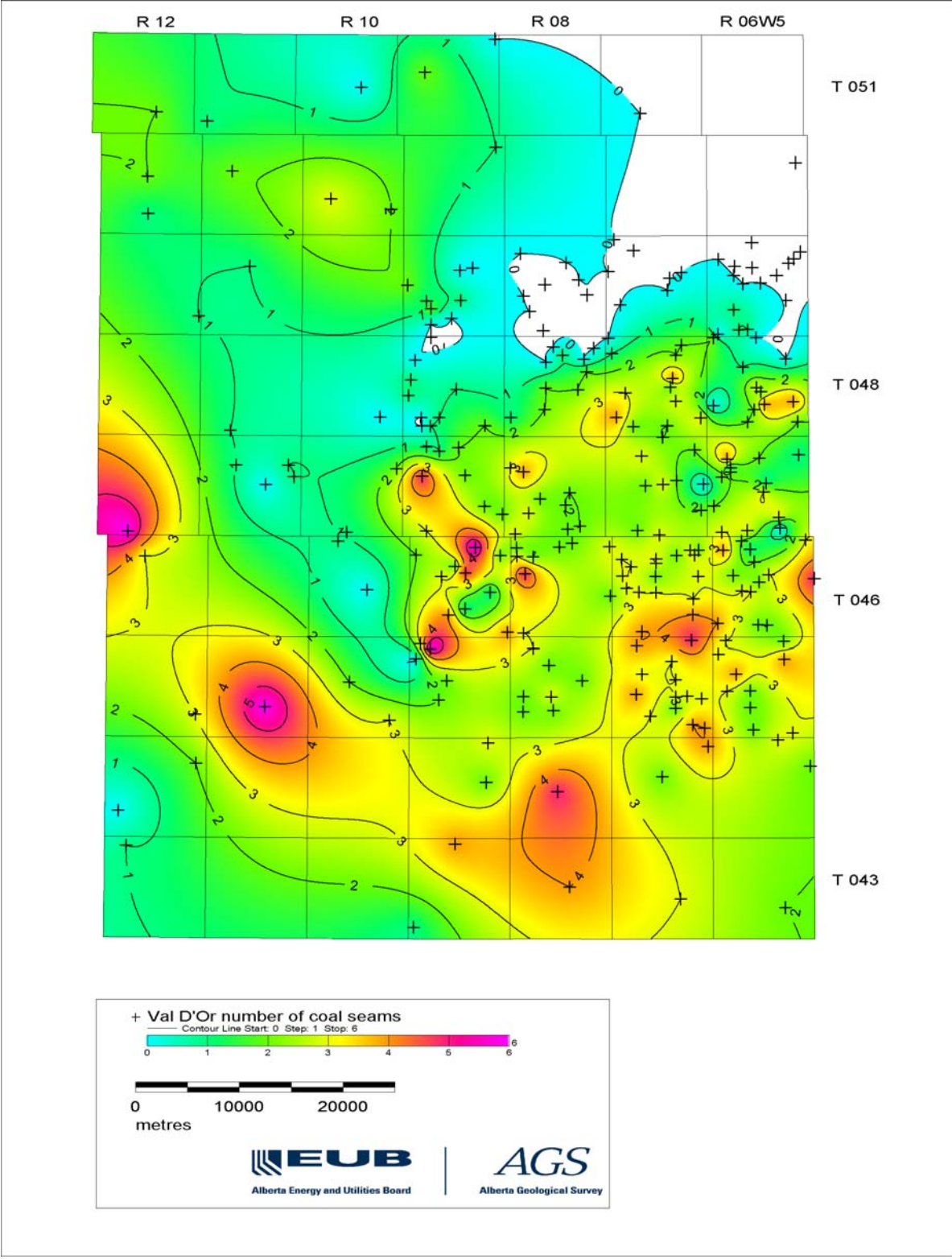


Figure 54. Number of Val D'Or coal seams, Pembina study area.

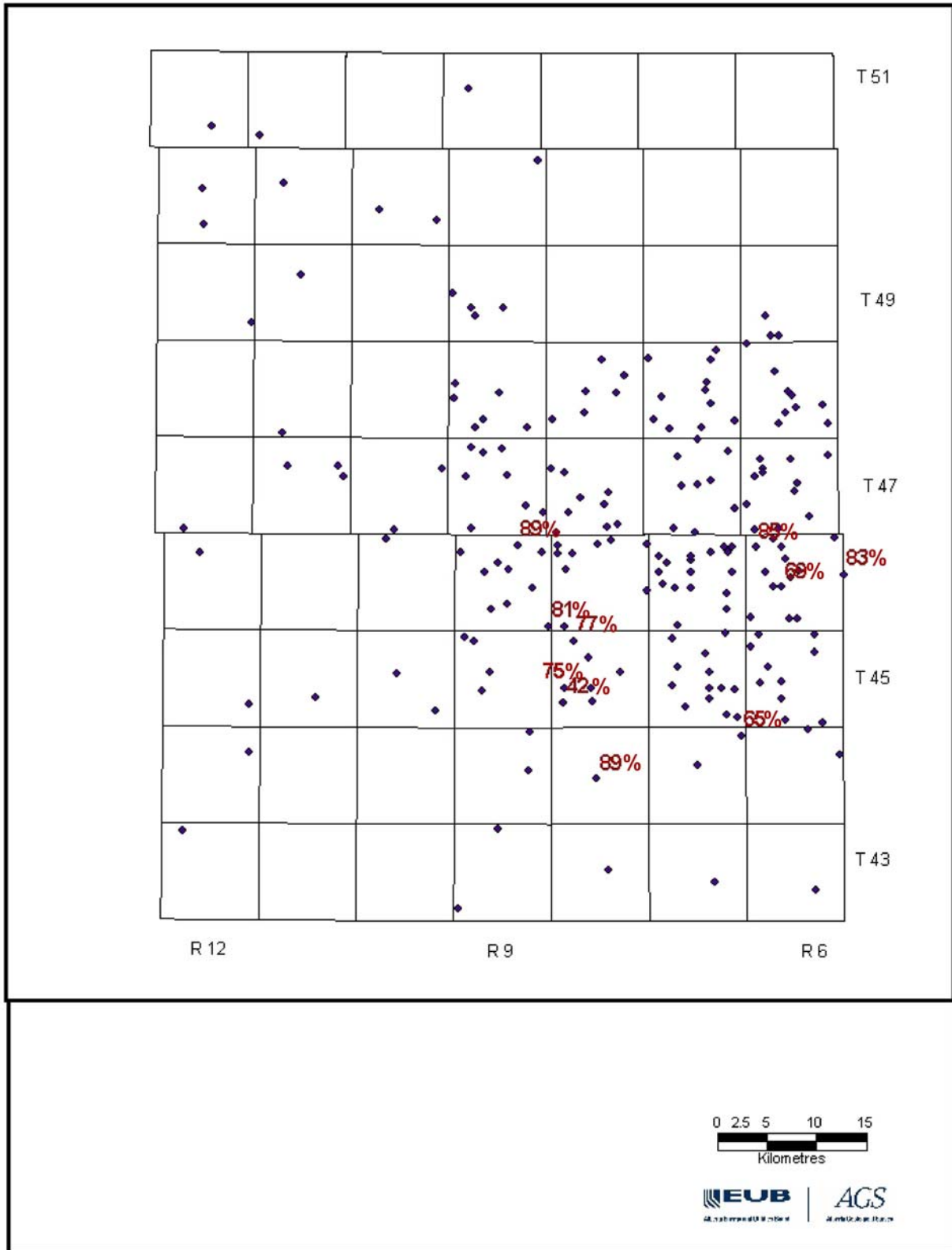


Figure 55. Distribution of 'clean coal' (in per cent) in the Val D'Or subzone, Ardley Coal Zone, Pembina study area.

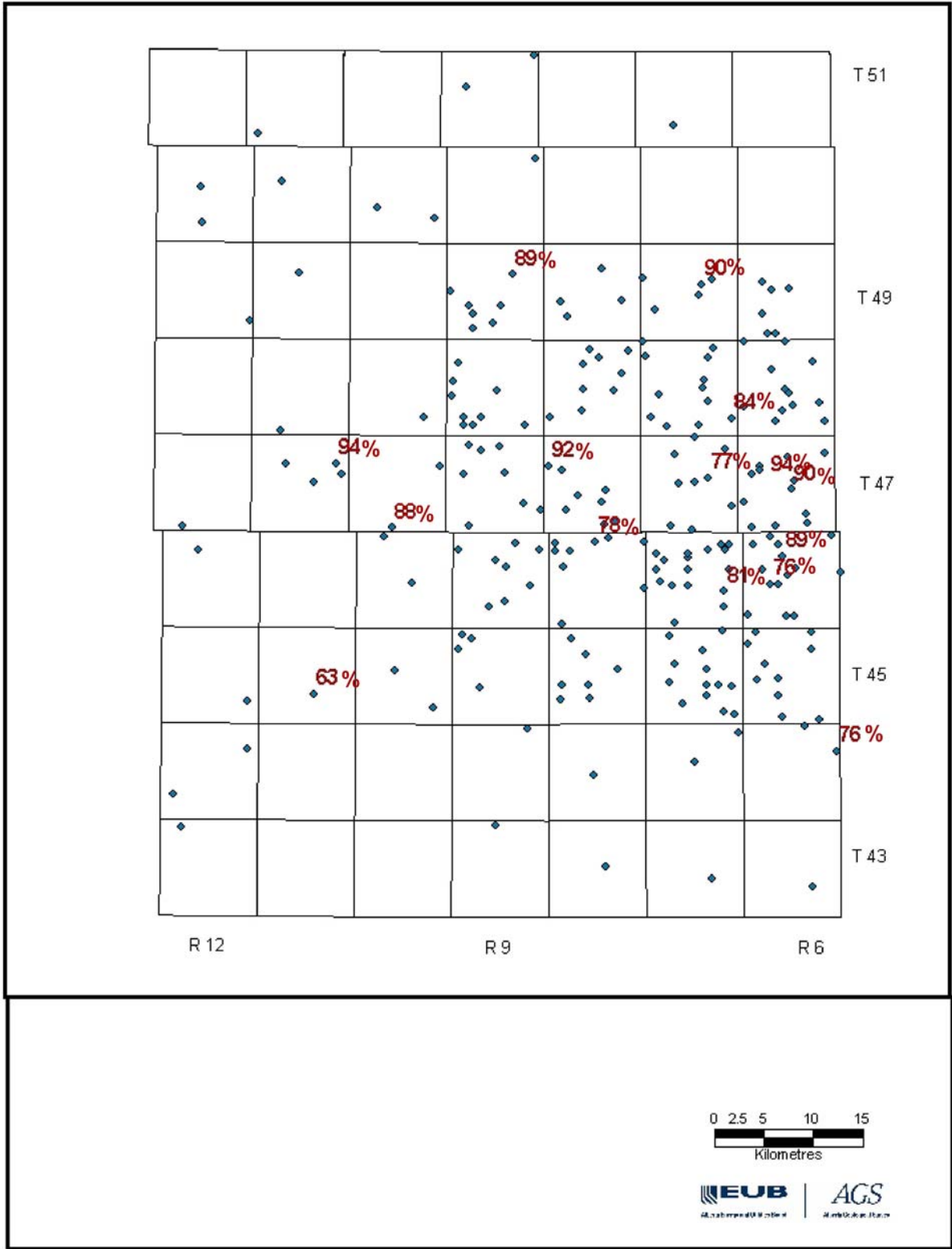


Figure 57. Distribution of 'clean coal' (in per cent) in the Silkstone subzone, Ardley Coal Zone, Pembina study area.

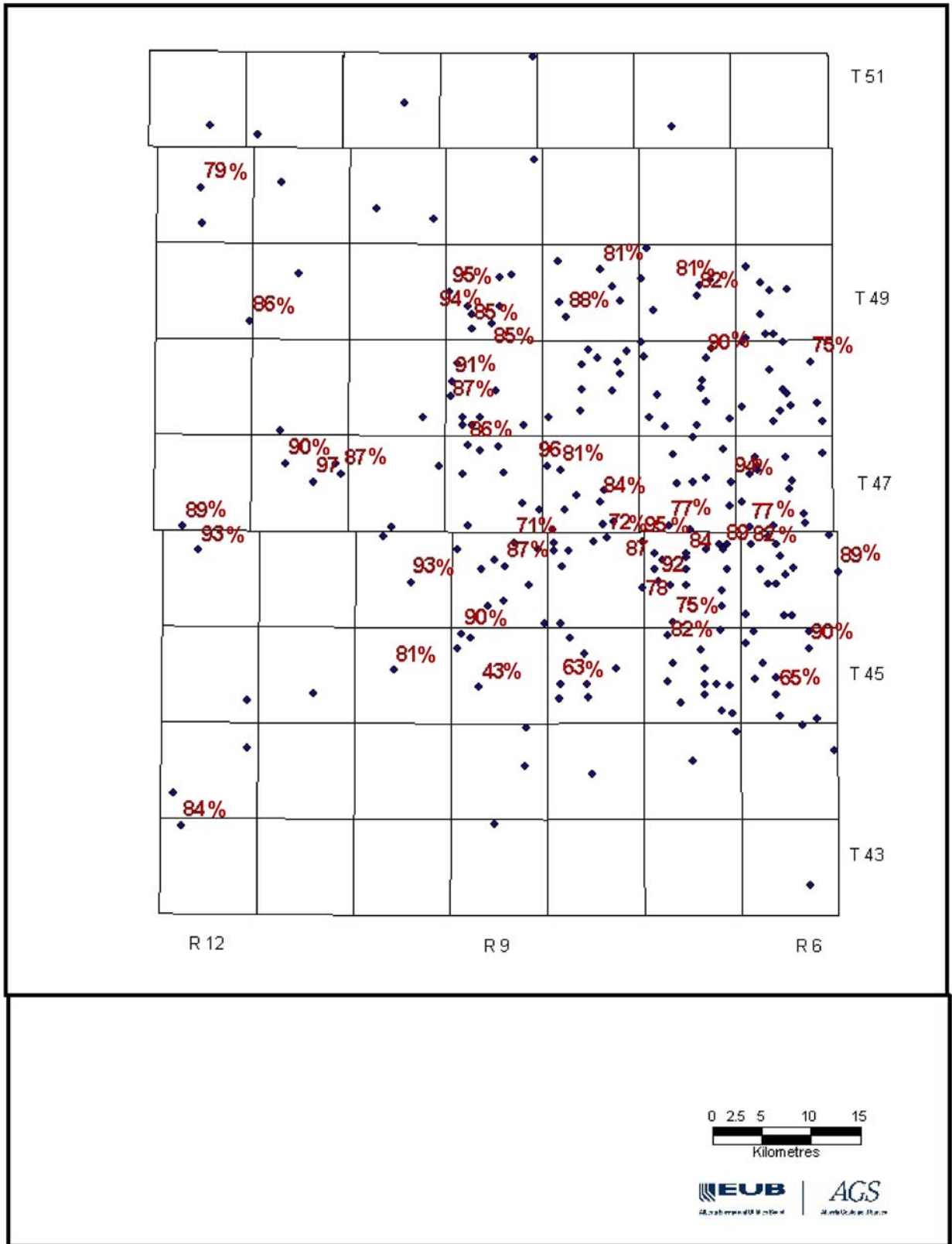


Figure 58. Distribution of 'clean coal' (in per cent) in the Mynheer subzone, Ardley Coal Zone, Pembina study area.

RANK SCALE		REFL. Rm	VOL. M. d.a.f. %	CARBON d.a.f. VITRITE	BED MOISTURE	CAL. VALUE BLU/lb (kcal/kg)	APPLICABILITY OF DIFFERENT RANK PARAMETERS		
GERMAN	USA								
Turf	Peat	-0.2							
		-0.25							
		-0.3		ca. 60	ca. 75				
Weich-	Lignite	-0.35							
Matt-		sub-bit.	-0.4		ca. 35	7200 (4000)			
	Sub-bit.	-0.45							
		C	-0.5						
	B	-0.55		ca. 71	ca. 25	9900 (5500)			
		A	-0.6						
Glanz-	C	-0.65							
		A	-0.7		ca. 77	ca. 8-10	12600 (7000)		
Flamm-	B	-0.75							
		A	-0.8						
Gasflamm-	A	-0.85							
		High vol. bituminous	-0.9						
Gas-	Medium volatile bituminous	-1.0							
			-1.1						
Fett-	Low volatile bituminous	-1.2		ca. 87		15500 (8650)			
			-1.3						
Ess-	Semi-anthracite	-1.4							
			-1.5						
Mager-	Anthracite	-1.6							
			-1.7						
Anthrazit	Meta A.	-1.8		ca. 91		15500 (8650)			
			-1.9						
Meta-Anthr.		-2.0							
		-2.1							
		-2.2							
		-2.3							
		-2.4							
		-2.5							
		-2.6							
		-2.7							
		-2.8							
		-2.9							
		-3.0							
		-3.1							
		-3.2							
		-3.3							
		-3.4							
		-3.5							
		-3.6							
		-3.7							
		-3.8							
		-3.9							
		-4.0							

Figure 59. Coal rank chart (Bustin et al., 1983).

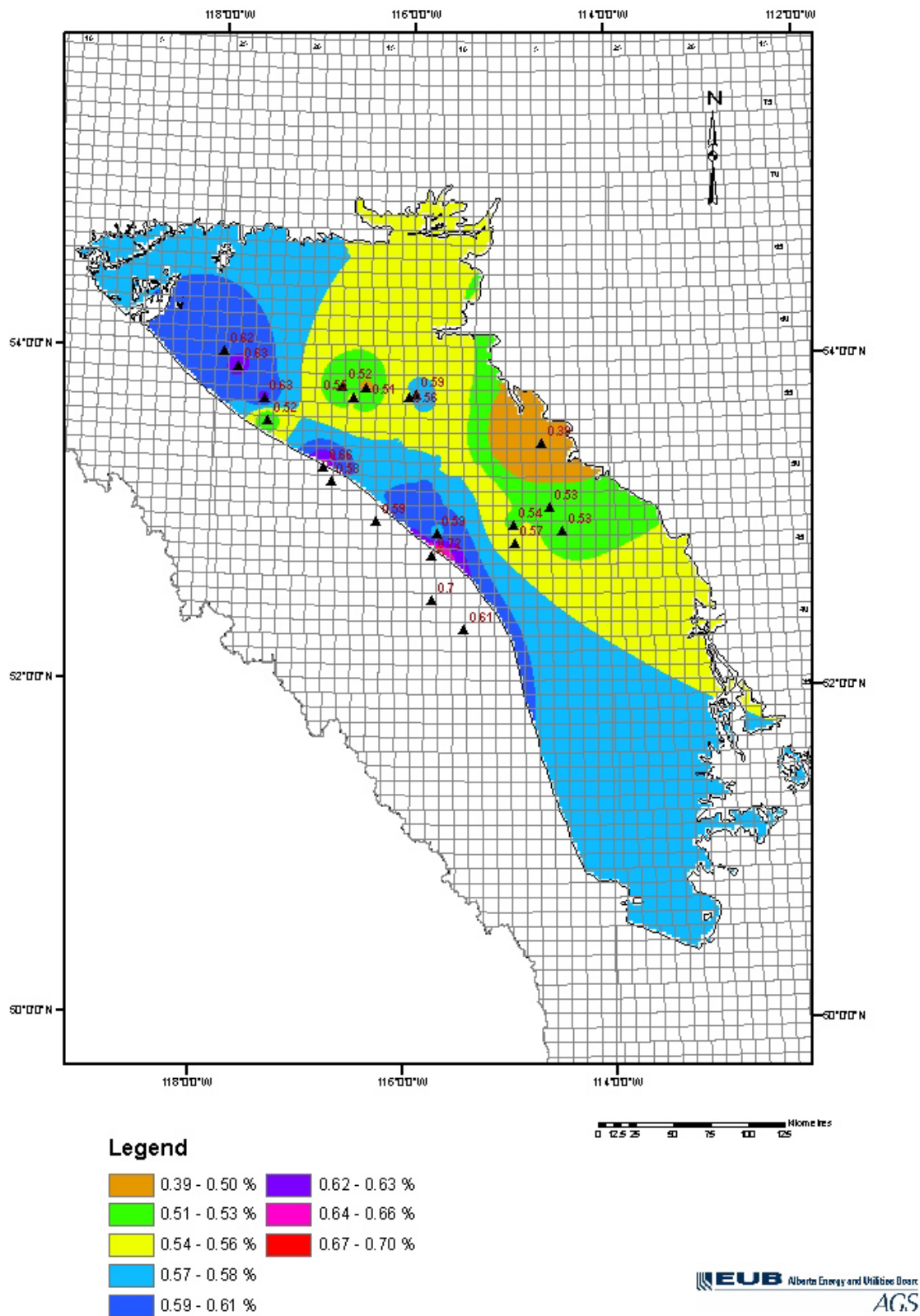


Figure 60. Distribution of vitrinite reflectance in the Ardley Coal Zone, Alberta.

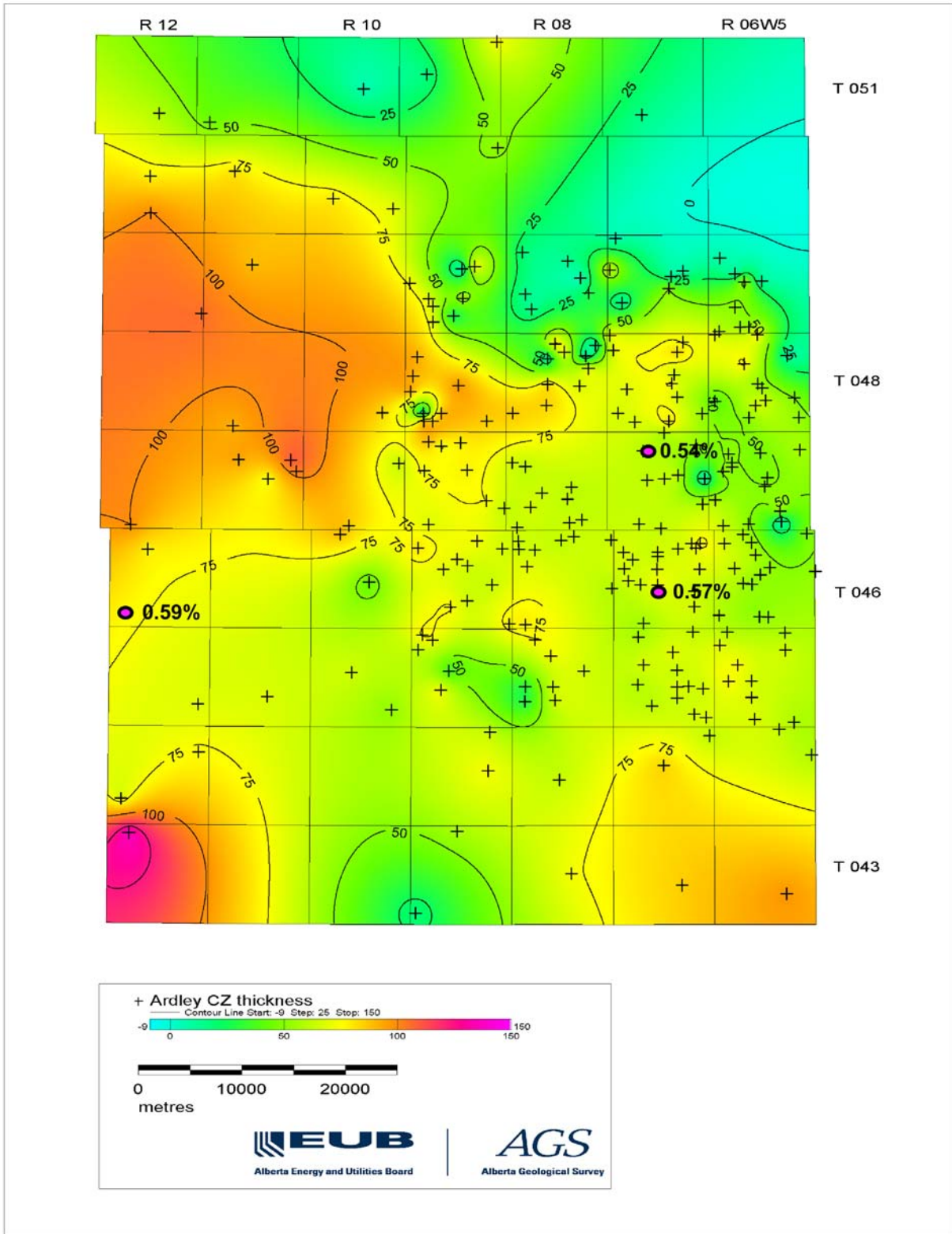


Figure 61. Distribution of vitrinite reflectance in the Ardley Coal Zone in the Pembina study area.

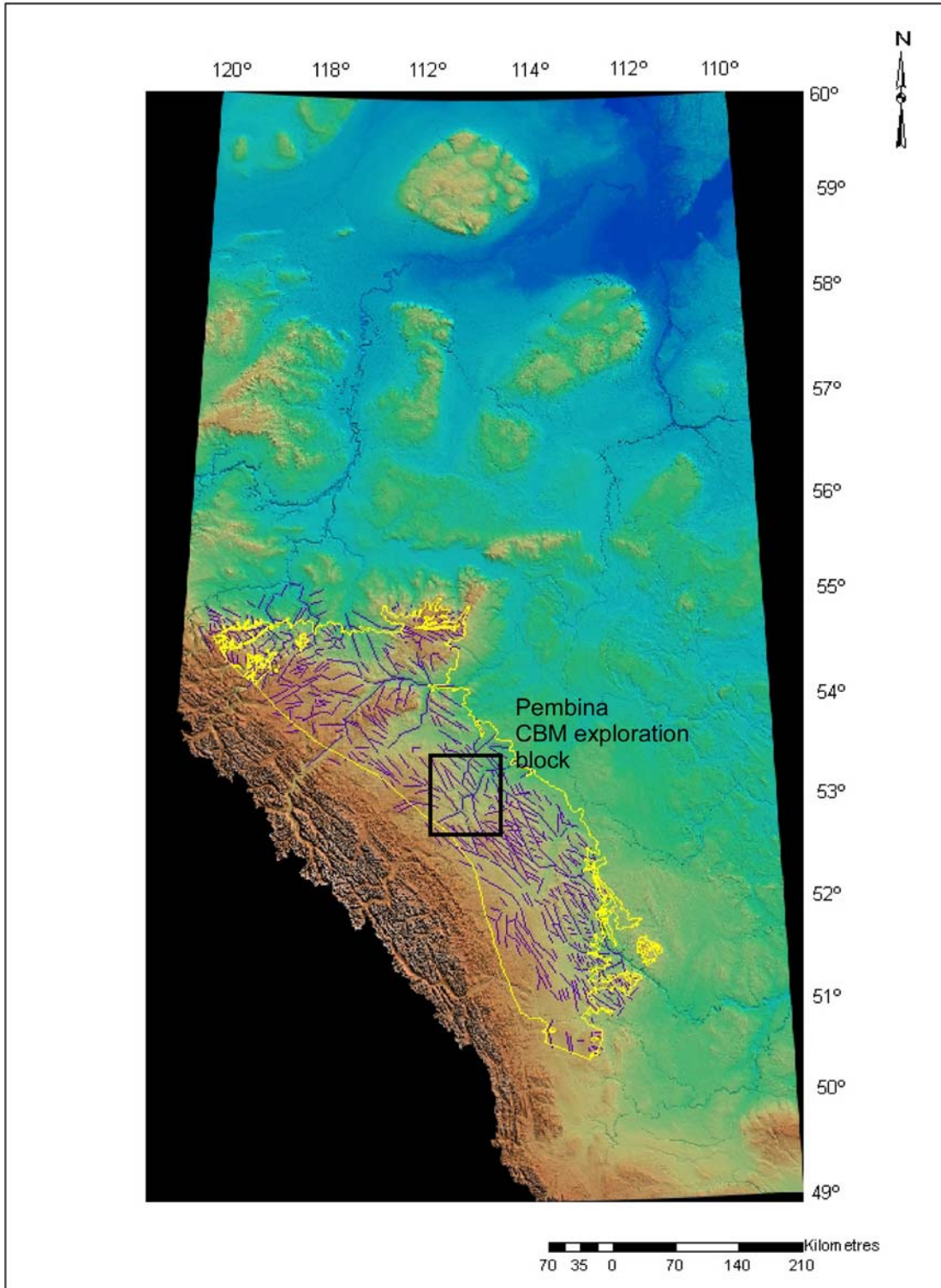


Figure 63. Interpretation of surface lineaments from the Alberta digital elevation model.

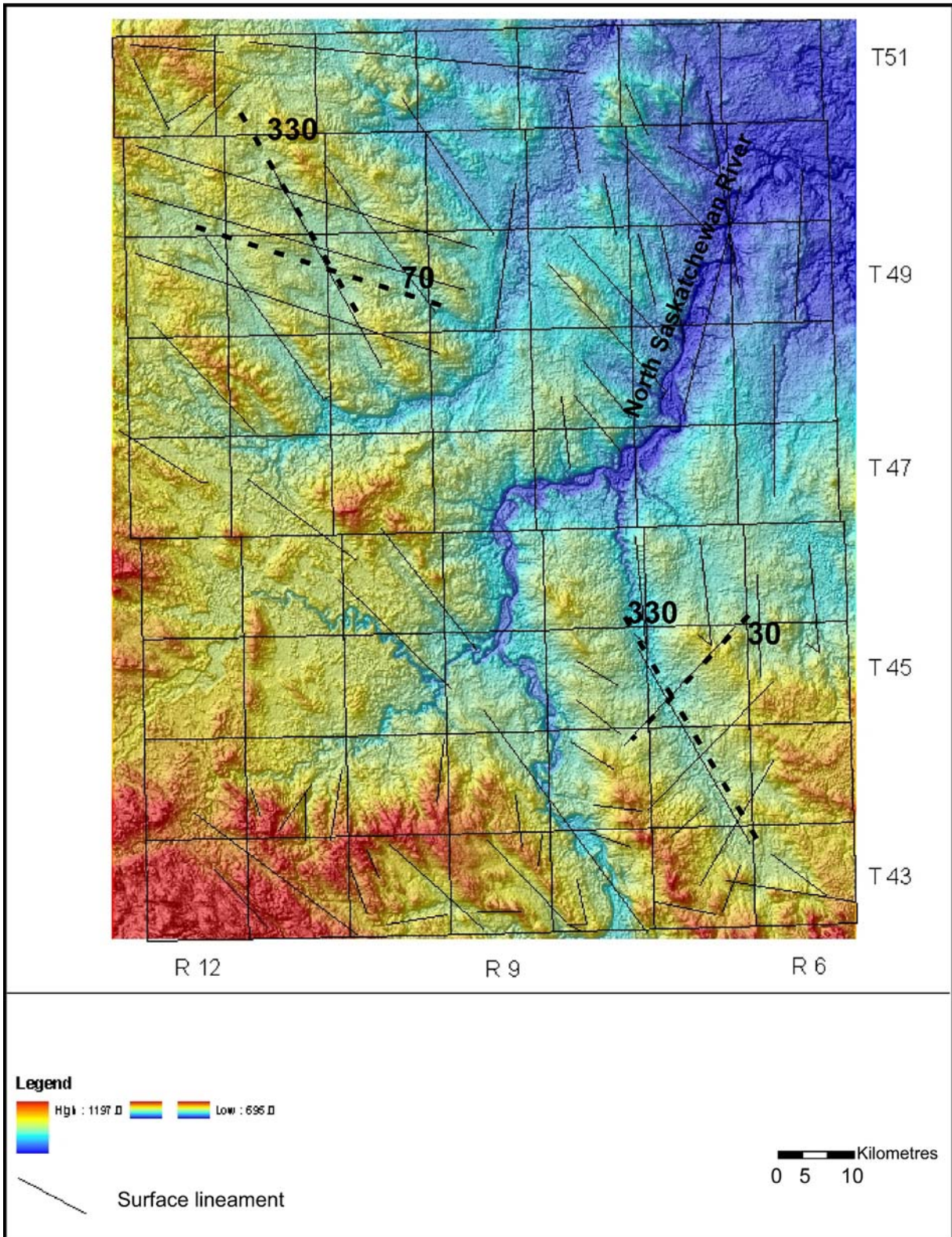


Figure 64. Interpretation of surface lineaments from the digital elevation model of the Pembina CBM exploration block.

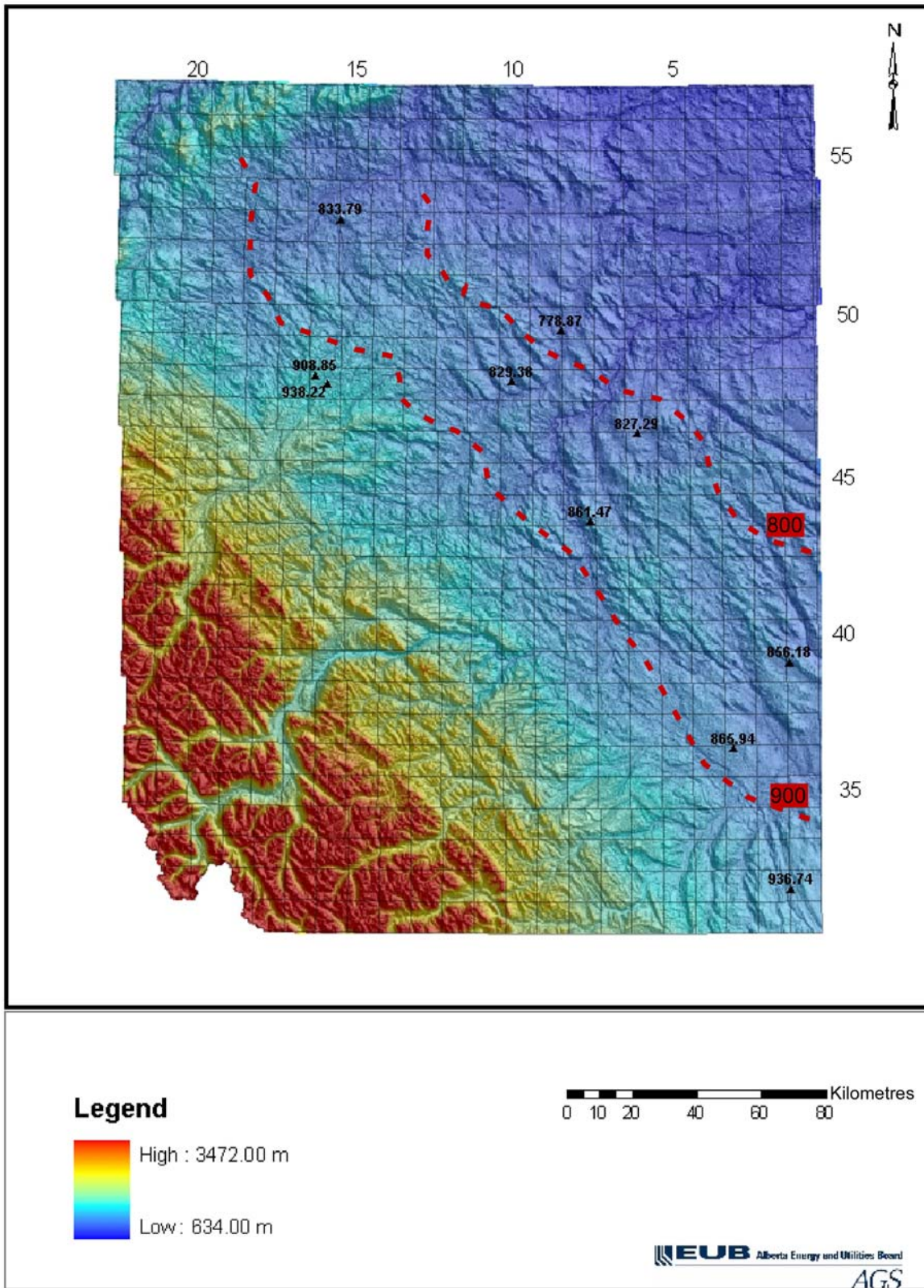


Figure 65. Potentiometric contours of hydraulic head data for the Paskapoo Formation plotted on the digital elevation model.

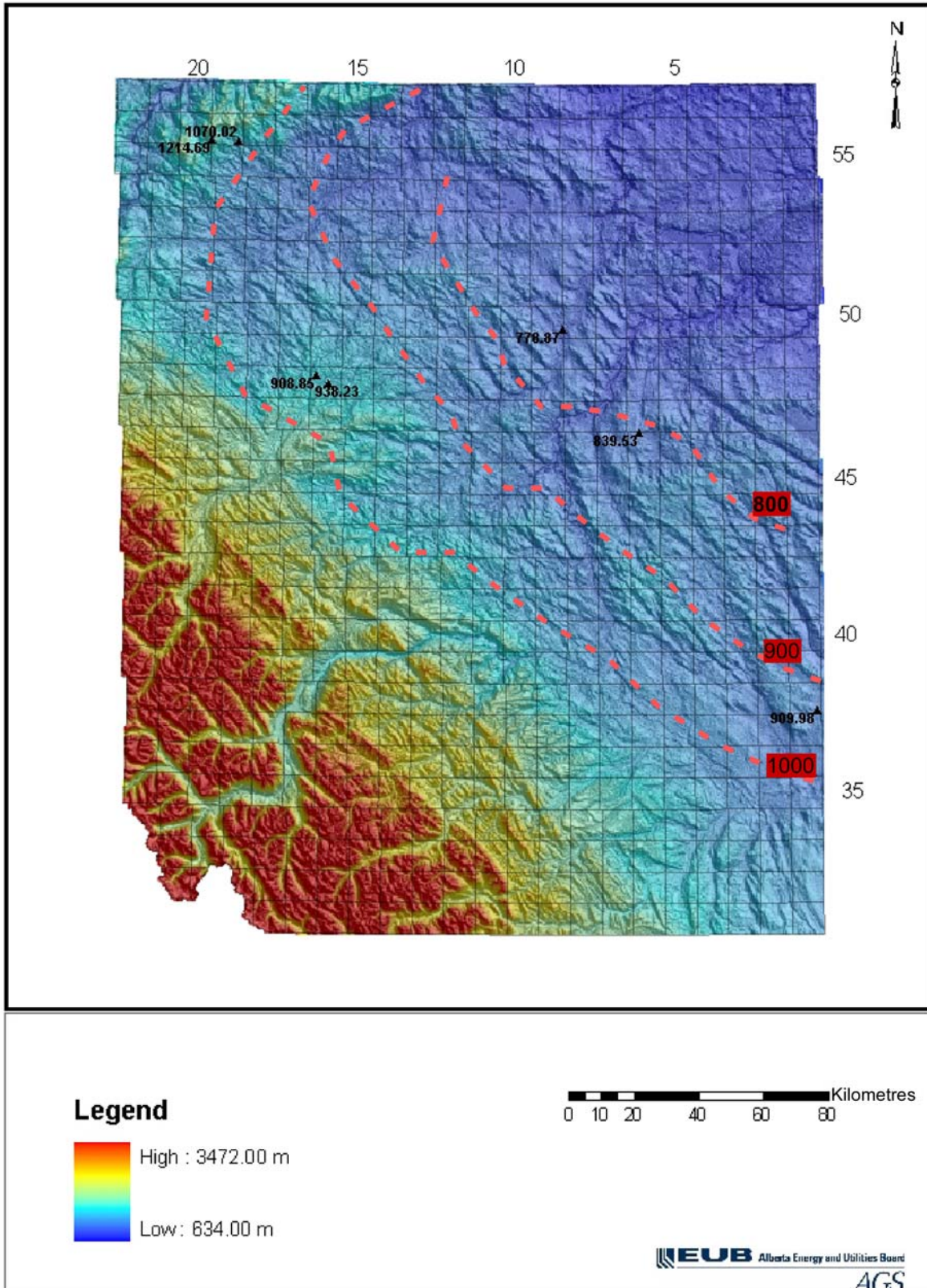


Figure 66. Potentiometric contours of hydraulic head data for the Scollard Formation plotted on the digital elevation model.

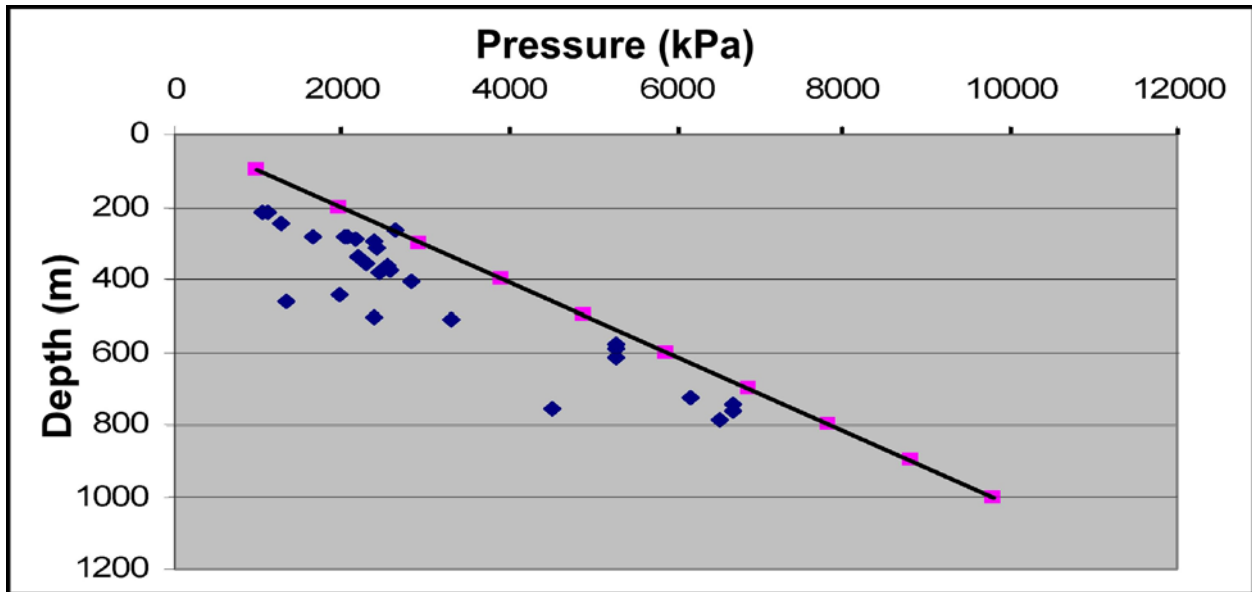


Figure 67. Formation pressure versus depth, Scollard and Paskapoo formations, regional scale. Trend line represents equivalent freshwater hydrostatic pressures.

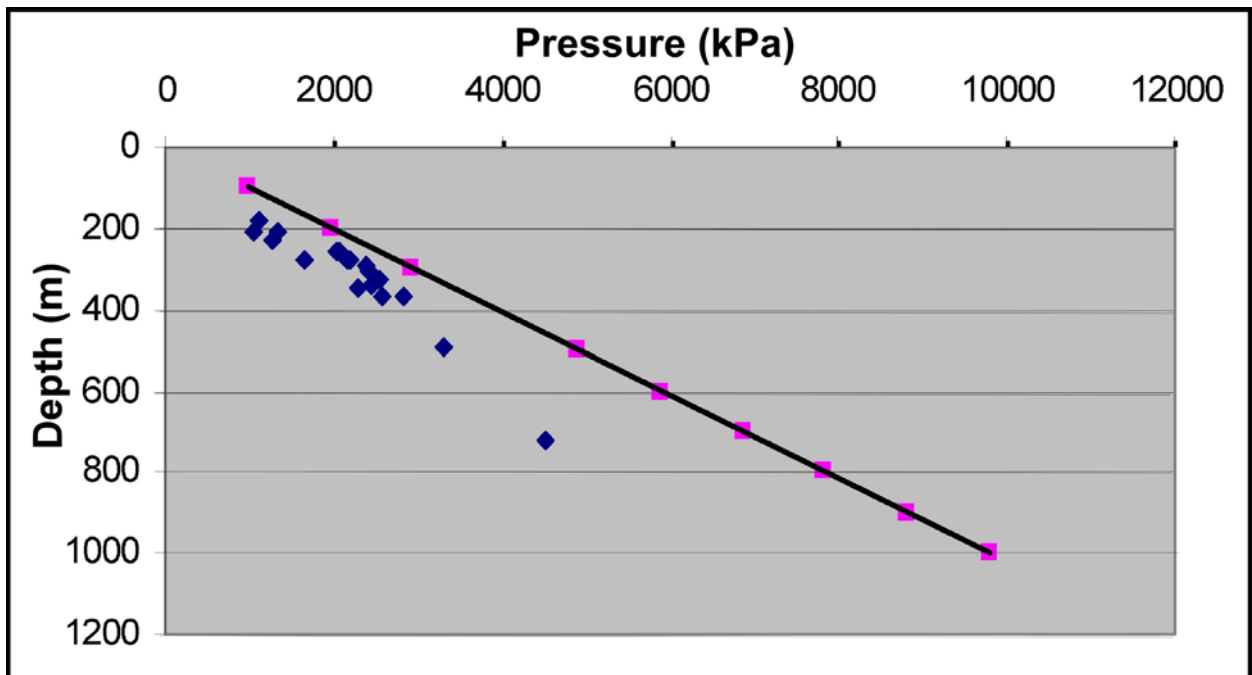


Figure 68. Formation pressure versus depth, Paskapoo Formation, regional scale. Trend line represents equivalent freshwater hydrostatic pressures.

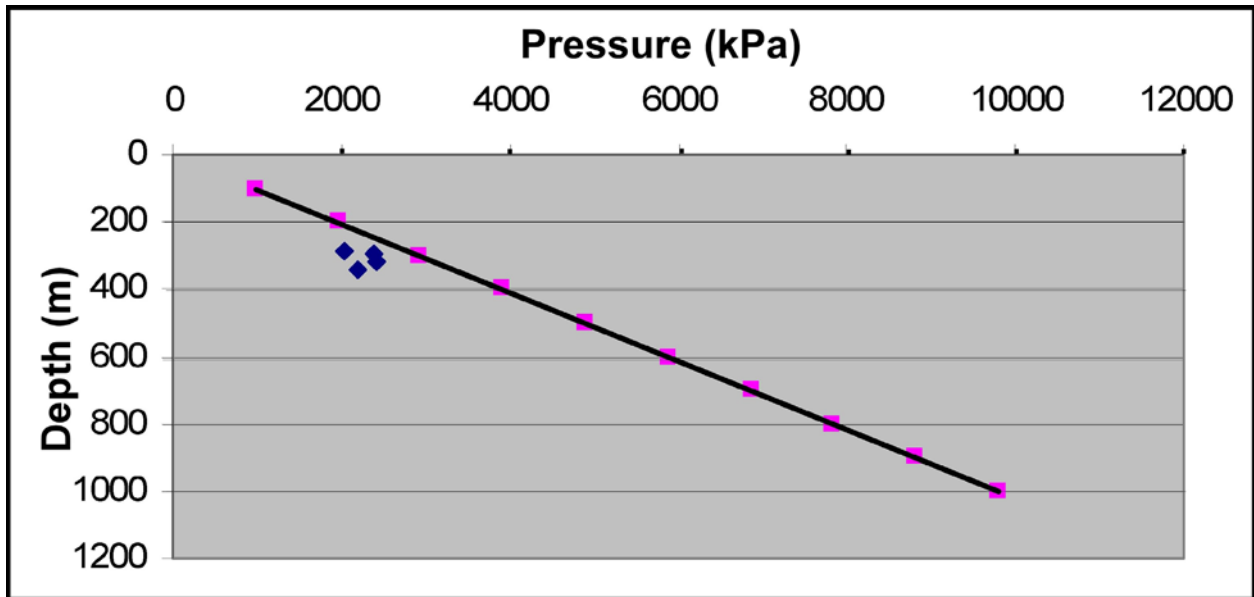


Figure 69. Formation pressure versus depth, commingled Paskapoo basal sandstone channels and upper Ardley coal beds, regional scale. Trend line represents equivalent freshwater hydrostatic pressures.

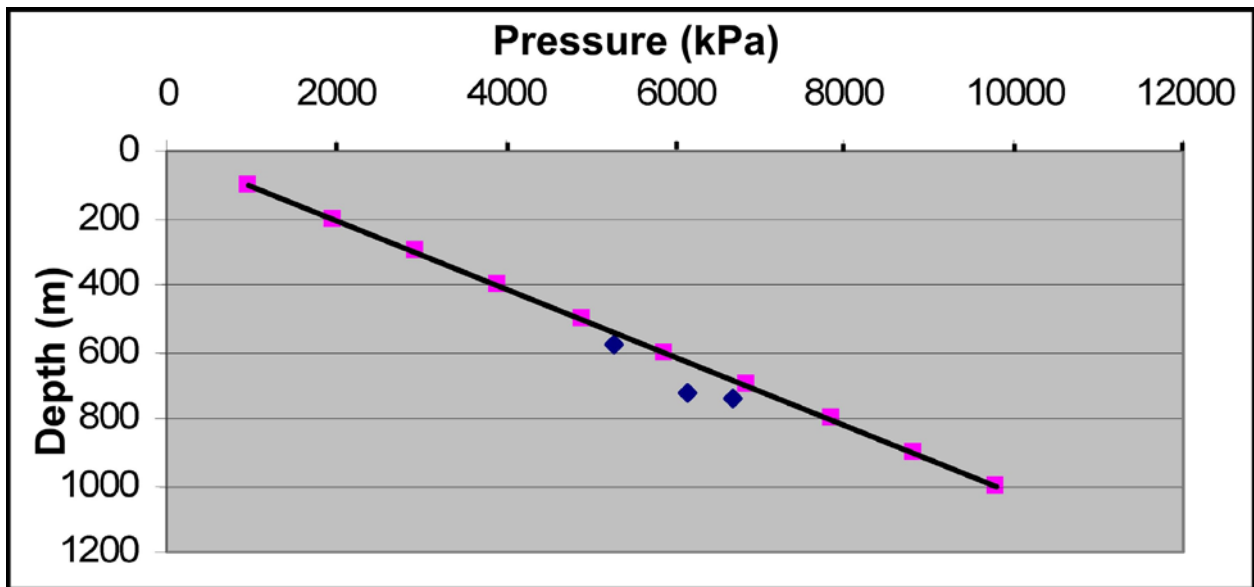


Figure 70. Formation pressure versus depth, upper Ardley coal subzones. Trend line represents equivalent freshwater hydrostatic pressures.

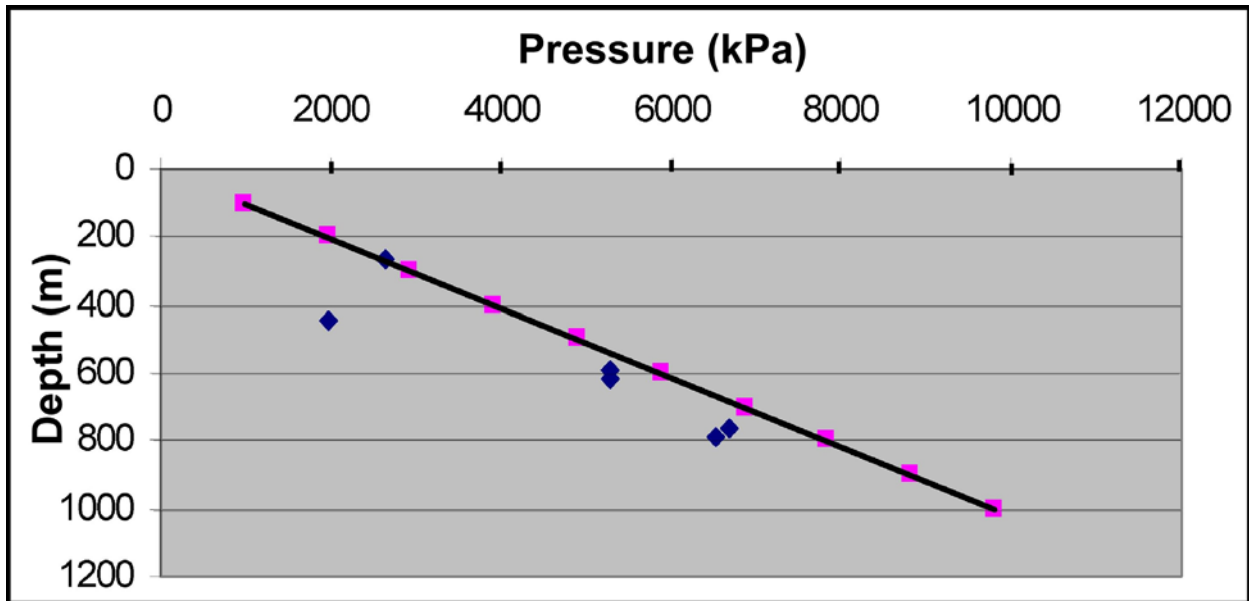


Figure 71. Formation pressure versus depth, lower Ardley coal subzones. Trend line represents equivalent freshwater hydrostatic pressures.

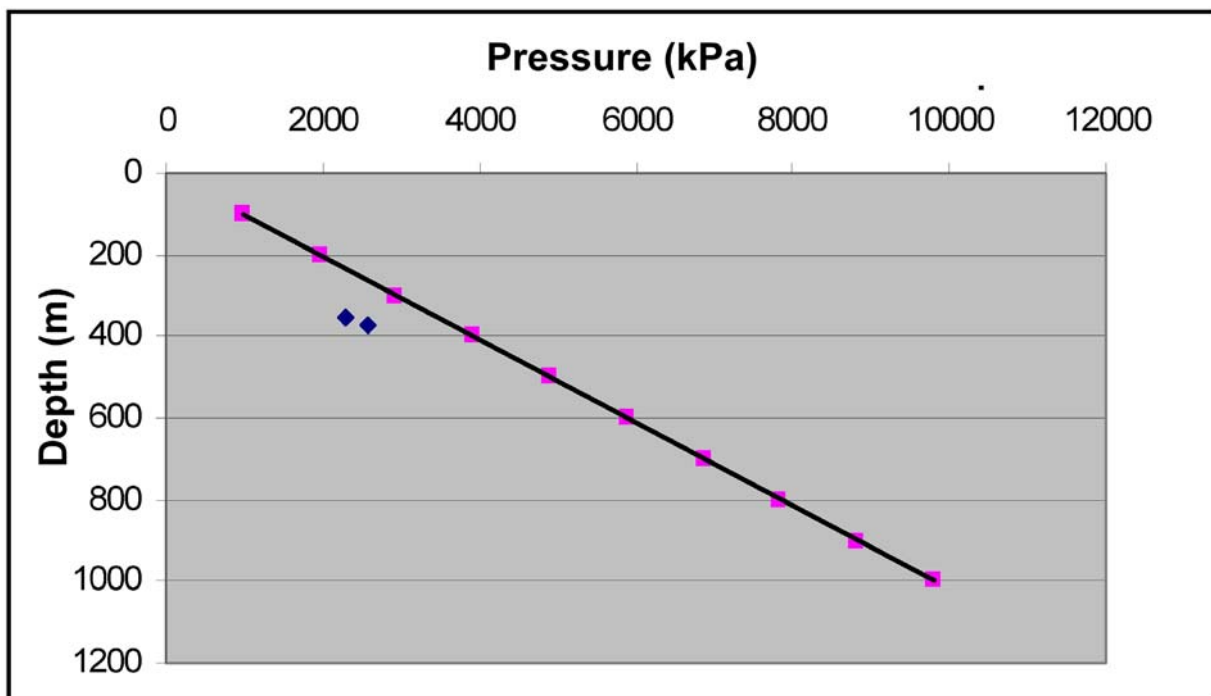


Figure 72. Formation pressure versus depth, Paskapoo Formation, well 02/07-32-036-03W5/0. Trend line represents equivalent freshwater hydrostatic pressures.

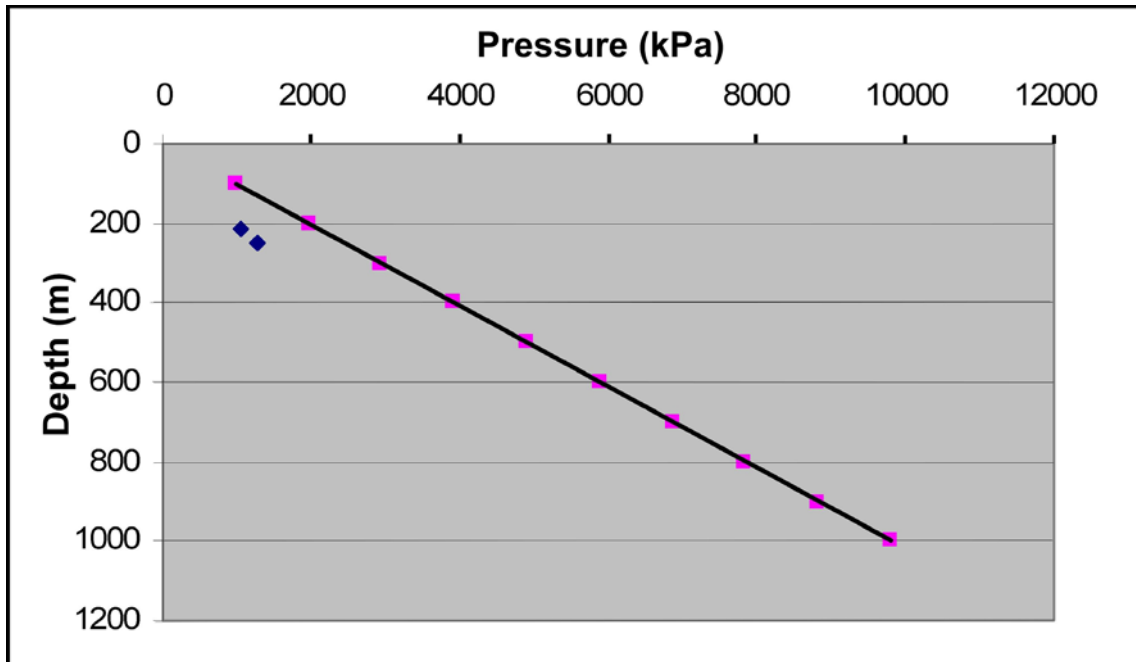


Figure 73. Formation pressure versus depth, Paskapoo basal sandstone channels, well 00/06-34-052-09W5/0. Trend line represents equivalent freshwater hydrostatic pressures.

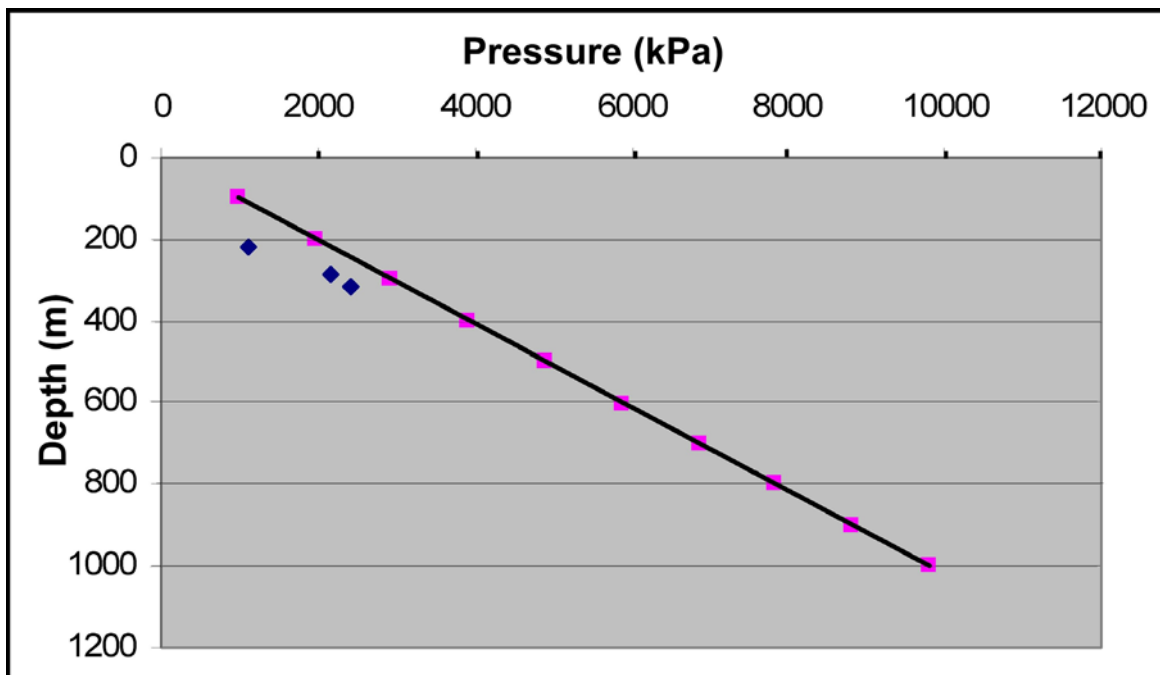


Figure 74. Formation pressure versus depth, upper Paskapoo and Paskapoo basal channels. Trend line represents equivalent freshwater hydrostatic pressures.

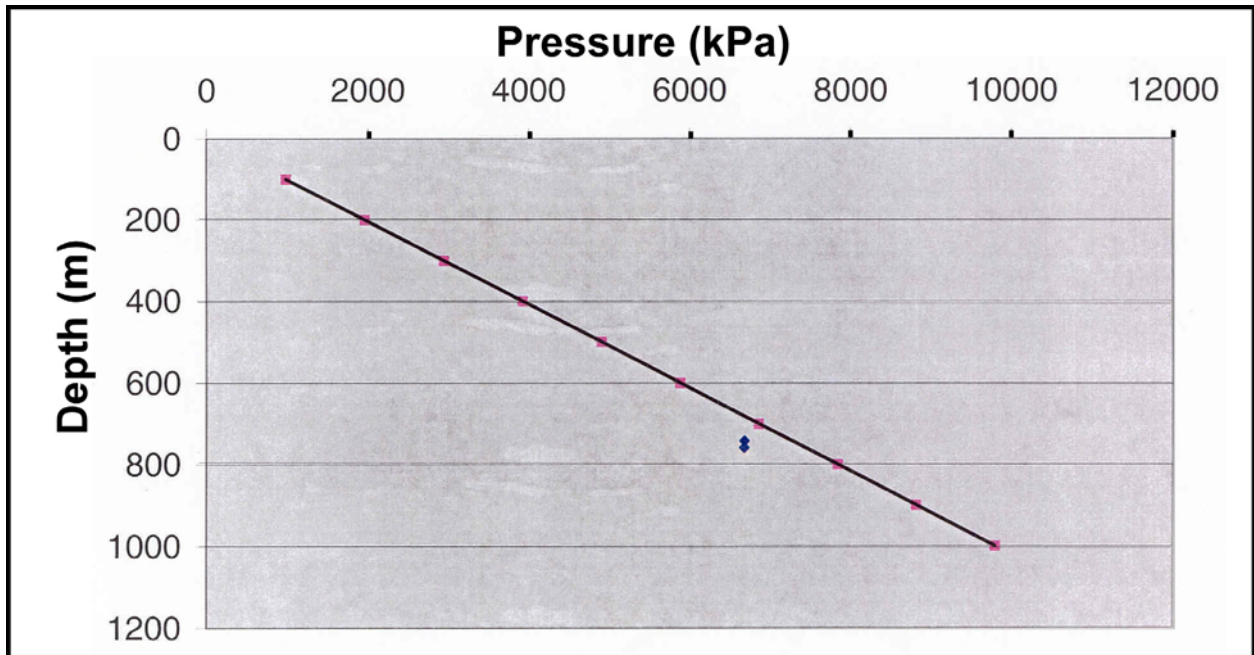


Figure 75. Formation pressure versus depth, MU and MI coal subzones, well 02/11-06-056-19W5/0, Edson coalbed methane exploration block.

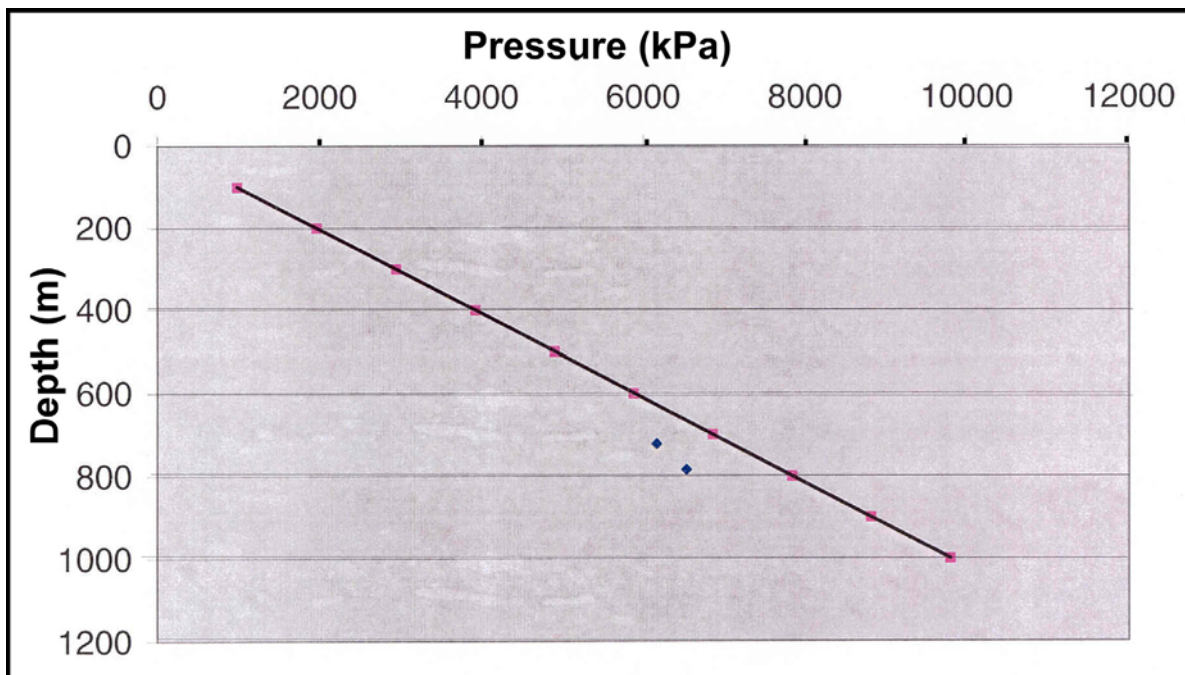


Figure 76. Formation pressure versus depth, Val D'Or, Arbour and Silkstone coal subzones, well 00-10-16-048-14W5/0, Pembina coalbed methane exploration block.

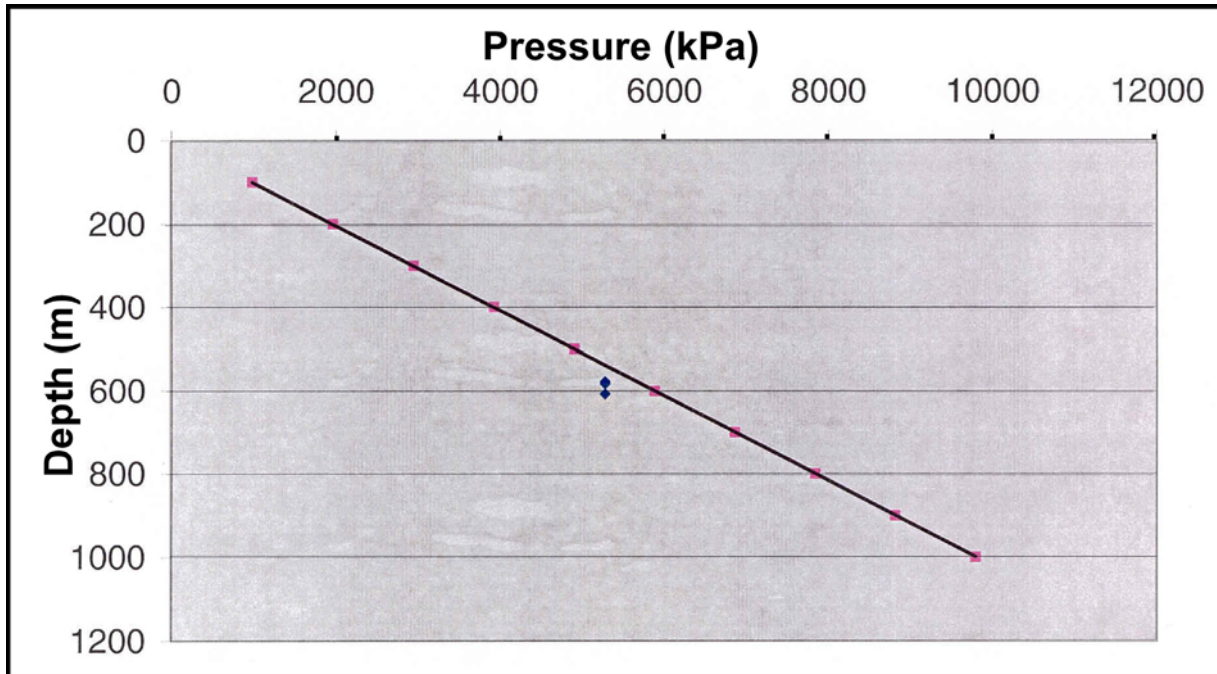


Figure 77. Formation pressure versus depth, 'S', 'Ml' and 'N' coal subzones, well 00/11-01-056-19W5/0, Edson coalbed methane exploration block.

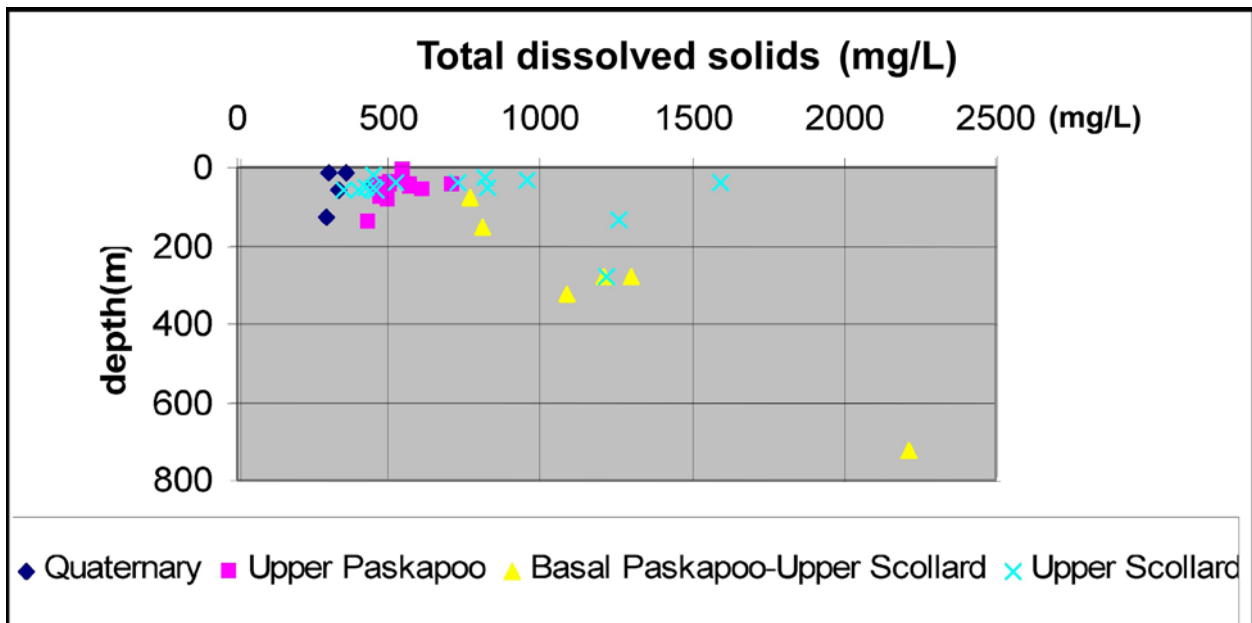


Figure 78. Total dissolved solids (TDS), Quaternary, Paskapoo and Scollard succession, regional data.

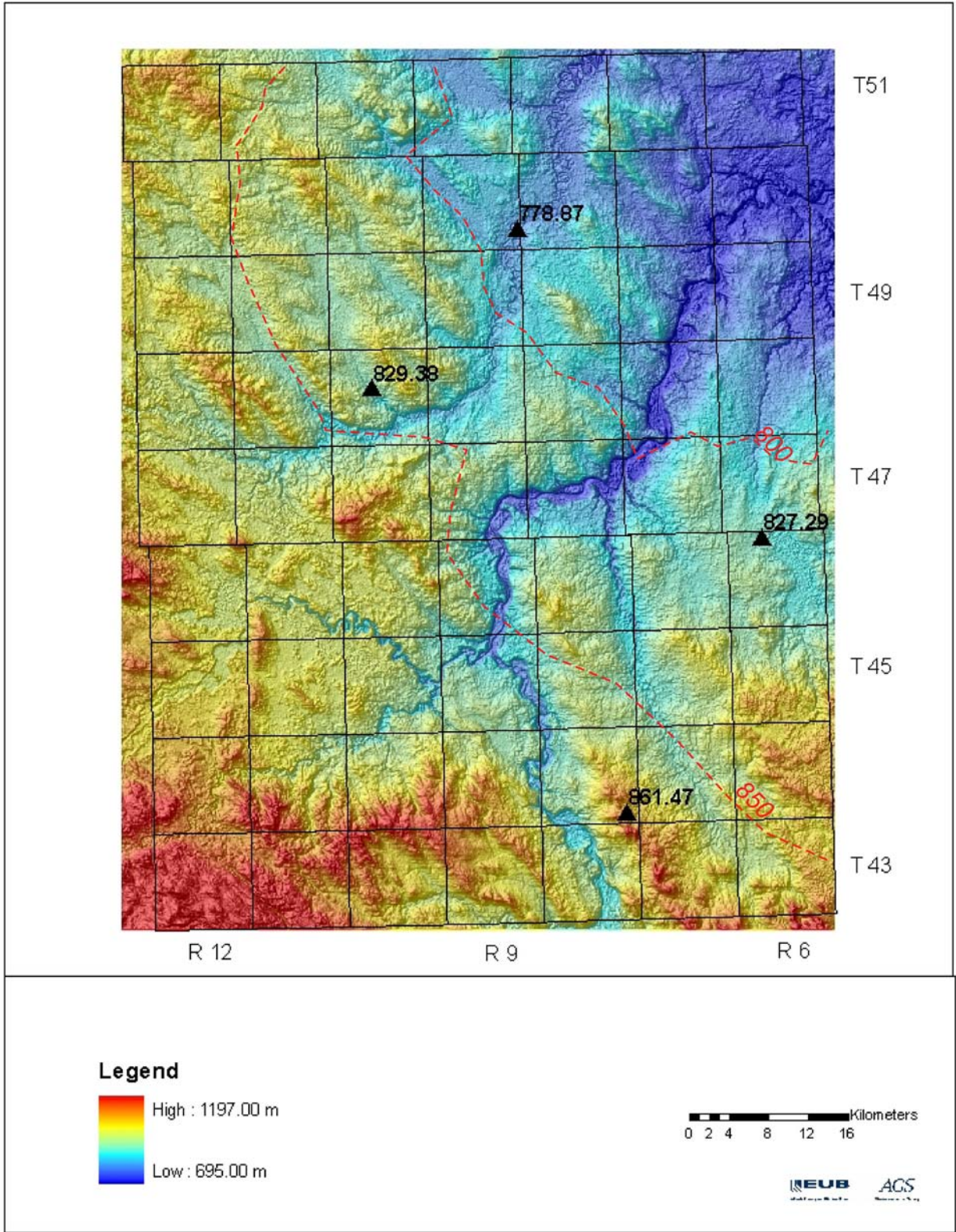


Figure 79. Potentiometric surface, Paskapoo Formation, Pembina study area.

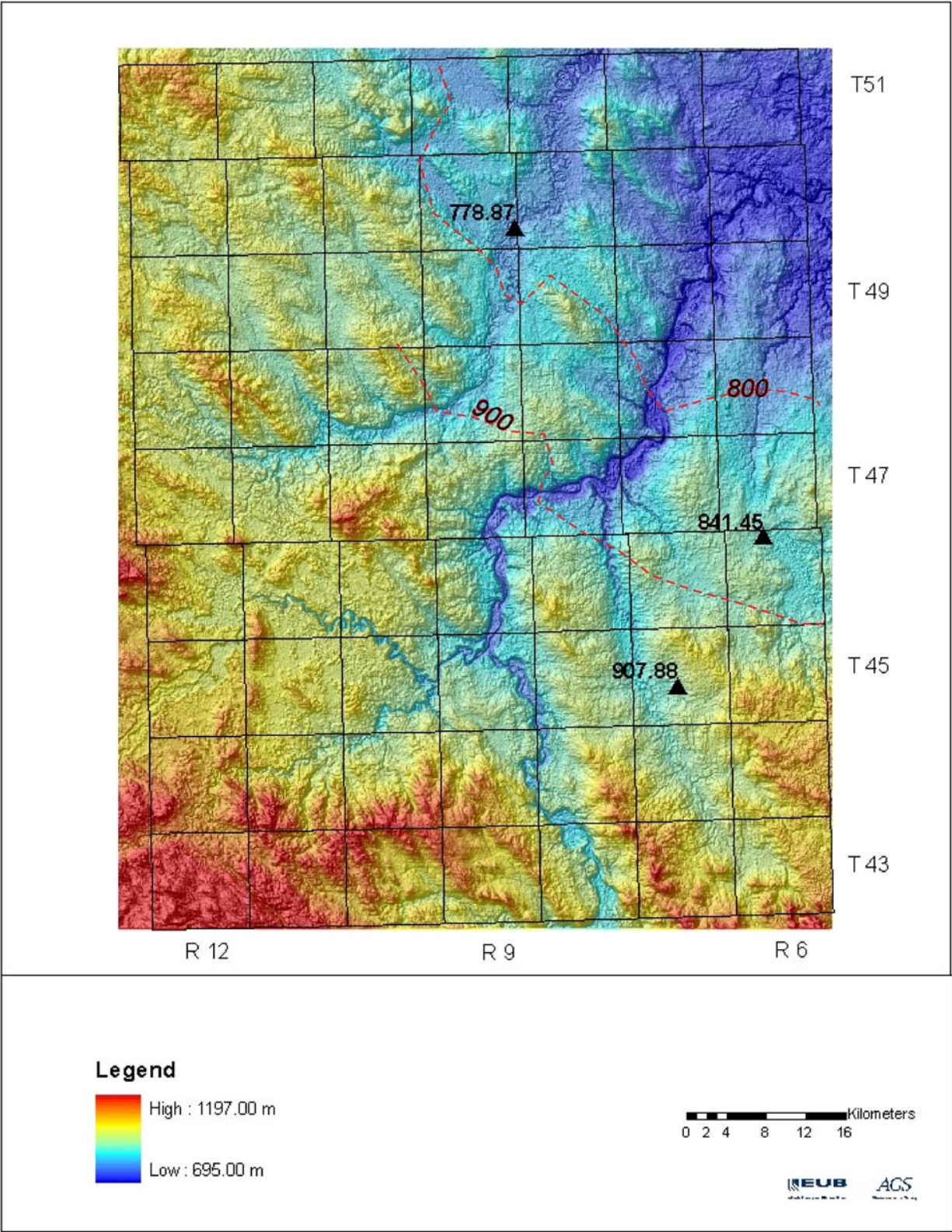


Figure 80. Potentiometric surface, Scollard Formation, Pembina study area.

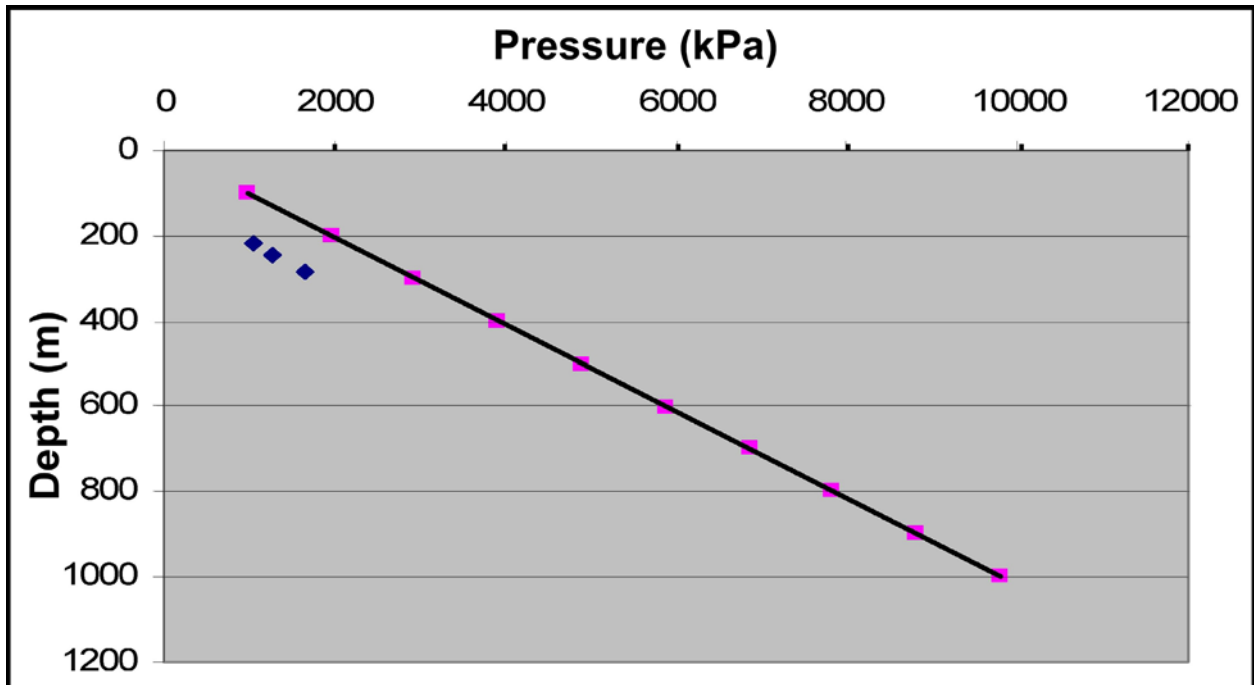


Figure 81. Formation pressure versus depth, Paskapoo Formation, Pembina study area. Trend line represents equivalent freshwater hydrostatic pressures.

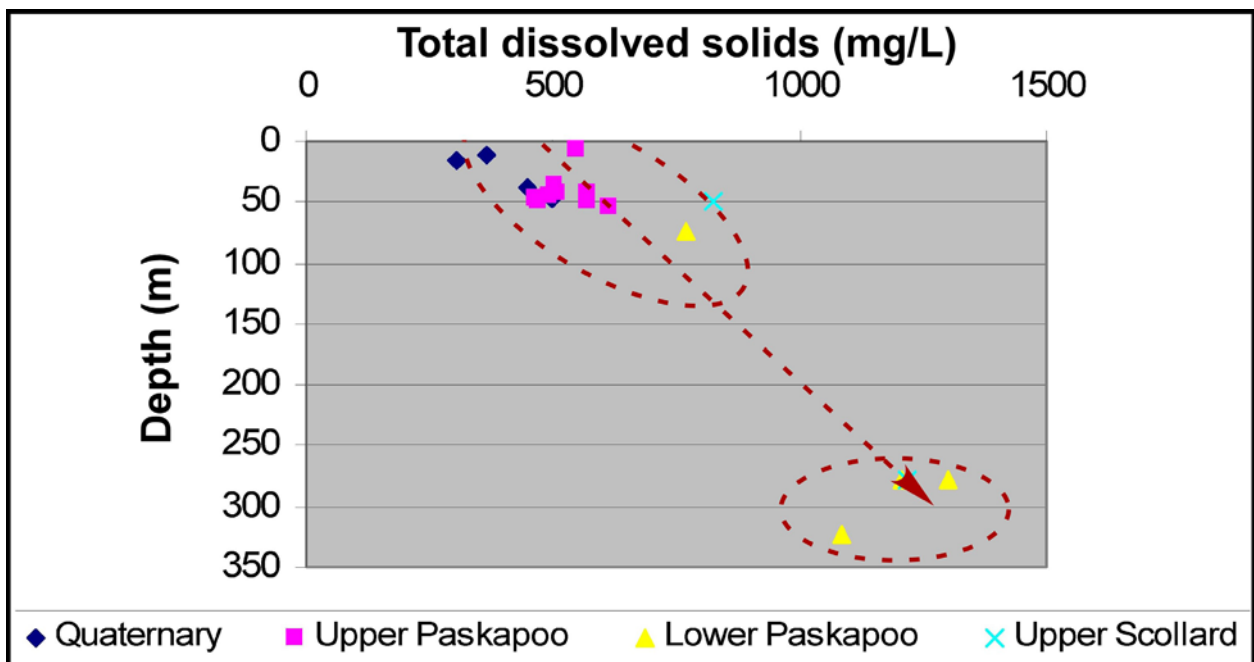


Figure 82. Total dissolved solids (TDS), Pembina study area.

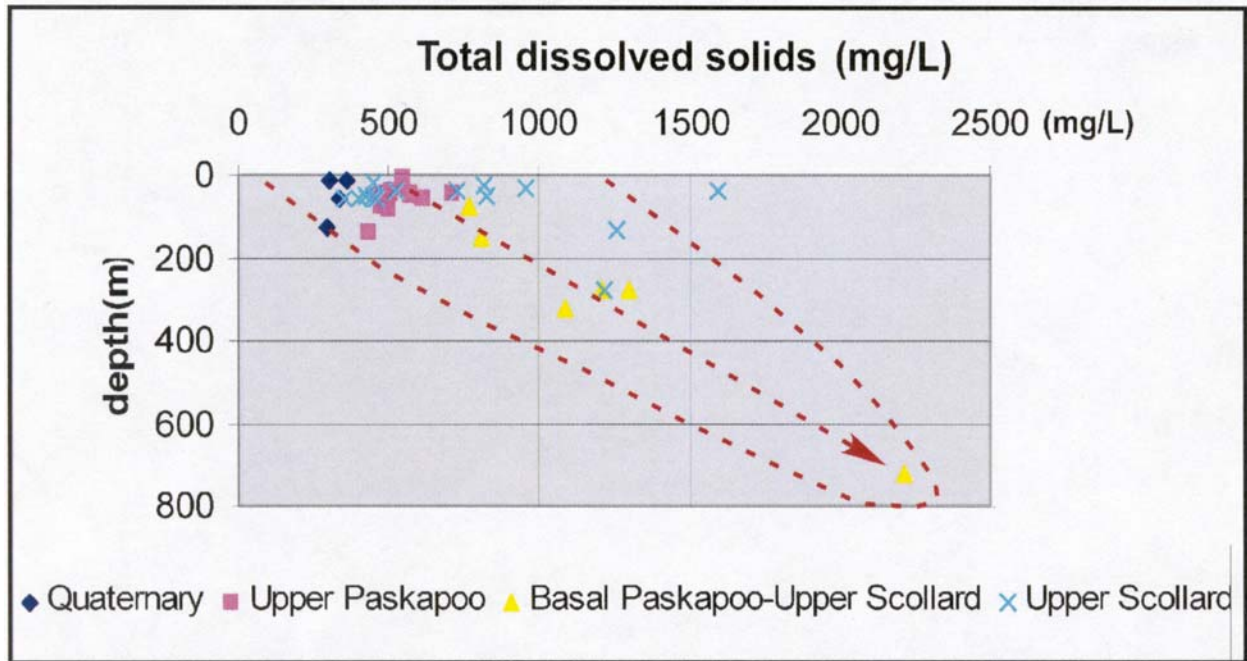


Figure 83. Total dissolved solids (TDS), regional data including the TDS trend.

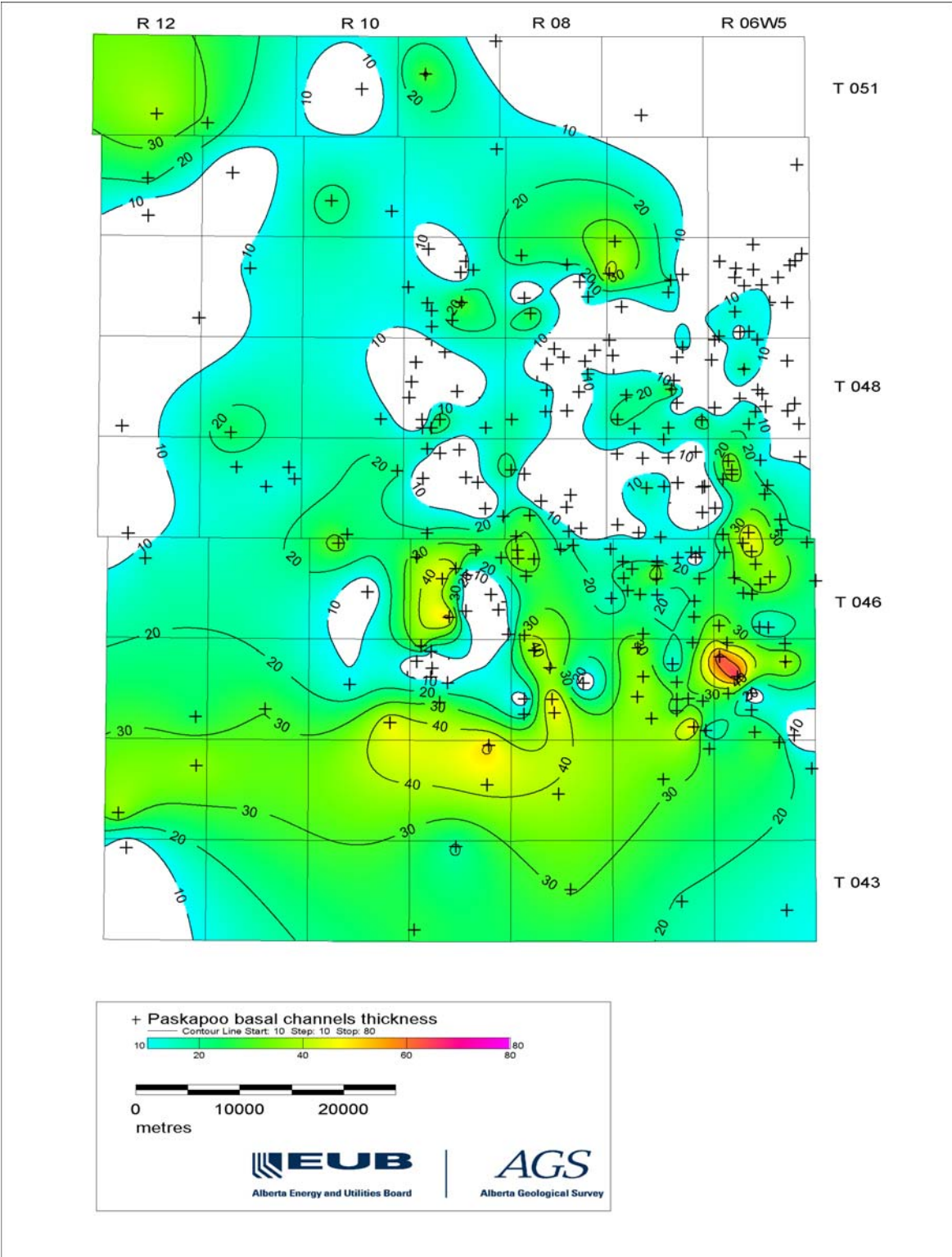


Figure 84. Isopachs of the Paskapoo basal sandstone channels (>10 m), Pembina study area.

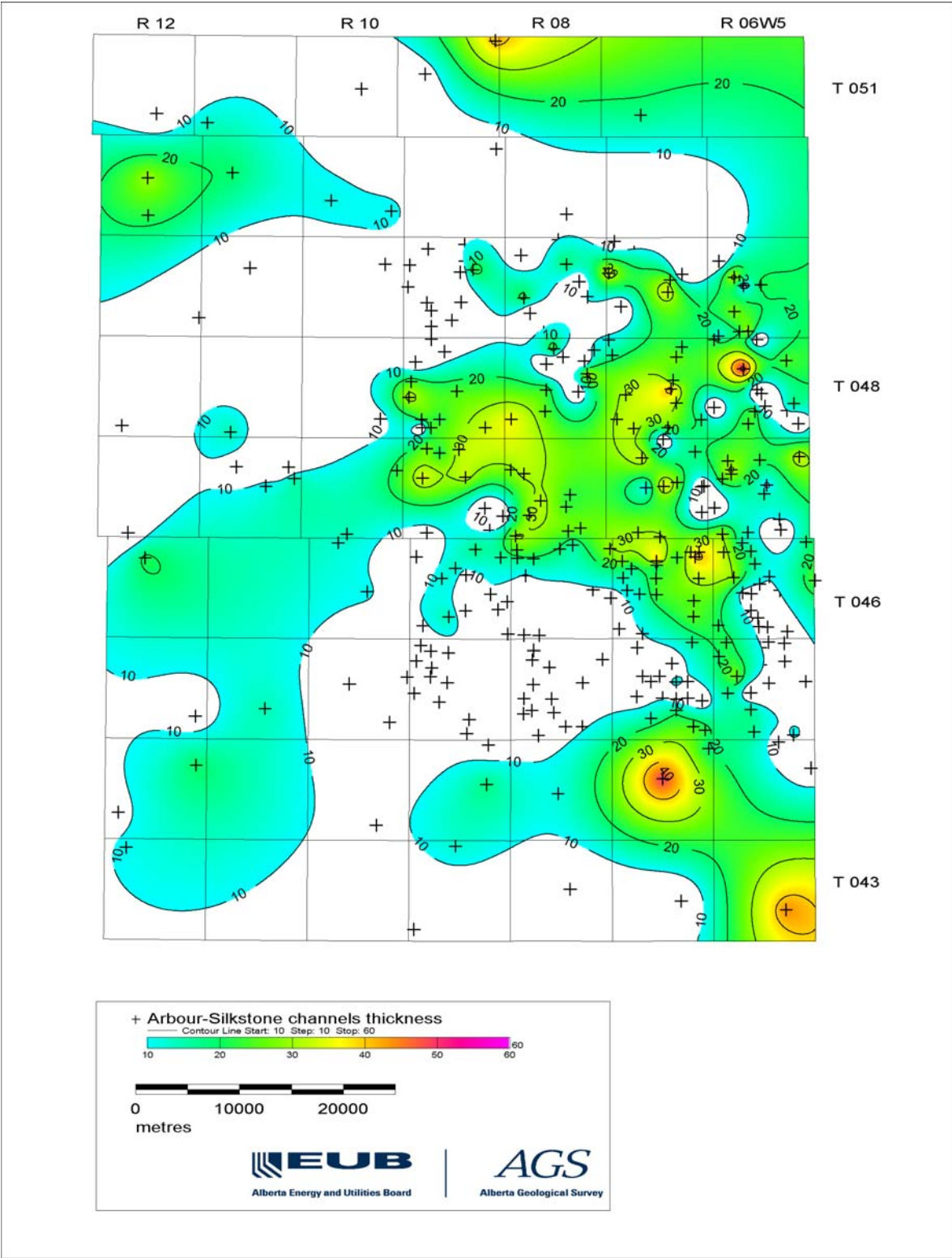


Figure 85. Isopachs of the Arbour-Silkstone sandstone channels (>5 m), Pembina study area.

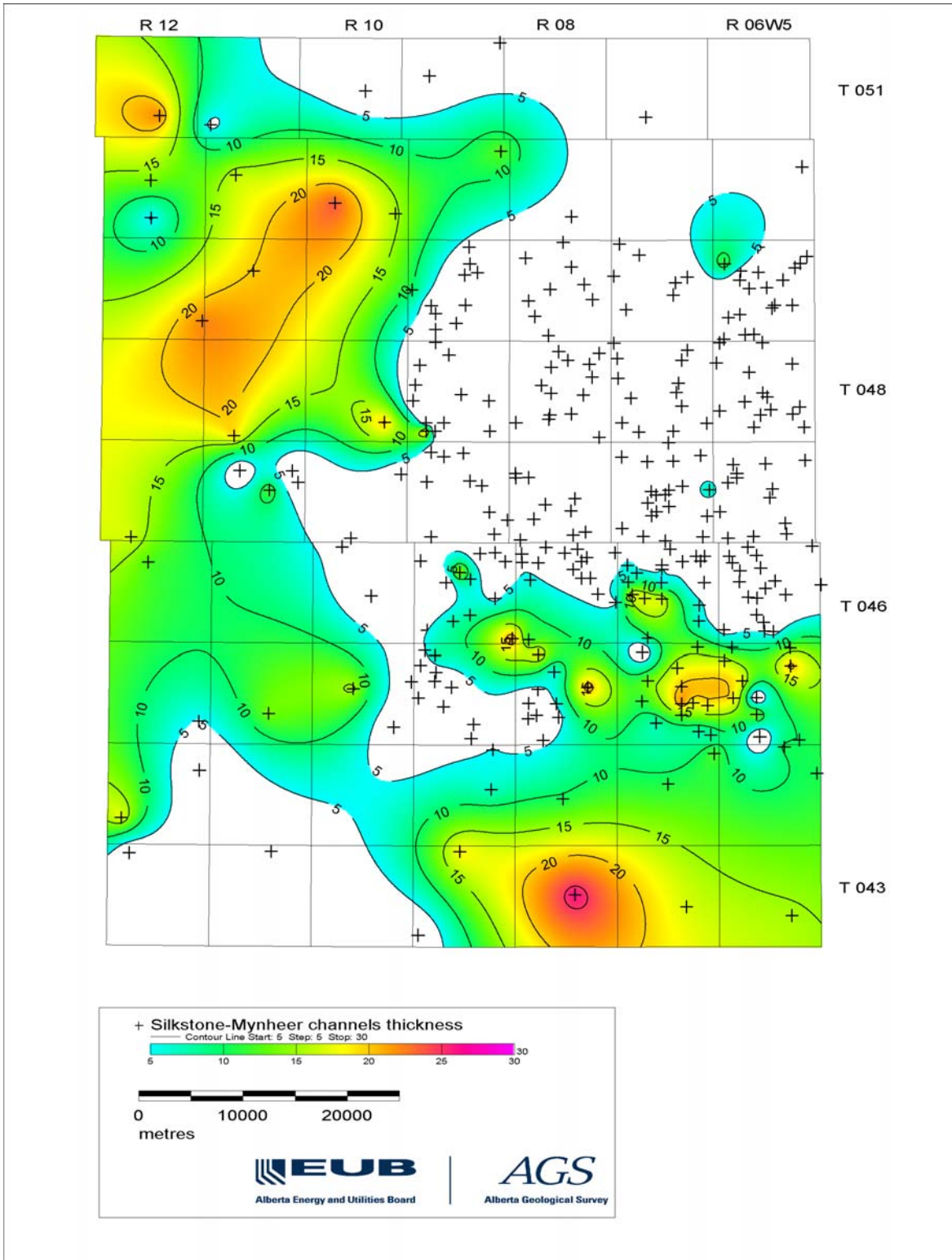


Figure 86. Isopachs of the Silkstone-Mynheer sandstone channels (>5 m), Pembina study area.

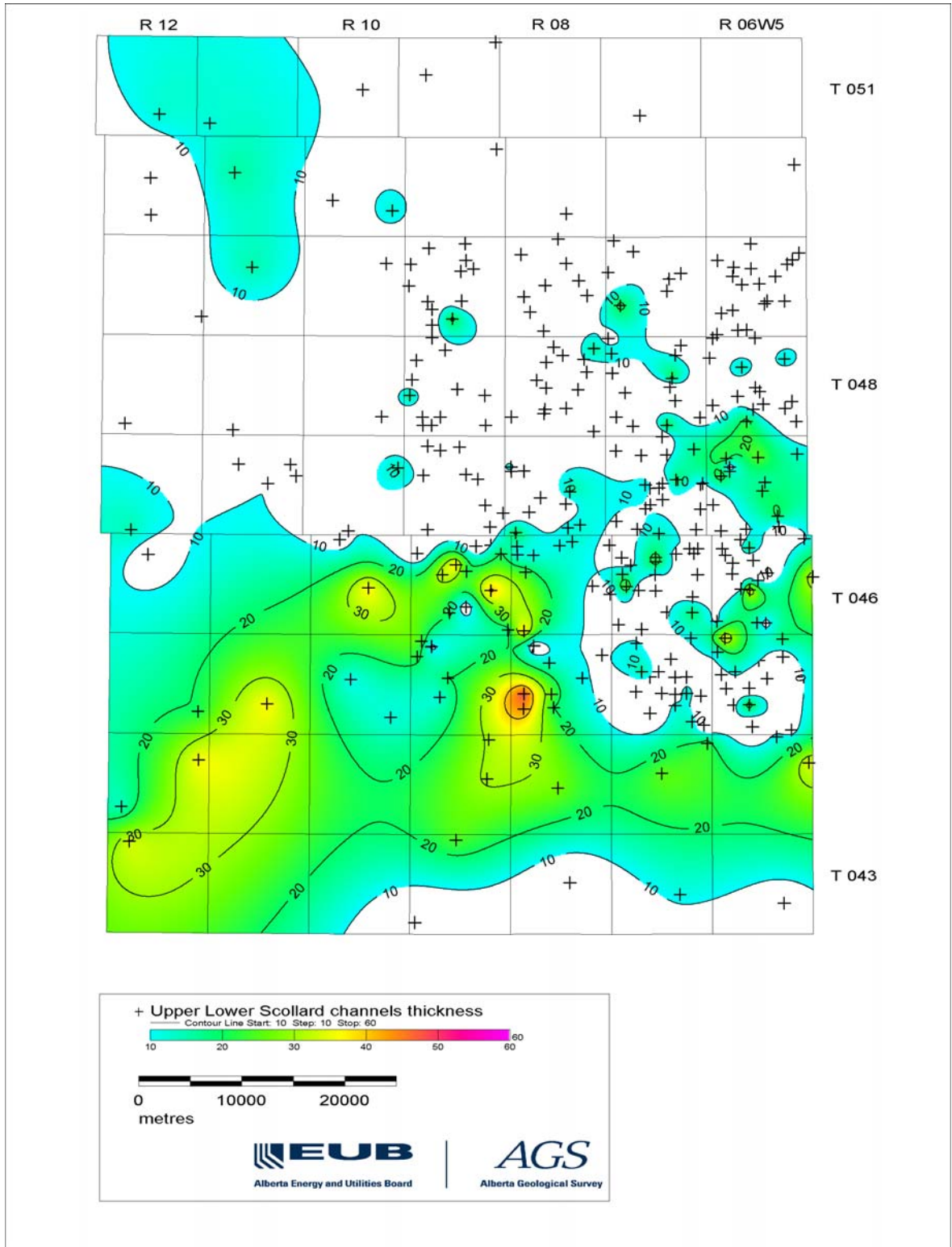


Figure 87. Isopachs of the upper sandstone channels (>5 m) of the lower Scollard Formation, Pembina study area.

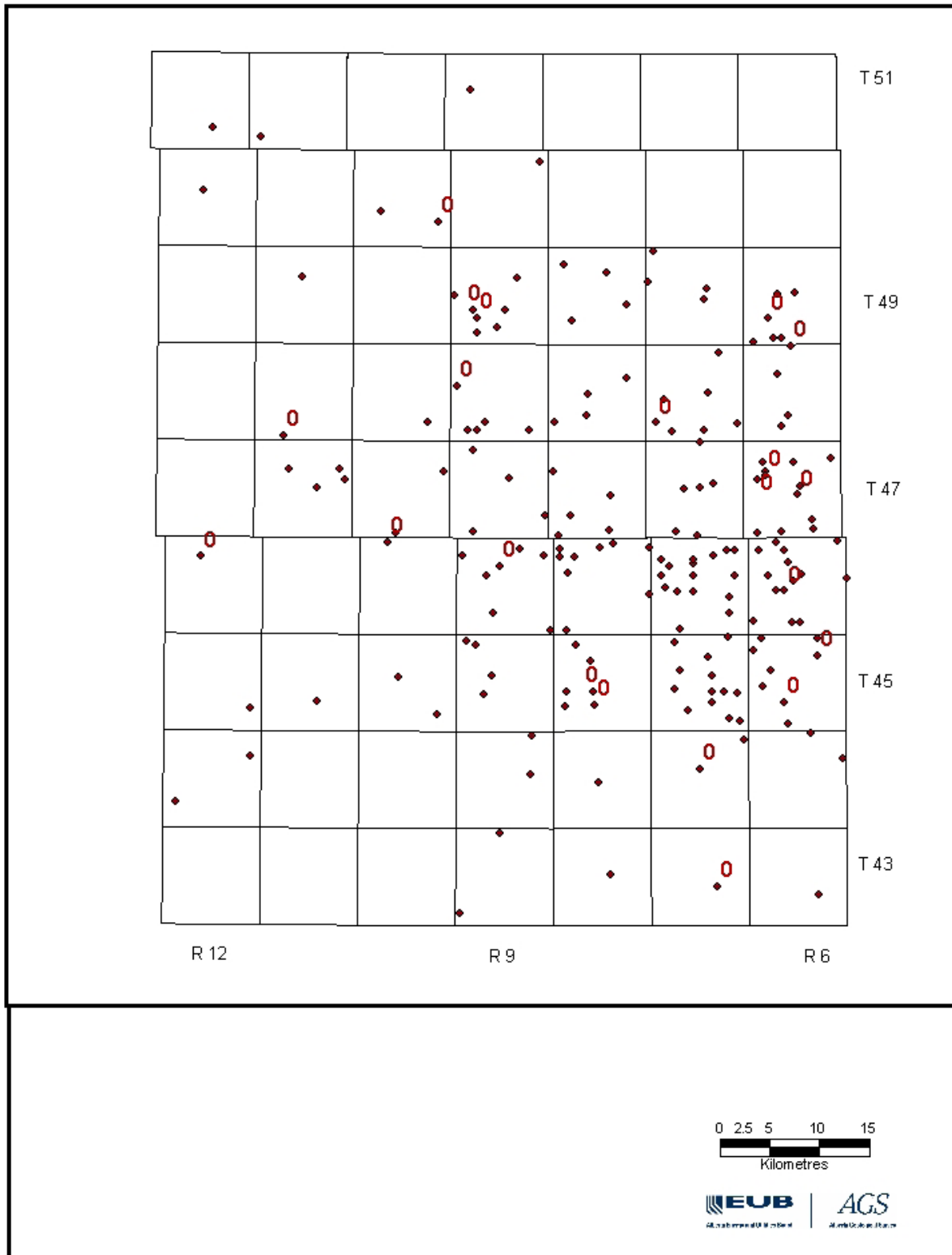


Figure 88. Locations where Paskapoo basal channels are in direct contact with the uppermost Ardley coal seams (indicated in red), Pembina study area.

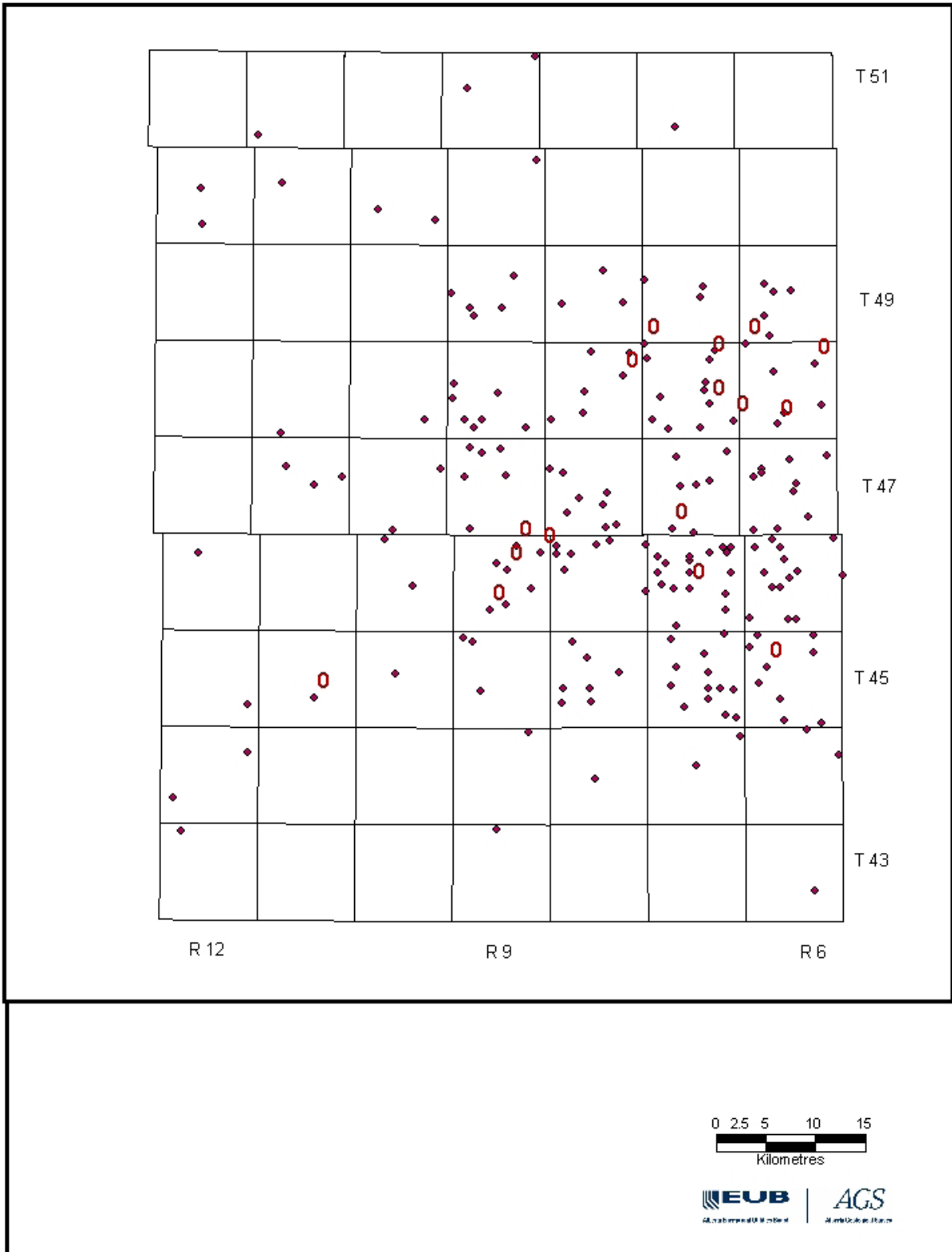


Figure 89. Locations where Arbour-Silkstone channels are in direct contact with the Silkstone coal seams (indicated in red), Pembina study area.

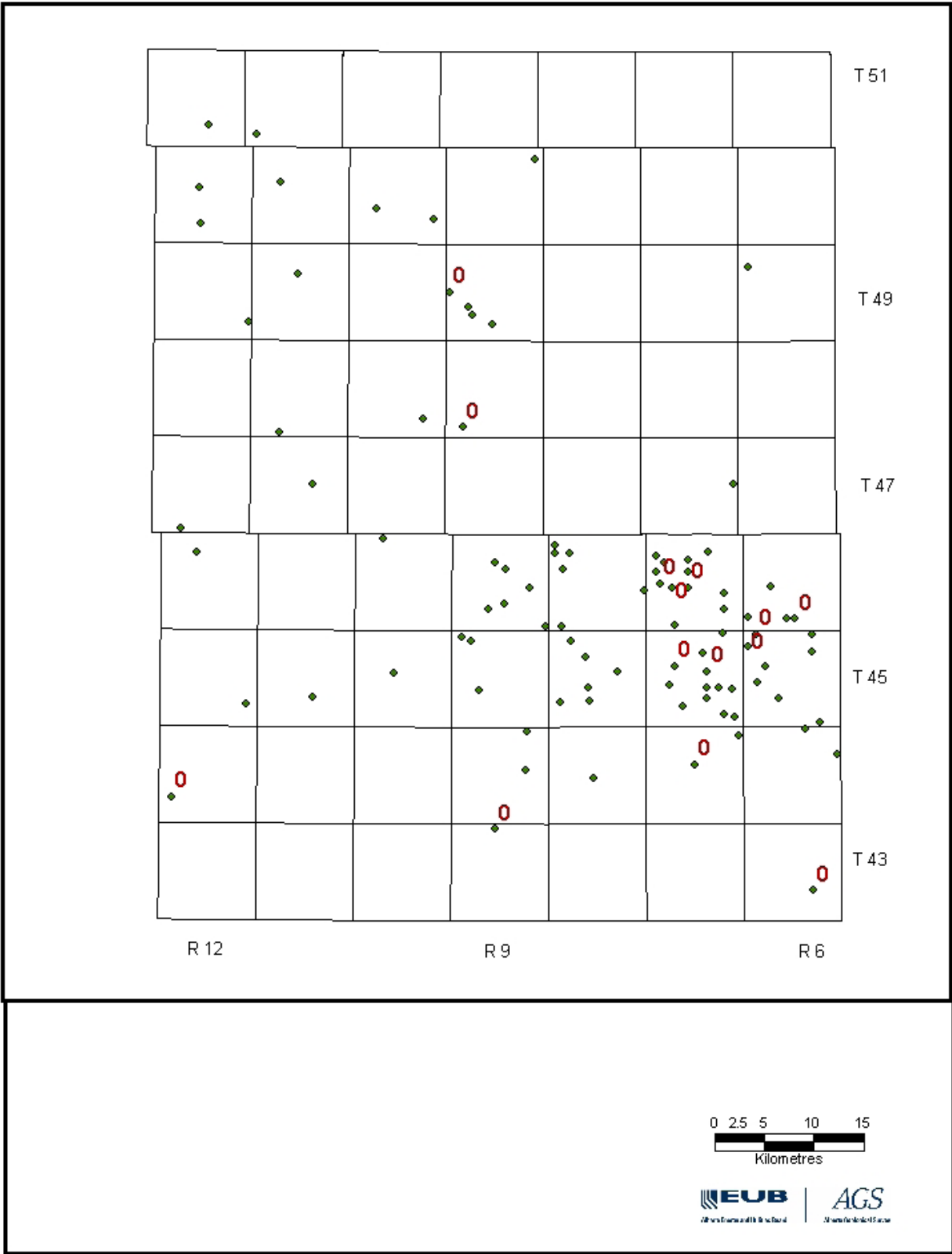


Figure 90. Locations where upper channels are in direct contact with the lowermost Mynheer coal seams (indicated in red), Pembina study area.

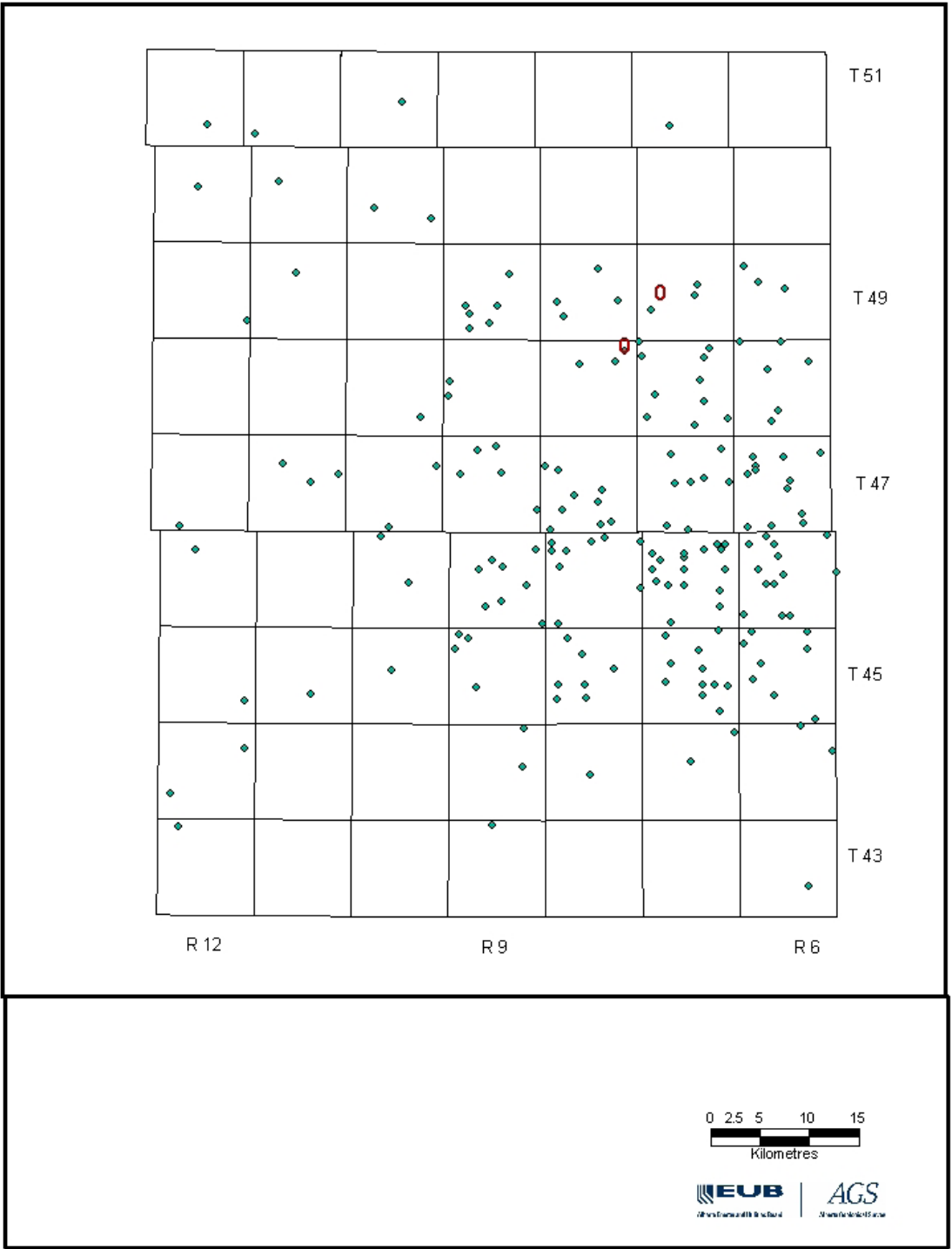


Figure 91. Locations where Silkstone-Mynheer channels are in direct contact with the Mynheer coal seams (indicated in red), Pembina study area.

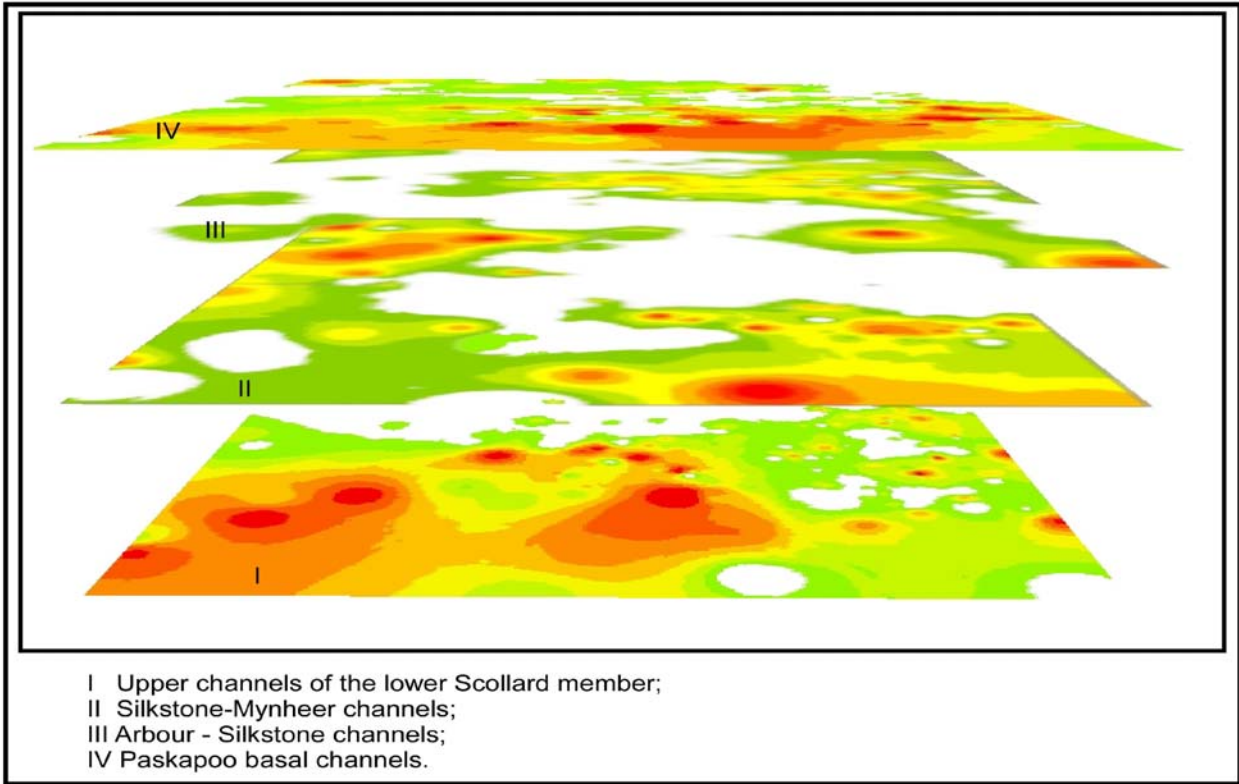


Figure 92. Three-dimensional image of the channel succession, Pembina study area.

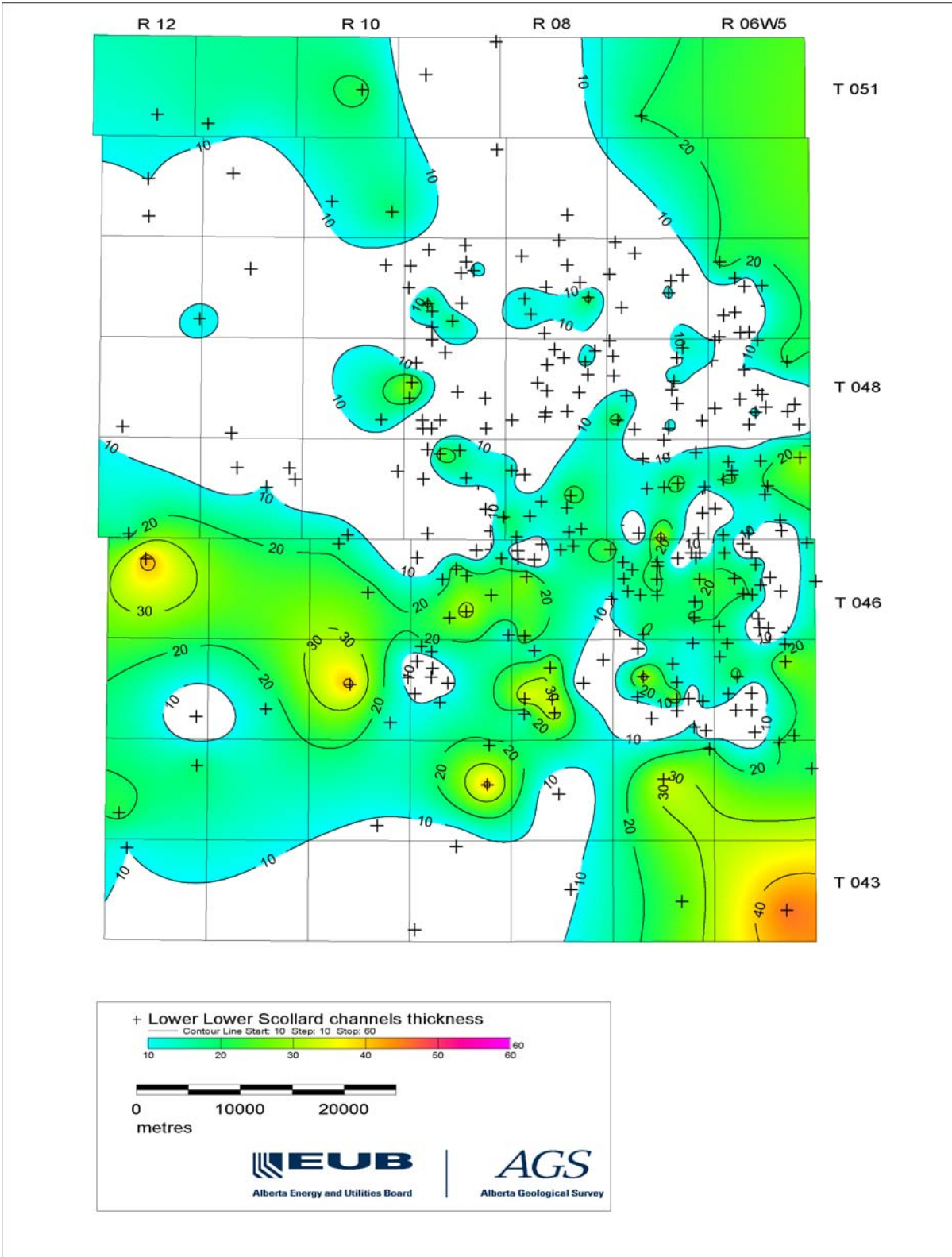


Figure 93. Isopachs of the lower channels of the lower Scollard Formation, Pembina study area.

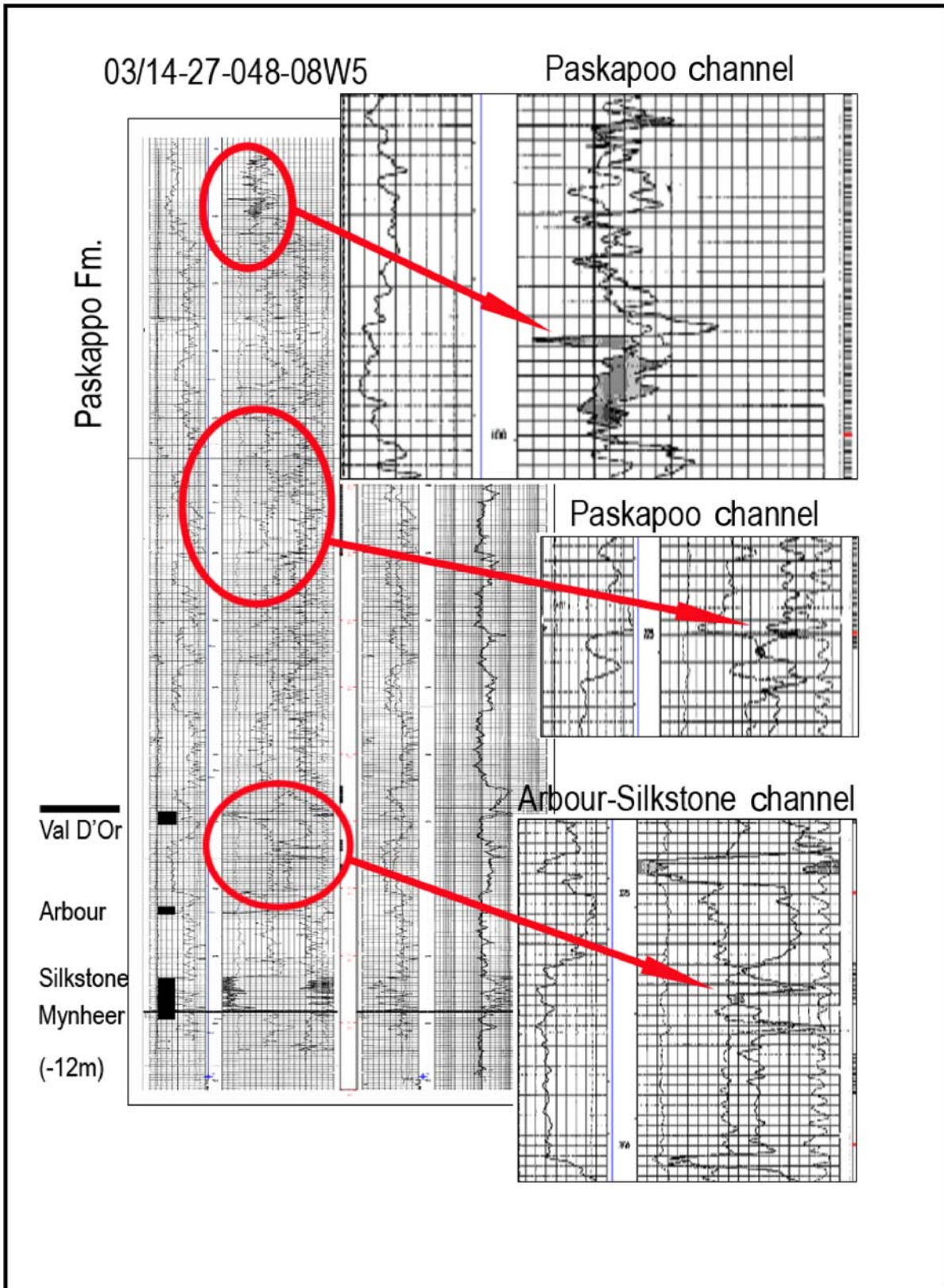


Figure 94. Multiple small gas accumulations in the basal Paskapoo and Arbour-Silkstone sandstone channels, well 03/14-27-048-08W5, Pembina study area.

00/16-16-044-08W5

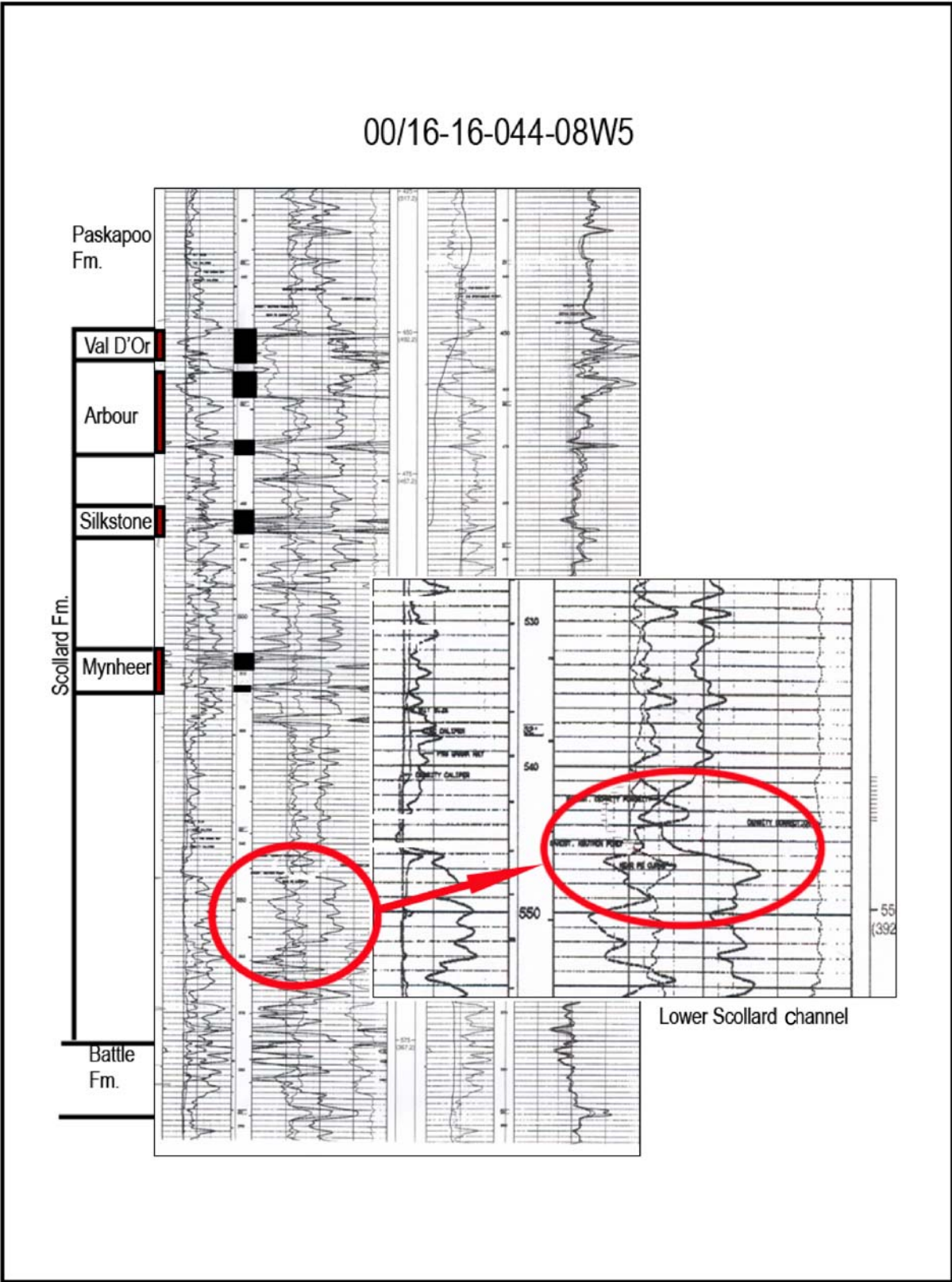
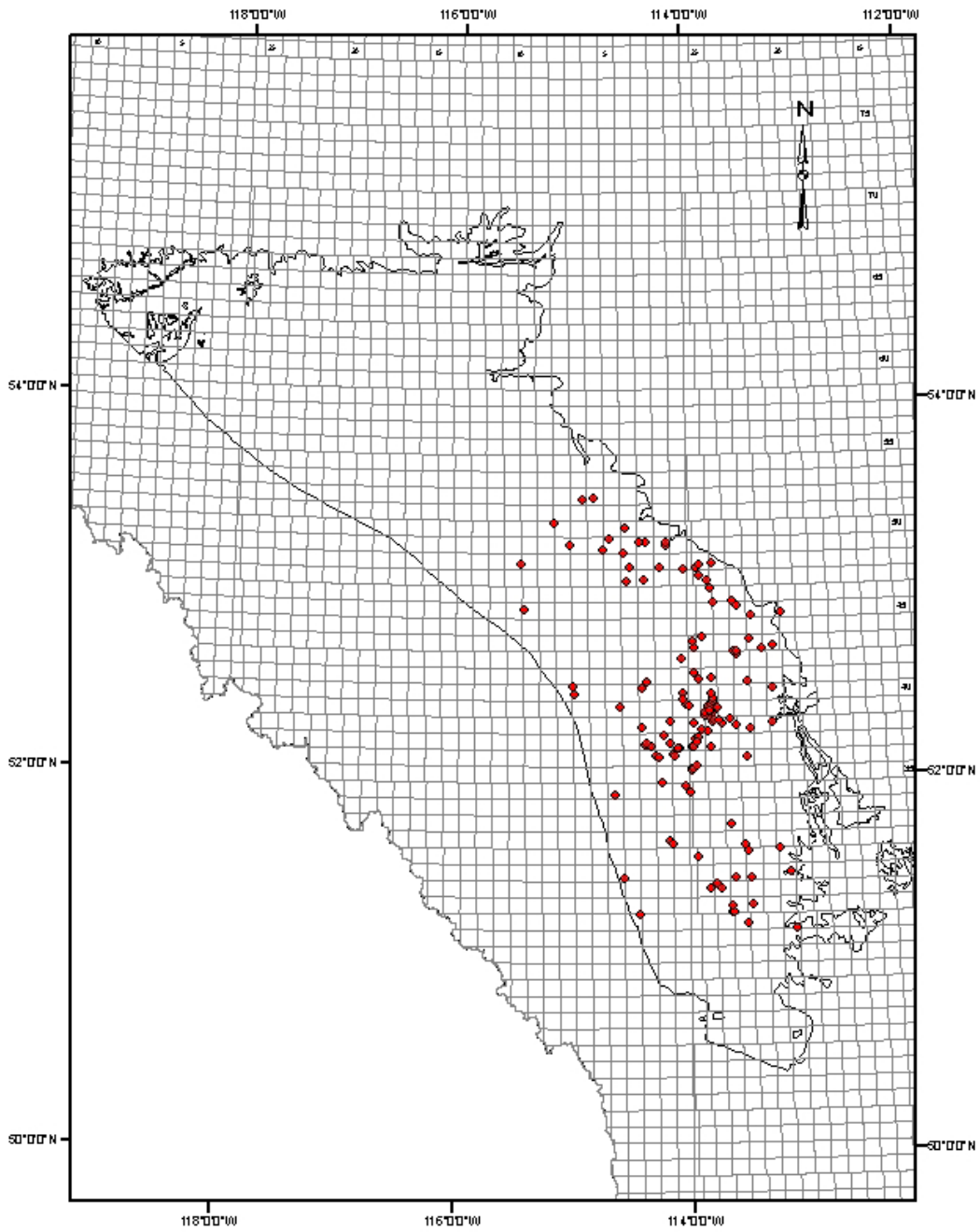


Figure 95. Small gas accumulation in the lower sandstone channel of the Scollard Formation, Pembina study area.



Legend

- ◆ shallow gas well



Figure 96. Shallow gas wells map (Alberta Environment, 2005).

Appendix 2. Core Photographs

Plate 1

- Figure A Medium-grained lithic sandstone with oblong conglomerate pebbles of variable size (00/14-15-046-10W5/00, 458 m, base of Val D'Or-Arbour channel).
- Figure B Medium to fine-grained lithic sandstone with oblong conglomerate pebbles of variable size and rare associated coal streaks (02/10-10-047-07W5/00).
- Figure C Medium to fine-grained lithic sandstone with rare coal clasts (02/09B-26-047-11W5/00, 496 m, Arbour-Silkstone channel).
- Figure D Medium to fine-grained lithic sandstone with 2 cm thick of vitrain bands. (02/09B-26-047-11W5/00, 468 m, top of Arbour-Silkstone channel).
- Figure E Medium to fine-grained lithic sandstone interbedded with subparallel, thin, light grey silt beds associated with rare and fine dark grey shale; low-angle crossbedding (02/09B-26-047-11W5/00, 472 m, Arbour-Silkstone channel).
- Figure F Very fine grained lithic sandstone interbedded with rippled, laminar, dark grey shale (02/09B-26-047-11W5/00, 483 m, Arbour-Silkstone channel).
- Figure G Medium-grained, dark grey, burrowed sandy shale; possible lacustrine environment. (02/09B-26-047-11W5/00, 514 m, Silkstone-Mynheer channel).

Plate 2

- Figure A Medium to fine-grained lithic sandstone (00/14-15-046-10W5/00, 566 m, upper channel of the lower part of Scollard Formation).
- Figure B Medium to fine-grained lithic sandstone (00/14-15-046-10W5/00, 575 m, upper channel of the lower part of Scollard Formation).
- Figure C Erosional contact at the top of the Ardley coal zone (02/09B-26-047-22W5/00, 490 m, top of Silkstone coal subzone).
- Figure D Erosional contact at top of Ardley coal zone (00/14-15-046-10W5/00, 502 m).
- Figure E E1 – Longitudinal view of fining-upward thin unit; E2 – transverse view of conglomerate pebbles (00/14-15-046-10W5/00, 502 m, Paskapoo channel).

Plate 3

- Figures A, B and C Light grey silty mudstone unit with rare root traces and coal streaks, more frequent towards the top (B and C; 02/10-10-047-07W5/00, paleosol unit within Val D'Or-Arbour interval).
- Figure D D1 – dark grey mudstone with slickensides; D2 – detail view of D1 (02/10-10-047-07W5/00, 379 m, top paleosol unit at base of Arbour coal subzone).
- Figure E Dark brownish grey, massive carbonaceous mudstone with preserved plant fragments (02/10-10-047-07W5/00, 436 m, top of Arbour coal subzone).
- Figure F Slickensides in dull coal (02/09B-26-047-11W5/00, 536 m, Mynheer coal subzone).
- Figure G Slickensides in banded dull coal (00/14-15-046-10W5/00, 507 m, Arbour coal subzone).

Plate 4

- Figure A (core and detail view) A1 – siltstone-mudstone succession (02/09B-26-047-11W5/00, 433–436 m, base of Paskapoo Formation); A2 – mudstone unit with root traces (top paleosol unit).
- Figure B (core view) Siltstone-mudstone succession, with root traces and slickensides becoming more frequent towards the top (top paleosol unit; 02/09B-26-047-11W5/00, 437–438 m).
- Figure C C1 – fragment of carbonaceous mudstone; C2 – core view of succession of mudstone (paleosol unit) and coal (02/09B-26-047-11W5/00, 438–440 m, top of Val D'Or coal subzone and 442–444m, base of Val D'Or coal subzone).
- Figure D Detailed view of dark brownish grey paleosol unit with gradual increase in organic matter, both showing slickensides (02/09B-26-047-11W5/00, 438 m).

Plate 5

- Figure A (external view of core) Banded dull coal alternating with banded bright coal intensely infilled with calcite (02/10-10-047-07W5/00, 427–430 m, Mynheer coal subzone).
- Figure B (external view of core) Banded coal (02/10-10-047-07W5/00, 427–430 m, Mynheer coal subzone).
- Figure C (inside view of core) Banded coal, banded dull and dull coal; mainly horizontal calcite infillings; good vertical open cleats (02/10-10-047-07W5/00, 370 m, Val D’Or coal subzone).
- Figure D D1 – inside view of the core; D2 – external view of the core. Banded bright coal; mainly horizontal calcitic infillings but also isolated vertical cleats infilled with calcite; good vertical open cleats (02/10-10-047-07W5/00, 370 m, Val D’Or coal subzone).
- Figure E (external view of core) Banded bright coal; rare and discontinuous cleats infilled with calcite; good vertical open cleats; amber granules (02/10-10-047-07W5/00, 427–430 m, Mynheer coal subzone).
- Figure F (internal and external view of core) Banded bright coal with mainly horizontal calcitic infillings (right) and banded coal (left; 02/10-10-047-07W5/00, 427–430 m, Mynheer coal subzone).
- Figure G (internal view of core) Dull coal with open vertical cleats (02/10-10-047-07W5/00, 427–430 m, Mynheer coal subzone).
- Figure H (internal view of core) Banded dull coal with mainly horizontal calcitic infillings (02/10-10-047-07W5/00, 427–430 m, Mynheer coal subzone).
- Figure I (internal view of core) Dull coal, banded coal and banded bright coal succession with isolated calcitic infillings; good vertical open cleats (02/10-10-047-07W5/00; 375–378 m; Arbour coal subzone).

Plate 6

- Figure A (external view of core) Banded bright coal (02/10-10-047-07W5/00, 429 m, Mynheer).
- Figure B (external view of core) Banded bright coal (02/10-10-047-07W5/00, 429 m, Mynheer).
- Figure C (external view of core) Banded and banded bright coal with open cleats more frequent within the banded bright coal interval (02/10-10-047-07W5/00, 429 m, Mynheer).
- Figure D (internal and external view of core) Banded and banded bright coal with rare but continuous open vertical cleats; more frequent short cleats are present within the banded bright coal interval (02/10-10-047-07W5/00, 429 m, Mynheer).
- Figure E (internal view of core) Banded coal and banded bright coal with more frequent vertical cleats within the bright banded coal interval (02/10-10-047-07W5/00, 429 m, Mynheer coal subzone)
- Figure F (external view of core) Banded bright coal showing linear face cleats which the aperture becomes wider within the higher organic intervals (02/10-10-047-07W5/00, 424 m, Silkstone coal subzone).
- Figure G (external view of core) Banded bright coal with vertical change into banded coal and banded dull coal showing linear face cleats which the aperture becomes wider within the higher organic intervals (02/10-10-047-07W5/00, 424 m, Silkstone coal subzone).

Plate 7

- Figure A (transverse and interior view of core fragment) Banded coal with open coal cleats and dull coal with no visible cleats (02/10-10-047-07W5/00, 429 m, Mynheer coal subzone).
- Figure B (exterior view of core) Banded bright coal with multiple horizontal and vertical calcite infillings (02/10-10-047-07W5/00, 427 m, Mynheer coal subzone).
- Figure C (exterior view of core) Banded bright coal with small vertical cleats and only minor calcite infillings (02/10-10-047-07W5/00, Arbour coal subzone).
- Figure D (exterior view of core) Banded coal and banded bright coal with small vertical cleats and only minor calcite infillings (02/10-10-047-07W5/00, 428 m, Mynheer coal subzone).

Figure E (exterior view of core) Banded coal and banded bright coal with small vertical cleats and only minor calcite infillings (02/10-10-047-07W5/00, 428 m, Mynheer coal subzone).

Figure F (exterior view of core) Banded bright coal with multiple horizontal calcite infillings grading into dull coal and coaly shale (02/10-10-047-07W5/00, 427 m, Mynheer coal subzone).

Plate 8

Figure A (interior view of the core fragment) Banded bright coal with vitrain lenses (00/14-15-046-10W5/00, 503 m, Val D'Or coal subzone).

Figure B (interior view of the core fragment) Banded coal (00/14-15-046-10W5/00, 503 m, Val D'Or coal subzone).

Figure C (transverse view of the core fragment) Bright coal with strong rectangular cleats and slickenside surface (00/14-15-046-10W5/00, 503 m, Val D'Or coal subzone).

Figure D (interior view of the core fragment) Banded bright coal and vitrain characterized by shiny lustre on irregular break surface (00/14-15-046-10W5/00, 503 m, Val D'Or coal subzone).

Figure E (exterior view of the core) Dark grey carbonaceous mudstone with fine and isolated fractures infilled with calcite perpendicular to bedding (00/14-15-046-10W5/00, 524 m, uppermost coal seam of Silkstone coal subzone).

Plate 9

Figure A (transverse view of core fragment) Rare but continuous face cleats at the fusain–dull coal interface (00/14-15-046-10W5/00, 504 m, Val D'Or coal subzone).

Figure B (transverse view of core fragment) Frequent face cleats (<1 cm interspaces) free of calcite recorded by a fusain layer (00/14-15-046-10W5/00, 504 m, Val D'Or coal subzone).

Figure C (transverse view of core fragment) Frequent face cleats (~1 cm interspaces) free of calcite within dull coal (02/10-10-047-07W5/00, 473 m, Val D'Or coal subzone).

Figure D (transverse view of core fragment) Rare face cleats (~3 cm interspaces) free of calcite recorded by a fusain layer (02/10-10-047-07W5/00, 429 m, Mynheer coal subzone).

Figure E (transverse view of core fragment) Rare face-cleats (~3 cm interspaces) free of calcite recorded by fine banded coal (00/14-15-046-10W5/00, 505 m, Val D'Or coal subzone).

Figure F (interior view of core fragment) 'Spider-web' fine system of calcite infillings (02/09B-26-047-11W5/00).

Figure G (transverse view of core fragment) Banded bright coal with thick (0.2 mm) calcite infillings (00/14-15-046-10W5/00, 526 m, Upper Silkstone coal seam).

Figure H (interior view of core fragment) Continuous print of vertical cleat within dull coal and shaly coal mostly free of calcite (02/10-10-047-07W5/00, 473 m, Val D'Or coal subzone).

Figure I (interior view of core fragment) Banded dull coal with continuous cleats free of calcite (02/10-10-047-07W5/00, Mynheer coal subzone).

Figure J (transverse view of core fragment) Frequent face cleats (<1 cm interspaces) free of calcite recorded by fusain layer (00/14-15-046-10W5/00, 503 m, Val D'Or coal subzone).

Plate 10

Figure A (inside view of core fragment) Banded bright coal with thick vitrain intervals (00/14-15-046-10W5/00, 535 m, base of Silkstone coal subzone).

Figure B (inside view of core fragment) Carbonaceous mudstone (00/14-15-046-10W5/00, 544 m, Mynheer coal subzone).

Figure C (inside view of core fragment) Banded coal with long vertical open cleats (00/14-15-046-10W5/00, 549 m, Mynheer coal subzone).

Figure D (inside view of core fragment) Banded bright coal with thick (~1 cm) bands of vitrain (00/14-15-046-10W5/00, 547 m, Mynheer coal subzone).

Figure E (exterior view of core fragment) Banded bright coal with longitudinal open cleats and an isolated lenticular area of calcite infilling in 'spider-web' system (00/14-15-046-10W5/00, 534 m, Silkstone coal subzone).

- Figure F (inside view of core fragment) Banded bright coal with thick bands of vitrain and local calcite infillings (00/14-15-046-10W5/00, 539 m, top of Mynheer coal subzone).
- Figure G (inside view of core fragment) Shaly coal (00/14-15-046-10W5/00, 544 m, Mynheer coal subzone).
- Figure H (transverse view of core fragment) Carbonaceous mudstone (00/14-15-046-10W5/00, Mynheer coal subzone).
- Figure I (exterior view of core fragment) Mudstone–shaly coal contact (00/14-15-046-10W5/00, 550 m, Mynheer coal subzone).

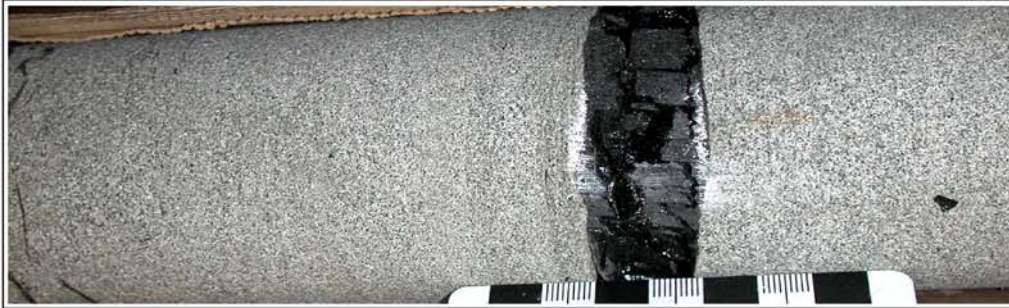
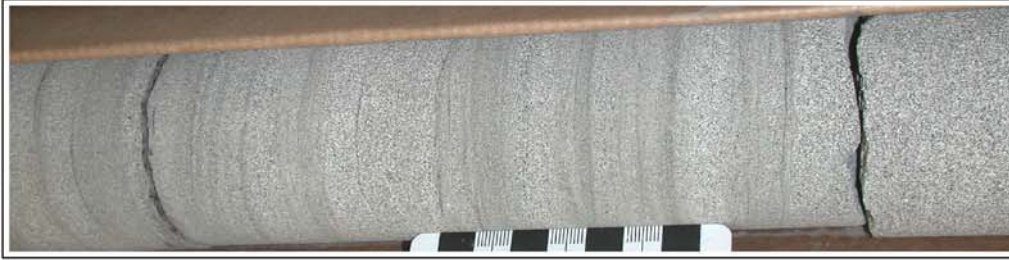
Plate 11

- Figure A (external and inside view of core fragment) Banded bright coal with multiple, small, open vertical cleats and isolated intervals of calcite infilling (02/10-10-047-07W5/0, 371 m, Val D'Or coal subzone).
- Figure B (inside view of core fragment) Banded coal with open vertical cleats and isolated intervals of calcite infilling (02/10-10-047-07W5/0, 375 m, Arbour coal subzone).
- Figure C (external view of core fragment) Banded bright coal with multiple, small, open vertical cleats and isolated intervals of calcite infilling (02/10-10-047-07W5/0, 371 m, Val D'Or coal subzone).
- Figure D (inside view of core fragment) Dull coal and banded dull coal in gradual transition (02/10-10-047-07W5/0, 375 m, Arbour coal subzone).
- Figure E (inside view of core fragment) Banded bright coal with multiple open vertical cleats and isolated intervals of calcite infilling (02/10-10-047-07W5/0, 371 m, Val D'Or coal subzone).
- Figure F (external view of core fragment) Banded bright coal with multiple, small, open vertical cleats and isolated intervals of calcite infilling (02/10-10-047-07W5/0, 424 m, Silkstone coal subzone).
- Figure G (external view of core fragment) Gradational transition from dull coal to banded coal to carbonaceous mudstone to mudstone (02/10-10-047-07W5/0, 429 m, Mynheer coal subzone).
- Figure H (inside view of core fragment) Banded coal and banded dull coal with open cleats (02/10-10-047-07W5/0, 374 m, Arbour coal subzone).
- Figure I (external view of core fragment) Banded bright coal with multiple, small, open vertical cleats and isolated intervals of calcite infilling (02/10-10-047-07W5/0, 424 m, Silkstone coal subzone).
- Figure J (external view of core fragment) Banded coal with open vertical cleats and isolated intervals of calcite infilling (02/10-10-047-07W5/0, 424 m, Silkstone coal subzone).
- Figure K (inside view of core fragment) Dull coal and banded dull coal (02/10-10-047-07W5/0, 423 m, Silkstone coal subzone).
- Figure L (inside view of core fragment) Shaly coal with distinguishable big plant cells (02/10-10-047-07W5/0, 430 m, Mynheer coal subzone).

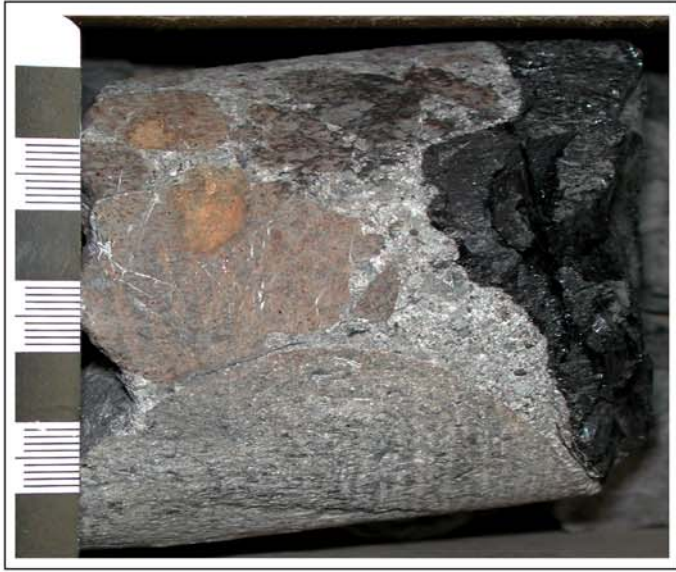
Plate 12

- Figure A (external view of core fragment) Shaly coal consisting of interbedded thin coal layers and mudstone (00/14-15-046-10W5, 375 m, Arbour coal subzone).
- Figure B (external view of core fragment) Coal-tonstein contact (02/09B-26-047-11W5/00, 427 m, Mynheer coal subzone).
- Figure C (external view of core fragment) Coal-tonstein contact (02/10-10-047-07W5/00, 427–432 m, Mynheer coal subzone).
- Figure D (external view of core fragment) Thin tonstein layer within coal (02/10-10-047-07W5/00, 427–432 m, Mynheer coal subzone).
- Figure E (external view of core fragment) Coal-tonstein contact (02/10-10-047-07W5/00, 376 m, Arbour coal subzone).

- Figure F (external view of core fragment) Shaly coal (00/14-15-046-10W5/00, 526 m, uppermost coal seam of Silkstone coal subzone).
- Figure G (external view of core fragment) Tonstein layer interpreted as Arbour top marker (02/10-10-047-07W5/00, 374 m, Arbour coal subzone).



A





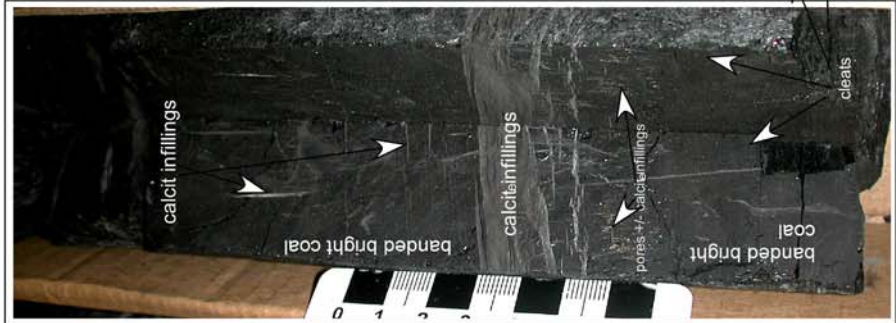


A2



A1





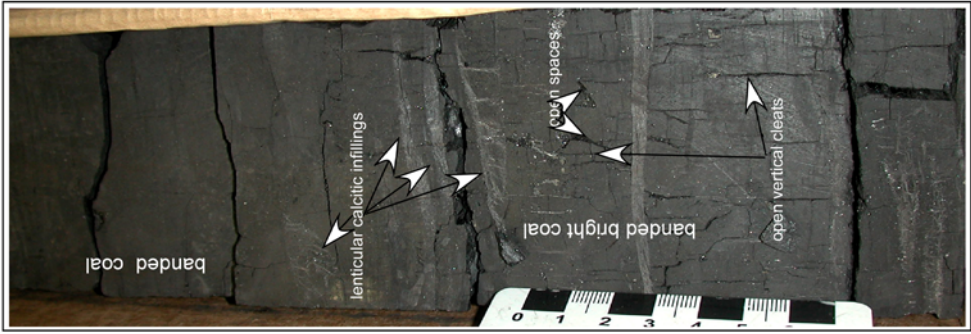
D2

D1

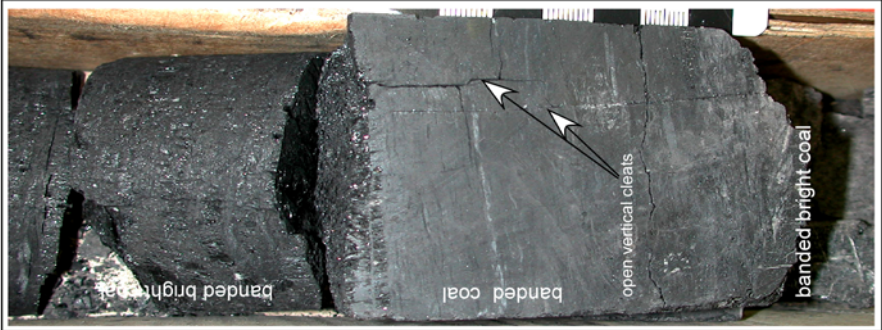
C

B

A



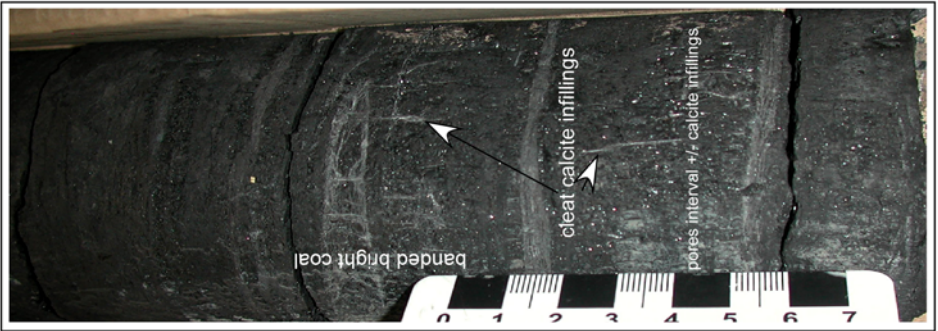
D



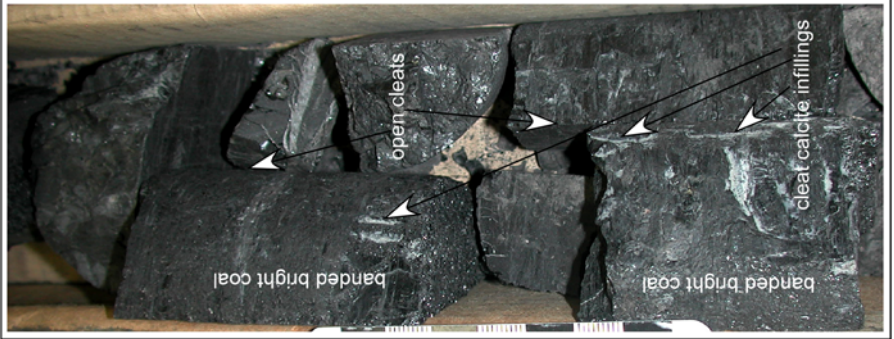
C



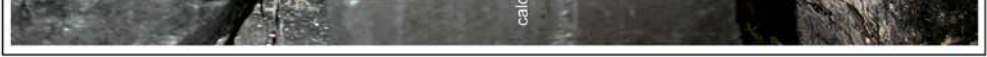
B



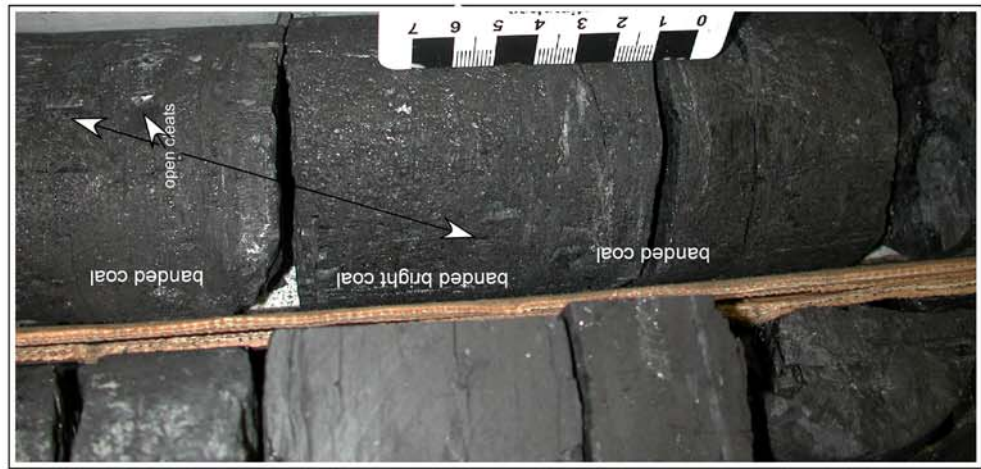
A



E



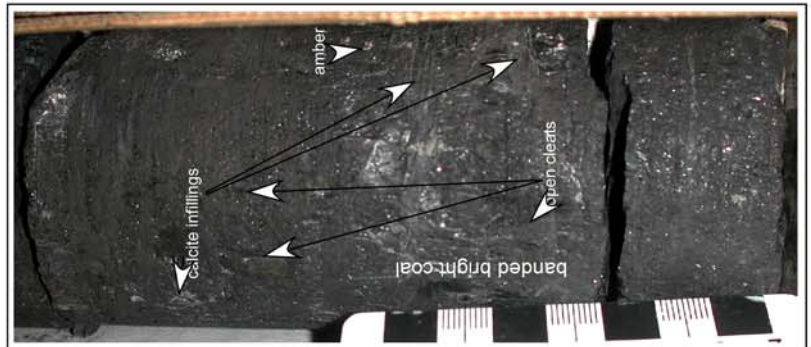
E



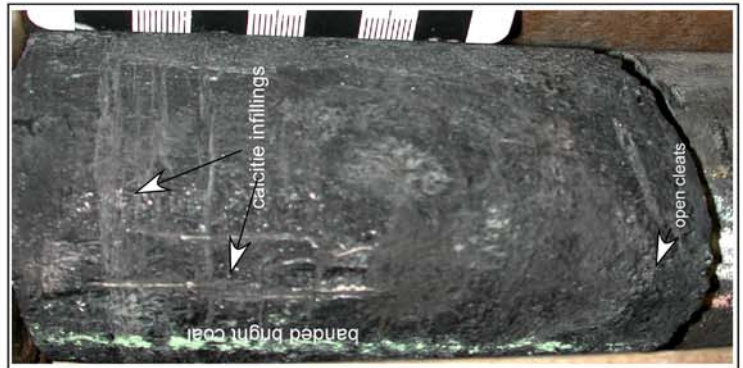
D



C



B

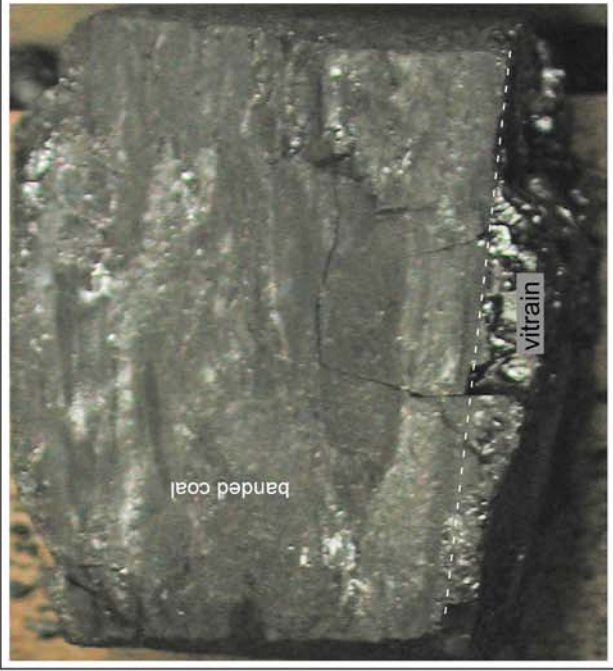


A

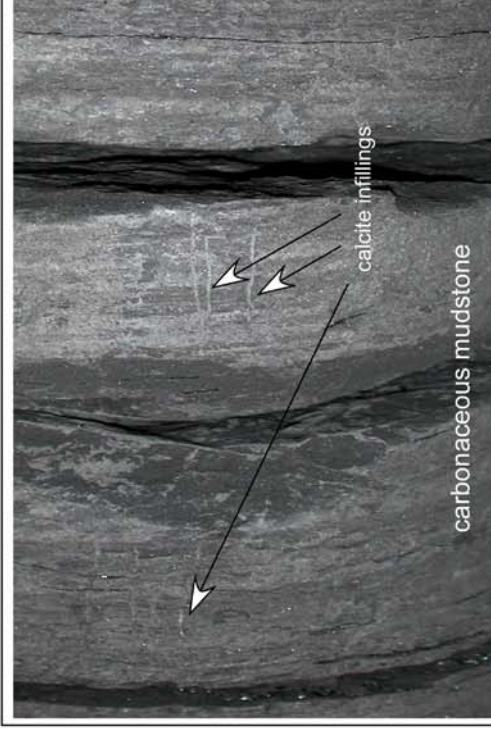
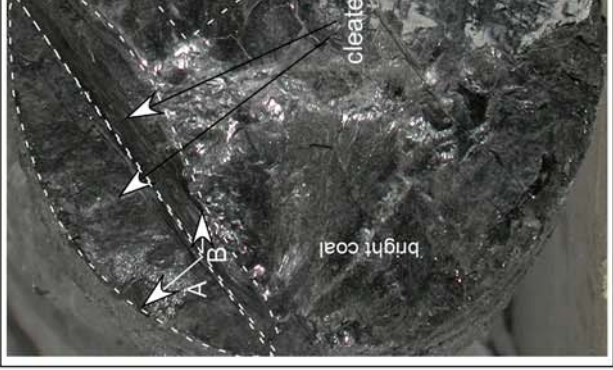


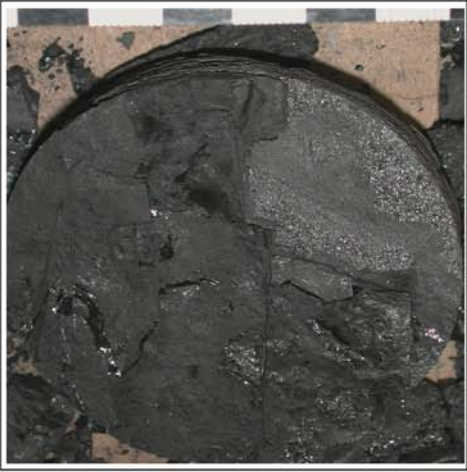


A



B





A



B



D



E



F

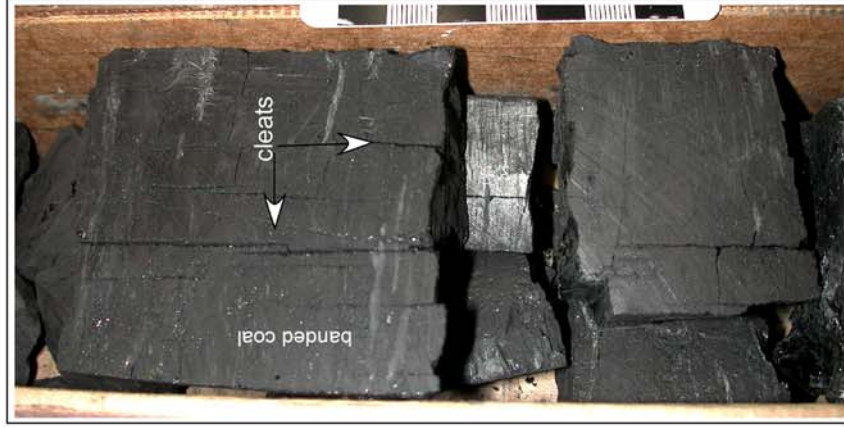




A



B



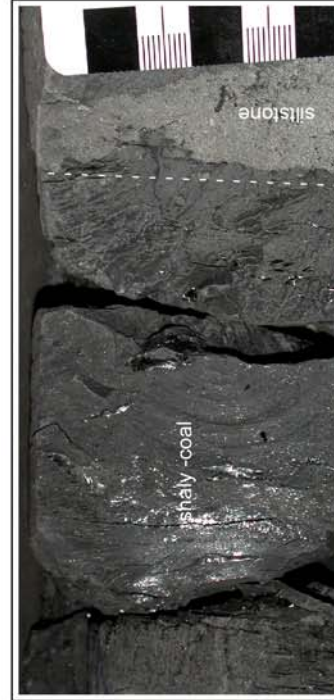
C



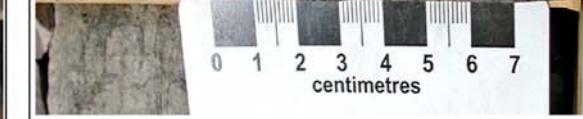
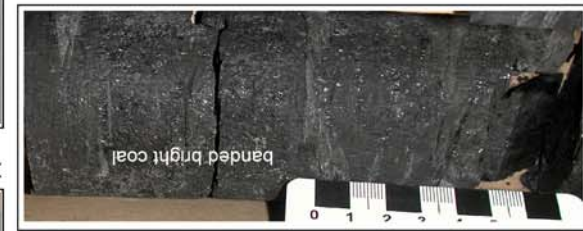
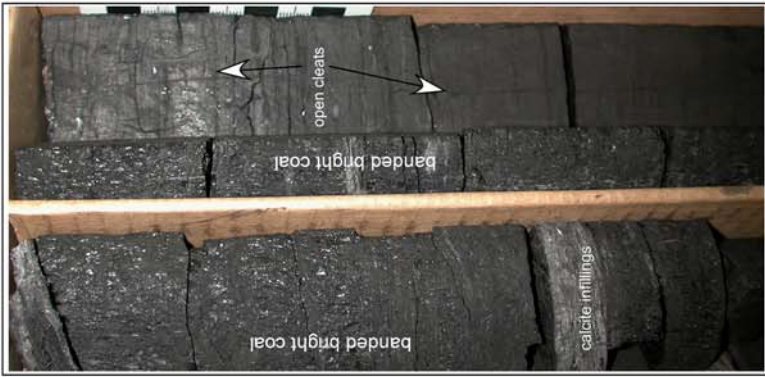
D



E



siltstone





D



A



B

